#1 Oceanog. Lab. Meteorol. Res. Inst.
Collected Reprints

COLLECTED REPRINTS

VOLUME 1

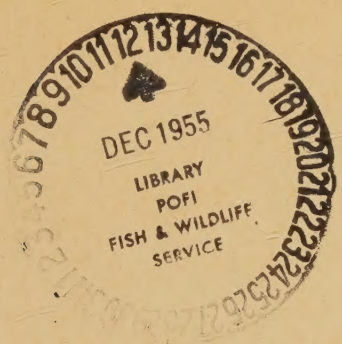

OCEANOGRAPHICAL LABORATORY,
METEOROLOGICAL RESEARCH INSTITUTE
MABASHI, SUGINAMI,
TOKYO, JAPAN.

April 1954

Digitized by the Internet Archive
in 2025

https://archive.org/details/oceanographical-laboratory-meteorological-research_1954-04

Preface

Our Oceanographical Laboratory was newly established in August 1952. Since the establishment it has been one year and a half, and during this period members of the laboratory have published their papers in various journals, of which offprints are here collected and issued as the Business Report Series No. 1. If this series might be more or less helpful to oceanographical researchers, we shall be very happy.

This volume owes much to those societies and publishers who have permitted the use of their copyrights on a condition that this volume should not be for sale.

February 1954

Masito NAKANO, DR. SC.
Chief of the Oceanographical Laboratory
Meteorological Research Institute

Contents

1) NAN'NITI, T. : A theory on the transparency of sea water.
Papers Met. Geophys. **3** (3), Jan. 1953.

2) NAN'NITI, T. : A current meter using a phototube (1).
Papers Met. Geophys. **3** (4), March 1953.

3) NAN'NITI, T. : A current meter using a phototube.
Rec. Oceanogr. W. Japan **1** (N. S.) (1), March 1953.

4) WADA, S. K. & R. WADA: On a new pearl oyster from the Pacific coast of Japan, with special reference to the cross-fertilization with another pearl oyster, Pinctada Martensii (Dunker).
Jour. Oceanogr. Soc. Japan 8 (3/4): 127, March 1953.

5) UNOKI, S. and M. NAKANO: On the Cauchy-Poisson waves caused by the eruption of a submarine volcano (1st Paper).
Oceanogr. Magaz. **4** (4), March 1953.

6) UNOKI, S. and M. NAKANO: On the Cauchy-poisson waves caused by the eruption of a submarine volcano.
Rec. Oceanogr. W. Japan **1** (N. S.) (1), March 1953.

7) KOIZUMI, M. : On the annual variation in oceanographical elements at a fixed point (39°N, 153°E) in the Pacific Ocean.
Rec. Oceanogr. W. Japan **1** (N. S.) (1), March 1953.

8) WADA, S. K. : Notes on the ecology of a plankton copepod, Labidocera pavo Giesbrecht.
Rec. Oceanogr. W. Japan **1** (N. S.) (1): 100, March 1953.

9) UNOKI, S. and M. Nakano: On the Cauchy-Poisson waves caused by the eruption of a submarine volcano (2nd paper).
Oceanogr. Magaz. **5** (1), June 1953.

10) ABE, T. : A study on the foaming of sea water (5th report)
On the foaming of sea water and inorganic electrolyte solutions. (in Japanese with English abstract).
Oceanogr. Report, CMO, **3** (1/2), 1953.

11) ABE, T. : A study on the foaming of sea water (6th report). On the mechanism of decay of the foam layer in sea water. (in Japanese with English abstract).
Oceanogr. Report. CMO, **3** (1/2), 1953.

12) NAN'NITI, T. : On the fluctuation of the Kurosiwo and the Oyasiwo (II). Proc. 8th Pacific Sci. Congr., Quezon City, Philippines.

13) NAKANO, M., M. KOIZUMI & F. FUKUOKA: On the oceanographical conditions of the sea near the fixed point, 153°E, 39°N, in the north Pacific Ocean. Proc. 8th Pacific Sci. Congr., Quezon City, Philippines.

14) NAN'NITI, T. : An improvement on the case of Forel's sea color scale.
Papers Met. Geophys. **4** (2), Sept. 1953.
15) NAN'NITI, T. : How to select the observation points.
Papers Met. Geophys. **4** (2), Sept. 1953.
16) NAN'NITI, T. : A current meter using a phototube (II).
Papers Met. Geophys. **4** (2), Sept. 1953.
17) ABE, T. : A study on the foaming of sea water (7th report). On the mechanism of decay of the foam layer of sea water (Part 2) (in Japanese with English abstract),
Jour. Oceanogr. Soc. Japan, **9** (2) 1953.
18) NAKANO, M., S. UNOKI & Y. KUGA: On the result of wave observations at Jogashima Island and its application to wave forecasting (I).
Papers Met. Geophys. **4** (3/4), Dec. 1953.
19) WADA, S. K. : Spawning of the tridacnid clams.
Jap. Jour. Zool. **11** (2)
20) UNOKI, S. & M. NAKANO: On the Cauchy-poisson waves caused by the eruption of a submarine volcano. (3rd paper).
Papers Met. Geophys. **4** (3/4), Dec. 1953.
21) ABE, T. : A study on the faming of sea water. On the mechanism of the decay of foam layer of sea water.
Rec. Oceanogr. W. Japan **1** (N. S.) (2), 1953.
22) KOIZUMI, M. : On the oceanographic and meteorological conditions at the fixed station "Extra" in the North Pacific Ocean.
Rec. Oceanogr. W. Japan **1** (N. S.) (2), 1953.
23) WADA, S. K. : Larviparons oysters from the west tropical Pacific.
Rec. Oceanogr. W. Japan **1** (N. S.) (2), 1953.

Reprinted from the *Papers in Meteorology and Geophy ics* Vol. I No. 3, 1953
Published by the Meteorological Research Institute

A Theory on the Transparency of Sea Water

by

T. Nan'niti

Published by the Meteorological Research Institute,
Mabashi, Suginami, Tokyo, Japan
January 1953

551.460.189:551.463

A Theory on the Transparency of Sea Water

by

T. Nan'niti

Meteorological Research Institute

(Received October 30, 1952)

Abstract

The present author derived theoretically the equation for the transparency of water as follows,

$$h=\frac{1}{2k(\lambda)}\log_e\frac{\left(1-\rho_0(\lambda)\right)^2\cdot\left(\frac{\rho(\lambda)}{\pi}-\frac{3}{16\pi}\frac{\alpha(\lambda)}{k(\lambda)}\right)}{\left\{\frac{3}{16\pi}\cdot\frac{\alpha(\lambda)}{k(\lambda)}\cdot\left(1-\rho_0(\lambda)\right)^2+\rho_0(\lambda)\right\}C(\lambda)},$$

and by the above equation discussed the relation between transparency and the oceanographical elements which have effects on it.

1. Theoretical consideration

Let us suppose a sea which has an infinite depth. Suppose that the solar radiation $J_0(\lambda)$ falls into water, then the light reflected back from the water surface is given by

$$(1)\qquad B_w(\lambda)=\left[\left\{\frac{\sin(\varphi-\chi)}{\sin(\varphi+\chi)}\right\}^2+\left\{\frac{\tan(\varphi-\chi)}{\tan(\varphi+\chi)}\right\}^2\right]J_0(\lambda)$$
$$=\rho_0(\lambda)J_0(\lambda),$$

where λ, φ and χ are the wave length of light, the incident and refractive angles respectively. The intensity of light penetrating into water is respresented by

$$(2)\qquad I_0(\lambda)=J_0(\lambda)-B_w(\lambda)=(1-\rho_0(\lambda))J_0(\lambda).$$

The vertical intensity of scattered light at the depth z is given by $\{3\alpha(\lambda)/8\pi\}\cdot I_0(\lambda)\cdot e^{-k(\lambda)z}$, where $\alpha(\lambda)$ and $k(\lambda)$ are respectively the scattering and extinction coefficient of water [1].

When we observe the scattered light through the water column the length of which is z, the light is exposed to extinction by the column and to reflection by the water surface. So on the surface we can see the scattered light at depth z as

$$\{3\alpha(\lambda)/8\pi\}\{1-\rho_0(\lambda)\}^2J_0(\lambda)e^{-2k(\lambda)z}.$$

Now, we must integrate the above quantity from 0 to z, since we measure actually

the integrated intensity of light from all parts in the water column. Thus the intensity of scattered light from the water column is expressed as follows,

$$\{3\alpha(\lambda)/8\pi\}\{1-\rho_0(\lambda)\}^2 J_0(\lambda)\int_0^z e^{-2k(\lambda)z}\,dz$$
$$=\{3\alpha(\lambda)/16\pi k(\lambda)\}\{1-\rho_0(\lambda)\}^2 J_0(\lambda)(1-e^{-2k(\lambda)z}).$$

Next, the intensity of light reflected from the surface of the Secchi disc at the depth z is given by $\{\rho(\lambda)/\pi\}I_0(\lambda)e^{-k(\lambda)z}$ where $\rho(\lambda)$ is the albedo of the disc, and the disc is regarded as perfectly rough. We observe this reflected light as $\{\rho(\lambda)/\pi\}\{1-\rho_0(\lambda)\}^2 J_0(\lambda)e^{-2k(\lambda)z}$. Thus, the apparent intensity of light coming from the disc in water is expressed by the next formula;

$$(3)\qquad B(\lambda)=B_w(\lambda)+\frac{3\alpha(\lambda)}{16\pi k(\lambda)}\{1-\rho_0(\lambda)\}^2 J_0(\lambda)(1-e^{-2k(\lambda)z})$$
$$+\frac{\rho(\lambda)}{\pi}\{1-\rho_0(\lambda)\}^2 J_0(\lambda)e^{-2k(\lambda)z}.$$

The scattering light from the water around the disc is given by

$$(4)\qquad A(\lambda)=B_w(\lambda)+\frac{3\alpha(\lambda)}{8\pi}\{1-\rho_0(\lambda)\}^2 J_0(\lambda)\int_0^\infty e^{-2k(\lambda)z}\,dz$$
$$=B_w(\lambda)+\frac{3\alpha(\lambda)}{16\pi k(\lambda)}\{1-\rho_0(\lambda)\}^2 J_0(\lambda).$$

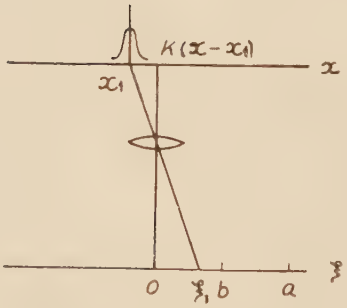

Fig. 1. The pattern of the image of Secchi disc under water upon the retina.

Now, if an observer looks upon the disc in water, the intensity distribution of light on his retina is expressed by $K(x-\xi_1)$, where ξ and x axes are the sea surface and the retina respectively [2], and the function $K(x)$ will depend on the character of his eyes as shown in Fig. 1. Now, the radii of the Secchi disc and the visual field are *ob* and *oa* respectively, then the image of the point ξ_1 on the retina is expressed by $K(x-x_1)$ and $x_1=\xi_1$.

So we recognize the disc as

$$\int_0^{2\pi}\int_\lambda\int_0^b e(\lambda)K(x-\xi)B(\lambda)\xi\,d\xi\,d\lambda\,d\theta,$$

where $e(\lambda)$ is the sensitivity of eyes. Thus the transparency of water can be calculated by the next equation

$$(5)\qquad \frac{\int_0^{2\pi}\int_\lambda\left\{\int_0^b e(\lambda)K(x-\xi)B(\lambda)\xi\,d\xi-\int_b^a e(\lambda)K(x-\xi)A(\lambda)\xi\,d\xi\right\}d\lambda\,d\theta}{\int_0^{2\pi}\int_\lambda\int_b^a e(\lambda)K(x-\xi)A(\lambda)\xi\,d\xi\,d\lambda\,d\theta}=C, \qquad [3]$$

where the constant C depends on the sensitivity of the observer's eyes and also the sea surface conditions. But then, we know little about $K(x-\xi)$, so we put

approximately the above equation (5) as follows,

$$\frac{B(\lambda)-A(\lambda)}{A(\lambda)}=C(\lambda)\,. \tag{6}$$

Putting the equations (3) and (4) into (6), we get

$$e^{-2k(\lambda)z}=\frac{\left\{\frac{3}{16\pi}\frac{\alpha(\lambda)}{k(\lambda)}\{1-\rho_0(\lambda)\}^2+\rho_0(\lambda)\right\}C(\lambda)}{\{1-\rho_0(\lambda)\}^2\left(\frac{\rho(\lambda)}{\pi}-\frac{3}{16\pi}\frac{\alpha(\lambda)}{k(\lambda)}\right)}.$$

So the transparency of water can be expressed by the following formula;

$$h=\frac{1}{2k(\lambda)}\log_e\frac{\{1-\rho_0(\lambda)\}^2\left(\frac{\rho(\lambda)}{\pi}-\frac{3}{16\pi}\frac{\alpha(\lambda)}{k(\lambda)}\right)}{\left\{\frac{3}{16\pi}\frac{\alpha(\lambda)}{k(\lambda)}\{1-\rho_0(\lambda)\}^2+\rho_0(\lambda)\right\}C(\lambda)}. \tag{7}$$

If we take $\varphi=0$,

$$\rho_0(\lambda)=\left(\frac{n_{12}-1}{n_{12}+1}\right)^2=\left(\frac{n_2-n_1}{n_2+n_1}\right)^2,$$

which we may use approximately until $\varphi=30°$, where n is a refractive index.

Then,

$$h=\frac{1}{2k(\lambda)}\log_e\frac{\left\{\frac{4n}{(n+1)^2}\right\}^2\left(\frac{\rho(\lambda)}{\pi}-\frac{3}{16\pi}\frac{\alpha(\lambda)}{k(\lambda)}\right)}{\left[\frac{3}{16\pi}\frac{\alpha(\lambda)}{k(\lambda)}\left\{\frac{4n}{(n+1)^2}\right\}^2+\left(\frac{n-1}{n+1}\right)^2\right]C(\lambda)}. \tag{8}$$

2. Numerical calculation

The scattering coefficient of pure water is given by RAMAN, EINSTEIN and SMOLUKOWSKY [1] as follows

$$\alpha(\lambda)=\frac{\sigma RT}{N}(\mu^2-1)(\mu^2+1)\frac{1}{\lambda^4}\,.$$

Putting $\lambda=5200\,\mathring{A}$, $T=288\,°K$, $\sigma=49\times10^6$ C.G.S., $\mu=1\cdot34$, $R=22\cdot4\times10^3\,\mathrm{cm^3/mol}$, $N=6\cdot06\cdot10^{23}\,\mathrm{mol^{-1}}$, we get $\alpha=0.00223$. SAWYER [4] [5] got the value of $k=0\cdot019$ at $\lambda=5200\,\mathring{A}$ in distilled water. In natural water, VERCELLI [5] obtained the values $\alpha=0\cdot002$, $k=0\cdot06$, $0\cdot11$ at $\lambda=5300\,\mathring{A}$ and $5720\,\mathring{A}$. The refractive index is given as $n=1\cdot33524$ at $\lambda=5269\cdot978\,\mathring{A}$, $t=20°C$, so we get the values $\rho_0=0\cdot02$.

Assuming that the albedo of the white Secchi disc is 0.6 and the value of C is 1/100, we shall get the value of transparency for pure water, $h=173\,m$.

In Sargasso Sea, the value of the extinction coefficient $k=0.050$ was reported by G. L. CLARKE [5]. Using these quantities, we get $h=67.2\,m$. In fact, the transparency in Sargasso Sea was observed as $h=66.5\,m$. So we can say that the above calculation agrees well with the observation despite a simple assumption that the sea is homogeneous, i.e., $k=$const. and $\alpha=$const. In other words, in Sargasso sea the water is quite transparent and homogeneous.

Now as seen in the equation (7), transparency is governed by $k(\lambda)$ and $\alpha(\lambda)$. So we can represent the nature of transparency as a function of $\alpha(\lambda)/k(\lambda)$. For, if we assume approximately that extinction is the sum of absorption and scattering, and that the absorption is equal to that in pure water, we get the equation $\alpha(\lambda)/k(\lambda)=1-0.019/k(\lambda)$ [6], which varies from zero to one as water becomes turbid. Next, for the value of $C(\lambda)$, different estimations are made by different authors, so here we take it to be 1/100 and 1/57 [1]. In actual observation, the ratio of light reflected back from the water surface such as 5% [1] is somewhat larger than the calculated one. We calculated hk by the equation (7). The results are given in the follwing table and Fig. 2.

The Table of hk

ρ/π \ α/k	0	0.02	0.2	0.4	0.6	0.8	1.0	Remarks
0.20	3.4	3.4	3.2	3.0	2.8	2.7	2.6	$C=\frac{1}{100}$, $\rho_0=0.02$
0.15	3.3	3.3	3.1	2.8	2.6	2.4	2.3	
0.20	3.1	3.1	2.9	2.7	2.5	2.3	2.2	$C=\frac{1}{57}$, $\rho_0=0.02$
0.15	3.0	3.0	2.8	2.5	2.3	2.1	2.0	
0.15	2.6	2.6	2.4	2.2	2.0	1.9	1.8	$C=\frac{1}{57}$, $\rho_0=0.05$

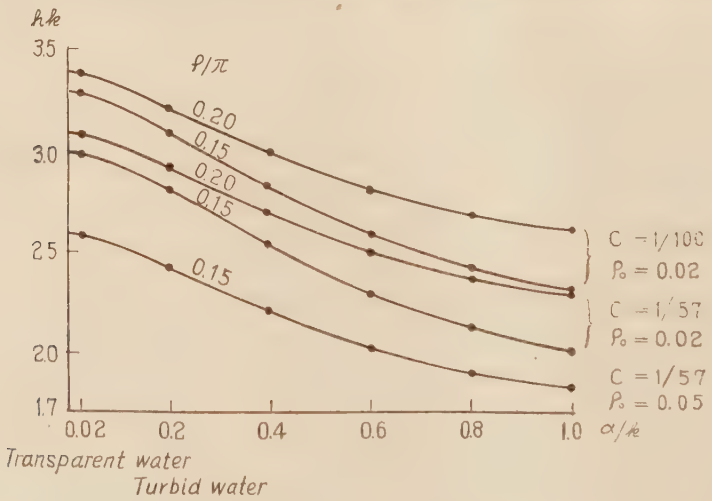

Fig. 2. Relation between (transparency × extinction coefficient) and (scatting coefficient/extinction coefficient)

We know as C and ρ_0 becomes larger and as ρ becomes smaller, the values of hk become smaller, and if ρ/π and ρ_0 are constant, the curve expressing hk gradually goes downwards keeping its form as C becomes larger. So if the albedo of the Secchi disc and the sea surface are constant, the relation between hk and α/k, or k is constant by any observer by shifting the coordinate axis, but if the albedo of

the disc or the sea surface is not constant, the above relation of hk and α/k is different even by the same observer, i.e., in the case when C is constant. And as water becomes more turbid, i.e., α/k becomes closer to 1, the value of hk becomes smaller. Formerly, a formula such as $h=1.7/k$ or $hk=$const [7] was deduced. If it is true, the value of C will be smaller, as the water becomes more turbid, i.e., it will become difficult to recognize the difference of brightness between the disc and its circumference, that is, our power of recognition of the difference of brightness will be lowered than in transparent water. Consequently transparency depends much on the difference of colour sensation as TAKENOUTI [1] says. And we should take secondary effects into consideration as water becomes more turbid, which generate the various colours of sea.

In conclusion, for the observation of the transparency of water, we must conduct further researches on $\alpha(\lambda)/k(\lambda)$, which plays a great role in the transparency of water, and we must be careful about the sea surface conditions which influence value of ρ_0 and C, and also we must keep the albedo of the disc ρ constant.

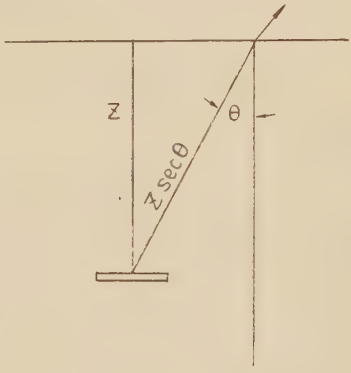

Fig. 3. Situation of a Secchi disc when a wire inclines.

3. Correction to the transparency when a wire inclines

When a wire suspending the Secchi disc has an inclination θ to the sea surface, and the disc keeps its plane horizontal as shown in Fig. 3, then, we are obliged to see the disc in an oblique direction; the intensity of scattered light from the water column is given by

$$\int_0^z \frac{3\alpha(\lambda)}{16\pi} J_0(\lambda)\{1-\rho_0(\lambda)\}e^{-k(\lambda)z}(1+\cos^2\theta)e^{-k(\lambda)\frac{z}{\cos\theta}}\{1-\rho_0'(\lambda)\}dz$$
$$= \frac{3}{16\pi}\frac{\alpha(\lambda)}{k(\lambda)}\frac{1+\cos^2\theta}{1+\frac{1}{\cos\theta}}\{1-\rho_0(\lambda)\}\{1-\rho_0'(\lambda)\}J_0(\lambda)\left(1-e^{-k(\lambda)\left(1+\frac{1}{\cos\theta}\right)z}\right).$$

When the angle θ is smaller than 30°, $\rho_0(\lambda)=\rho_0'(\lambda)=\{(n_{12}-1)/(n_{12}+1)\}^2$ and as θ is larger than 30°, the above equation holds approximately. The intensity of light reflected by the disc is given by

$$\frac{\rho(\lambda)}{\pi}\cos\theta\{1-\rho_0(\lambda)\}^2 J_0(\lambda)e^{-k(\lambda)\left(1+\frac{1}{\cos\theta}\right)z}.$$

So, we have the next equation for the apparent intensity of light coming from the disc in water instead of the equation (3),

$$(9)\quad B(\lambda)=B_w(\lambda)\cos\theta+\frac{3}{16\pi}\frac{\alpha(\lambda)}{k(\lambda)}\frac{1+\cos^2\theta}{1+\frac{1}{\cos\theta}}\{1-\rho_0(\lambda)\}^2 J_0(\lambda)\left(1-e^{-k(\lambda)\left(1+\frac{1}{\cos\theta}\right)z}\right)$$
$$+\frac{\rho(\lambda)}{\pi}\cdot\cos\theta\{1-\rho_0(\lambda)\}^2 J_0(\lambda)e^{-k(\lambda)\left(1+\frac{1}{\cos\theta}\right)z}.$$

The scattering light from the water around the disc is also given by

$$(10) \qquad A(\lambda)=B_w(\lambda)\cos\theta+\frac{3}{16\pi}\frac{\alpha(\lambda)}{k(\lambda)}\frac{1+\cos^2\theta}{1+\frac{1}{\cos\theta}}\{1-\rho_0(\lambda)\}^2J_0(\lambda).$$

So, putting equations (9) and (10) into (6), we get the next formula instead of equations (7) and (8):

$$(11) \qquad z=\frac{\cos\theta}{k(\lambda)(1+\cos\theta)}\log_e\frac{\{1-\rho_0(\lambda)\}^2\left(\frac{\rho(\lambda)}{\pi}-\frac{3}{16\pi}\frac{\alpha(\lambda)}{k(\lambda)}\frac{1+\cos^2\theta}{1+\cos\theta}\right)}{\left(\frac{3}{16\pi}\frac{\alpha(\lambda)}{k(\lambda)}\{1-\rho_0(\lambda)\}^2\frac{1+\cos^2\theta}{1+\cos\theta}+\rho_0(\lambda)\right)C(\lambda)}.$$

Then we have

$$z \fallingdotseq \frac{\cos\theta}{k(\lambda)(1+\cos\theta)}\log_e\frac{\{1-\rho_0(\lambda)\}^2\left(\frac{\rho(\lambda)}{\pi}-\frac{3}{16\pi}\frac{\alpha(\lambda)}{k(\lambda)}\right)}{\left(\frac{3}{16\pi}\frac{\alpha(\lambda)}{k(\lambda)}\{1-\rho_0(\lambda)\}^2+\rho_0(\lambda)\right)C(\lambda)}$$

$$= \frac{2\cos\theta}{1+\cos\theta}\cdot h.$$

So we have

$$h \fallingdotseq \frac{1+\cos\theta}{2\cos\theta}z=\frac{1+\cos\theta}{2}h_\theta,$$

where h_θ and h are respectively the length of the wire in water and the transparency of water. We have Fig. 4 which shows the increase in the length of the wire when it inclines in water.

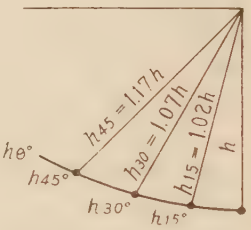

Fig. 4. Relation between apparent and true transparency when a wire inclines.

4. Seasonal variation

Assuming $\alpha(\lambda)=k(\lambda)-\text{const.}(\lambda)$, we have $\alpha(\lambda)/k(\lambda)=1-\text{const.}(\lambda)/k(\lambda)$. When the transparency varies periodically, the extinction coefficient also changes with the same period from the equation (7). Assuming that the colour of the sea is caused by the scattering and absorption of light, we can expect also that the colour of the sea will change annually with the same period of the extinction coefficient, or the variation of transparency. We can see the fact in actual observations, for example, in those reported by Koizumi [8].

Acknowledgement The author expresses his best thanks to Dr. Y. Miyake, Dr. Y. Takenouti and Mr. K. Sekihara for their kind advices.

References

[1] Takenouti, Y., 1950: On the Transparency of Sea Water. The Oceanographical Magazine, 2, p. 129.

[2] Hidaka, K., 1941: Integral Equations. Tokyo, Kawade-shobo, p.3.

[3] Suda, K., 1943: The Science of the Sea (Kaiyo Kagaku). Tokyo, Kokin-shoin, p. 284.

[4] Sawyer, W.R., 1931: The Spectral Absorption Light by Pure Water and Bay of Fundy Water. Contr. Canad. Biol. Fish., N.S, **7** (8) Dl, p. 75.

[5] Takenouti, Y., 1939: On the Under Water Illuminations. Bulletin of the Japanese Society of Scientific Fisheries, **8**, p.194.

[6] Takenouti, Y., 1944: On the Extinction Coefficient of Sea Water. Journal of the Oceanographical Society of Japan, **3**, p. 181.

[7] Sverdrup, H. U., Johnson, M. W. and Fleming, R. H., 1949: The Oceans. New York, Prentice-Hall Inc. p.82.

[8] Koizumi, M., 1951: On the Oceanographical Conditions around the Fixed Point "X". The Oceanographical Report, Central Meteorological Observatory of Japan. **2**, p. 163.

Reprinted from the *Papers in Meteorology and Geophysics* Vol. III No. 4, 1953
Published by the Meteorological Research Institute

A Current Meter Using a Phototube* (I)

— Test Manufacture of a New Current Meter and Some Experiments on the Sea —

by

T. Nan'niti

Published by the Meteorological Research Institute,
Mabashi, Suginami, Tokyo, Japan
March 1953

551.460.183

A Current Meter Using a Phototube* (I)

— Test Manufacture of a New Current Meter and Some Experiments on the Sea —

by

T. Nan'niti

Meteorological Research Institute

(Received December 25, 1952)

Abstract

To measure velocities of currents automatically, the author has made a recording current meter using a phototube, in which the intermittent photoelectric current is depicted on a chart of a recorder on deck. The speed and direction of water current can be measured respectively by the time intervals and by the intensity of photoelectric current. Experiments on the sea have shown that by using the current meter, the actual under-water conditions can be immediately observed, and fine, accurate and rapid observations of water current have been made possible.

1. Introduction

Most of the types of the recording current meter, hitherto devised, require a water-tight chamber equipped with a propeller which rotates in accordance with the velocity of current. Since the shaft of the propeller penetrates the wall of the chamber, it becomes very difficult to keep the chamber water-tight under a hydrostatic pressure. In the new current meter here described, this difficulty is eliminated by using a beam of light in place of the shaft of a propeller. Furthermore, by using a phototube and a cylindrical mirror specially designed with a magnet, minute variations in both speed and direction of current can be measured.

2. A principle of the photoelectric method

In the present current meter, a light of constant intensity is emitted from a light source, and is reflected by a cylindrical mirror into a phototube producing photoelectric current.

A disc with holes which rotates in accordance with the current by means of a propeller is placed in the path of the light between the light source and the mirror.

---

* The preliminary study on this subject was published in "Umi-to-Sora" [1].

Therefore, an intermittent flash of light is produced by a rotating disc, the frequency of flashes being proportional to the speed of the current. Thus, the latter can be measured from the frequency of flashes.

The shape of the mirror is an equilateral triangle, more exactly, a trapezoid, girt around a cylinder like a belt, the apex of the triangle being slightly overlapping the base. The cylinder is attatched with a magnet at the bottom, which keeps it in constant direction to the geomagnetic co-ordinate.

Since the light source moves with the direction of current, a light with certain intensity is reflected by the triangular mirror in accordance with the current direction. In other words, a certain value in the intensity of the reflected light corresponds to a certain value in the direction of current. Therefore, the latter can also be found from the measurement of the intensity of the reflected light.

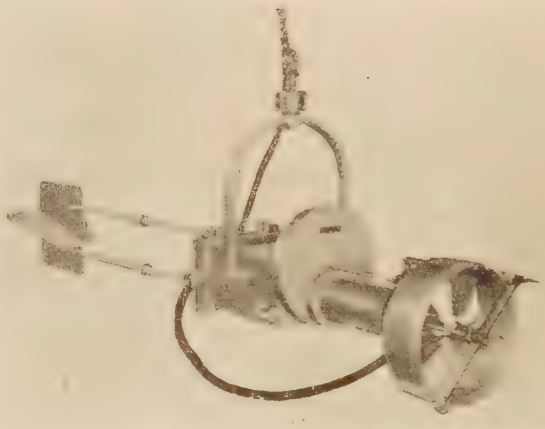

Fig. 1. The under-water portion of the current meter, which sends photoelectric signals.

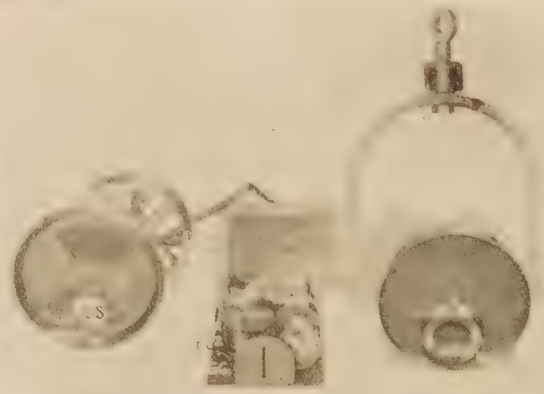

Fig. 2. The inner parts of the current meter shown in Fig. 1.

3. The details of the design

The current meter is shown in Figs. 1 and 2. C_1 and C_2 are brass cases, each with a glass window, GW_1 or GW_2, and their interior are kept water tight, but water freely passes through between two glass windows, GW_1 and GW_2. The light source, LS is an electric lamp which is lit by a battery on deck; from the light source, a parallel ray is thrown through the window GW_1 into C_2. A disc, D, with holes, is rotated with a speed proportional to that of current by means of a propeller P. So intermittent beams of light are thrown on the window of the case C_2 by the rotation of the disc. As the light penetrates into the case C_2 through the window GW_2, it is restricted by a slit S, and a narrow linear beam of light is obtained, then it is reflected toward a phototube PT by a cylindrical mirror CM. The mirror is always kept in the constant geomagnetic direction by an attatched magnet.

Now, since the current meter with the lamp and the slit is kept in the direction of current by its rudder, while the cylindrical mirror remains in a constant direction, the relative position of the slit to the mirror will be changed according to the direction of current. Consequently, the intensity of the light reflected by the mirror will be varied in accordance with the current direction, when the intensity of an incident light thrown into the case C_2 is kept constant. Hence the intermittent photoelectric current, with different intensities corresponding to the current direction, is produced by a phototube PT. In order to keep constant the intensity of the incident light, a variable resistance is inserted in the electric circuit, with which the voltage applying to the lamp is kept constant. However, if the extinction coefficient of water between the cases C_1 and C_2 varies during an observation the intensity of light upon the mirror will be changed, and it will cause an error in the observed values of the direction of current. In order to eliminate this error, two electric coils, EC_1 and EC_2, are set respectively in parallel and normal to the principal line of the instrument. By these coils, four kinds of electromagnetic fields, each differring by 90° in the direction, can be formed, when necessary. Therefore, the relation between the intensity of photoelectric current and the direction of water current can be readily recorded on the chart. Since the direction of the electromagnetic fields produced by the coils are either parallel or normal to the principal axis of the instrument, that is, the direction of the current, and a linear relationship exists between the photoelectric intensity and the direction of the cylindrical mirror (see Section 5), the direction of the water current can be determined, even when the intensity of incident light changes.

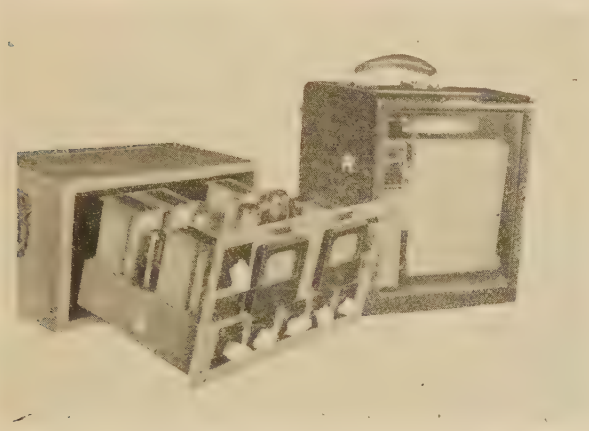

Fig. 3. The amplifier (A) and the recorder (R).

The photoelectric current is amplified by a vacuum-tube UZ-6C6 and then led to a micro-ammeter on deck by a cable. The speed of water current can be measured by reading the time intervals of intermittent photoelectric current, its direction being determined by measuring the electric current intensity.

Furthermore, automatic recording is also possible, by further amplifying the photoelectric current, for instance, by means of modulation. The amplifier and the recorder are shown in Fig. 3.

4. Instrumentation

The schematic block and circuit diagram of the photoelectric measurment process are shown in Figs. 4 and 5. Each part of the instruments will be described in the following.

a. Under-water portion This part is shown in Fig. 1. It is immersed into the water during observation. It sends the signal to the recorder on deck by way of a ten-fold rubber-covered cable 50 meters long. For detailed description, see the above section.

b. Amplifier on deck This part is shown in Figs. 3, 4 and 5. The upper part in Fig. 5 is an oscillator to generate a carrier wave. The direct photoelectric current is amplified by modulation method. The output current can be controlled by the grid bias voltage, noise limitter volume and output current regulator, all the voltages of the power supply being kept constant.

The characteristics of the instrument above mentioned are given in the following figures (Figs. 6 and 7). In Fig. 6, the relation between the grid bias voltage and the plate current of the vacuum-tube UZ-6C6 is

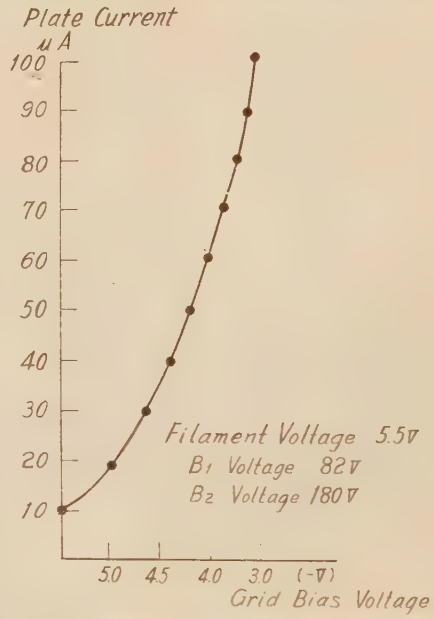

Fig. 6. Relation between the plate current and the grid bias voltage.

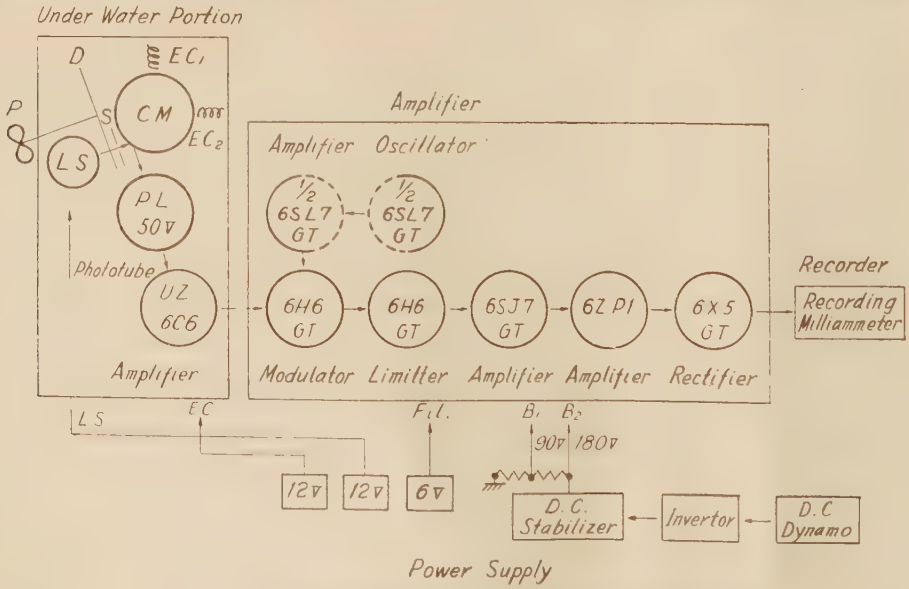

Fig. 4. Schematic block diagram of the instrument.

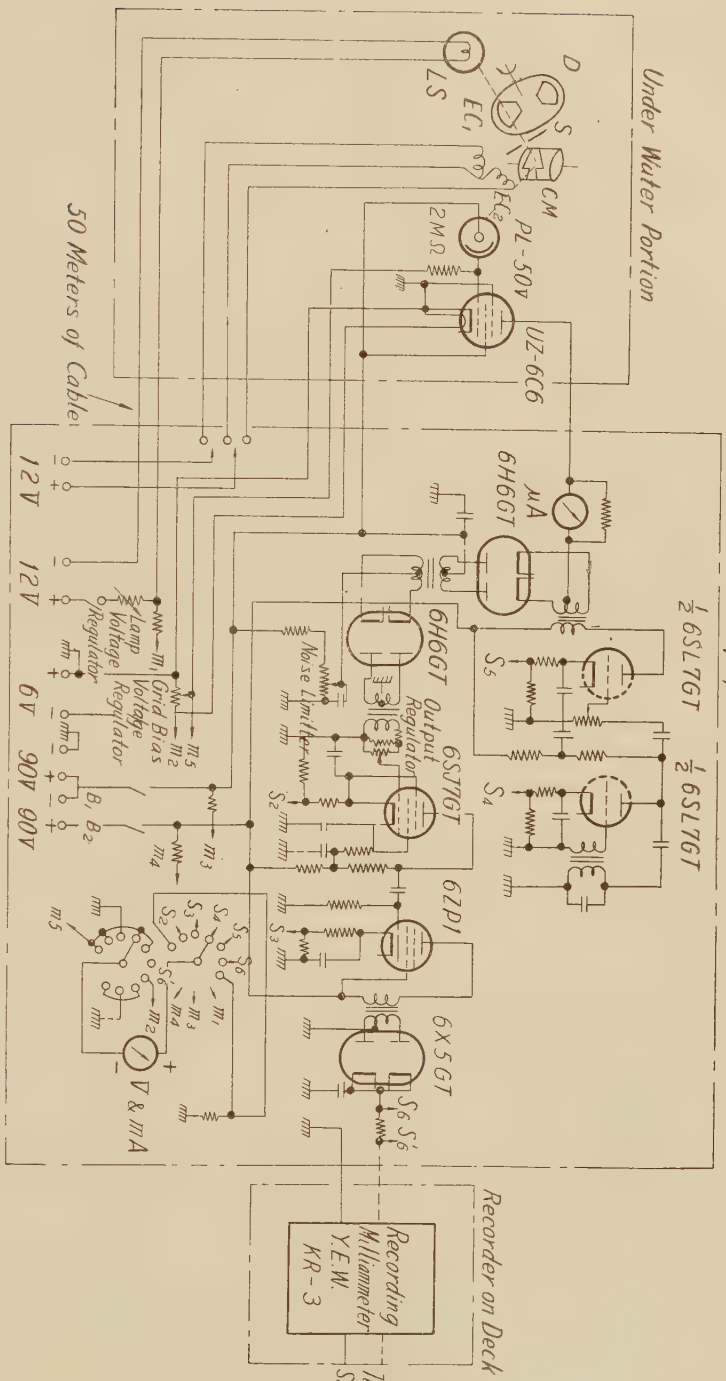

Fig. 5. Schematic circuit diagram of the instrument.

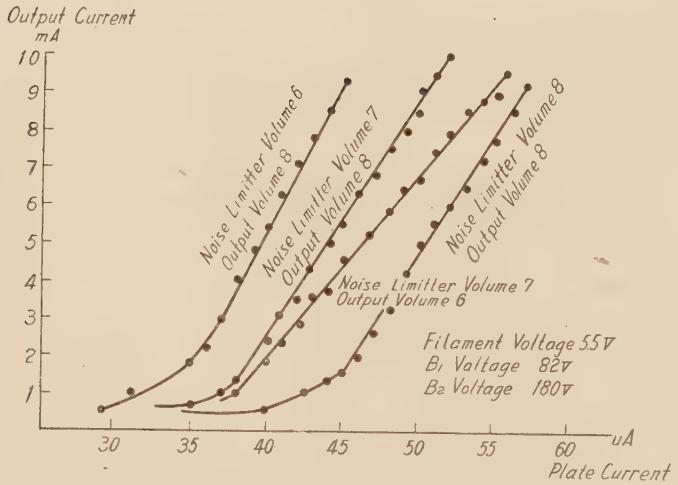

Fig. 7. Relation between the output and the plate current.

presented. The relation between the plate current and the resultant recording current is shown in Fig. 7. These lines in the figure will be changed by the values of noise limitter volume and output current regulator. From the facts shown in Figs. 6 and 7, an adjustment of the instrument to obtain the linear relation between the photoelectric current and the recording current is found possible.

c. Recorder and power supply Yokogawa's recording milliammeter, type KR-3, was used, in which the chart was rolled with a speed of 2 cm/min. At this rate of advance, a ten-meter chart roll will last 8 hours, and the batteries for the electric lamp, the electric coils and the filaments of the vacuum-tubes will last more than 10 hours. Furthermore, the electric power required for the instrument is of the direct 90 volts and 180 volts. Since the direct current of 100 volts was available on board the ship, where the experiments were carried out, the direct current was first changed into the alternating one by an invertor; further, it was changed into the direct current of 180 and 90 volts by a direct current stabilizer, the diagram of which is shown in Fig. 8.

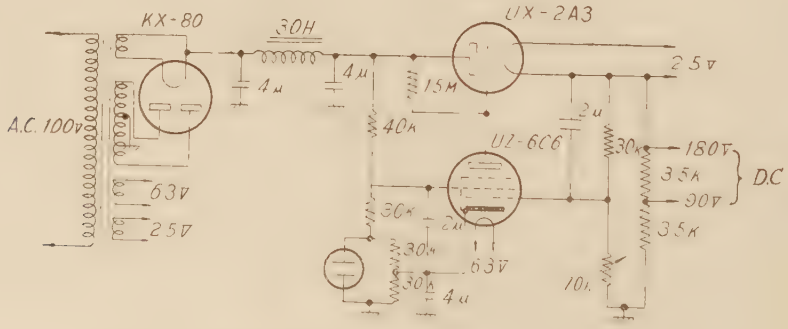

Fig. 8. Schematic circuit diagram of D. C. stabilizer.

5. Theoretical consideration

Now let current speed of water be v cm/sec and the number of flashes of light be n times/sec, then we have

$$v=an^2+bn+c\,,$$

where a,b and c are constants. Two holes are made in the disc, which turns once whenever water has run 20 meters. Therefore, the light path is opened once per 10 meter running of water. Assuming that it requires t seconds and l cm of chart to record N times of the intermittent photoelectric current, we have,

$$n=N/t=N/30\,l\,,$$

then,

$$v=a(N/30\,l)^2+b(N/30\,l)+c\,.$$

Next, let the breadth of the slit S be B, and the vertical length of the mirror, CM, be $\alpha\theta+\beta$, $0^\circ \leq \theta \leq 360^\circ$, where both α and β are constants, and θ is the angle around the axis of the cylinder. The intensity of light reflected by the mirror is given by $I_0 e^{-kz}\rho B(\alpha\theta+\beta)$, where I_0 is the intensity of the original light, k is the combined extinction coefficient of the glass windows and water, z is its optical length, and ρ is the albedo of the mirror. So the photoelectric current i will be proportional to the angle θ, that is $i=K\theta$, provided that the quantities above mentioned are kept constant. From Figs. 6 and 7, we can expect a linear relation between the recording electric current and direction of oceanic current. Indeed, for example, it is seen in Fig. 9.

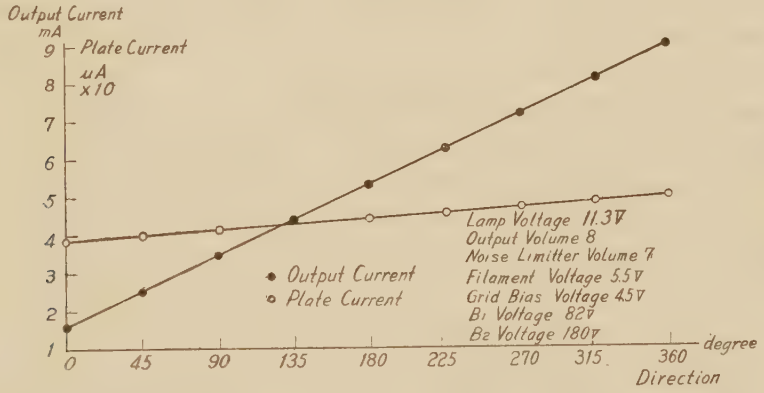

Fig. 9. Relation between the direction of the current meter and the intensity of the photoelectric current.

6. Experimental results

The experiments were performed in Tokyo Bay on board the research ship "Asasiwo Maru", on June 26th and September 17th, 1952. The hull of the ship is made of wood. The results are compared with those obtained by an Ekman-Merz current meter. Comparative measurements sometimes revealed augular disagreements as high as 82°; since the measurements were done in shallow waters of only

three meters' depth, the instruments could be seen through the sea surface. The disagreements were recognized always to be due to the errors caused by the Ekman-Merz current meter although the sea was very calm.

The observation which was performed at Lat. 35°27.5′ N, Long. 139°44.3′ E in Tokyo Bay on September 17th will be considered in the following. The record which was obtained at the depth of 1.75 m is shown in Fig. 11. The current direction fluctuated with an amplitude 40° and a period 8 minutes, its main direction being S 30°W(210°) and speed 27.5 cm/sec. Though the speed calibration was not done, the values for the speed would almost be correct. The measurement was often interrupted by disturbances in the propeller caused by jelly fish. The minute fluctuation on the record, with the period of 2 or 3 seconds and the amplitude 2° or 3° (the maximum being 10°) might be caused by Kármán vortex in the water.

Another record in the same experimental run is shown in Fig. 12. The current direction fluctuated with the amplitude of 30°, the period from 3.5 min. to 5 min., its main direction was S 60° W (240°), and the speed 29.1 cm/sec.

A simultaneous observation with an Ekman-Merz's and the new current meter was performed, the two instruments being set as near as possible to each other (Fig. 10). At 21h58m, according to the Ekman-Merz current meter, the direction of the current was 169°, the speed 31.7 cm/sec, while the record obtained by the new current meter showed that the current direction was 250°, the speed 30.0 cm/sec. Further, the old instrument measured a current of 178° in the direction, and the speed 16.2 cm/sec at 22h38 m, while at 22h39m, a current of 260° and 14.4 cm/sec was recorded by the present current meter.

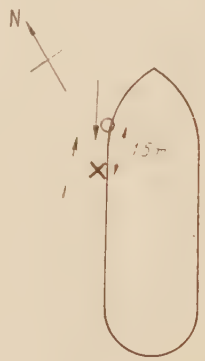

Fig. 10. Position of the new and Ekman Merz current meter in the comparative experiment.
The arrows show the direction of current as observed by vision.
Heavy arrow: 1.75 m layer
Broken arrow: 3 m layer

Since the current meter under-water could be seen from above the water surface, the direction of current in situ was cleary determined by visual observation from the situation of the meter. The current direction visually observed (SW or WSW) as shown in Fig. 10 agreed well with the record of the new instrument; whereas the directions observed by the current meter of the Ekman-Merz type frequently showed disagreements with visual observation.

Observation at a layer of 3 m depth was commenced at 23h15m. The direction

of current, as seen from the deck, was found, at first, equal with that at 1.75 m layer, that is, it was S or SW at about 23h50m and turned to NE or E thereafter (Fig. 13). At 00h23m, 18 th, values of 58° and 13.6 cm/sec were obtained by the Ekman-Merz's, while, the record by the new instrument showed that the current was of 80° and 11.9 cm/sec at 00h20m.

The fluctuation in the current direction, of the order of several minutes, which was observed in the upper layer, could not be detected in the record obtained at the layer 3 meters deep, although the measurements were performed successively. Therefore, it seems highly probable that the fluctuation in the pattern of current as recorded in the observation at 1.75 m layer really occurs, although it is also possible that the fluctuation arose from the turbulence which might be caused by the side of the ship, since the draft of the ship was 2~3 meters.

Acknowledgement The author wishes to express his hearty thanks to Dr. Y. Miyake and Dr. Y. Takenouti for their encouragement, to Mr. K. Kawamura for his kind advice, and to the members of the Oceanographical Division of the Central Meteorological Observatory for their help during the observations. His thanks are also due to the members of Turumi Seiki Co. and of Toho Denki Co., for the construction of the instrument.

This work was made possible by a grant in aid for research of test manufacture in 1951 from the Ministry of Transportation.

Reference

[1] Nan'niti, T., 1947 : A Current Meter Using a Photocell (I). Umi-to-Sora, **25**, No. 5, p. 64 (in Japanese).

A CURRENT METER USING A PHOTOTUBE

T. NAN'NITI

Meteorological Research Institute, Tokyo

A CURRENT METER USING A PHOTOTUBE

T. NAN'NITI

Meteorological Research Institute, Tokyo

1. *Physical Principles and Details of the Design.* The current meter is shown in Figs. 1 and 2. C_1 and C_2 in the figures are brass cases, each with a glass window GW_1 or GW_2, and the inner parts are kept water tight though water freely passes through between the glass windows. Light of constant intensity is emitted from a light source LS, reflected by a cylindrical mirror CM and produces a photoelectric current in a phototube PT. A disc D with holes which rotates in accordance with the speed of water current by means of a propeller P is placed in the path of light between the light source LS and the mirror CM. Therefore, intermittent light is

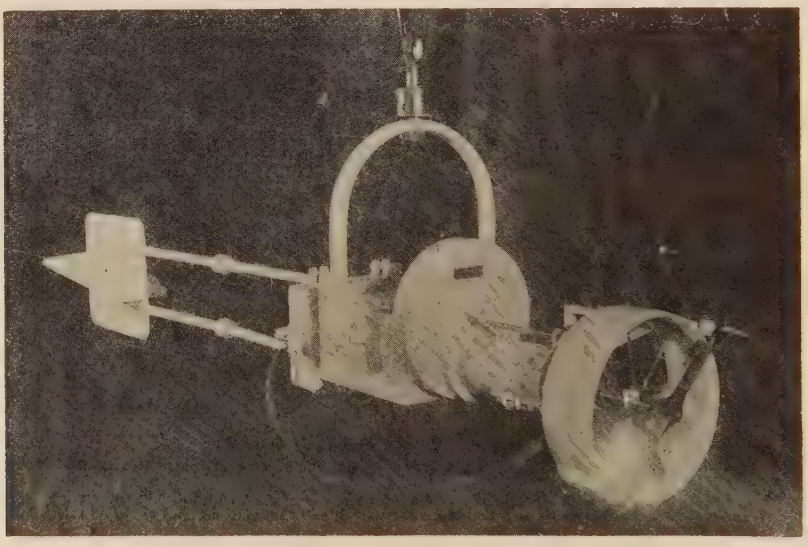

Fig. 1. Under water portion of current meter.

produced by the rotating disc D, the frequency of the flash being exactly proportional to the speed of the oceanic current. Consequently, the speed of current can be measured from the frequency of flash. The shape of the mirror CM is an equilateral triangle, more exactly a trapezoid, rolled around a cylinder like a belt. The cylinder is fitted with a magnet at the bottom, which keeps it in constant direction to the geomagnetic co-ordinate. The light is narrowed by a slit S and forms a line light, and it swivels with the direction of water current, so light of a certain intensity, reflected

by the triangular mirror in accordance with the current direction. Therefore, the current direction can be known also from the measurement of the intensity of the reflected light. However, if the extinction coefficient of water between the glass windows

Fig. 2. Inner part of current meter shown in Fig. 1.

varies during an observation, the intensity of light upon the mirror will be altered, and it causes an error in the observed values of the direction of the current. In order

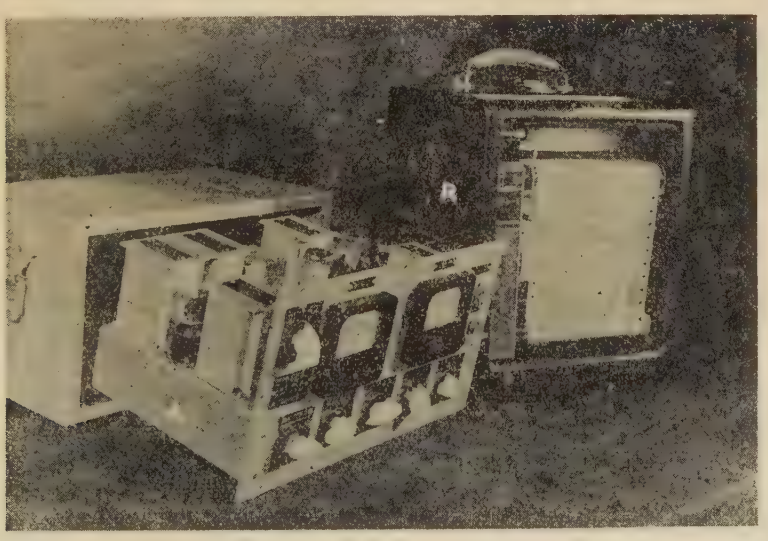

Fig. 3. Amplifier and Recorder.

to avoid this error, two electric coils, EC_1 and EC_2 are set respectively parallel and normal to the principal line of the instrument. By these coils, four kinds of electro-

magnetic fields, each differing 90° in direction from one another, can be formed. Therefore, relation between the intensity of photoelectric current and the direction of the instrument can be readily recorded on the chart, and as a linear relation exists between the photoelectric intensity and the direction of the instrument (see the following section), the direction of the water current can be determined, irrespective of the intensity of incident light of the mirror.

Next, the photoelectric current is amplified by a vacuum-tube UZ-6C6 and then led to a microammeter on deck by a cable. It is further amplified by means of modulation and led to a recording milliammeter. The amplifier A and the recorder R are shown in Fig. 3. Yokogawa's recording milliammeter, type KR-3, was used, in which the chart is rolled with a speed of 2 cm/min.

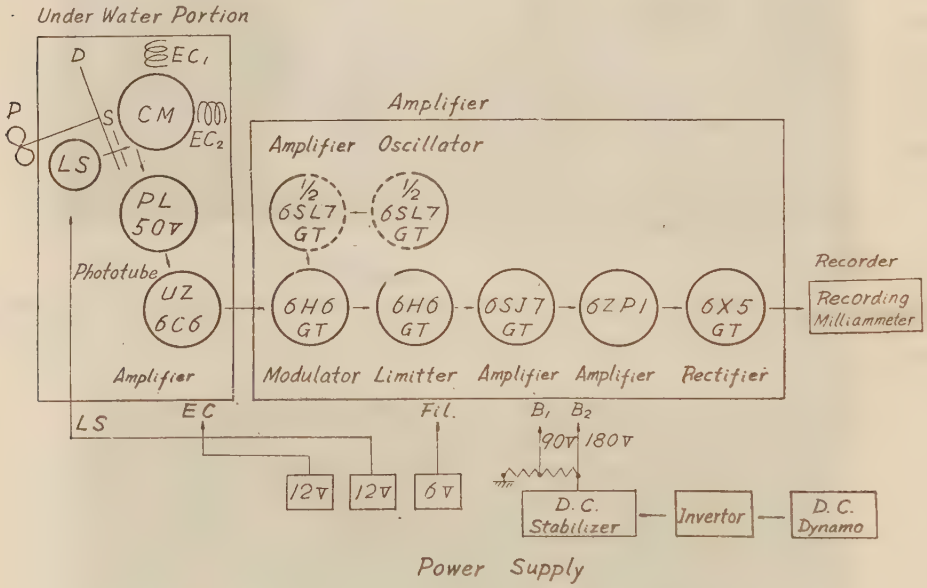

Fig. 4. Schematic block diagram of the instrument.

The schematic block and circuit diagram of the photoelectric measurement process are shown in Figs. 4 and 5.

The relation between the grid bias voltage and the plate current of the vacuum-tube UZ-6C6 is shown in Fig. 6, and the relation between the plate current and the resultant recording current is shown in Fig. 7. The lines in the figure will be changed by the values of noise limitter volume and output current regulator. From the facts shown in Figs. 6 and 7, adjustment of the instrument to the linear relation between the photoelectric current and the recording current is found to be possible.

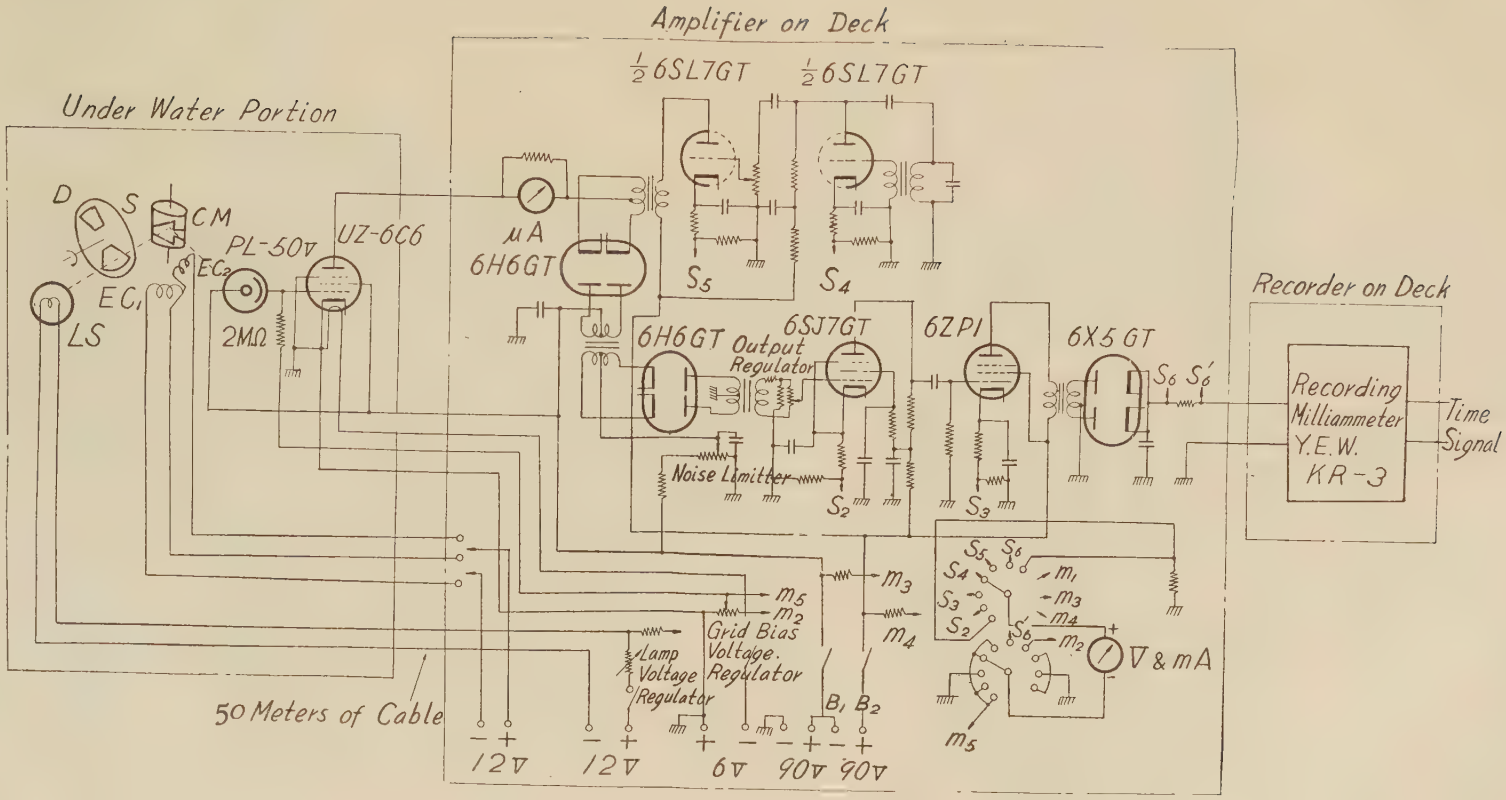

Fig. 5. Schematic circuit diagram of the instrument.

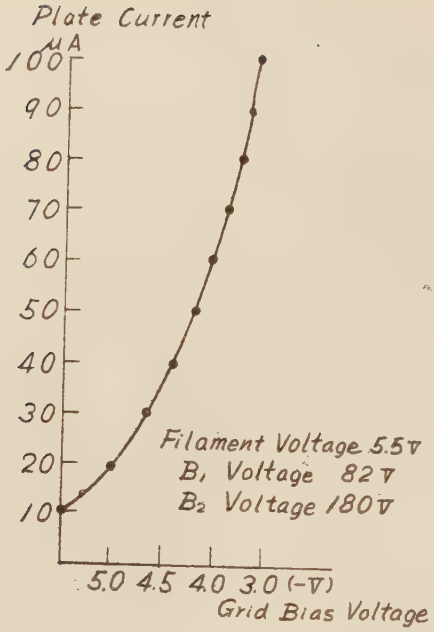

Fig. 6. Relation between the plate current and the grid bias voltage.

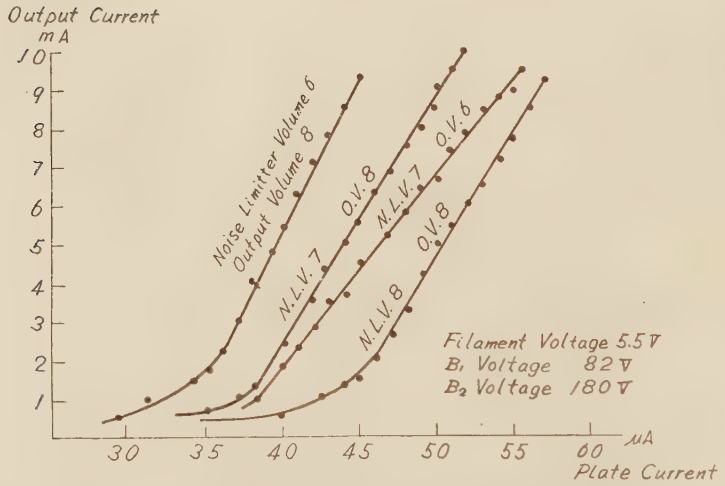

Fig. 7. Relation between the output and the plate current.

2. *Theoretical Consideration.* Now, let the current speed be v cm/sec and the number of flash of light be n time/sec, then we have

$$v = an^2 + bn + c$$

where a, b and c are constant. Two holes are made in the disc, which turns one cycle as the wate runs 20 meters. Therefore, the light path opens once per 10 meters movement of water. As it requires t sec and l cm of chart length to record N times of intermittent photoelectric current, then we have

$$n = \frac{N}{t} = \frac{N}{30\,l}$$

So we have

$$v = a\left(\frac{N}{30\,l}\right)^2 + b\left(\frac{N}{30\,l}\right) + c\,.$$

Next, let the breadth of the slit S be B, and the vertical length of the mirror CM be $\alpha\theta+\beta$, $0^\circ \leq \theta \leq 360^\circ$, where both α and β are constant, and θ is the angle around the axis of the cylinder. The intensity of light reflected by the mirror is then given by $I_0 e^{-kz}\rho B(\alpha\theta+\beta)$, where I_0 is the intensity of original light, k is the combined extinction coefficient of the glass windows and the water, z is its optical path and ρ is the albedo of the mirror. So the photoelectric current i will be proportional to the angle θ, that is $i = K\theta$. From the above figs. 6 and 7, we expect the linear relation between the recording electric current and the direction of the instrument. Indeed, for example, it is seen in Fig. 8.

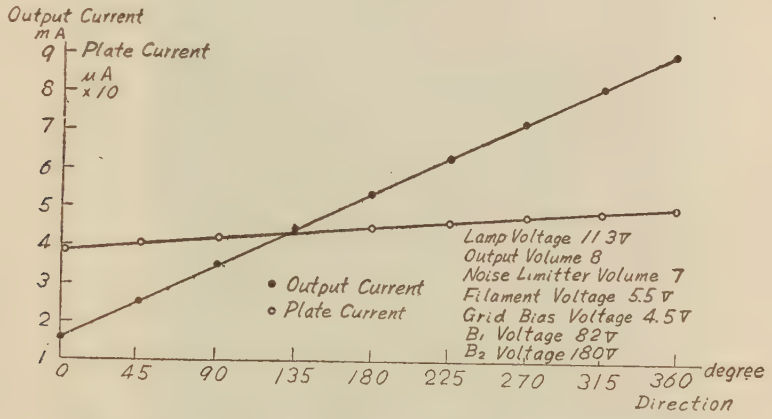

Fig. 8. Relation between the direction of the current meter and the intensity of the photoelectric current.

3. *Experimental Results.* Experiments were performed in Tokyo Bay on board the research ship "Asasiwo Maru" on June 26th and September 17th, 1952. The results are compared with those obtained by the Ekman-Merz current meter, and the new current meter is better than the old one in the respect that it can record the oceanic current more minutely and accurately. For instance, we can see even the fluctuation of oceanic current in Fig. 9, of which amplitude and period are about 40° and several minutes, respectively. The main current direction was S 30°W, the speed being 27.5 cm/sec.

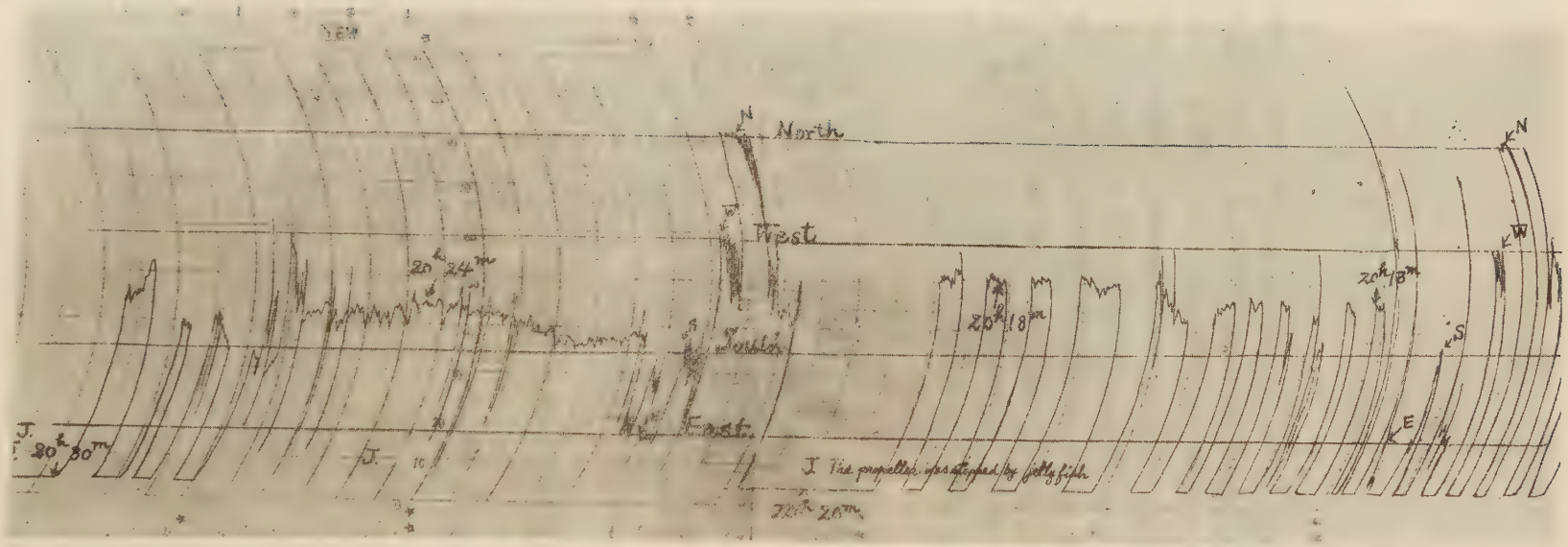

Fig. 9. A record of current obtained at a 1.75 m layer. Note the fluctuation in both speed and direction, and the minute fluctuation in the latter which seems to be caused by vortices. (The width of the chart paper is 12 cm)

Acknowledgement. The author wishes to express his hearty thanks to Dr. Y. Miyake and Dr. Y. Takenouti for their encouragements, to Mr. K. Kawamura for his kind advice, and also to the members of the Oceanographic Division of the Central Meteorological Observatory for their help during the observations. His thanks also due to the members of the Toho Denki Co. and of the Turumi Seiki Co. for the construction of the instrument. This work was made possible by a grant for research for test manufacture in 1951 from the Ministry of Transportation.

References

T. Nan'niti: A Current Meter using a Photocell. Umi-to-Sora **25**, 5 (1947). (in Japanese)
T. Nan'niti: A Current Meter using a Phototube. Papers in Meteorology and Geophysics MRI. **3**, 4 (1952).

PRINTED BY
KASAI SHUPPAN INSATSUSHA
MINATO-KU, TOKYO, JAPAN
東京都港區芝南佐久間町1－53
笠井出版印刷社印行

On a new pearl oyster from the Pacific coast of Japan, with special reference to the cross-fertilization with another pearl oyster, *Pinctada martensii* (Dunker)

By

Seiji K. WADA

(Oceanographical Laboratory, Meteorological Research Institute, and Fisheries Institute, Tokyo University)

and

Renji WADA

(Laboratory of Pearl Culture, San Miguel, Panama)

In Japanese waters, several species of pearl oysters have been found. Of these, the commonest is the Japanese pearl oyster, *Pinctada martensii*, which is widely cultivated for the production of pearls on the southern coasts of the country. Recently, a pearl culture company was established at Shimizu, Shizuoka Prefecture, and extensive fishing for pearl oysters has been carried out in the harbor of Shimizu (location: Long. 138°30′E; Lat. 35°0′N). In a collection of pearl oysters from bottom beds near the entrance of the harbor, a new form of pearl oyster has been found by one of the writers (R. Wada).

Even at a casual glance, the new form is distinguished from the typical form of *P. martensii* by the shape of the shell-valves. On considering the shell variation which occurs in the latter species, however, it cannot be determined whether the new form is a distinct species or a variety of the Japanese pearl oyster.

In order to obtain clear-cut evidence which would show whether there is a systematic difference between them, cross-fertilization experiments were attempted by the other of the writers (S. K. Wada). The work was carried out at the Misaki Marine Biological Station, in the summer of 1952. The materials, the two forms of pearl oyster, were collected in the harbor of Shimizu, and transferred to Misaki in the spring of the same year.

Results

1. *Cross-fertilization.* It has been shown by one of the authors (Wada, 1941, 1947) that, in *P. martensii* and *P. maxima*, although artificaial fertilization with sex cells from dissected gonads is generally not successful in normal sea water,

it is readily accomplished in ammoniacal sea water ($0.4\text{-}1.0\times10^{-3}$N NH_4OH), and that the development ensues normally, provided that the eggs are transferred to normal sea water after fertilization. In the ammoniacal sea water, sperm, otherwise inactive, are made intensely active, and cytoplasmic maturation of eggs which involves germinal vesicle break-down and further cytoplasmic changes is also induced.

Eggs were washed several times with fresh sea water, using a hand-centrifuge. Sperm were employed in subequal concentration as far as possible, if not otherwise stated. Fertilization was accomplished in the ammoniacal sea water, the concentration of which was $0.5\text{-}1.0\times10^{-3}$N NH_4OH, when the eggs of *P. martensii* were used, and $1.0\text{—}2.0\times10^{-3}$N NH_4OH, in the majority of the cases in which the eggs of the new pearl oyster were employed. Eggs, totalling from 100 to 400 in number, were counted 2-3 hours after insemination, when the embryos had developed into the morula or early blastula stage, and the rate of development was calculated.

Although, when eggs are fertilized in ammoniacal sea water, the percentage of development is various according to the condition of the eggs, in the Japanese pearl oyster, it has usually been found to be over 50% in the foregoing experiments, and practically a 100% rate of development is not infrequently attained when the ova are in a favorable condition.

The results of cross-fertilization with eggs of *P. martensii* are presented in Table 1. As shown in the table, in cases of straight-fertilization of *martensii*×*martensii*, 60-90 per cent of the eggs develop, while in the cross, *martensii* ♀× new form ♂, only 10-15 per cent at most of the eggs develop, the rate usually being less than 1%. The differences in the rate of development between the experiments of each pair, in which the eggs of the same individual were emloyed, ranges from 45% to 92%. If the cases in which *martensii*×*martensii* gave above 70% rate of development are selected, the differences amount to 72-92%.

The results of experiments on the cross-fertilization of the new pearl oyster eggs are summarized in Table 2.

Although it is expected that further varying of the conditions will reveal a method for obtaining a high rate of artificial fertilization, the experiments so far have shown only that very concentrated ammoniacal sea water seems to be necessary to accomplish fertilization. In contrast to the case of cross-fertilization using eggs of *P. martensii*, the results seem to be somewhat confused. On some occasions, as in Exp. Nos. 24 and 27, the percentage of developing eggs is de-

Table 1. Results of cross-fertilization in *P. martensii* egg.
Species: M, *P. martensii*; S, the new form.
Fertilization was performed in $0.5\text{-}1.0\times10^{-3}$N ammoniacal sea water; temperature: 24°-29°C.

Exp. No.	Straight-fertilization		Cross-fertilization		Difference	Remarks
	Individuals employed ♀ ♂	Rate of develop.	Individuals employed ♀ ♂	Rate of develop.		
21	$M_0\times M_2$	94	$M_0\times S_1$	1.5	92	10 min. exp. to a.s.w.
	$M_0\times M_2$	94	$M_0\times S_1$	10	84	30 min. exp. to a.s.w.
22	$M_1\times M_3$	75	$M_1\times S_2$	0	75	
			$M_1\times S_3$	0	75	
			$M_1\times S_4$	0	75	
			$M_1\times S_5$	0	75	
			$M_1\times S_6$	0	75	
26	$M_7\times M_8$	73	$M_7\times S_{12}$	1	72	In 1.0×10^{-3}N a.s.w.
	$M_7\times M_8$	55	$M_7\times S_{12}$	0	55	In 0.5×10^{-3}N a.s.w.
28	$M_7\times M_9$	85	$M_7\times S_{13}$	41		High sperm concentration
29	$M_{10}\times M_9$	60	$M_{10}\times S_{13}$	15	45	
			$M_{10}\times S_{12}$	1≫	60	
32	$M_{10}\times M_{11}$	72	$M_{10}\times S_{15}$	0	72	
			$M_{10}\times S_{15}$	50		High sperm concentration

Table 2. Comparison of the results of straight- and cross-fertilization in the new pearl oyster eggs.

Exp. No.	Straight-fertilization		Cross-fertilization		Remarks
	Individuals employed ♀ ♂	Rate of develop.	Individuals employed ♀ ♂	Rate of develop.	
23	$S_7\times S_8$	1>			Shed eggs
	$S_7\times S_9$	0	$S_7\times M_4$	28	Ovarian eggs; shed sperm
			$S_7\times M_5$	15	Ovarian eggs; spermarian sperm
24	$S_7\times S_{10}$	16	$S_7\times M_6$	0	
27	$S_{11}\times S_{12}$	26	$S_{11}\times M_8$	1	
31	$S_{14}\times S_{15}$	30	$S_{14}\times M_{11}$	30	High sperm concentration
	$S_{14}\times S_{15}$	10	$S_{14}\times M_{11}$	18	Lower sperm concentration
33	$S_{14}\times S_{15}$	31			
			$S_{14}\times M_{11}$	53	Relatively high sperm concentration

Species: S, the new form; M, *P. martensii*. Temperature: 25°-29°C. Concentration of ammoniacal sea water: pH 8.8 in Exp. 23; pH 9.2 in Exp. 24; 2×10^{-3}N in Exp. 27; in Exp. Nos. 31 and 33, insemination in 1×10^{-5}N immediately after breakdown of germinal vesicles in 2×10^{-5}N. Duration of exposure to 2×10^{-5}N ammon. s.w. was 35 minutes in Exp. 31 and 27 minutes in Exp. 33.

finitely higher in straight-fertilization than in heterogenous fertilization; whereas, on other occasions, the reverse result was obtained. However, the percentage of developing eggs so far obtained has never amounted to over 30%, although the break-down of germinal vesicles occurred in almost all eggs in the ammoniacal sea water.

In cross-fertilization, the concentration of sperm employed is of paramount importance. When *martensii* eggs are fertilized by sperm of the new pearl oyster in a very high concentration, the percentage of resultant developing embryos rises as high as 40-50, as shown in experiments Nos. 28 and 32. Further, when eggs of the new oyster are inseminated by sperm in dense concentration, in both straight- and cross-fertilization, the number of resultant developing eggs increases markedly, the percentage reaching around 50.

In order to obtain some comparable evidence concerning cross-fertilization in other bivalve molluscs, experiments have been carried out with two species of oviparous oysters, *Ostrea laperousei* Schrenk and *O. echinata* Quoy et Gaimard, which are classified into different subgenera. These experiments were performed in normal sea water.

When sperm are employed in the usual concentration, of an order of 10^6 times dilution of dry sperm, cross-fertilization as measured by the resultant developing eggs occurs in a very low percentage; on the other hand, when sperm are used in a slightly higher concentration, of the order of 10^5 times dilution of dry sperm, the percentage of developing embryos increased very markedly. Especially in the cross *laperousei* ♀ × *echinata* ♂, no differences are perceptible from the batches of *laperousei* × *laperousei*; development ensues in almost all eggs. Moreover, it has been found that this is not a result of mere activation by sperm; syngamy of male and female nuclei, and formation of normal cleavage asters can be readily observed under a phase contrast microscope, when the eggs are slightly compressed. No cases of polyspermic development have been observed, and farther development is normal in all respects, apparently normal D-shape veligers resulting. However, in case of the cross *echinata* ♀ × *laperousei* ♂, with dense sperm, the percentage of development so far obtained has been 15% at most.

Cases of successful fertilization brought about by high concentration of sperm are also reported by various authors; for example, by Lillie (1921) and by Oka (1952) in a interspecific cross of sea urchins; by Kupelwieser (1909) in the cross, *Strongylocentrotus* ♀ × *Mytilus* ♂; and by Fuchs (1914) in self-fertilization in *Ciona*.

2. *Characters of sex cells.* The eggs of the proposed new pearl oyster are not morphologically distinguishable from those of *P. martensii*. The ovarian eggs are more or less polygonal in shape, with clearly visible germinal vesicles; on maturing, they take on a spherical form, averaging 51 μ in diameter; the eggs of *martensii* average 52 μ in diameter. On the other hand, the spermatozoon of the new oyster is somewhat different from that of *martensii* in the shape of the head; the acrosome is slightly longer and more distinct in the latter than in the former. Moreover, the head tapers slightly toward the posterior in *martensii* sperm, while in the sperm of the new oyster, it is of roughly equal width throughout the head proper.

The new oyster sperm can be more readily activated by egg sea water than those of *P. martensii*, and it is frequently observed that the sperm obtained from the dissected testes move very actively in normal sea water; such conditions have been never met with in the sperm of *P. martensii*, although hundreds of males have been examined.

Like the case of *P. martensii*, spawning in the male oyster can be readily induced by a sudden rise of water temperature, and in the female, by the combined effects of increased temperature and addition of sperm suspension.

3. *Conchological features.* The proposed new species is distinguished from *P. martensii* by a prominent development of the posterior process of the hinge, and also by the marked indentation just ventral to it.

Although only 21 animals were available for examination, the size is definitely larger than that of *P. martensii*; the latter species commonly attains 7 cm in dorse-ventral length, animals over 7 cm generally showing features of agedness in various respects, while many of the new oysters were over 8 cm in dorso-ventral length, the largest measuring 9.1 cm in D–V length and 8.1 cm in antero-posterior length. Furthermore, even in the largest forms, there was no evidence of retardation in growth, the surface of the prismatic layer inside the shell being as broad as in the young specimens.

In the new oyster, the hinge length is longer than that of *P. martensii*. In fully-grown animals of the latter species, the dorso-ventral length is definitely longer than the hinge length, while it is roughly equal in relatively young animals. For specimens measuring 6.0–7.6 cm in D–V length, the ratio of hinge length to D–V length is 0.84 ± 0.01, on an average (mean of 266 animals). On the other hand, in the new the forms, the hinge length is subequal to D–V length in fully-grown animals. The mean of the ratios of hinge length to D–V length in 20 individuals, which measured 6.5–9.1 cm in D–V length, is 0.97 ± 0.04.

In Fig. 1 is depicted a line showing the relation between the D-V length and the thickness (width) of the shell, according to the measurements of about 1000 individuals of *P. martensii* from Ago Bay, Mie Prefecture. On the figure are also plotted the data obtained from the 21 new oysters. As shown in the figure, comparing these with those of *P. martensii*, the flatness of the shell-valve in the present oyster is very marked. The flatness is mainly due to that of the right valve. The ratio of thickness to D-V length for the fully grown Japanese pearl oyster is 0.38±0.016 (mean of 266 animals measuring 6.0-7.6 cm in D-V length) ; while the same ratio for the new forms is 0.29±0.020 (mean of measurements in 21 animals).

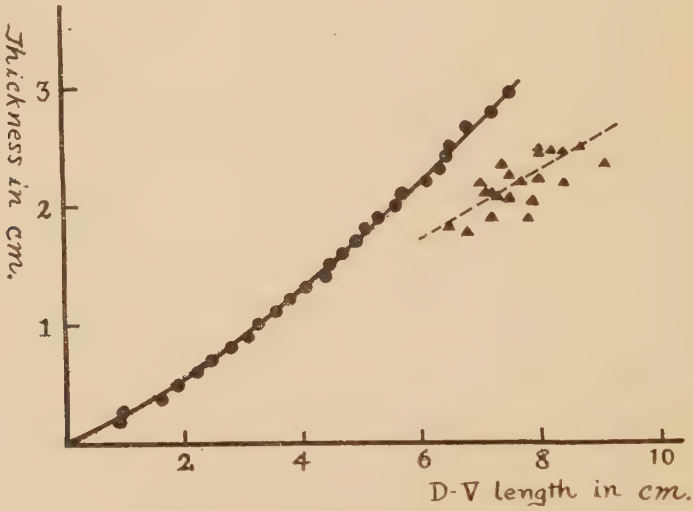

Fig. 1. Relation between the D-V length and the thickness of the shell-valves in *P. martensii* and the new form.
Solid circle and full line: *P. martensii* (1001 individuals, each circle represents from 10 to 74 individuals) ; triangular and broken line: the new pearl oyster (21 individuals).

The weight of the shell valves is definitely less in the new species than in *P. martensii*, especially in the larger specimens.

In the Japanese pearl oyster, a linear relationship is observed between D-V length and A-P length, as expressed by the equation,

$$(\text{D-V length}) = 1.08 \times (\text{A-P length}).$$

In the new forms also, the relation seems to be similar to that in *P. martensii*, so far as the presently available data indicate.

The ground color of the prismatic layer is generally yellowish gray, with pink tint near the outside surface; sometimes, especially in young forms, the

outside is tinged with blackish green or brownish red. The radial bands of sepia color, which are so characteristically found in *P. martensii*, are completely lacking. The newly secreted lip processes are markedly tinged with pink to red; the transverse bands on them being absent. The processes are of roughly equal width from the base to the tip; in *P. martensii*, they are generally tapered towards the tip, and definite transverse bands are usually, though not always, present.

The nacre is lustrous silvery white, resembling that of the silver-lip variety of *P. maxima*.

Discussion

It is generally believed that the rate of development depends largely on the physiological condition of the eggs, if ripe, fresh sperm are employed. As stated above, the difference in the rate of development between the batches of *martensii*× *martensii* and those of *martensii* ♀× new oyster ♂ amounts to more than 70%. If the two forms are assumed to belong to the same species, such a large difference cannot be explained by the probable difference in the fertilizing power of the sperm of different individuals, although it is true that the condition of the sperm may effect the development rate to the extent of around 10 or 20 per cent. The opinion that the two forms are local varieties is rejected because the materials have all come from the same locality. The most plausible explanation for the cause of this difference in the rate of development is that the sperm employed in the experiments were from oysters of different species.

The results of the experiments in which eggs of the new oysters were used, as shown in Table 2, do not indicate any difference between the physiological activity of the sperm of the two species on the new oyster eggs. However, this cannot be considered as a valid objection against the systematical separation of the two forms, since, in these cases, the conditions can hardly be normal, with a less than 30 per cent rate of fertilization. Nevertheless, it is worth while to mention that better results in the rate of development were not infrequently obtained in the case of new oyster ♀×*martensii* ♂ than in the straight-fertilization with the new species eggs.

When the eggs of *P. martensii* which have been expressed from the excised gonad are kept standing in normal sea water, the germinal vesicles of the majority soon break down, and an exposure to 0.1×10^{-3}N ammoniacal sea water of from 10 seconds to a few minutes is sufficient for the accomplishment of fertilization; whereas, the ovarian eggs of new oysters retain the germinal vesicles intact for

a long time in normal sea water, and, in the majority of the eggs, the breakdown of the germinal vesicles requires about half an hour's exposure (temperature: ca. 28°C) to 2×10^{-3}N ammoniacal sea water. Moreover, the germinal vesicles of the discharged eggs of *martensii* are in the course of breaking down, while in the freshly shed eggs of the new species, it was found that the germinal vesicles are clearly visible, although they are soon broken down on standing in sea water.

Judging by these facts, it is supposed that the ovarian eggs of *P. martensii* are in a more advanced stage of cytoplasmic maturation than those of the new species. This will partly account for the greater facility of fertilization in *martensii* eggs.

From the evidence obtained in the cross-fertilization experiments and also from other morphological characteristics described above, it is concluded that the present pearl oyster represents a new species, distinct from the Japanese pearl oyster, *P. martensii*.

The fact that, in cross-fertilization, the rate of development can amount to about 50 per cent when a high sperm concentration is employed cannot be a valid objection against this conclusion, since in the inter-subgeneric fertilization of oysters, as stated above, 100% of the eggs develop into normal larvae when dense sperm are employed.

Cases of successful interspecific fertilization between oysters have also been reported by Seno and Hori (1929), Galstoff and Smith (1932) and Miyazaki (1939), although nothing has been stated about the concentration of the sperm which theses authors employed.

The pearl oysters hitherto reported from the waters around Japan, are, other than *P. martensii*, *P. fucata* (Gould), *P. panasesae* (Jameson), *P. scheepmacheri* (Dunker), *P. cheminitzii* (Philippi), *P. maxima* (Jameson) and *P. margaritifera* (Linné) (Kuroda and Habe, 1952; Nishikawa, 1904; Habe, 1951). The pearl oyster here described cannot be identified with any of these, since it differs in conchological characteristics. Although the taxonomy of pearl oysters has been hotly disputed, the new pearl oyster is not supposed to belong to any of the previously described species of the genus *Pinctada*. References have been made to Gould (1862), Dunker (1873, 1880), Reeve (1858), Jameson (1901), Iredale (1939), and Dall, Bartch, and Rehder (1938).

Conclusion

From the evidence presented above, it is concluded that the present pearl

oyster belongs to a new species. We, herewith, denominate it *Pinctada shimizuensis* n. sp. with the following description.

Pinctada shimizuensis n. sp. (Fig. 2).

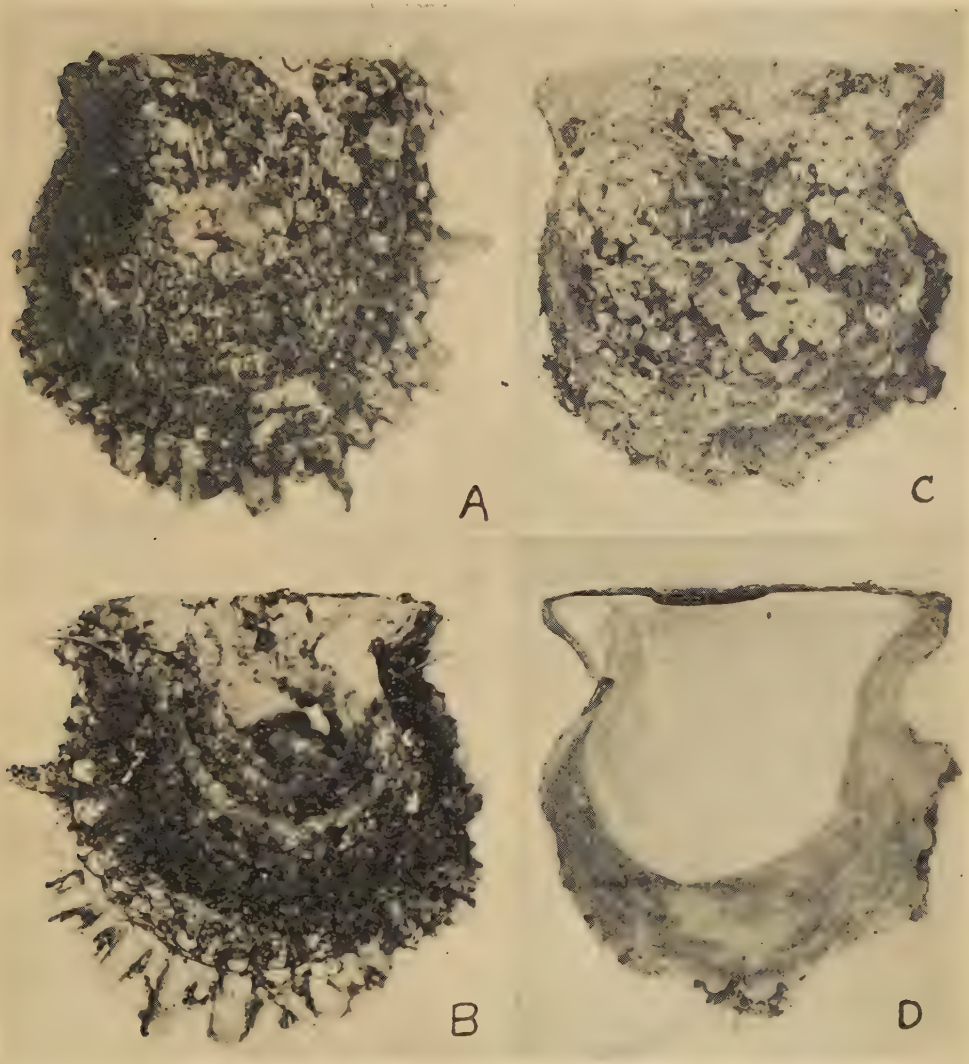

Fig. 2. *Pinctada shimizuensis* n. sp.*

A, B. Outside view of the left (A) and right (B) valves of one living specimen. Size of the animal: 8.4×8.3 cm.

C. Outside view of the left valve of another specimen. Size of the animal: 8.4×8.0 cm.

D. Inside view of the right valve of the same specimen as C.

* In printing these photographs, thanks are due to Miss K. Okazaki for her assistance.

Description.—Shell of medium size, attaining 9 cm in diameter, shape subquadrate, rather compressed, right valve markedly flat. Hinge rather long and shallow; a pair of anterior teeth present, though obscure; lateral teeth not sharp. Posterior process of hinge generally very marked, with a prominent indentation ventral to it. The outside of the shell generally yellowish grey, tinged with pink on the surface; sometimes, especially in young forms, blackish green or brownish red coloration is added. The sepia black radial bands completely absent; the laminae prominent at outer edge of shell; free edges of laminae deeply and irregularly scalloped; with pink tinge. The nacre of the inside is lustrous silvery white, similar tint extending throughout the whole surface of the nacre.

Type locality.—Shimizu, Suruga Bay (location: Long. 138°30′E; Lat. 35°0′N); 10-12 meters deep.

Measurements of some of the specimens are given in Table 3. A specimen which is believed to belong to this species has been found at Buton, Celebes I.

Table 3. Measurements of specimens of the new pearl oyster.

Dorso-ventral length (cm)	Antero-posterior length (cm)	Hinge-line (cm)	Thickness (cm)
9.1	8.1	8.0	2.35
8.4	8.0	7.9	2.45
8.4	8.3	8.0	2.20
8.7	7.8	9.3	2.50
8.2	7.8	8.1	2.45
8.0	7.4	7.3	2.45
8.0	7.5	7.1	2.47
8.0	8.0	7.5	2.23
7.9	7.2	7.9	2.03
7.8	7.6	6.3	1.90
7.7	7.5	7.4	2.20
7.5	7.1	8.3	2.25
7.5	6.8	7.0	2.05

Judging from the lustre and color of nacre and the size of the shells, the present pearl oyster will become one of the important molluscs for pearl cuture if they can be effectively cultivated.

Summary

1. A new form of pearl oysters has been found at Shimizu, Suruga Bay.
2. When sperm of this form were used to fertilize the eggs of *P. martensii*,

a very marked difference (over 70%) was observed between the rate of development of these hybrids and that of *P. martensii* eggs fertilized with self sperm. Fertilization was accomplished in ammoniacal sea water ($0.5\text{–}1.0^{-3} \times$N NH_4OH).

3. The rate of development in cross-fertilization increases markedly when sperm are employed in a high concentration.

4. In the breeding season, it is supposed that the ovarian eggs of *P. martensii* are in a more advanced stage of cytoplasmic maturation than those of the new species.

5. The new pearl oyster, being 8–9 cm in diameter, attains a larger size than *P. martensii*, and differs conchologically from the latter in various other respects: especially, longer hinge line, presence of a prominent posterior indentation, flatter shell valves, coloration of the prismatic layer, etc.

6. It is concluded that newly found mollusc belongs to a new species, and it is denominated *Pinctada shimizuensis* n. sp. A description is given.

The writers wish to express their indebtedness to the director of the Misaki Marine Biological Station for the use of laboratory facilities. Their thanks are also due to Dr. Jean C. Dan for her kind guidance in the preparation of the manuscript.

References

Dall, W. H., Bartch, P., and H. A. Rehder. 1938: A manual of the recent and fossil marine pelecypod mollusks of the Hawaiian Islands. B. P. Bishop Mus. Bull. 153. 233 pp.

Dunker, W. 1872: Die Gattung *Avicula*. Conch.-Cab. **7** (3): 1–84.

Dunker, W. 1882: Index molluscorum maris japonici. 301 pp. Cassellis Cattorum.

Fuchs, H. M. 1914: The action of egg-secretions on the fertilizing power of sperm. Arch. f. Entw.-Mech., **40**: 205–252.

Galtsoff. P. S., and R. O. Smith. 1932: Stimulation of spawning and cross-fertilization between American and Japanese oysters. Science, N. S., **76** (1973): 371–372.

Gould, A. A. 1862: Otia conchologica. 256 pp. Boston.

Habe, T. 1951: Genera of Japanese shells. Pelecypoda No. 1. pp. 62–63. (in Japanese).

Iredale, T. 1939: Mollusca. Part I. Sci. Rep. Great Barrier Reef Exped. 1928–29, **5** (6): 1–425.

Jameson, H. L. 1901: On the identity and distribution of the mother-of-pearl oysters; with a revision of the subgenus *Margaritifera*. Proc. Zool. Soc. London, **1** (25): 372–394.

Kupelwieser, H. 1909: Entwicklungserregung bei Seeigeleiern durch Molluskensperm. Arch. f. Entw.-Mech., **27**: 434–462.

Kuroda, T., and T. Habe. 1952: Check list and bibliography of the recent marine mollusca of Japan. 210 pp. Tokyo.

Lillie. F. R. 1921: Studies of fertilization. VIII. On the measure of specificity in fertilization between two associated species of the sea-urchin genus *Strongylocentrotus*. Biol. Bull., **40**: 1–22.

Miyazaki, I. 1939: Some notes on the cross-fertilization of Japanese oysters. Bull. Jap. Soc. Sci. Fish., **7** (5) : 257-261.

Nishikawa, T. 1904: Pearls. Zool. Magazine (Tokyo), **16**: 203-214. (in Japanese)

Oka, T. B. 1952: Studies on reciprocal hybrids in the sea urchins, *Pseudocentnotus* and *Strongylocentrotus*, *Strongylocentrotus* and *Heliocidaris*. (I). Annot. Zool. Jap., **25** (1/2) : 225-237.

Reeve, L. A. 1858: Monograph of the genus *Avicula*. Conch. Icon., **10**.

Seno, H., and J. Hori. 1929: Studies on the cross-fertilization between *Ostrea gigas*, *O. spinosa* and *O. circumpicta*. Zool. Magazine (Tokyo), **41**:406-407. (in Japanese)

Wada, S. 1941: On the artificial fertilization and development of the silver-lip pearl oyster, *Pinctada maxima* (Jameson) Kagaku Nan'yo (Science in the South Seas), **4** (3) : 202-208. (in Japanese).

Wada, S. 1947: Artificial fertilization of the Japanese pearl oyster in ammoniacal sea water. Bull. Japan. Soc Sci. Fish. **13** (2) : 59. (in Japanese).

On the Cauchy-Poisson Waves Caused by the Eruption of a Submarine Volcano. (1st paper)*

By

Sanae UNOKI

(Oceanographical Section, C.M.O., Tokyo)

and Masito NAKANO

(Oceanographical Laboratory, Meteorological Research Institute, Tokyo)

Abstract: Tsunami waves produced by an eruption of a submarine volcano were recorded three times by a self-registering wave guage installed on Hachijo Island about 130 km distant from the valcano. The period of the tsunami waves was about 95 sec at the beginning, and an hour later about 30 sec, gradually decreasing with the lapse of time. The variation of the wave height was also conspicuous, showing a distinct "beat" phenomenon. Solving the Cauchy-Poisson wave problem for the case when an initial impulse or an initial elevation is given to a finite area, and comparing the theory with observations, it was found that the agreement is excellent in the period, variation of wave height and interference phenomenon. Thus it was made clear that the Cauchy-Poisson wave can actually exist in the ocean with its form almost the same as the theory demands. Moreover, the intensity and scale of the eruption were estimated from the comparison of theory and observations.

§1. *Preface.*

From the middle to the last decade of September 1952, submarine eruptions occured at the reef (which was subsequently called Myojinsho) about 300 km distant to the south of Honshu, Japan. On these occasions, peculiar tsunami waves were recorded by the self-registering wave guage installed on Hachijo Island about 130 km distant to the north of this reef. As the characteristics of these waves were quite similar to those of the Cauchy-Poisson waves, investigations were made on the relation between both waves, and it was ascertained that these tsunami waves are really nothing but the Cauchy-Poisson waves. The results of investigation are stated in the following.

Originally, Cauchy and Poisson had a dissatisfaction with the fact that their predecessors had dealt only with the problem of waves which had been already formed, and they, independently to each other, discussed the problem of "generation of a wave" when a local disturbance is given to the surface of deep water in an instant. The wave thus created is the so-called "Cauchy-

* This investigation has been carried out as a part of the "Microseism and Ocean Wave Research Project" of C.M.O. during 1951~1953.

Poisson Wave"[1] and has conspicuous characteristics as follows: in the matter of space, the farther distant from the disturbance source, the longer the wave length is; and in the matter of time, the periods of the waves coming one after another are gradually shorter; and moreover, since the wave length becomes longer as the wave goes away from the disturbance source, the phase in question travels over the surface with a constant acceleration.

Thus the theory of the Cauchy-Poisson wave problem is an elegant one, but the existence of the Cauchy-Poisson wave in reality in the ocean has been doubted by many practitioners as Scott-Russel and others,[2] and not sufficiently testified for a long time. Meanwhile, the experiment made by Weber[3] seems to have reached no satisfactory results. However, according to the recent experimental results of atomic bomb at Bikini Atoll,[4] it is reported that the period, wave length and phase velocity of the sea waves caused by the explosion were, for the second wave and the waves thereafter, increasing with the distance from the explosion center; and that at a given point these values of each wave were smaller than those of the preceding wave. And it is also stated that the wave with largest height in a wave group has advanced with the group velocity. Consequently, this report enables us to consider that the Cauchy-Poisson wave exists in reality, but the authors were not able to know the details sufficiently.

At any rate, thus the Cauchy-Poisson wave has been made artificially, and it would be fully significant to know that the Cauchy-Poisson wave occurs not only artificially nor experimentally, but also actually in nature.

§ 2. *Observation data.*

The positions of the point where the eruption of the submarine volcano occurred (31°56.7′N, 140°0.5′E) and of Hachijo Island where the waves were observed are shown in Fig. 1. As for the position within Hachijo Is. of the wave gauge (33°5.7′N, 139°46.5′E), Fig. 4 shall be refered to. The eruption of this submarine volcano and the appearance of a new island (Myojinsho) have become a problem of both scientific and social interest, and the details are stated in other reports.

Fig. 1.

The first eruption began on September 16, 1952, and the eruptions continued until almost the end of the month, and it seems that eruptions are seen still now intermittently. Their occurrences were discon-

tinuous and several times a day in the most frequent period. Dr. NIINO, one of the members of the investigation party which went on board the training ship "Shinyo-maru" (229 tons) of the Tokyo University of Fisheries forMyojinsho, made detailed observations of the eruption which occurred at the time 13h 40m, 23rd. According to his observations, "when the eruption occurred, the sea surface which had been even till that time heaved up suddenly to a water dome, whose dimension was 300 m wide and less than 5 m high immediately after the eruption, 1000 m wide after 10 seconds, and 1500 m wide after 60 seconds." It seems therefore that this water dome was generated not instantaneously at the moment of eruption, but was developed gradually by continuous supply of energy for a period of time. Dr. KUMAGORI,[5] another member of the investigation party, says that "block, thin smoke rose on the water surface, sea water heaved up more than 5~6 m high, and instantly an eruption took place at 13h 40m, when explosion noises were heard and slight vibration of the air was felt. The water which had heaved up collapsed into waves of 50~60 m wave length, the wave height decreased before our eyes and became only about 1 cm when the waves reached our ship which was at a distance of about 1600 m. Such waves came twice, and the third wave was not to be perceived. The period was 12~13 seconds." Moreover, Dr. TSUYA[5] says that "on both the occasions of eruptions at 13h 12m and 13h 40m on the 23rd the water dome was 1 km wide and 50~60 m high. The collapse of this dome into waves and their propagation are just as Dr. KUMAGORI says." The observations of these investigators regarding the height of water dome are very different from each other, and which of them is correct remains uncertain. Whether the waves of short length and of small height which are generated as the water dome collapses correspond to tsunami waves of our consideration or not is doubtful, but anyhow, it can be naturally conceived that a certain kind of wave will be generated by the collapse of this enormous water dome.

On the other hand, it is assumable that a strong impulse acts upon sea water at the moment of explosion; namely, this assumption is testified by the vigorous projection of eruptives and the feeling of vibrations in the air accompanied with explosions, and by the fact that noises due to the eruptions at Myojinsho Reef were recorded frequently and conspicuously by the SOFAR hydrophone[6] of U.S. Navy installed on the Pacific coast of U.S.A. almost a thousand kilometer distant. Consequently it is also conceivable that waves would be produced by such strong impulse.

Moreover, according to wave records and other facts, it is known that the

eruption of 23rd was not so strong and that the eruptions of 16th, 24th and 26th which caused conspicuous tsunami waves were by far stronger.

A party of hydrographical investigators went on board the "Kaiyo-Maru, No. 5." (220 tons) of the Hydrographic Office of the Maritime Safety Agency for the purpose of scientific investigations on Myojinsho Reef, and the ship was unfortunately lost since the 24th of September and is finally supposed to have been sunken by an eruption of the submarine volcano. For determination of the cause and time of that disaster, the recordings of the wave gauge as mentioned in the following have played an important rôle.

Hachijo Island is situated 130 km north of Myojinsho Reef. As its position is favorable for observation of waves caused by typhoons and cyclones, wave observation on that island had been planned by the present authors, and the observation was commenced fortunately on September 15, the previous day of the beginning of eruption. The self-registering wave guage is a reconstruction of a statoscope for measuring microbarometric changes and is of the pressure recorder type using a bellows. Its self-recording part sends out roll-recording paper at the average speed of 33 cm an hour, and winds it up on the drum, enabling to obtain a continuous record of wave during ten and odd hours. Its reducing scale for ordinary waves is about 1/70, but since a slow-leak apparatus for eliminating long period waves of tides and so on is attached to it, the reducing scale for tsunami waves of our consideration with period of about 1 minute seems to have been somewhat smaller than that for ordinary waves.

This observation has been made by the members of the Hachijojima Weather Station under control of the Central Meteorological Observatory. During the period of eruption, as it was just the testing period, the wave guage operated not very fully, and satisfying wave records were obtained only for several hours a day.

Notwithstanding, these wave records showed three remarkable tsunami waves and one probable tsunami wave. *A*, *B* and *C* in Fig. 2 indicate the formers and the forms of waves are very evident. *D* indicates the latter case where the form is not clear. For the convenience of comparison, moreover, the wave record of ordinary days is shown in *E*. As the wind waves and swells in these records are superposed on tsunami waves, smoothed curves extracting tsunami waves only are shown in *A*, *B* and *C* of Fig. 7. In the original record of Fig. 2 the former and latter parts of each wave record are separated and they would be considered as the waves owing to different causes, but in the smoothed curve of Fig. 7 it is evidently recognized that they are not separated ones, but continuous

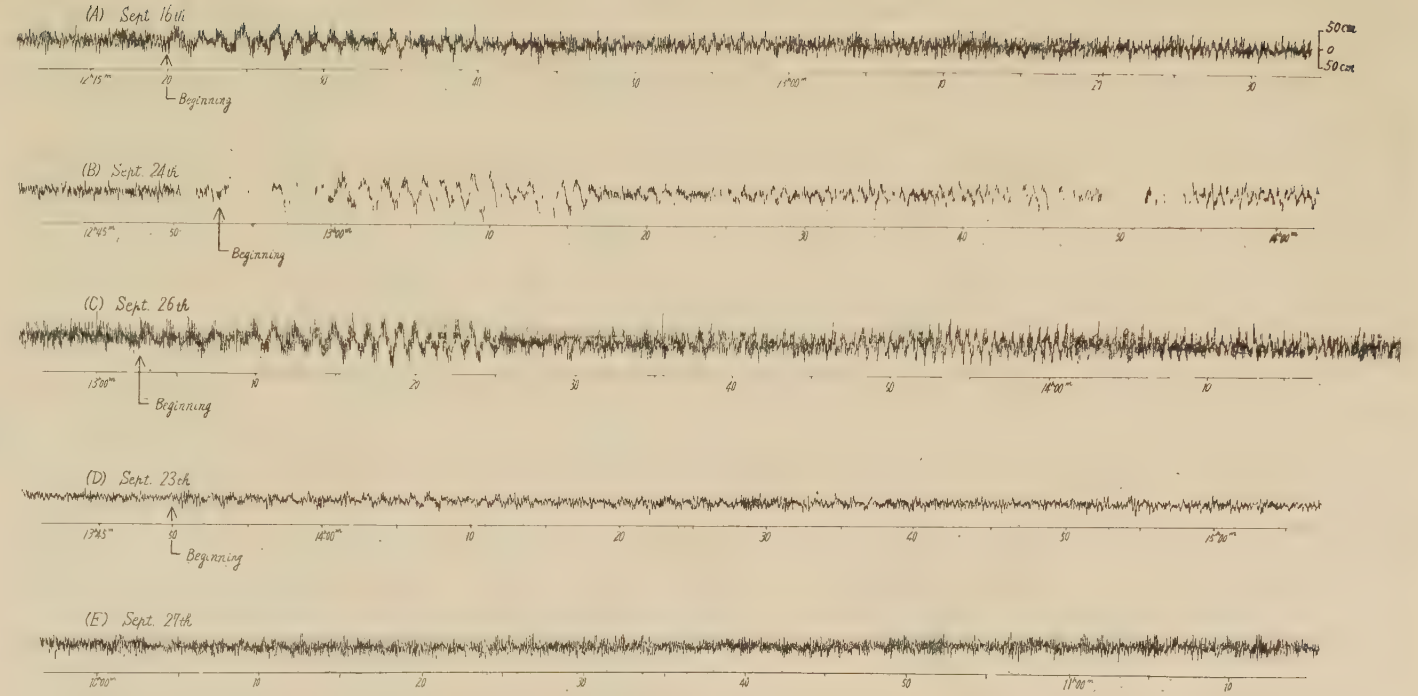

Fig. 2. The wave records at Hachijo Island.

A, *B* and *C* represent the remarkable tsunamis caused by the eruption of a submarine volcano at Myojinsho. *D* indicates a probable tsunami wave.

waves, only appearing so because of the interference wave form. Moreover, owing to the lack of a master clock for time checking, it was impossible to obtain exact time marks in this period. Accordingly, the time marks on the wave records are afterwards plotted appropriately and it is probable that there might be errors of the order of magnitude ±3 min, which should be born in mind in the following discussions.

Now, on September 16 when Fig. 2. *A* (or Fig. 7. *A*) was obtained, no one witnessed the eruption, but by the portable seismograph of the Hachijojima Weather Station a microseismic wave (rather, surface wave) with maximum amplitude 5 μ and average period 4.1 sec was perceived at 11h 52m. According to seismologists, this microseismic wave seems to have been caused not by wind waves but by the eruption at Myojinsho Reef. Assuming the velocity of this wave to be several kilometers per second as in ordinary seismic surface waves, the eruption can be assumed to have occurred also at about 11h 52m. On the other hand, the time when the tsunami wave began at Hachijo Island is 12h 20m, thus the time necessary for propagation of this wave from Myojinsho to Hachijo Is. is 12h 20m−11h 52m=28m. The maximum wave height of this wave was 56 cm.

On the 24th of September when Fig. 2. *B* (or Fig. 7. *B*) was obtained,—perhaps by the eruption which produced this tsunami wave the "Kaiyo-maru, No. 5" met with her disaster,—no one witnessed the eruption. The beginning time of this tsunami wave was 12h 53m, and its maximum height 92 cm.

On September 26 when Fig. 2. *C* (or Fig. 7. *C*) was obtained, the maximum wave height was 71 cm, and the attack of tsunami wave at 13h 03m. On this occasion, that the eruption occurred at 12h 35m was ascertained by a patrol ship searching for the "Kaiyo-maru, No. 5." By this, the travel time of this wave is 13h 03m−12h 35m=28m, which is the same value as in the case *A*.

On September 23 of Fig. 2. *D*, eruptions were observed at 13h 12m and 13h 40m, as previously mentioned. On the other hand, the record shows that a tsunami-like wave was beginning at about 13h 50m. Comparing this record with those of *A*, *B* and *C*, there are many differences in regard to the variation of periods and wave heights; namely, this wave seemes to be a tsunami wave at a glance, but it also can be regarded as a special wave type seen on the approach of a typhoon or a cyclone, or as "surf beats" stated by W. H. Munk.[7] And, as to the beginning time of 13h 50m, considerable doubts may be entertained for various reasons. On consideration of these circumstances, we do not treat the case *D* here.

On other days than 16th, 24th and 26th, tsunami waves were caused by the eruptions, but owing to the lack of wave observation, the data were not obtained. For example, the tsunami wave caused by the eruption at about 7h 25m, 17th, was perceived by fishermen of Hachijo Island. On the other hand, there are the cases when no tsunami waves were caused, though eruptions were recognized. It is uncertain, however, what grade of eruption can produce what grade of wave.

Moreover, wave observations like these at Hachijo Island have been done also at Jogashima and Omaesaki shown on the map of Fig. 1, but at these places no tsunami waves accompaning the eruptions were seen. And even at Hachijo Island where there is a tidal station at a point on the opposite side of the island to the position of the wave gauge, tsunami waves were not seen on the mareograms. This seems to be due to the fact that the station is situated in the shade of the island in the progressing direction of the waves and therefore the wave height have been diminished. (see Fig. 4)

§ 3. *Travel time of tsunami wave.*

In regard to the time necessary for propagation of a tsunami wave, it is a question whether this wave progresses with phase velocity or with group velocity. ROSSBY[8] states that the phase of largest energy progresses with group velocity, and MUNK[9] says also that individual waves should be considered as progressing with group velocity. Moreover, concerning the sea waves caused by explosion of atomic bomb,[4] it was said that the wave with maximum wave height in a wave group progresses with group velocity. We shall see whether or not these theories and facts should be confirmed by the tsunami waves produced by the recent eruptions.

In the case of the tsunami wave under consideration, as the depth is 200～1000 m and its period 30～100 sec, it is evident that we should, considering its relative depth, treat it as a medium wave (elliptic trochoidal wave), not as a deep water wave nor long wave.

For medium waves, if we take the period τ, the wave length λ and the depth to the bottom d,

$$\text{phase velocity}: \quad c=\{(g\lambda/2\pi)\tanh(2\pi d/\lambda)\}^{1/2} \tag{1}$$

$$\text{group velocity}: \quad c_g=\frac{c}{2}\{1+(4\pi d/\lambda)/\sinh(4\pi d/\lambda)\}, \tag{2}$$

where there exists the relation $\lambda=c\tau$ naturally. As the examples where the values of c and c_g are calculated for various values of d and τ seem to be

seldom, an example is shown in Fig. 3 for reference. But, in the extent of our consideration we cannot find so much difference between the phase velocity c of medium wave, the group velocity c_g of medium wave and the group velocity of deep water wave.

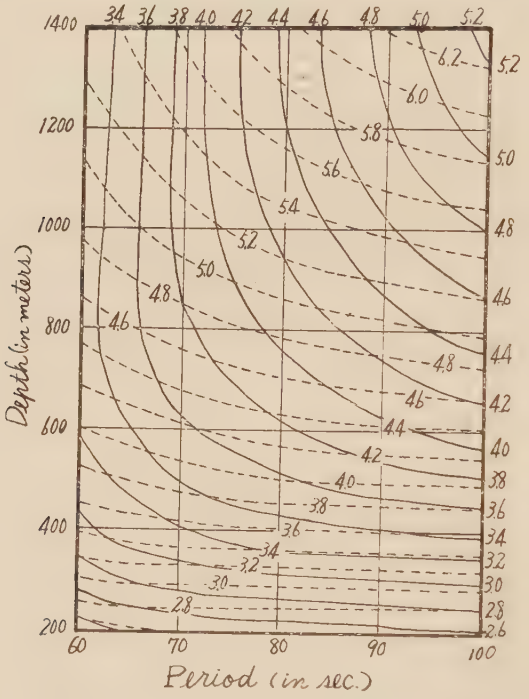

Fig. 3. The group and phase velocities of surface wave corresponding to various values of the period and the depth. The full and the broken lines show the group velocity and the phase velocity in km/min, respectively.

According to A, B and C of Fig. 2 (or Fig. 7), the period of the wave which first arrived is about 95 sec. So, a refraction diagram is shown in Fig. 4 when the wave of the period 95 sec progresses with group velocity. From this figure, it is seen that in the vicinity of Hachijo Is. orthogonal lines converge, thus especially the wave heights become larger, and that we may consider the wave which came from Myojinsho to the wave recorder of Hachijo Is. to have progressed almost linearly. Therefore, when we calculate the travel time numerically by the formula

$$t=\int\frac{ds}{c_g}=\sum\frac{\Delta s}{c_g}$$

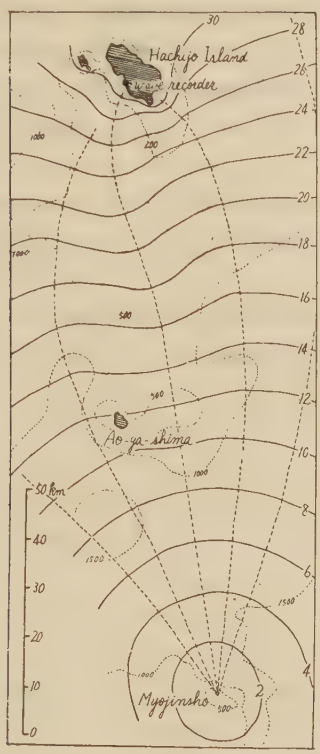

Fig. 4. The refraction diagram of the progressive wave, of the period of 95 seconds, travelling with the group velocity. The full lines show the lines of equal travel time in minutes. The broken lines show the orthogonals and the dotted lines the lines of equal depth in meters.

using the seachart, the values of Table 1 are obtained. On Table 1 are shown also the values when the wave of the period 95 sec progresses with phase velocity of medium wave or with group velocity of deep water wave.

Table 1.

Classification of velocities	Group velocity of medium wave (c_g)				Phase velocity of medium wave (c)	Group velocity of deep water wave
Period τ (sec)	60	80	95	100	95	95
Travel time (min)	41.5	34.3	32.1	31.6	28.5	30.1

Namely, the travel time is 32.1 min in the case of group velocity and 28.5 min in the case of phase velocity for the wave with the period of 95 sec.

The actual travel time was, as mentioned in § 2, about 28 minutes in both the cases of Sept. 16 and Sept. 26, being accompanied with errors of the order

of magnitude 3 min. It is difficult, therefore, to decide distinctly whether the waves in the present problem have progressed with phase velocity or with group velocity. In the ranges of period and depth of our consideration, it was necessary to have more accurate time-marks in order to make the difference of travel time clear. Moreover, the fact that the travel time of a deep water wave progressing with group velocity is very near to the value of actual travel time suggests that we can go on with our discussion not so unreasonably by assuming the wave to be a deep water one.

The next question to be solved is when the volcanic explosion should have occurred that caused the sinking of the "Kaiyo-maru, No. 5" on September 24. Comparing the waves of *A* (Sept. 16) and *C* (Sept. 26) of Fig. 2 (or Fig. 7) with that of *B* (Sept. 24), we can, from the similarity in the values of periods of the first stages and in the variations of periods and wave heights, guess that the travel time in the case *B* would be about 28 min, as well as in the cases *A* and *C*. Accordingly, the disaster of the "Kaiyo-maru, No. 5" is presumed to have occurred at

$$24\text{th}\ 12\text{h}\ 53\text{m} - 28\text{m} = 24\text{th}\ 12\text{h}\ 25\text{m} \pm 6\text{m}$$

From the noises of SOFAR hydrophone,[6] U.S. Navy, the explosion on 24th is presumed to have occurred at about 12h 20m, and this result is approximately in accord with the value obtained by us.

§ 4. *Cauchy-Poisson wave problem when a local disturbance is given to a limited extent of the sea surface.*

The theory of the waves produced in deep water by a local disturbance of the surface was investigated in two classical memoirs by Cauchy and Poisson. And, as this theory is systematically and comprehensibly described in "Hydrodynamics" of LAMB, we shall go on with our discussion, following the method and notations of LAMB.[1] For simplification of the problem, the sea is considered to be spreading infinitely, and the depth to be very large. We neglect the effect of friction and treat the problem as one-dimensional, the origin of co-ordinates being taken on an undisturbed surface and y-axis in the vertical direction upwards. η represents the elevation, ϕ the velocity potential, ρ the density of sea water and g the acceleration of gravity. Then, the impulse acting upon the sea surface is shown by $\rho\phi_0$, where zero suffix indicates surface-value ($y=0$).

According to what is said in § 2, the tsunami waves produced by the explosion of submarine volcano can be considered as produced by simultaneous actions of initial elevation and initial impulse on the sea surface. Therefore, we shall

obtain the elevation, when the initial conditions are given by

$$\rho\phi_0=F(x),\ \eta=f(x)\ ;\ \text{at}\ \ t=0. \tag{3}$$

Now, when the surface impulse only acts upon the undisturbed water surface, then assuming the initial conditions

$$\rho\phi_0=F(x),\ \eta=0, \tag{4}$$

the elevation η_i is given by[1]

$$\eta_i=\frac{1}{g}\frac{\partial\phi_0}{\partial t}=-\frac{1}{\pi g\rho}\int_0^\infty \sigma\sin\sigma t\,dk\int_{-\infty}^{\infty}F(\alpha)\cdot\cos k(x-\alpha)\,d\alpha. \tag{5}$$

And when the initial elevation only acts, without any impulse, namely

$$\rho\phi_0=0,\qquad \eta=f(x), \tag{6}$$

we have[1]

$$\eta_e=\frac{1}{\pi}\int_0^\infty\cos\sigma t\,dk\int_{-\infty}^{\infty}f(\alpha)\cos k(x-\alpha)\,d\alpha. \tag{7}$$

In (5) and (7), there is a relation

$$\sigma^2=gk. \tag{8}$$

Then, the elevation η under the initial condition (3) may be given by

$$\eta=\eta_i+\eta_e \tag{9}$$

approximately.

1. The case of initial impulse.

The assumption in Lamb's "Hydrodynamics" for the initial impulse $F(x)$ is

$$\lim_{\varepsilon\to0}\int_{-\varepsilon}^{\varepsilon}F(\alpha)\,d\alpha=1, \tag{10}$$

namely, the initial impulse is concentrated to the immediate neighbourhood of the origin, so that $F(\alpha)$ vanishes for all but infinitesimal value of α.

For large values of $\frac{1}{2}gt^2/x$, under the above assumption, (5) becomes

$$\eta_i=\frac{g^{1/2}t^2}{2^{5/2}\pi^{1/2}\rho x^{5/2}}\left(\cos\frac{gt^2}{4x}-\sin\frac{gt^2}{4x}\right) \tag{11}$$

approximately,[1] which was studied by Cauchy and Poisson. In this solution, the period decreases with time, but the wave height increases with time infinitely, and the "beat" phenomenon does not appear.

On the other hand, in the wave records of A, B and C of Fig. 7, the beat-phenomenon appears conspicuously, while the period of individual waves regularly decreases with time. Accordingly, instead of the condition (10), we should consider that the initial impulse has to be of finite intensity in order that the wave height may be finite, and that for the appearance of beat a disturbance source of finite width should be assumed, as suggested by Lamb. Such a pro-

blem is likely to have been treated by BURNSIDE,[10] but we could not know what kind of disturbance source was assumed by him.

Now, we consider the case when an impulse of constant intensity has acted upon a certain extent of the sea surface at the moment of explosion of a submarine volcano. Then, since the impulse is considered as acting only upon the extent of $-l \leqq x \leqq l$, the initial impulse is

$$\rho\phi_0 = P(-l \leqq x \leqq l), \quad \rho\phi_0 = 0 \quad (|x| > l). \tag{12}$$

Accordingly, from (5)

$$\eta_t = -\frac{P}{\pi\rho g}\int_0^\infty \sigma \sin\sigma t\, dk \int_{-l}^{l} \cos k(x-\alpha)\, d\alpha$$

$$= \frac{P}{\pi\rho}\left[\int_0^\infty \frac{\sin\sigma t \sin k(x-l)}{\sigma}\, dk - \int_0^\infty \frac{\sin\sigma t \sin k(x+l)}{\sigma}\, dk\right]. \tag{13}$$

Now, we shall calculate

$$I = \int_0^\infty \frac{\sin\sigma t \sin k\xi}{\sigma}\, dk. \tag{14}$$

Considering (8),

$$I = \frac{2}{g}\int_0^\infty \sin\sigma t \sin\frac{\sigma^2}{g}\xi\, d\sigma = \frac{1}{g}\int_0^\infty \left\{\cos\left(\frac{\sigma^2}{g}\xi - \sigma t\right) - \cos\left(\frac{\sigma^2}{g}\xi + \sigma t\right)\right\} d\sigma$$

$$= \frac{1}{g^{1/2}\xi^{1/2}}\left[\int_{-\omega}^{\infty} \cos(\zeta^2-\omega^2)\, d\zeta - \int_{\omega}^{\infty} \cos(\zeta^2-\omega^2)\, d\zeta\right] = \frac{1}{g^{1/2}\xi^{1/2}}\int_0^\omega \cos(\zeta^2-\omega^2)\, d\zeta$$

$$= \frac{2}{g^{1/2}\xi^{1/2}}\left[\cos\omega^2 \int_0^\omega \cos\zeta^2 d\zeta + \sin\omega^2 \int_0^\omega \sin\zeta^2 d\zeta\right],$$

where we put, as in "Hydrodynamics" of LAMB,

$$\zeta = \frac{\xi^{1/2}}{g^{1/2}}\left(\sigma \pm \frac{gt}{2\xi}\right), \quad \omega = \left(\frac{gt^2}{4\xi}\right)^{1/2}.$$

Accordingly, we have

$$\eta_t = \frac{2P}{\pi\rho g^{1/2}}\left[\frac{1}{(x-l)^{1/2}}\left\{\cos\omega_1^2 \int_0^{\omega_1} \cos\zeta^2 d\zeta + \sin\omega_1^2 \int_0^{\omega_1} \sin\zeta^2 d\zeta\right\}\right.$$

$$\left. - \frac{1}{(x+l)^{1/2}}\left\{\cos\omega_2^2 \int_0^{\omega_2} \cos\zeta^2 d\zeta + \sin\omega_2^2 \int_0^{\omega_2} \sin\zeta^2 d\zeta\right\}\right], \tag{15}$$

where

$$\omega_1 = \left\{\frac{gt^2}{4(x-l)}\right\}^{1/2}, \quad \omega_2 = \left\{\frac{gt^2}{4(x+l)}\right\}^{1/2}. \tag{16}$$

(15) is a strict solution. The definite integrals in it $\int_0^\omega \cos\zeta^2 d\zeta$ and $\int_0^\omega \sin\zeta^2 d\zeta$ are shown by the curves I and II of Fig. 5, and are well-known as FRESNEL'S integrals in optics. An example of numerical calculation of (15) is shown in Fig. 7. *E*. In order to render the characteristics of the solution comprehensible, let us make an approximation. If we use

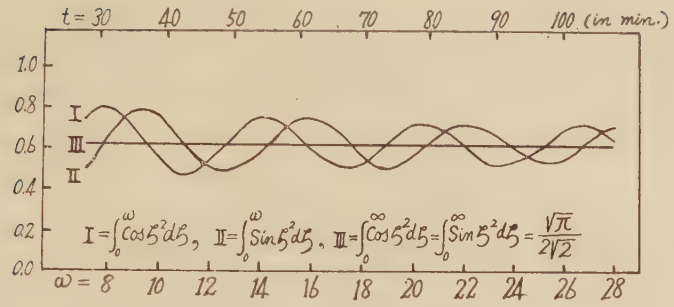

Fig. 5. Fresnel's Integral.

The values of t in the upper row are calculated by $\omega=(gt^2/4x)^{1/2}$ in the case of $x=130$ km.

$$\int_0^\infty \cos\zeta^2 d\zeta = \int_0^\infty \sin\zeta^2 d\zeta = \frac{\sqrt{\pi}}{2\sqrt{2}}, \tag{17}$$

(15) becomes, in case of $\omega_1, \omega_2 \gg 1$,

$$\begin{aligned}
\eta_t &= \frac{P}{\pi\rho}\Bigg[\frac{\pi^{1/2}}{2^{1/2}g^{1/2}(x-l)^{1/2}}\left\{\cos\frac{gt^2}{4(x-l)}+\sin\frac{gt^2}{4(x-l)}\right\} \\
&\quad - \frac{\pi^{1/2}}{2^{1/2}g^{1/2}(x+l)^{1/2}}\left\{\cos\frac{gt^2}{4(x+l)}+\sin\frac{gt^2}{4(x+l)}\right\}\Bigg] \\
&= \frac{P}{2^{1/2}\pi^{1/2}\rho g^{1/2}x^{1/2}}\Bigg[\left\{1+\frac{3}{8}\left(\frac{l}{x}\right)^2+\cdots\cdots\right\} \\
&\quad \times\left\{\cos\frac{gt^2}{4(x-l)}+\sin\frac{gt^2}{4(x-l)}-\cos\frac{gt^2}{4(x+l)}-\sin\frac{gt^2}{4(x+l)}\right\} \\
&\quad +\left\{\frac{1}{2}\left(\frac{l}{x}\right)+\frac{5}{16}\left(\frac{l}{x}\right)^3+\cdots\cdots\right\} \\
&\quad \times\left\{\cos\frac{gt^2}{4(x-l)}+\sin\frac{gt^2}{4(x-l)}+\cos\frac{gt^2}{4(x+l)}+\sin\frac{gt^2}{4(x+l)}\right\}\Bigg] \\
&= -\frac{2P}{\pi^{1/2}\rho g^{1/2}x^{1/2}}\Bigg[\left\{1+\frac{3}{8}\left(\frac{l}{x}\right)^2+\cdots\cdots\right\}\sin\left(\frac{gt^2}{4}\cdot\frac{l}{x^2-l^2}\right)\sin\left(\frac{gt^2}{4}\cdot\frac{x}{x^2-l^2}-\frac{\pi}{4}\right) \\
&\quad -\left\{\frac{1}{2}\left(\frac{l}{x}\right)+\frac{5}{16}\left(\frac{l}{x}\right)^3+\cdots\cdots\right\}\cos\left(\frac{gt^2}{4}\cdot\frac{l}{x^2-l^2}\right)\cos\left(\frac{gt^2}{4}\cdot\frac{x}{x^2-l^2}-\frac{\pi}{4}\right)\Bigg].
\end{aligned} \tag{18}$$

This approximation means the replacement of the curves I and II with the curve III of Fig. 5.

In the region where this formula holds, at any assigned epoch, the changes in length and height from wave to wave in the two functions $\sin\left(\frac{gt^2}{4}\cdot\frac{l}{x^2-l^2}\right)$ $\cos\left(\frac{gt^2}{4}\cdot\frac{l}{x^2-l^2}\right)$ and $\sin\left(\frac{gt^2}{4}\cdot\frac{x}{x^2-l^2}\right)$ $\cos\left(\frac{gt^2}{4}\cdot\frac{x}{x^2-l^2}\right)$ of (18) are gradual, so that a considerable number of consecutive waves may be represented approximately by a sine or cosine curve. The circumstances are, in fact, all approximately reproduced when

$$\Delta\frac{gt^2}{4}\cdot\frac{l}{x^2-l^2}=2\pi \quad \text{and} \quad \Delta\frac{gt^2}{4}\cdot\frac{x}{x^2-l^2}=2\pi. \qquad (19),\ (20)$$

Hence, if we vary t alone, we have, putting $\Delta t=\tau_1$ or τ_2, the periods of oscillation:

$$\tau_1=\frac{4\pi(x^2-l^2)}{glt}, \qquad \tau_2=\frac{4\pi(x^2-l^2)}{gxt} \qquad (21),\ (22)$$

respectively. Especially, in the case when $x\gg l$, (18) becomes

$$\eta_i=-\frac{2P}{\pi^{1/2}\rho g^{1/2}x^{1/2}}\sin\left(\frac{gt^2}{4x}\cdot\frac{l}{x}\right)\sin\left(\frac{gt^2}{4x}-\frac{\pi}{4}\right). \qquad (23)$$

The periods in this case are, for $\sin\left(\frac{gt^2}{4x}\cdot\frac{l}{x}\right)$ and $\sin\left(\frac{gt^2}{4x}-\frac{\pi}{4}\right)$,

$$\tau_1=\frac{4\pi x}{gt}\cdot\frac{x}{l} \qquad \text{and} \qquad \tau_2=\frac{4\pi x}{gt} \qquad (24),\ (25)$$

respectively, and hence

$$\tau_1=\tau_2\times\frac{x}{l}. \qquad (26)$$

The wave lengths corresponding to them are respectively

$$\lambda_1=\frac{8\pi x^2}{gt^2}\cdot\frac{x}{2l}, \qquad \lambda_2=\frac{8\pi x^2}{gt^2}, \qquad (27),\ (28)$$

and hence

$$\lambda_1=\lambda_2\cdot\frac{x}{2l}. \qquad (29)$$

Comparing the solution (11) of Cauchy and Poisson with the solution (23) obtained by us, it will be found that $\sin\left(\frac{gt^2}{4x}\cdot\frac{l}{x}\right)$ appears in the latter. So, we shall show that (11) is a special case of (23). If Cauchy-Poisson's assumption (10) for an impulse is to be applied to our case, the impulse P becomes larger and larger, while l becomes smaller and smaller, so as to make

$$\lim_{l\to 0}\int_{-l}^{l}Pd\alpha=\lim_{l\to 0}(P\times 2l)=1.$$

Then, (23) becomes

$$\eta_i=-\frac{2}{\pi^{1/2}\rho g^{1/2}x^{1/2}}\sin\left(\frac{gt^2}{4x}-\frac{\pi}{4}\right)\times\left\{\lim_{l\to 0}P\times\sin\left(\frac{gt^2}{4x}\cdot\frac{l}{x}\right)\right\}$$
$$=\frac{g^{1/2}t^2}{2^{-1/2}\pi^{1/2}\rho x^{5/2}}\left(\cos\frac{gt^2}{4x}-\sin\frac{gt^2}{4x}\right),$$

which perfectly coincides with (11).

The period τ_2 of (25) has already been obtained by Cauchy and Poisson by assuming a point source of disturbance, but it is noteworthy that, when the source is of limited width, the period has, strictly speaking, a relation to the

width l of the disturbance source, as is indicated by τ_2 of (22). The larger the width of disturbance source is, the larger its effect upon the period is. In (23) the period τ_1 of newly added factor $\sin\left(\frac{gt^2}{4x}\cdot\frac{l}{x}\right)$ is, as is shown in (26), by far larger than the period τ_2 of individual waves. For example, if we take $x=130$ km, $l=1$ km, Table 2 is obtained.

Table 2.

t min	ω	τ_1 hours	τ_2 sec	λ_1 km	λ_2 km	c_1 km/min	c_2 km/min
30	7.81	3.4	93	871	13.4	4.32	8.64
60	15.63	1.7	47	218	3.3	2.16	4.32
90	23.44	1.1	31	97	1.5	1.44	2.88

The elevation in this case is shown in Fig. 7. G, and indicates apparently the wave form of "beat." This beat is caused, as LAMB has pointed out, by mutual interference of the waves generated from various parts of the initial disturbance source of finite extent.

The grade of this interference depends upon the ratio of the distance x from the source and the dimension l of the source, and in case when x is constant, the larger l makes the grade of interference larger. This is evident from the form of τ_1.

And from (25) and (28) it is known that, at a given point, the period of an individual wave decreases gradually with t, and that the wave length increases with the distance x from the origin. The same can be said about τ_1 and λ_1 of the interference wave form.

Next, the phase velocity of an individual wave comes to be

$$c_2=\frac{\lambda_2}{\tau_2}=\sqrt{\frac{g\lambda_2}{2\pi}} \tag{30}$$

which accords with the phase velocity of deep water wave. Hence, the velocity of a wave with constant wave length, namely the group velocity, is

$$c_g=\frac{x}{t}=\frac{1}{2}\sqrt{\frac{g\lambda_2}{2\pi}}=\frac{1}{2}c_2. \tag{31}$$

On the other hand, the velocity of interference wave shown by $\sin\left(\frac{gt^2}{4x}\cdot\frac{l}{x}\right)$ is

$$c_1=\frac{\lambda_1}{\tau_1}=\frac{x}{t}=\frac{1}{2}c_2 \tag{32}$$

which is entirely equal to the group velocity c_g of individual waves. This relation lies in a similar circumstance to the fact that the velocity of the interference wave form obtained by superposing two sine waves with slightly different

periods and lengths is equal to the group velocity of individual sine waves. These values are shown in Table 2.

2. The case of initial elevation.

Here we consider the case when the elevation Q of a constant height is given to an extent $(-L \leqq x \leqq L)$ of the sea surface at $t=0$. Then, (6) can be rewritten as

$$\rho\phi_0=0\,;\quad \eta=Q\,(-L\leqq x\leqq L),\quad \eta=0\,(|x|>L), \tag{33}$$

and an appromixmate solution which satisfies these conditions is given by

$$\eta_e=\frac{4Qx^{1/2}}{\pi^{1/2}g^{1/2}t}\sin\left(\frac{gt^2}{4x}\cdot\frac{L}{x}\right)\cdot\cos\left(\frac{gt^2}{4x}-\frac{\pi}{4}\right), \tag{34}$$

which will be proved in the following. Comparing (5) with (7), we obtain

$$\frac{1}{g\rho}\frac{\partial}{\partial t}\eta_e=\eta_i \tag{35}$$

by equating $f(x)=F(x)$. Hence, considering

$$\begin{aligned}\frac{1}{g\rho}\frac{\partial}{\partial t}\eta_e=-\frac{2Q}{\pi^{1/2}\rho g^{1/2}x^{1/2}}\Big\{&\sin\left(\frac{gt^2}{4x}\cdot\frac{L}{x}\right)\cdot\sin\left(\frac{gt^2}{4x}-\frac{\pi}{4}\right)\\&-\frac{L}{x}\cos\left(\frac{gt^2}{4x}\cdot\frac{L}{x}\right)\cdot\cos\left(\frac{gt^2}{4x}-\frac{\pi}{4}\right)\\&+\frac{2x}{gt^2}\sin\left(\frac{gt^2}{4x}\cdot\frac{L}{x}\right)\cdot\cos\left(\frac{gt^2}{4x}-\frac{\pi}{4}\right)\Big\},\end{aligned} \tag{36}$$

we can neglect the second and third terms in comparison with the first one in our case. Accordingly, putting $Q=P$, $L=l$, and comparing with η_i of (23), it is apparent that (35) holds then (34) is the solution required. Moreover, if we obtain the limiting value of (34) in order that $\lim_{L\to 0}\int_{-L}^{L}Qd\alpha=1$ may hold we get

$$\eta_e=\frac{g^{1/2}t}{2^{3/2}\pi^{1/2}x^{3/2}}\left(\cos\frac{gt^2}{4x}+\sin\frac{gt^2}{4x}\right), \tag{37}$$

which is equal to the result obtained in LAMB's "Hydrodynamics" for the case of point source and of initial elevation.

Now, in the solution (34) above obtained, the period, the wave length and characteristics concerning interference phenomenon are quite the same as in the solution (22) for the case of initial impulse. Namely, the period of individual wave is shown by (25) and that of interference wave form will be shown by replacing L with l in (24). But, in regard to wave height, the circumstances are considerably different; $x^{1/2}$ is contained in the numerator, while t is newly added to the denominator. Accordingly, the wave height at a given point decreases with

time, and finally it vanishes. In the case of initial impulse, such a phenomenon does not occur as has been seen.

3. Thus, when the distributions of initial impulse and initial elevation are simultaneously given by

$$\begin{cases} \rho\phi_0 = P(-l \leqq x \leqq l), & \rho\phi_0 = 0 \quad (|x| > l), \\ \eta = Q(-L \leqq x \leqq L), & \eta = 0 \quad (|x| > L), \end{cases} \tag{38}$$

the elevation is given by

$$\eta = \eta_i + \eta_e = -\frac{2P}{\pi^{1/2}\rho g^{1/2} x^{1/2}} \sin\left(\frac{gt^2}{4x} \cdot \frac{l}{x}\right) \sin\left(\frac{gt^2}{4x} - \frac{\pi}{4}\right) + \frac{4Qx^{1/2}}{\pi^{1/2} g^{1/2} t} \sin\left(\frac{gt^2}{4x} \cdot \frac{L}{x}\right) \cdot \cos\left(\frac{gt^2}{4x} - \frac{\pi}{4}\right) \tag{39}$$

approximately, from (9), (23) and (34). When l is not equal to L, the interference wave form is considerably complicated, but the period of individual waves is known to vary according to (25), also.

§ 5. *Comparison of the theory with observations.*

First, we shall consider the period. Strictly speaking, the period of individual waves depends upon the width (l or L) of disturbance source, as shown by (22). But when the point of observation is very far from the disturbance source, the period is approximately represented by

$$\tau = \frac{4\pi x}{gt}, \tag{25}$$

where x denotes the distance from the central part of disturbance source, and t the time since the explosion. This equation is always consistent, when initial elevation only, or initial impulse only has acted, or when both of them have simultaneously acted. The theoretical curves, obtained by calculation of (25), taking t as abscissa, τ as ordinate, and putting $x = 130$ km, are shown in Fig. 6 as A, B and C respectively. The points plotted in Fig. 6 at the same time are the reading values of the period of actual tsunami waves from the wave records shown by A, B and C of Fig. 7. Comparison of the theoretical curves with observational values shows a very good accordance between all the cases of 16th, 24th and 26th in the value itself of period and in the aspect of decrease with time of the period.

Next, we investigate the variation of wave height. In the wave records of Fig. 7 A, B and C, there are appearing conspicuous "beats", and with variations similar to each other. Namely, in every case the wave began to occur

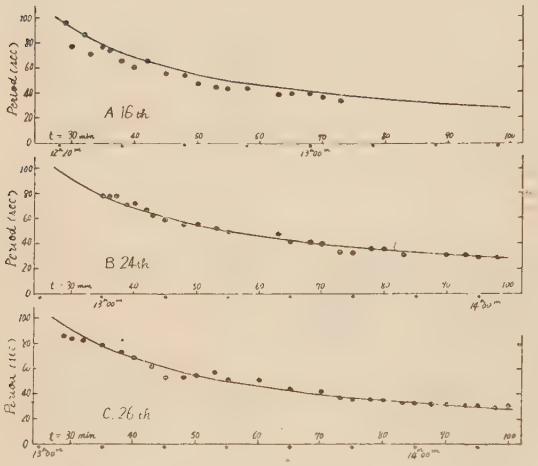

Fig. 6. Comparison of periods between theory and observations. The curves are theoretical ones calculated by $\tau=4\pi x/gt$. Dots show the observed period.

at the time $t=28$ min (actually observed in the cases of 16th and 26th, assumed in the case of 24th), and the first node at $t=58$ min. The position of this node corresponds to 16th 12h 50m in the case *A*, 24th 13h 23m in the case *B*, and 26th 13h 33m in the case *C*. Moreover, the wave height as the whole is gradually decreasing with time, while it is showing the beats.

1. For simplicity, we first assume that the wave has been produced by initial impulse alone, and investigate, to what extent then we can explain the observed facts. In this case the strict solution is given by (15), and the approximate one by (23). From (23), the nodes of beats are determined by

$$\frac{gt^2}{4x}\cdot\frac{l}{x}=n\pi\,;\qquad (n=1,2,3,\cdots\cdots)$$

namely, because of

$$l=\frac{4n\pi x^2}{gt^2} \tag{40}$$

we can know the width of initial impulse, when the time of node is known. This is naturally recognized by consideration of the cause of interference. Hence, putting $x=130$ km and executing the calculation of l from $t=58$ min of the first node ($n=1$), we obtain $l=1.8$ km. Therefore, the range to which the impulse is applied is $2l=3.6$ km for every case of 16th, 24th and 26th. If consideration is made on the report of the explosion on 23rd stated in § 2, on the fact that the explosions on 16th, 24th and 26th are supposed to be of the scale by far larger than that of the explosion on 23rd, and on the possibility that the impulse can, even when the submarine crater is small, make funnel-shaped propagation and act upon the wide area of the sea surface, the above-mentioned values will be generally recognized.

Now, the result of numerical calculation of the strict solution (15), putting $l=1.8$ km, is shown in Fig. 7 *E*, and that of approximate solution (23) in *F*.

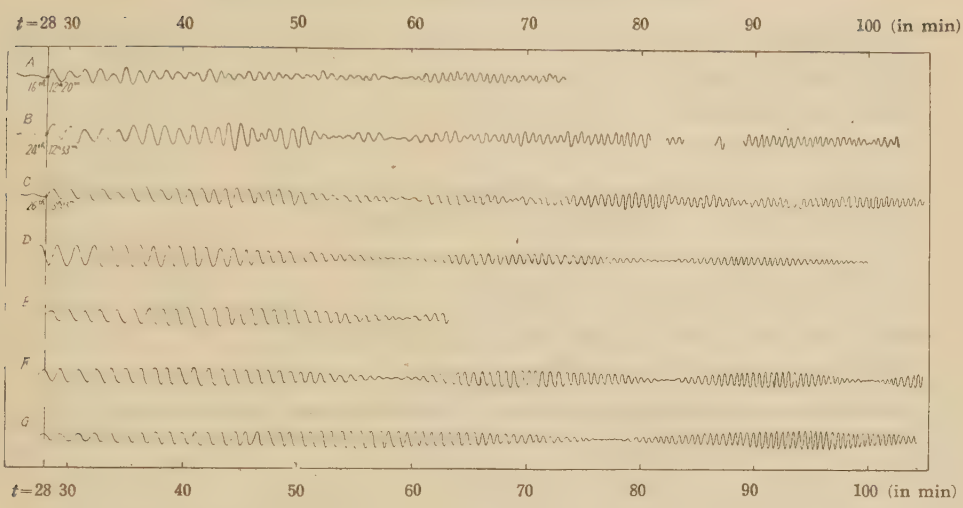

Fig. 7. Wave records A, B and C are the actual tsunamis obtained by smoothing A, B and C in Fig. 2 in order to eliminate swells and wind waves. D is the theoretical wave caused by an initial elevation, calculated in the case of $L=1.8$ km by (34). E, F and G represent the theoretical waves caused by initial impulse; E and F are calculated in the case of $l=1.8$ km by (15) and (23) respectively, and G in the case of $l=1$ km by (23).

Hence it is plain that the essence of the strict solution (15) can be sufficiently represented by the approximate solution (23). Comparison of these theoretical curves with the observed records A, B and C shows a good accord in the aspect of variation of wave. For instance, the number of waves contained in the first beat from $t=28$ min to $t=58$ min is almost the same in every case. For purpose of reference, the theoretical elevation in the case of $l=1$ km, $x=130$ km is shown in Fig. 7. G. The position of the first node in this case is $t=77.5$ min, and by a small difference in l the position of node may be very much displaced. Namely, the value l can be sharply fixed by the position of node. However, after the first node of $t=58$ min, the theory and the observations are not so in good accord. Naturally the beats have occurred, but not so conspicuously as in the beginning, and irregularly. Solely in the case B (or 24th), the second node seems to have occurred at about $t=82\sim85$ min, though it is not very clear owing to the lack of record, and this is in accord with the theoretical value of $t=82$ min. The third node has occurred at about $t=100$ min, also in accord with the theory. Especially on 24th, as the decrease of wave height as the whole is small, it may be considered that in the explosion on 24th the effects of initial impulse are conspicuous. For other cases, this can not be said definitely. In this regard it will be discussed later.

Furthermore, assuming that these tsunami waves have been caused by initial impulse, the intensity P of impulse per unit area is obtained by knowing the maximum wave height.

According to (23),

$$\eta_{i,\max}=\frac{H_{\max}}{2}\div\frac{2P}{\pi^{1/2}\rho g^{1/2}x^{1/2}}$$

i.e.

$$P=\frac{1}{4}\pi^{1/2}\rho g^{1/2}x^{1/2}\cdot H_{\max} \tag{41}$$

Actual values are shown in the third line of Table 3.

Table 3.

Sept. 1952	*A*. 16th	*B*. 24th	*C*. 26th
$H_{\max}$ (cm)	56	92	71
P (dyne·sec/cm²)	2.8×10^6	4.6×10^6	3.6×10^6
Q (m)	3.1	5.1	3.9

Whether these values of P are recognizable or not is uncertain owing to the lack of observed data. However, as our theory is treating a one-dimensional problem, the intensity P of impulse in the actual case of two dimensions is considered to be of the values pretty larger than the one obtained here. And, strictly speaking, as is seen from the refraction diagram of Fig. 4, the effect of convergence of orthogonal lines on the wave height in the neighbourhood of Hachijo Is. should be taken into account in calculating the intensity of impulse.

2. Next, we shall investigate the case when the wave is produced by initial elevation alone. Comparing (34) with (23), the positions of the nodes of beat phenomenon are entirely the same as in the case of initial impulse shown by (40). Hence, the range of initial elevation is $2L=2\times1.8=3.6$ km, which is somewhat larger than what was observed on 23rd, as stated in § 2, but may be seemingly a reliable value.

Then, putting $L=1.8$ km, an approximate solution η_e is calculated by (34), and Fig. 7 *D* is obtained. According to this, we can to some extent well explain the aspect of gradual decrease of actual wave height as the whole. Especially, the wave *A* of 16th quite resembles to *D*. Namely, the tsunami wave of 16th can be considered as largely affected by an initial elevation.

And we can, if the maximum wave height is known, obtain the quantity Q of initial elevation. By (34), we have

$$Q=\frac{1}{8}\cdot\pi^{1/2}g^{1/2}t_0x^{-1/2}H_{\max}, \tag{42}$$

where t_0 is the time whose value enables η_0 to be maximum in (34) and which satisfies $\tan\left(\frac{gt_0^2}{4x}\cdot\frac{L}{x}\right)\Big/\left(\frac{gt_0^2}{4x}\cdot\frac{L}{x}\right)=2$ approximately. Putting $x=130$km, $L=1.8$km, then $t_0=35$min, and if Q is numerically searched for, it becomes as shown in the fourth line of Table 3. These values are in accord with the height of water dome observed immediately after the eruption of 23rd, as is said in §2, but are considerably smaller than what was observed at a short time later. It is necessary to pay attention to the fact that the values obtained here may be considerably smaller than the actual values in the case of two dimensions, as is emphasized in the case of initial impulse also.

3. Hitherto, consideration has been made on the cases when initial impulse or initial elevation has acted on the surface independently. But, as is said in §2, it should be considered that in reality they both act simultaneously. The elevation in this case is given by (39), where unknown constants P, Q, l and L can be determined by comparing the observed data with the theory. If these four unknown quantities have been appropriately determined, the actual wave form with considerably complicated interference will be explained quite exactly. However, it seems to be very difficult to find the magnitude and scale of impulse and elevation actually from wave records.

From the above discussions, we may conclude without great errors that the tsunami wave of 16th was caused mainly by the initial elevation accompanying the explosion, and that the tsunami wave of the 24th showed conspicuous effects of the initial impulse at the moment of explosion. The result of the latter will give a suggestion to the causes of the "Kaiyo-maru, No. 5" disaster. In the case of 26th it is not so simple. And as there can be cases where tsunami waves have not been produced by the explosion, the three cases stated above will belong to remarkable explosions. Particularly, the explosion of 24th which caused the sinking of the "Kaiyo-maru, No. 5" is evidently known from Table 3 to have been especially intense.

From the actual wave records, however, it is seen that the theory and the observations may disagree with each other in the later parts of records where the wave period is very short, even though the values of P, Q, l and L are correctly fixed. We may consider the causes of this disagreement as follows: (a) when t becomes large, the period of waves becomes very short and finally comparable with the periods of swells and wind waves, so that it is impossible to take out tsunami waves alone independently, (b) thus, the tsunami waves interfere with swells and wind waves, (c) the effect of friction, which has not been considered in the discussions hitherto, is especially conspicuous for waves

of short period.

We have used several suppositions in order that the problem may be discussed easily. Nevertheless, the theory and the observations show a satisfactory agreement in the essence of our problem, as is shown by Fig. 6 and 7. In this regard, noteworthy points are as follows; (a) there is no essential difference between the characteristics of solutions obtained in the cases of one-dimension and two-dimensions, as is seen from the results in LAMB's "Hydrodynamics" (§ 238–9 and § 255). But the absolute values of initial impulse or elevation obtained on Table 3 must be corrected in the actual case of two-dimensions; (b) it is not an essential problem to our case whether the depth to the bottom is limited or unlimited; namely, whether the wave is supposed to be a medium wave or deep water wave, as is stated in § 3; (c) for the waves of long period in the earlier stage, the effect of friction is small.

In the near future, we intend to investigate on the cases of two-dimensions, of limited water-depth, or on the case when the effects of frictional force are considered.

§ 6. *Summary*.

From the above discussions, it can be concluded that the tsunami waves recorded recently at Hachijo Island are the Cauchy-Poisson waves produced by the initial impulse and initial elevation acted upon the sea surface of limited area at the moment of explosion of a submarine volcano. And it has become possible to know the scale and magnitude of initial local disturbance, by knowing the time of occurrence of node of interference wave form and the maximum wave height.

And the existence of such a wave with longer period of about 1 min is of significance in many respects. Namely, we may consider that such a longer wave can be produced not only by explosion of a submarine volcano, but also by abrupt change of air pressure in the active region of a typhoon, cyclone or front. For example, according to what was formerly studied by one of the authors, M. NAKANO,[11] it was seen that, when a developed cyclone passes through south of Honshu, Japan, characteristic waves with longer period of 1~3 min are recorded on the mareograms and these waves are most dependent upon the changes of pressure gradient with time, *i.e.* $\frac{\partial G}{\partial t}=\frac{\partial}{\partial x}\left(\frac{\partial p_0}{\partial t}\right)$. Accordingly, these waves may be supposed to be a kind of Cauchy-Poisson wave produced by an abrupt microbarometric change in the central part of a cyclone. If so, other than the forerunner due to wind stated by MUNK[9] and others, forerunner of

different kind is to exist. Furthermore, as one of the important causes of secondary undulations of tides in a bay, it has been often considered that waves of the long period corresponding to that of free oscillations of the bay may exist in the open ocean. This may be recognizable when we consider the Cauchy-Poisson waves caused by atmospheric disturbances.

Acknowledgement.

In conclusion the authors wish to express their thanks to the members of Hachijojima Weather Station by whose eager observations valuable wave records were obtained, to Dr. H. NIINO who instructed the authors of the condition of the sea at the moment of Myojinsho explosion, to Dr. Y. KAWABATA, Dr. Y. SAITO and to Mr. K. KAJIURA who gave advices, and to Mr. T. YUSA who assisted in numerical calculation. And the authors pray heartily for the heavenly bliss of all the investigators and crewmen on board the "Kaiyo-maru, No. 5" whose precious lives were sacrificed in the southern sea of Japan to the progress of science.

Literature.

(1) H. LAMB: *Hydrodynamics*, sixth edition, §§ 238, 239, 240, 1932.
(2) THORADE: *Probleme der Wasserwellen.* § 2, Hamburg, 1931.
(3) THORADE: *l.c.* § 16.
(4) Los Alamos Scientific Laboratory: *The Effect of Atomic Weapons*, Chapter 4, 1950.
(5) The Report presented by the Investigation Committee for the cause of the "Kaiyo-maru, No. 5" disaster, (in Japanese), Hydrogr. Office, 1952.
(6) R. S. DIETZ: On the "SOFAR" Hydrophone. (Lecture delivered on the 25th of November, 1952 at the Hydrographic Office of Japan.)
(7) W. H. MUNK: Surf Beats. *Trans. Amer. Geophys. Union.* Vol. 30, No. 6, 1949.
(8) C.-G. ROSSBY: On the Propagation of Frequencies and Energy in Certain Types of Oceanic and Atmospheric Waves. *Journ. Met.* Vol. 2, No. 4, 1945.
(9) W. H. MUNK: Tracking Storms by Forerunners of Swell. *Journ. Met.* Vol. 4, No. 2, 1947.
(10) H. LAMB: *l.c.* foot-notes on p. 393.
(11) M. NAKANO: On the Secondary Undulations of Tides Caused by Cyclonic Storms (1st paper). *Oceanogr. Mag.* Vol. 1, No. 1, pp. 13~32, 1949.

Postscript.

While this paper was going to be sent to press, the authors could find out the treatise of W. BURNSIDE ("On deep-water waves resulting from a limited original disturbances", Proc. Lond. Math. Soc. (1), XX. 22, 1888). He discussed only the case of initial elevation, and not the case of initial impulse which the present authors have studied especially in detail. First, BURNSIDE gave solutions for the case when the initial elevation is given in the forms of $c\alpha^2/(\alpha^2+x^2)$ and $c\{\alpha^2/(\alpha^2+x^2)\}^{3/4}\cdot\cos\{(3/2)\cdot\tan^{-1}x/\alpha\}$, and next, he investigated the problem where an initial elevation with a constant height is given to a limited area. The solution for the latter case is naturally coincident with the solution (34) obtained by the present authors, but his method in solving was different from that of the present authors.

ON THE CAUCHY-POISSON WAVES CAUSED BY THE ERUPTION OF A SUBMARINE VOLCANO.*

S. UNOKI

Oceanographical Section, Central Meteorological Observatory, Tokyo

and M. NAKANO

Oceanographical Laboratory, Meteorological Research Institute, and Geophysical Institute, Tokyo University

Reprinted from
Records of Oceanographic works in Japan, vol I. No. 1 (new series), March, 1953

ON THE CAUCHY-POISSON WAVES CAUSED BY THE ERUPTION OF A SUBMARINE VOLCANO.*

S. UNOKI

Oceanographical Section, Central Meteorological Observatory, Tokyo

and M. NAKANO

Oceanographical Laboratory, Meteorological Research Institute, and Geophysical Institute, Tokyo University

1. *Preface.* The theory of the waves produced in deep water by a local disturbance of the surface was investigated by Cauchy and Poisson independently in the case of one dimension. The similar problem in two dimensions was dealt with by Dr. H. Lamb[1] and Dr. K. Terazawa[2], but their investigations are insufficient for our purpose. Though the theory of the Cauchy-Poisson wave problems is an elegant one, the existence of such a wave in reality in the ocean has been doubted by many practitioners. Recently, however, the report of the experimental results of an atomic bomb explosion enables us to consider that the Cauchy-Poisson wave may exist in reality[3]. Here, we shall show that the Cauchy-Poisson wave occurs not only artificially and experimentally, but also actually in nature.

The position of the point where the eruption of the submarine volcano occurred and the position of Hachijo Island, where the wave was observed, are shown in Fig. 1. From the middle to the end of September, 1952, submarine eruptions occurred at a reef which is located about 300 km south of Honshu, Japan. Tsunami waves caused by some of these eruptions which were observed on September 16th, 24th and 26th, 1952 respectively are shown in Fig. 2, A, B, C. Wave observations were made at Hachijo Island, about 130km north of the submarine volcano (Myojinsho), using a self-registering wave gauge of a pressure recorder type. Wave records A, B and C in Fig. 2 are not actual data, but data adjusted to eliminate wind waves and swells, and the time

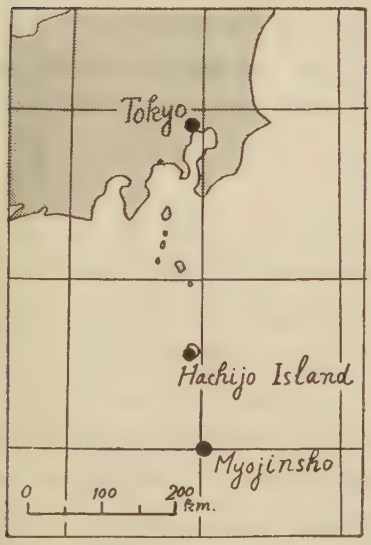

Fig. 1.

* Full discussion of this problem will be made in the *Oceanographical Magazine;* first paper-Vol. IV, No. 4, second paper.-Vol. V, No. 1, 1953.

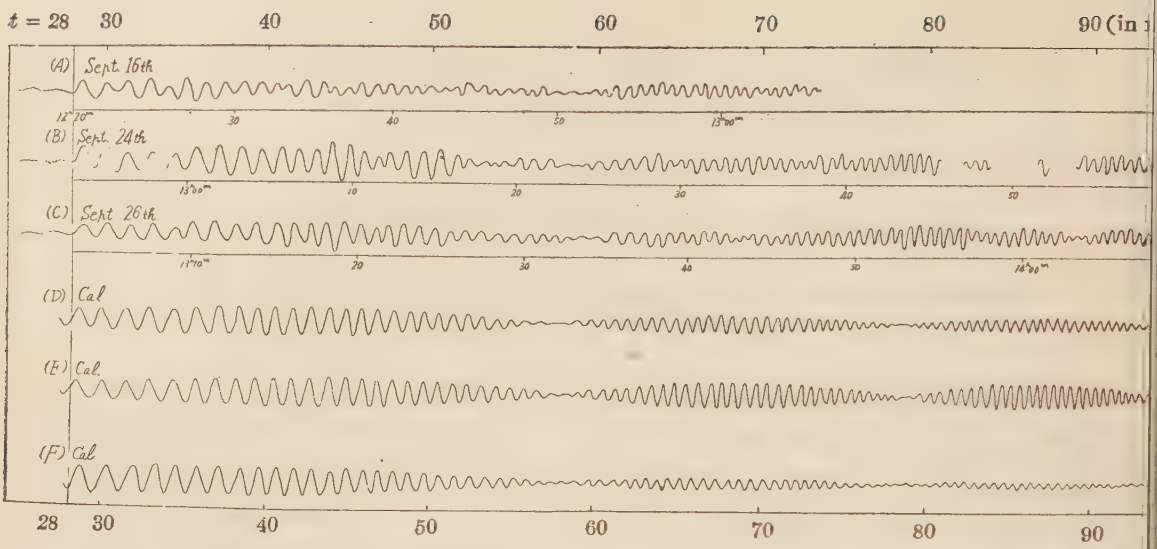

Fig. 2. Wave records A, B and C are the tsunamis obtained by adjusting the observed data in order to eliminate swells and wind waves. Curves D and E represent the theoretical waves caused by initial impulse, and F is the theoretical wave caused by initial elevation.

marks on wave records may have errors of the order of magnitude ±3 min. owing to the lack of a master clock for time checking. The maximum wave heights on the 16th, 24th and 26th were 56cm, 92cm and 71cm respectively, and the time necessary for propagation of tsunami from Myojinsho to Hachijo Island was 28 min. on both the 16th and the 26th. On the 24th, when the tsunami shown in Fig. 2, B was recorded—perhaps caused by the same eruption which brought disaster to the "Kaiyo-maru No. 5" of the Hydrographic Office as the ship was engaged in scientific investigation of Myojinsho —the travel time is not known because no one witnessed the eruption.

Valuable observations on the eruption at 1340 hours on the 23rd were made by members of the Myojinsho investigation party. According to their report, when the eruption occurred the sea surface, which had been even till that time, heaved up suddenly to a water dome whose dimensions were 300m wide and less than 5m high immediately after the eruption. Following this the dome became 1.5km wide and and 50～60m high, and resembled a fountain. The water which heaved up collapsed into waves of 50～60m wave length, but the wave height decreased as the party watched and was only about 1 cm when the waves reached their ship, a distance of about 1600 m. Such waves came only twice and the period was 12～13 seconds. Whether or not these waves of short wave length and small wave height correspond to the tsunami waves of our consideration is doubtful, but regardless, it can be conceived

that a particular type of wave will be generated by the collapse of such an enormous water dome.

On the other hand, it can be assumed from many facts that a strong impulse acts upon sea water at the moment of an explosion. Consequently, it is also conceivable that waves would be produced by this strong impulse.

2. *Travel time of tsunami waves.* In regard to the time necessary for the propagation of a tsunami wave, a question exists whether the wave travels with a phase velocity or with a group velocity as stated theoretically by Rossby, W.H. Munk and others. We shall here consider the problem. In our case, as the depths are 200～1400 m and the periods 30～100 sec., we should imagine the wave as a medium (elliptic trochoidal) wave rather than as a deep water wave or a long wave, considering the relative depth. For a medium (elliptic trochoidal) wave if we take period τ, the wave length λ and the depth d,

$$\text{phase velocity:} \quad C = \left\{\frac{g\lambda}{2\pi}\tanh\left(\frac{2\pi d}{\lambda}\right)\right\}^{\frac{1}{2}}, \qquad (1)$$

$$\text{group velocity:} \quad C_g = \frac{C}{2}\left\{1+\left(\frac{4\pi d}{\lambda}\right)\Big/\sinh\left(\frac{4\pi d}{\lambda}\right)\right\}, \qquad (2)$$

where $\lambda = C\tau$. According to A, B and C of Fig. 2, the period of the wave which first arrived is about 95 sec. On Table 1 are shown the travel times when the wave has progressed with the group velocity of a medium wave, and when a wave of a 95 sec period has progressed with the phase velocity of a medium wave and with the group velocity of a deep water wave.

The travel time is 32.1 min. if the wave has progressed with group velocity, and 28.5 min. if with phase velocity. The actual travel time, as mentioned in § 1, was about 28 min. in both the cases of 16 and 26 September.

Table 1

Classification of velocities	C_g			C	Group velocity of deep water wave
Period τ (sec.)	60	80	95	95	95
Travel time (min.)	41.5	34·3	32.1	28.5	30.1

As this value, however, can be accompanied by errors of the order of magnitude of 3 min, and it seems that the wave which first arrived has not always progressed with a constant wave form, it is difficult to determine whether the wave in the present problem has progressed with phase velocity or with group velocity. Moreover, the fact that the travel time of a deep water wave progressing with group velocity is

very near to the value of actual travel time suggests that we may most reasonably continue our discussion by assuming the wave to be a deep water one.

3. *Cauchy-Poisson wave problems in two horizontal dimensions when a local disturbance is given to a limited extent of the sea surface.* For simplification of the problem, the sea is considered to be spreading infinitely, and the depth to be very great. As a frictional force which affects wave motion, we shall take up the frictional force proportional to the velocity of fluid particles instead of eddy viscosity. S. Unoki,[4] one of the authors, has already proved that this assumptiou is almost valid in the case of waves with comparatively longer periods, and found the value of the proportional coefficient (2μ) of the frictional force to be 5.5×10^{-4} c.g.s.

First, let us consider the wave caused by an initial local impulse, follwing Prof. Lamb's notation.[1] The origin of co-ordinates is taken on an undisturbed surface and cylindrical co-ordinates z and ω are used, z being positive upwards. Considering the above frictional force, when the initial conditions are given as

$$\zeta = 0\,, \qquad \rho\phi_0 = F(\omega), \tag{3}$$

the solution to be satisfied is

$$\phi_t = \frac{e^{-\mu t}}{\rho}\int_0^\infty\left(\cos\sigma t - \frac{\mu}{\sigma}\sin\sigma t\right)e^{kz}J_0(k\omega)kdk\int_0^\infty F(\alpha)J_0(k\alpha)\alpha d\alpha, \tag{4}$$

$$\zeta_t = -\frac{e^{-\mu t}}{g\rho}\int_0^\infty\frac{\sigma^2+\mu^2}{\sigma}\sin\sigma t J_0(k\omega)kdk\int_0^\infty F(\alpha)J_0(k\alpha)\alpha d\alpha, \tag{5}$$

where the following relation must be satisfied

$$\sigma^2+\mu^2 = gk. \tag{6}$$

If the initial impulse is constant in the limited extent, then assuming

$$\rho\phi_0 = P(\omega \leqq l)\,, \qquad \rho\phi_0 = 0\ (\omega > l), \tag{7}$$

the elevation is given by

$$\zeta_t = -\frac{2^{\frac{1}{2}}\pi^{\frac{1}{2}}Ple^{-\mu t}}{\rho\omega^{\frac{1}{2}}}\Re\left[\frac{1}{2\pi}\int_0^\infty\frac{k^{\frac{1}{2}}}{\sigma}e^{i\left(\sigma t-k\omega-\frac{1}{4}\pi\right)}J_1(kl)dk\right.$$

$$\left.-\frac{1}{2\pi}\int_0^\infty\frac{k^{\frac{1}{2}}}{\sigma}e^{i\left(\sigma t+k\omega+\frac{1}{4}\pi\right)}J_1(kl)dk\right] \tag{8}$$

from (5) and (6), since

$$J_0(k\omega) \fallingdotseq \left(\frac{2}{\pi k\omega}\right)^{\frac{1}{2}}\sin\left(k\omega+\frac{1}{4}\pi\right), \text{ in case of } k\omega \gg 1\,.$$

Using Kelvin's method regarding the principle of stationary phase, we have approxomitely

$$\zeta_t = -\frac{Plt}{2^{\frac{1}{2}}\rho\omega^2}e^{-\mu t}\sin\left(\frac{gt^2}{4\omega}\right)\cdot J_1\left(\frac{gt^2}{4\omega}\cdot\frac{l}{\omega}\right), \tag{9}$$

in the case of $\omega \gg l$, $g^2t^2/4\omega^2 \gg \mu^2$ and $\mu \ll 1$. If the initial impulse is concentrated in the immediate neighborhood of the origin and the frictional force is neglected, (9) becomes

$$\zeta_t \sim \frac{gt^3}{27\pi\rho\omega^4} \sin \frac{gt^2}{4\omega}, \tag{10}$$

which coincides with what H. Lamb obtained[1]. By comparing the solution (10) obtained by H. Lamb when the initial disturbance is concentrated at the origin, with the solution (9) obtained by us, it will be found that $e^{-\mu t}$ and $J_1\left(\frac{gt^2}{4\omega} \cdot \frac{l}{\omega}\right)$ are augmented. The former is the effect of the frictional force, and the latter is the effect of mutual interference of waves generated from the various parts of a disturbing source of finite width, thus the wave shows a remarkable "beat" phenomenon. In (9), the period of individual waves is given by

$$\tau = \frac{4\pi\omega}{gt}. \tag{11}$$

The period of the interference wave form is larger by about (ω/l) times than τ. The nodes of interference waves are decided by

$$J_1\left(\frac{gt^2}{4\omega} \cdot \frac{l}{\omega}\right) = 0. \tag{12}$$

Similarly, in the case of an initial elevation applied to the undisturbed surface, with the initial conditions

$$\zeta = Q(\omega \leqq L),\ \zeta = 0(\omega > L) \text{ and } \rho\phi_0 = 0, \tag{13}$$

the elevation is given approximately by

$$\zeta_e = \frac{2^{\frac{1}{2}}QL}{\omega} e^{-\mu t} \cos\left(\frac{gt^2}{4\omega}\right) \cdot J_1\left(\frac{gt^2}{4\omega} \cdot \frac{L}{\omega}\right). \tag{14}$$

In this case also, (11) and (12) are consistent.

4. *Comparison of the theory and observed data.* The theoretical period is given by (11). The curves of the theoretical period, taking t as abscissa, τ as ordinate and putting $\omega = 130$ km, are shown in Fig. 3 as A, B and C respectively.

The points superimposed on the curve in Fig. 3 are the recorded values of the period of actual tsunami waves shown by A, B and C of Fig. 2. Comparison of the theoretical curves with the observed values shows a very good agreement in all cases, both in the value of the period and in the aspect of the decrease of period with time.

The position of the node of the beat is determined by (12), consequently we can know the radius of area on which initial disturbance acts when the time of occurrence of the node is known. Hence, putting the $\omega = 130$ km and $t = 58$ min. of the first

node into the equation, we obtain l (or L) = 2.2 km. If consideration is given to the many reports of the explosion on the 23rd stated in § 1 and to the fact that the explosions on the 16th, 24th and 26th were supposed to be of far greater magnitude, the above-mentioned values will be generally recognized as correct.

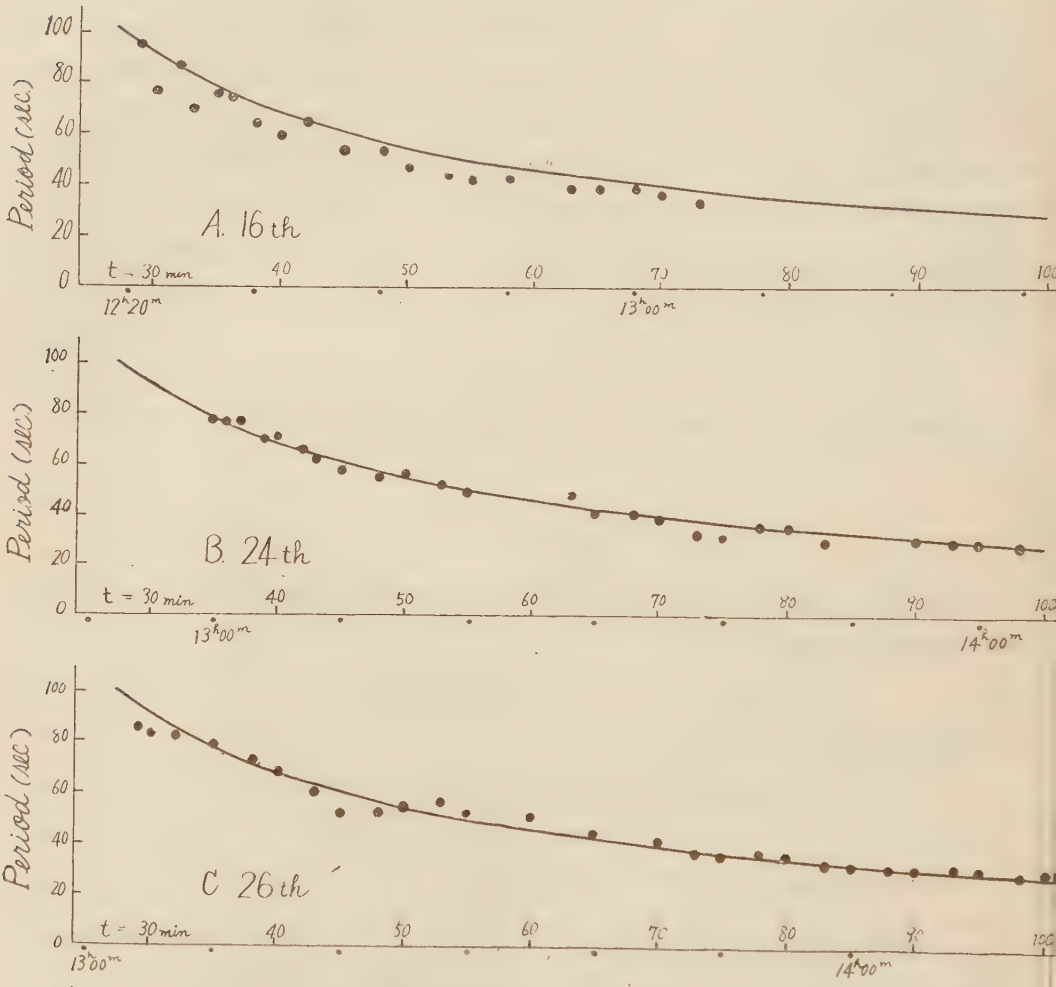

Fig. 3. Comparison of periods between theory and observation. The solid lines represent theoretical curves, while the dots represent observed values.

Now, the results of numerical calculation of solutions (9) and (14), using l (or L) = 2.2 km, are shown in Fig. 2, D and F respectively. For purpose of reference, the theoretical elevation in case of $\mu = 0$ in (9) is shown in Fig. 2, E. Comparison of these theoretical curves, especially D, with the observed wave records A, B and C shows good agreement with regard to the variation of waves. For instance, the number of waves contained in the first beat from $t = 28$ min. to $t = 58$ min., is almost the same in every case. However, after the first node of $t = 58$ min.

the beats occur less conspicuously, and irregularly. Especially, as the decrease of wave height generally was small, it is considered that in case of explosions the effect of the initial impulse on the generation of waves seems to be rather larger than that of the initial elevation.

Furthermore, the intensity P of the initial impulse per unit area or the height Q of the initial elevation is obtained by knowing the maximum wave height and the time of its occurrence, from (9) or (14) respectively. Calculated values are shown in Table 2.

Table 2

Sept. 1952	A (16th)	B(24th)	C(26th)
H_{max} (in cm)	56	92	71
P[in (dyne/cm^2) × sec]	4.2×10^7	7.0×10^7	5.4×10^7
Q (in meter)	38	62	48

The values of Q are in accord with the height of water dome in the observational report of § 1. On the other hand, according to the report on the cause of the disaster of the "Kaiyo-maru No. 5", it is concluded that her sinking may have occurred when the pressure 10 kg/cm^2 acted on the ship in the interval of 1/100 sec. Accordingly, the values of P obtained are recognized to be reliable. Whether the observed tsunami waves were generated by the action of initial impulse or initial elevation is not clear, but it seems to the authors that the action of initial impulse exerts much more effect than does the initial elevation.

In any case, it can be concluded that the tsunami waves recorded recently on Hachijo Island are the typical Cauchy-Poisson waves produced by an initial disturbance of the sea surface within a limited area at the moment of the explosion of a submarine volcano.

References

[1] H. Lamb: *Hydrodynamics*, sixth edition, 1932, § 255; or *Lond. Math. Soc. Proc.* Vol. **II**, (2), p. 371, 1904.

[2] K. Terazawa: *Proc. Roy. Soc.* A. XCII, 57, pp. 57–81, 1915.

[3] Los Alamos Scientitic Laboratory: *The Effect of Atomic Weapons*, § 4.40~4.57, 1950.

[4] S. Unoki: *Oceanogr. Mag.* Vol. **II**, No. 1, pp. 1–15, 1950.

PRINTED BY
KASAI SHUPPAN INSATSUSHA
MINATO-KU, TOKYO, JAPAN
東京都港區芝南佐久間町1－53
笠井出版印刷社印行

ON THE ANNUAL VARIATION IN OCEANOGRAPHICAL ELEMENTS AT A FIXED POINT (39° N, 153° E) IN THE PACIFIC OCEAN

M. KOIZUMI

Meteorological Research Institute, Tokyo.

ON THE ANNUAL VARIATION IN OCEANOGRAPHICAL ELEMENTS AT A FIXED POINT (39° N, 153° E) IN THE PACIFIC OCEAN

M. KOIZUMI

Meteorological Research Institute, Tokyo.

1. *Source material and methods.* The information has been taken from the data of the oceanographic observations which have been performed around the fixed point "EXTRA" (39° N, 153° E) in the Pacific Ocean by the Central Meteorological Observatory of Japan since October, 1947, where marine meteorological and aerological routine observations have been also carried out. Data obtained at about six hundreds stations, located within the area of 38° - 40° N and 152° - 154° E will be dealt with in this report. About 80% of the stations are distributed within the area of 38°40′-39°20′ N and 152°40′ - 153°20′ E; if the larger area of 38°30′ - 39°30′ N and 152°30′ -153°30′ E is taken, about 90% of them are included. The monthly mean values of several oceanographic elements have been computed, and on the basis of these means the characteristic features of the annual variation in oceanographic conditions have been investigated.

2. *Water temperature and chlorinity.* As station "EXTRA" is situated in the zone where two water masses, originating from Kuroshio and Oyashio, make contact with each other, it is covered sometimes with a water mass of Kuroshio origin, and sometimes with that of Oyashio origin. Therefore the oceanographic conditions fluctuate markedly. Even at a short distance or during a short time interval, quite different vertical distributions of water temperature and chlorinity are observed frequently. Hence, some of the individual values fluctuate markedly from the monthly mean. Since the variation caused by alternation of water mass is superimposed on the seasonal variation, monthly patterns of oceanographic elements are quite complicated.

In the upper layers, the annual variation in temperature had a maximum in late summer or early fall; the range of the variation decreases with depth, and the time of maximum temperature occurs later with increasing depth. This decrease of the range and the phase lag of maximum temperature were shown most clearly in 1948, while they were somewhat obscure in 1951. It may be concluded that the case of 1951 was due to the extraordinary variation caused by the alternation of water mass. The

thickness of the isothermal layer in late winter was 150～200 m. In late summer or early fall, the spring layer of temperature develops intensely, and at that time the gradient of 0.2°-0.3° C/m occurs between the 10 m and 25 m depths, or the 25 m and 50 m depths. During the months from April to September the temperature is higher at the surface than in the subsurface, and from October to March of the following year a reversed condition is observed. The annual variation in chlorinity in the upper layers has a maximum in spring, which is due to the effect of continued evaporation, and a minimum in fall, is caused by the heavy precipitation. The date of the extreme values occurs later with increasing depth.

The core of the intermediate water (Oyashio undercurrent) is generally decided by the layer of the minimum temperature or chlorinity in the vertical distribution. Around "EXTRA," the temperature minimum is not usually observed in the vertical distribution of monthly mean values, but in the vertical profiles of monthly mean chlorinity the minimum of 18.70‰～18.85‰ is usually found between the 400 m～500 m depths.

In the layers under the intermediate water the fluctuation becomes smaller and smaller with depth. Throughout the later two years (1950, 1951), the temperature differences between the highest and lowest temperatures in 500m, 600m, 800m 1000m, and 1500 m depth layer were about 2.5°, 1.5°, 0.8°, 0.5°, and 0.2° respectively, while the differences in chlorinity were less than 0.08‰ in any layer cited above.

3. *Colour of the sea, transparency, and plankton volume.* Although the individual values of the elements in question also fluctuate considerably for the same reasons as stated in the previous section, the characteristic features of the annual variation can be revealed when the monthly mean values are adopted.

Values of the plankton volume used here have been calculated from the settling volume of plankton collected from the 100 m depth to the surface with Kitahara's net (Hensen type, bolting silk XX13, diameter of the mouth: 25 cm).

The annual variation in the colour of the sea is similar to that of the transparency, both with two maxima, one in summer and the other in winter and two minima, occuring in spring and autumn. As to the seasonal variation in plankton volume, a very distinct maximum, a phenomenon of so called burst growth, occurs in spring and a less marked maximum in fall, and a marked minimum appears in winter, and also, in a less degree, in early fall. There are correlations between each of those three elements, and it is expected from features of their annual variations. An experimental formula $D=21.8V^{-0.25}$, where D represents transparency expressed in meter

and V, the plankton volume in cc/m^3, has been determined, although somewhat unsatisfactory conditions are involved such as the disregard of composition of plankton, inequality between the values of transparency and the depth of the net haul, etc. Functional relation between colour of the sea (F) and transparency, and also, between plankton

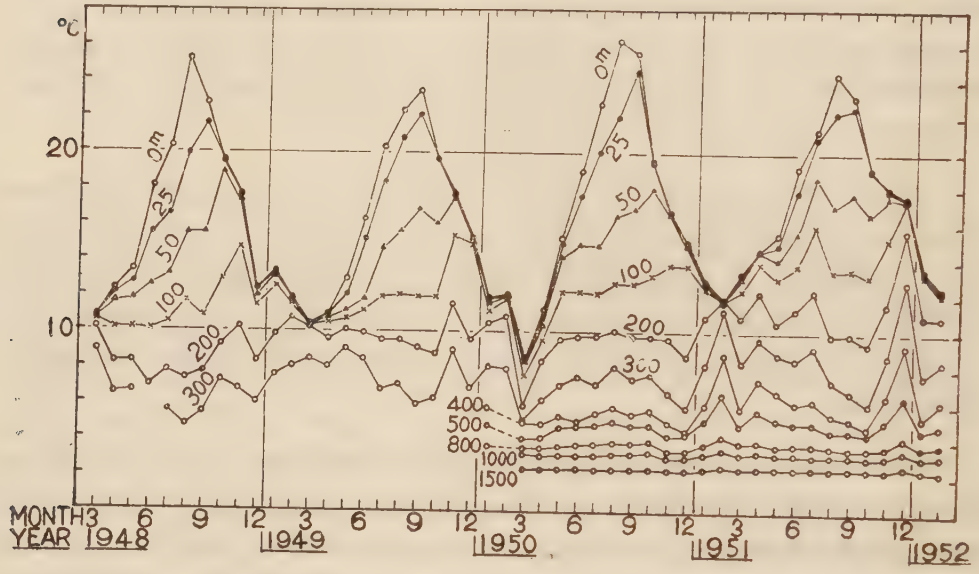

Fig. 1. Variation in water temperature at different depths.

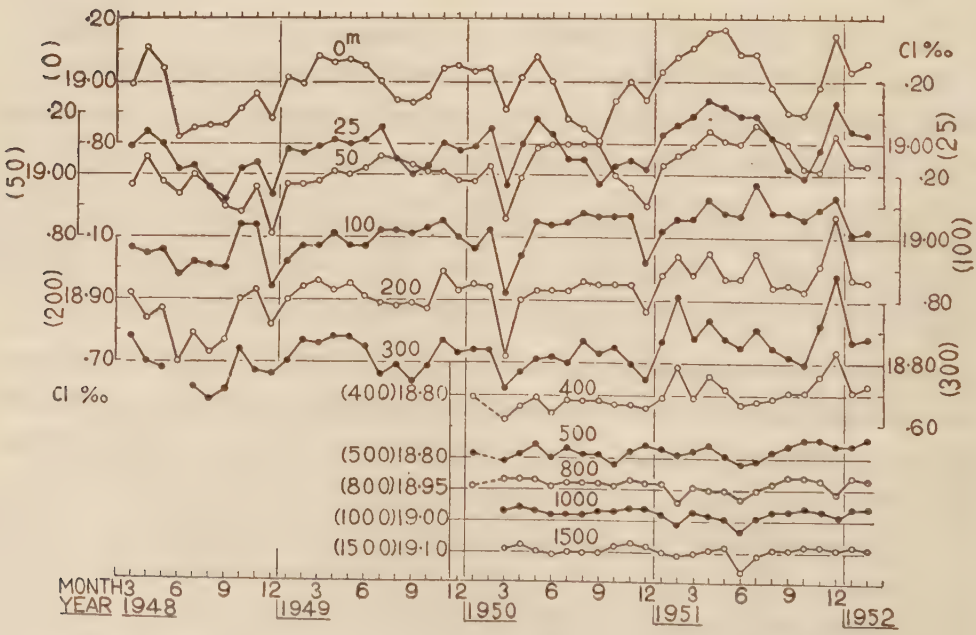

Fig. 2. Variation in chlorinity at different depths.

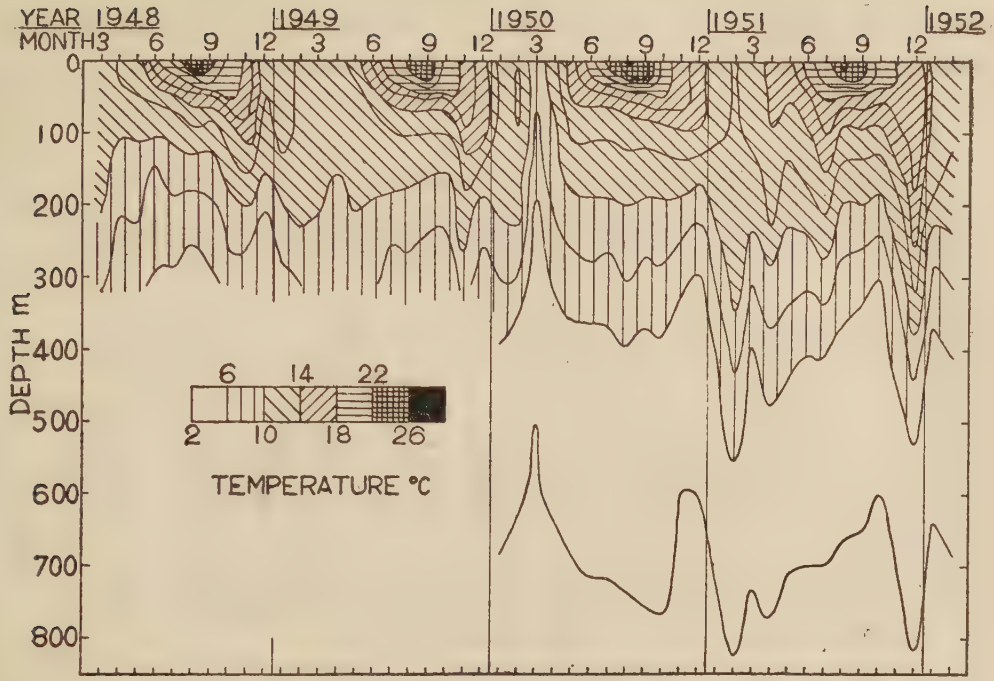

Fig. 3. Isopleth diagram of water temperature.

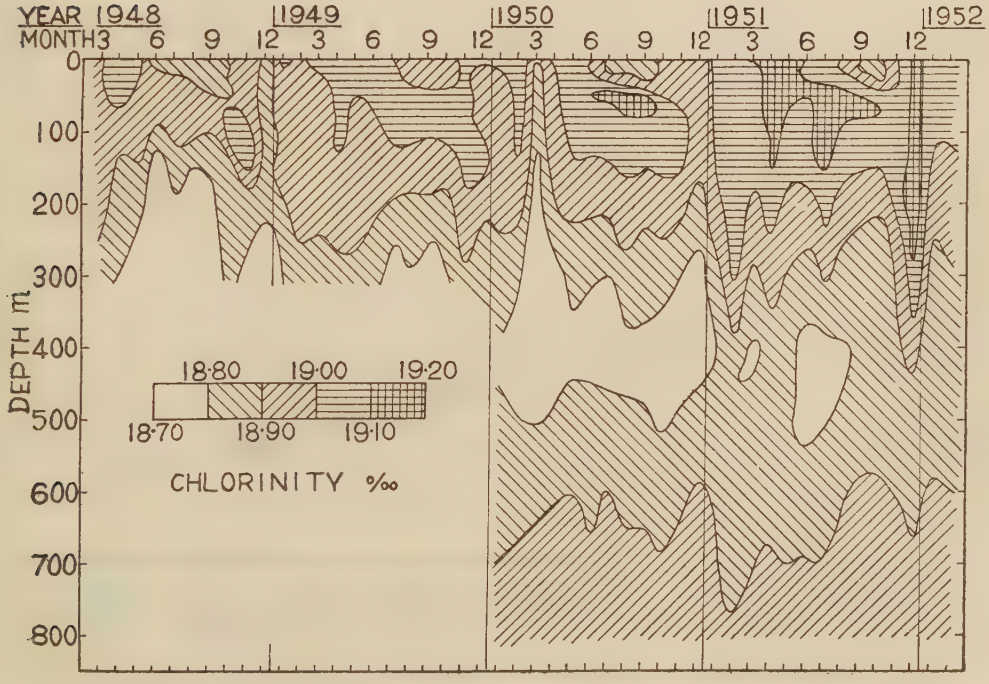

Fig. 4. Isopleth diagram of chlorinity.

volume and colour of the sea have not been determined, owing to the irregular scattering of the points on the F-D and the V-F diagrams. However, correlation coefficients have been computed to be: -0.67 and 0.37 respectively.

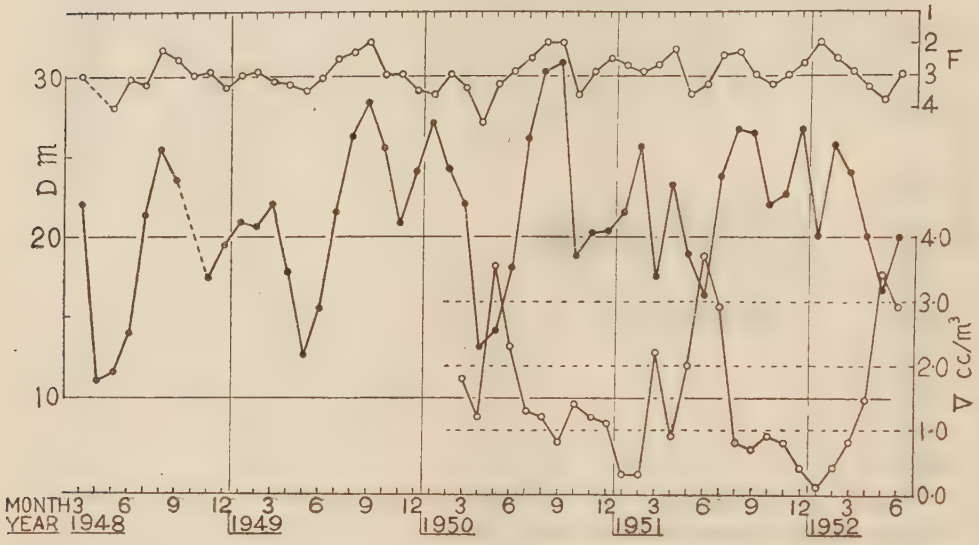

Fig. 5. Variation in colour of the sea (F), transparency (D), and plankton volume (V).

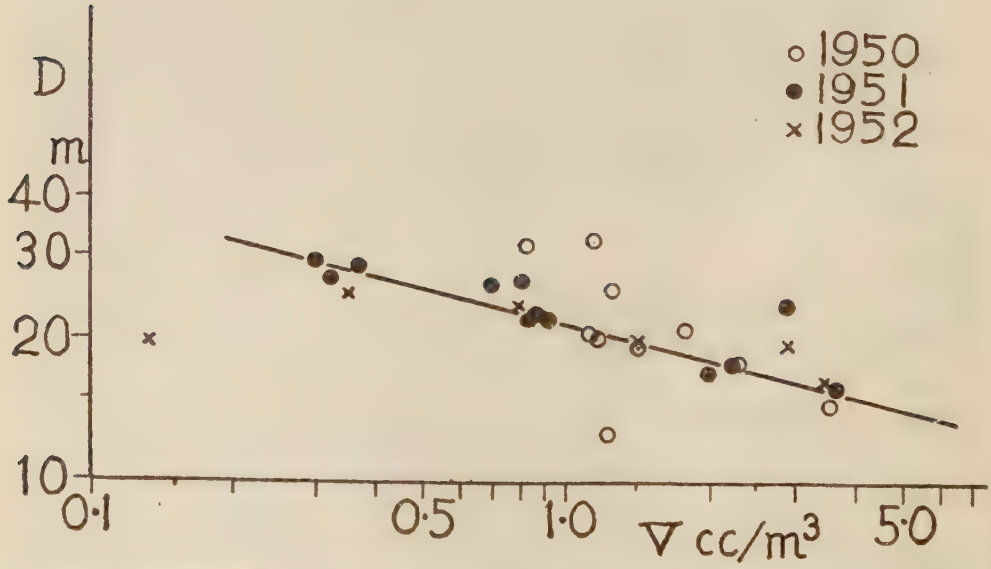

Fig. 6. Relation between transparency (D) and plankton volume (V) shown in logarithmic scale. The straight line represents $D=21.8V^{-0.25}$.

Table 1. Monthly mean values of water temperature at various depths (°C)

Year	Depth (m) \ Month	Jan.	Feb.	Mar.	Apr.	May	Jun.	Jul.	Aug.	Sep.	Oct.	Nov.	Dec.
1948	0	——	——	10.76	12.23	13.25	17.96	20.27	25.23	22.65	19.40	17.72	12.34
	10	——	——	10.84	12.16	13.09	17.44	19.80	24.82	22.15	19.56	17.76	12.46
	25	——	——	10.80	12.05	12.70	15.51	16.50	19.87	21.64	19.60	17.62	12.34
	50	——	——	10.74	11.63	11.83	12.61	13.18	15.50	15.54	18.89	17.31	12.04
	75	——	——	10.70	10.87	11.12	10.74	11.78	13.11	12.84	14.84	16.23	11.84
	100	——	——	10.65	10.17	10.18	10.06	10.54	11.69	10.90	12.92	14.66	11.53
	150	——	——	10.59	8.92	9.18	7.69	9.18	8.98	8.98	11.03	12.32	10.29
	200	——	——	10.03	8.17	8.26	6.93	7.69	7.33	7.70	9.19	10.23	8.34
	300	——	——	8.94	6.60	6.73	——	5.56	4.75	5.50	7.31	6.81	6.13
1949	0	12.98	11.67	10.22	10.94	12.85	16.18	20.34	22.31	23.38	19.58	17.42	15.12
	10	13.28	11.77	10.40	10.92	12.63	16.10	19.84	22.03	22.93	19.66	17.63	15.35
	25	13.20	11.76	10.41	10.88	12.05	15.23	18.26	20.81	22.06	19.61	17.61	15.29
	50	12.99	11.65	10.40	10.80	11.21	12.93	14.66	15.61	16.87	16.05	17.44	15.16
	75	12.78	11.62	10.34	10.52	10.96	11.87	13.02	13.44	13.43	13.32	16.86	15.11
	100	12.50	11.60	10.32	10.52	10.68	11.21	11.98	12.14	12.00	11.98	15.42	14.90
	150	11.72	11.34	10.30	10.12	10.34	10.40	10.75	10.58	10.26	10.09	12.87	11.67
	200	9.82	10.66	10.18	9.47	10.09	9.94	9.51	9.53	9.12	8.68	11.52	9.49
	300	7.62	8.13	8.45	8.09	9.06	8.51	6.75	7.12	6.02	6.31	8.99	6.85
1950	0	11.85	11.84	8.54	11.17	15.23	18.86	22.74	26.22	25.49	19.38	16.68	14.89
	10	11.89	12.02	8.56	11.09	15.09	18.63	22.41	25.82	25.05	19.52	16.72	15.00
	15	11.80	12.02	8.52	10.91	14.91	17.64	19.99	21.98	24.48	19.47	16.68	15.01
	50	11.62	11.96	8.28	10.39	14.17	14.93	14.90	16.47	16.94	18.03	16.56	14.81
	75	11.37	11.95	7.89	9.92	13.28	13.40	13.21	13.97	14.33	14.58	15.55	14.55
	100	11.16	11.91	7.57	9.60	12.34	12.29	12.20	12.85	12.77	13.23	13.77	13.82
	150	10.99	10.99	6.83	9.15	10.86	10.79	10.90	11.18	10.93	11.24	11.30	11.02
	200	10.43	10.76	5.79	8.32	9.51	9.68	9.67	10.02	9.65	9.74	9.59	8.61
	300	8.12	7.97	4.98	6.17	7.00	7.46	7.11	8.12	7.41	7.55	6.55	5.79
	400	5.82	——	4.94	4.88	5.34	5.13	5.47	5.89	5.47	5.71	4.95	4.55
	500	4.76	——	4.01	4.03	4.68	4.67	4.84	4.96	4.77	4.79	4.23	4.32
	600	4.27	——	3.94	4.11	4.30	4.40	4.44	4.57	4.41	4.38	3.96	4.02
	800	3.56	——	3.51	3.52	3.57	3.67	3.71	3.82	3.76	3.86	3.43	3.41
	1000	——	——	3.10	3.03	3.06	3.13	3.13	3.24	3.18	3.28	2.99	2.98
	1500	——	——	2.33	2.34	2.33	2.39	2.34	2.37	2.35	2.44	2.33	2.32
1951	0	12.80	11.65	13.22	14.53	15.35	19.10	21.21	24.28	23.08	19.06	17.89	17.19
	10	12.78	11.90	13.21	14.57	15.25	18.83	21.15	24.05	23.09	19.07	18.01	17.41
	25	12.68	11.92	13.22	14.54	14.89	17.79	20.80	22.24	22.51	19.00	17.99	17.43
	50	12.59	11.92	13.11	14.47	14.13	15.64	18.70	17.13	17.78	16.60	17.61	17.43
	75	12.56	11.92	12.70	14.20	13.58	14.55	17.13	14.74	15.02	14.80	16.88	17.42
	100	12.54	11.94	12.38	13.90	13.08	13.81	16.00	13.49	13.57	13.22	15.33	17.39
	150	11.93	11.88	11.67	13.37	11.60	12.57	14.15	11.52	11.34	11.12	13.17	16.64
	200	10.81	11.76	10.76	12.18	10.50	11.24	12.31	9.84	9.90	9.26	11.53	15.62
	300	8.13	11.17	8.30	9.56	8.83	8.48	9.22	7.33	6.65	6.04	8.73	12.79
	400	5.98	8.77	5.85	7.38	6.70	6.13	6.25	5.41	5.16	4.69	6.54	9.26
	500	5.03	6.51	4.84	5.64	5.07	4.91	4.87	4.49	4.53	4.30	5.04	6.38
	600	4.50	5.41	4.43	4.75	4.42	4.34	4.36	4.19	4.15	3.95	4.33	5.14
	800	3.73	4.17	3.76	3.92	3.68	3.71	3.65	3.64	3.53	3.43	3.61	4.07
	1000	3.15	3.45	3.16	3.29	3.18	3.20	3.13	3.12	3.09	3.00	3.11	3.40
	1500	2.37	2.50	2.40	2.43	2.38	2.39	2.37	2.37	2.35	2.33	2.35	2.52

Table 2. Montnly mean values of chlorinity at various depths (‰)

Year	Depth (m) \ Month	Jan.	Feb.	Mar.	Apr.	May	Jun.	Jul.	Aug.	Sep.	Oct.	Nov.	Dec.
1948	0	——	——	18.99	19.11	19.04	18.82	18.85	18.86	18.86	18.91	18.96	18.88
	10	——	——	19.00	19.06	19.01	18.87	18.83	18.83	18.82	18.89	18.95	18.85
	25	——	——	18.99	19.04	19.00	18.92	18.93	18.86	18.82	18.92	18.94	18.84
	50	——	——	18.97	19.06	18.98	18.94	19.00	18.96	18.90	18.88	18.96	18.81
	75	——	——	18.97	18.99	18.97	18.92	18.98	18.92	18.94	19.07	18.99	18.80
	100	——	——	18.97	18.95	18.96	18.88	18.92	18.91	18.90	19.04	19.04	18.84
	150	——	——	18.96	18.87	18.89	18.72	18.87	18.80	18.82	18.97	19.01	18.89
	200	——	——	18.92	18.84	18.87	18.70	18.79	18.73	18.77	18.90	18.93	18.82
	300	——	——	18.88	18.80	18.78	——	18.72	18.68	18.71	18.84	18.77	18.76
1949	0	19.01	18.99	19.08	19.06	19.07	19.05	19.00	18.94	18.93	18.95	19.04	19.05
	10	19.00	18.97	19.01	19.04	19.00	19.05	19.01	18.91	18.90	18.93	19.00	18.99
	25	18.98	18.97	18.99	19.01	19.00	19.01	19.05	18.95	18.90	18.93	19.00	18.98
	50	18.97	18.97	18.98	19.01	19.00	19.02	19.06	19.05	19.03	19.01	19.01	18.98
	75	18.97	18.96	18.97	19.00	18.98	19.00	19.04	19.05	19.05	19.04	19.01	18.96
	100	18.92	18.97	18.97	19.01	18.97	18.97	19.02	19.02	19.01	19.03	19.05	19.00
	150	18.93	18.96	18.97	18.99	18.96	18.94	18.96	18.95	18.94	18.94	19.05	19.01
	200	18.90	18.94	18.96	18.93	18.95	18.91	18.89	18.88	18.89	18.87	18.99	18.93
	300	18.80	18.87	18.86	18.88	18.88	18.85	18.76	18.79	18.74	18.79	18.87	18.83
1950	0	19.03	19.04	18.91	19.01	19.08	19.00	18.88	18.85	18.81	18.94	19.00	18.94
	10	19.00	19.04	18.88	19.00	19.08	18.99	18.85	18.84	18.80	18.93	18.95	18.93
	25	18.99	19.03	18.87	19.00	19.08	19.03	18.95	18.95	18.87	18.93	18.95	18.92
	50	18.98	19.03	18.86	18.99	19.09	19.10	19.10	19.10	19.10	19.00	18.96	18.90
	75	18.97	19.02	18.84	18.96	19.08	19.08	19.08	19.11	19.10	19.08	19.01	18.90
	100	18.96	19.02	18.82	18.94	19.05	19.04	19.05	19.08	19.07	19.07	19.07	18.92
	150	18.95	18.98	18.78	18.94	18.99	18.98	18.99	19.01	19.00	19.01	19.01	18.92
	200	18.95	18.94	18.72	18.90	18.93	18.93	18.93	18.96	18.95	18.95	18.95	18.86
	300	18.84	18.84	18.72	18.77	18.81	18.82	18.80	18.87	18.83	18.85	18.80	18.75
	400	18.79	——	18.72	18.76	18.79	18.74	18.78	18.78	18.78	18.77	18.77	18.76
	500	18.81	——	18.79	18.81	18.84	18.80	18.83	18.81	18.81	18.78	18.82	18.84
	600	18.86	——	18.87	18.89	18.90	18.87	18.90	18.87	18.87	18.85	18.88	18.91
	800	18.96	——	18.98	18.98	18.98	18.96	18.97	18.97	18.97	18.96	18.98	18.97
	1000	——	——	19.03	19.04	19.03	19.02	19.02	19.02	19.03	19.03	19.04	19.04
	1500	——	——	19.11	19.12	19.10	19.09	19.10	19.10	19.10	19.12	19.13	19.12
1951	0	19.03	19.08	19.11	19.16	19.17	19.09	19.09	18.98	18.90	18.89	18.98	19.15
	10	19.03	19.06	19.09	19.14	19.12	19.08	19.07	18.97	18.89	18.88	18.98	19.14
	25	19.03	19.06	19.09	19.14	19.12	19.09	19.09	19.02	18.92	18.89	18.98	19.13
	50	19.03	19.06	19.09	19.14	19.11	19.10	19.16	19.12	19.10	19.02	19.01	19.13
	75	19.03	19.06	19.07	19.13	19.09	19.09	19.18	19.11	19.11	19.10	19.07	19.14
	100	19.02	19.06	19.06	19.12	19.08	19.07	19.17	19.08	19.08	19.06	19.09	19.13
	150	19.01	19.06	19.03	19.10	19.02	19.02	19.11	19.01	19.01	19.00	19.07	19.18
	200	18.98	19.04	18.98	19.05	18.97	18.97	19.05	18.94	18.95	18.93	19.01	19.17
	300	18.87	19.01	18.88	18.94	18.88	18.85	18.91	18.85	18.82	18.80	18.92	19.08
	400	18.79	18.89	18.79	18.86	18.82	18.77	18.78	18.79	18.81	18.81	18.86	18.94
	500	18.83	18.81	18.82	18.84	18.81	18.78	18.79	18.82	18.84	18.86	18.86	18.84
	600	18.89	18.84	18.87	18.87	18.85	18.83	18.85	18.89	18.91	18.91	18.89	18.85
	800	18.97	18.91	18.96	18.95	18.95	18.92	18.95	18.97	18.99	18.99	18.98	18.94
	1000	19.02	18.99	19.03	19.02	19.01	18.97	19.01	19.03	19.03	19.04	19.03	19.01
	1500	19.10	19.09	19.10	19.11	19.12	19.04	19.09	19.11	19.11	19.12	19.12	19.11

Table 3. Monthly mean values of colour of the sea (*F*: Forel's scale), transparency (*D*: m), and plankton volume (*V*: cc/m³).

Year	Element \ Month	Jan.	Feb.	Mar.	Apr.	May	Jun.	Jul.	Aug.	Sep.	Oct.	Nov.	Dec.
1948	F	—	—	3.0	—	4.0	3.1	3.3	2.2	2 5	3.0	2.9	3.4
	D	—	—	22.0	11.0	11.5	14.0	21 3	25.4	23.5	—	17.4	19.4
	V	—	—	—	—	—	—	—	—	—	—	—	—
1949	F	3.0	2.9	3.2	3.3	3.5	3.1	2 5	2.3	2.0	3.0	3.0	3.5
	D	20.9	20.6	22.0	17.8	12.6	15.5	21.5	26.2	28.3	25.5	20.8	24.0
	V	—	—	—	—	—	—	—	—	—	—	—	—
1950	F	3.6	3.0	3.5	4.7	3.2	3.0	2 5	2.0	2.0	3.9	2.8	2.7
	D	27.0	24.2	21.1	12.8	14.7	18 0	25.6	31.2	30.8	19.4	20.1	20.7
	V	—	—	1.8	1.2	3.5	2.3	1.3	1.2	0.8	1.4	1.2	1.1
1951	F	3.0	2.6	2.7	2.0	4.0	3.5	2.3	2.3	3.0	3.0	3.2	2.6
	D	27.0	29.4	17.8	22.8	17.2	16.0	23 8	26.6	26.4	22.0	22.0	28.8
	V	0 3	0.3	2.2	0.9	2.0	3.7	2 9	0.8	0.7	0.9	0.8	0.4
1952	F	2.0	2.5	2.9	3.4	3.8	3.0						
	D	20.0	25.6	23.9	20.0	16.6	19.9						
	V	0.1	0.4	0.8	1.5	3.4	2.9						

PRINTED BY
KASAI SHUPPAN INSATSUSHA
MINATO-KU, TOKYO, JAPAN
東京都港區芝南佐久間町1－53
笠井出版印刷社印行

NOTES ON THE ECOLOGY OF A PLANKTON COPEPOD, *LABIDOCERA PAVO* GIESBRECHT

S. K. WADA

Oceanographical Laboratory, Meteorological Research Institute, Tokyo.

Reprinted from
Records of Oceanographic works in Japan. vol I, No. 1 (new series), March, 1953

NOTES ON THE ECOLOGY OF A PLANKTON COPEPOD, *LABIDOCERA PAVO* GIESBRECHT

S. K. WADA

Oceanographical Laboratory, Meteorological Research Institute, Tokyo.

Labidocera pavo was first described by Giesbrecht in 1889. The occurrence in the Red Sea and the Indian Ocean of this animal, although of females only, was reported by Giesbrecht (1891), Cleve (1901, 1903) and Thompson and Scott (1903). Males of this copepod were found for the first time by Sewell (1914) in the Gulf of Mannar, Ceylon. More recently, Mori (1932) found one male in a collection made in the vicinity of the Tokara Islands in the Eastern China Sea, and described the male as new to science. The occurrence of the copepod in the Yellow Sea was also reported by Mori in 1937.

This crustacean has been generally regarded as an oceanic warm water species, occurring rather sparsely; especially, the males have been supposed to be extremely rare. In the summer of 1936, swarms of *L. pavo* were observed at the pier of the Misaki Marine Biological Station, which is situated at the mouth of a small inlet on the eastern coast of Sagami Bay. The waters off the Station are under the alternate or mixed influences of warm oceanic current and neritic water from Tokyo Bay, the oceanic water rather predominating.

Between 1936 and 1952, swarms of the copepod have been observed at a definite season every year; observation was not made in 1945 because of military restrictions. The swarm can easily be recognized by the blue color of the animal. Swarms appear first in the middle of August, and the absence of the animal in the inshore water is generally affirmed for the first time after stormy weather in the middle of October. During this period, the presence of the swarm is always observable; at flood tides, the animals are observed jerking to and fro at the surface of water, sometimes jumping into the air; at ebb tides, the copepods are found swarming near the bottom.

The crustaceans appear in such abundance that they make excellent food for small fishes in the Aquarium of the Biological Station. Hundreds of grams of the copepods can readily be collected by one or two hauls of a small hand net.

Since 1948, daily observations of the water temperature have been made at the pier of the Station. Weekly averages of the temperature during the months from August to October were found to drop from 28° to 20° C. The chlorinity of the water at a station 50 m off the pier during these months, as observed in 1943, gave values of between 17.5‰ and 18.6‰ for the surface, and between 18.2‰ and 18.7‰ for the bottom water (5 m deep).

Swarms of *Labidocera* are found to be composed of adult female and male animals, as well as of various stages of copepodids. Almost all of the adult females are observed to be carrying a spermatophore on the ventral side of their abdominal segments. Adult males can readily be distinguished from the females by various characteristics: smaller size of the body, shape of the abdominal segments, geniculated right first antenna, stoutly modified fifth pair of legs, etc. The body length of the adult female is 2.2–2.3 mm, while that of the adult male is 1.7–1.8 mm (ten measurements each). Sewell (1914) reported that the total length of the adult male was 2.2 mm; the male animal collected by Mori (1932) was about 1.94 mm long.

At night a great many of the animals gather around an electric light. The common copepod animals in the collection, other than *Labidocera*, are usually *Acartia clausi* and a new species of *Tortanus*, both of which are naturally neritic inhabitants.

An aliquot sample of a collection made at night on September 22, 1950 was found to consist of 133 adult females, 304 adult males and 23 juvenile forms. The sex-ratio in adult animals was 1 to 2.3, with the males predominating considerably. All of the juvenile forms were found to be at a rather late stage (Stage V) of copepodid. All of the adult females were also found to be bearing spermatophores. This, of course, indicates the completion of copulation. Eggs which are believed to belong to this species were also found. Nauplius larvae were present in the collection, although, at present, species identification for these forms is difficult. Judging from these facts, it is highly probable that reproduction takes place during the swarming in coastal water.

An aliquot sample of another collection which was made in the daytime on September 1, 1944 was found to contain 119 adult females, 34 adult males and 121 juvenile forms. All of the adult females were carrying spermatophores; the juvenile forms, which constitute 44% of the whole population, consisted of various stages of copepodids, whose body lengths varied from 0.8 mm to 1.7 mm. The sex ratio, female to male, in adult animals was 3.5 to 1.

Judging by the above facts, it is postulated that swarms which are at first com-

posed of adult and copepodid forms develop and breed in inshore waters, dying away after the accomplishment of reproduction. Johnson (1935) reports that *L. jollae* and *L. trispinosa* reproduce during the summer and autumn in southern California waters.

At any rate, the two-months' sojourn in the coastal water of swarms of *Labidocera pavo* is one of the most outstanding events on the plankton calender in the neighboring waters of the Misaki Marine Biological Station. According to Dr. Y. Ohshima (verbal communication), swarms of copepods of this species were also observed in shallow waters in June and July of 1938 and 1939 at a point (Ikawazu) of the eastern coast of Atsumi Bay, about 180 nautical miles west from the Misaki Station. In this case, however, the swarm was found to consist of females alone.

In this connection, it should be noted that offshore planktonological observations which were performed at upper layers in, and in waters adjacent to Sagami Bay have failed to reveal the presence of any forms of this copepod. (Honjo, 1952; Central Meteorogical Observatory, 1951 a, b, c).

The writer is deeply indebted to the director of the Misaki Marine Biological Station, for the use of laboratory facilities, and to Dr. Jean C. Dan, for her kind guidance in the preparation of the manuscript.

Summary

Labidocera pavo makes its annual appearance in swarms in the coastal water around the Misaki Marine Biological Station. Swarms were observable for two months from the middle of August. Males of this species, which have hereto fore been considered rare, have been commonly found, sometimes exceeding the females in number. The copepods reproduce during their sojourn in the inshore waters.

References

Central Meteorological Observatory of Japan, 1951. The results of marine meteorological and oceanographical observations, No. 3; No. 5; No. 6.
Cleve, P. T. 1901. K. Sv. Vet. Ak. Handl., **35** (5).
—— 1903. Arkiv Zool., **1**; 327.
Giesbrecht, W. 1889. Atti Acad. Lincei. Roma (4) Rend., **5**.
—— 1891. Ibid., **7**.
Honjo, K. 1952. Journ. Oceanogr. Soc. Japan, **7** (3/4): 77.
Johnson, M. W. 1935. Biol. Bull., **68** (3): 397.
Mori, T. 1932. Zool. Magazine (Tokyo), **44** (523): 167.
—— 1937. The pelagic copepoda from the neighbouring waters of Japan. Tokyo.
Sewell, R. B. S. 1914. Spolia Zeylanica, **9** (35): 191.
Thompson J. C., and A. Scott. 1903. Ceylon Pearl Oyster Fisheries and Marine Biology, Pt. 1, Suppl. Rep. No. 7: 227.

PRINTED BY
KASAI SHUPPAN INSATSUSHA
MINATO-KU, TOKYO, JAPAN
東京都港區芝南佐久間町1－53
笠井出版印刷社印行

On the Cauchy-Poisson Waves Caused by the Eruption of a Submarine Volcano. (2nd paper)*

By Sanae UNOKI

Oceanographical Section, C.M.O., Tokyo

and Masito NAKANO

Oceanographical Laboratory, Meteorological Research Institute, Tokyo

Abstract:

We solved the Cauchy-Poisson wave problem in two horizontal dimensions for the case when an initial impulse or initial elevation is given to a finite area of the sea surface, considering the effect of a frictional force on the wave motion, and could show more precisely than in the case of one dimension that the Cauchy-Poisson wave can actually exist in the ocean with its form almost the same as the theory demands. Moreover, we could estimate an admissible value of initial disturbance and its energy from the comparison of the theory with observations.

§ 1. *Preface*

On the 16th, 24th, and 26th of September, 1952, peculiar tsunami waves were recorded by the wave gauge installed on Hachijo Island about 130 km distant to the north of Myojinsho Reef, where vigorous eruptions of a submarine volcano had been frequently recognized since the middle of September. In order to understand these waves, in our first paper[1] we discussed the Cauchy-Poisson wave problem for the case when an initial impulse and initial elevation acted upon the sea surface of limited area at the moment of explosion of a submarine volcano, and it was ascertained that these tsunami waves are really nothing but the Cauchy-Poisson waves. The agreement between the theory and observations was considerably satisfying in the period, variation of wave height with time and interference phenomenon. And it has become possible to know the scale and magnitude of initial local disturbance, by knowing the maximum wave height and the time when the node of a beat occurred.

However, as our theory treated a one-dimensional problem, the intensity and scale of initial disturbance obtained in the first paper are considered to be of the values pretty smaller than the values in the actual case of two dimensions. Moreover, in the first paper, the effect of friction was considered to be small in our

* This investigation has been carried out as a part of the "Microseism and Ocean Wave Research Project" of C.M.O. during 1951~1953.

case when the waves have the period of nearly one minute, and accordingly it was neglected. But this circumstance is not always existing, especialy not when the period becomes smaller. Hence, in the present paper, we shall discuss a Cauchy-Poisson wave problem in two dimensions, considering a frictional force acting on water particles.

Moreover, at this chance we shall again tell the explosion at 13h 40m on the 23rd of Sept. 1952 more precisely. According to what was said in the first paper, a disagreement with regard to the height of a water dome which occurred at the moment of that explosion was found between reports made by some of the members of the investigation party for Myojinsho. This question, however, has been dispelled by the recent reports made by Dr. H. Niino[2], where he says "as soon as the water surface which had been even till that time began to swell, it heaved up suddenly to a water dome whose dimension was about 5m high and 200m wide, and instantly it collapsed down in torrent. At this moment, the central part of the water dome began to boil up violently and its height became about 30m. In the mean time, another kind of blackish brown block erupted on the right of the water block and this and that blocks amalgamated at once. After that, from the middle of them, great amount of lava rushed up in the air with violent speed. These phenomena seemed to have occurred within 10sec only. — Moreover, immediately after the explosion, the complicated noises were heard and vibrations of the air felt, but the underwater shock which acted on the body of the ship was not felt so violently. — At the time about seven minutes later, the ship was suddenly joggled on the way going back at full speed in order to avoid the attacks of pumice stones and other eruptives, and instantly we could recognize abnormal waves, whose height was about 2m and whose length about 50m. They came several times, but the period was not observed carelessly." Moreover, according to him, the diameter of the crater of the volcano seemed to be 600～1000m. Consequently, it is seen that the water dome, whose height was said to be 50～60m by Dr. Kumagori and Dr. Tsuya in our first paper, is not the same one, which was said by Dr. Niino to be 5m high and had been found just at the moment of explosion. The former dome means what was observed a while later and may be a kind of columns of water and spray, which were spouting in the air.

§ 2. *Cauchy-Poisson wave problems in two dimensions*

The classical problem of ring wave produced in deep water by a local disturbance of the free surface was investigated by Cauchy and Poisson. H.

Lamb[3] completed the theory of wave propagation in two horizontal dimensions (and in one dimension too) when the initial disturbance is concentrated in the immediate neighbourhood of a point, assuming that Fourier's double integral theorem can be applied to such a case. Moreover, in another report[4], he dealt with some problems where the origin of disturbance lies beneath the water surface and its strength varies with time according to a prescribed law. Though the latter problems were suggested by a study of the phenomena of a submarine eruption, in the present paper we do not consider such problems, because the results have only a restricted application to our problems.

Dr. K. Terazawa[5] discussed a wave problem, especially the oscillations at the center of the disturbance, in the case when the initial disturbance is spread over a certain extent of the free surface in two horizontal dimensions. He dealt with the problems where the initial disturbances are given by

$$f(\tilde{\omega})=-A\cos m\theta/\tilde{\omega},\ A\cos m\theta/\sqrt{b^2+\tilde{\omega}^2}\ \text{and}\ Ab\cos m\theta/(b^2+\tilde{\omega}^2)^{3/2}$$

respectively. These assumptions of initial disturbance, however, are insufficient for our purpose. In the same paper, he also proposed to treat the case in which the initial disturbance source is situated at a finite depth from the free surface.

Now, we shall solve the problems where the initial disturbance of the free surface is spread over a limited area in two horizontal dimensions with a constant strength, taking account of a frictional force which acts on water particles. As such a frictional force, must be considered the eddy viscosity and the resistance of the air, in general. But it will be greatly difficult to consider their effects strictly.

However, since the wave length is very large and its steepness is very small in our case, the effect of friction of the air may be neglected. On the other hand, concerning the action of the eddy viscosity, S. Unoki[6], one of the present authors, showed that all the water particles on a vertical section to the direction of the propagation of a wave with long period are apt to get uniform resistance even when the eddy viscosity is considered, and he concluded that we may as the simplest form of resistance take up the frictional force proportional to the velocity of fluid particles, instead of the eddy viscosity. On the basis of this assumption, he could explain successfully the decrease of height of a wave, which was found by M. Nakano[7], one of the present authors, from the mareograms obtained in the case when a conspicuous cyclone passes through south of Honshu, Japan, and whose period is about 1~3 min.

The period of waves of our consideration caused by the eruption of a sub-

marine volcano is also 95~30 sec, and is near what was found by Nakano. Accordingly, it may be assumable in our case also that the frictional force proportional to the velocity of fluid particles is acting, instead of the eddy viscosity.

If the axes of x,y are taken on the undisturbed surface, and the axis of z is drawn vertically upwards, the components of force are given by

$$X=-2\mu u, \quad Y=-2\mu v, \quad Z=-g-2\mu w$$

respectively, where 2μ is the proportional coefficient of friction and $2\mu=5.5\times10^{-4}$ $\sec^{-1}$ according to Unoki[6]. Then, using Lamb's notations[3], we find

$$\frac{p}{\rho}=\frac{\partial\phi}{\partial t}-gz+2\mu\phi-\frac{1}{2}q^2+F(t)$$

as the pressure-equation. Hence, if ζ denotes the elevation of the surface, we shall have

$$\zeta=\frac{1}{g}\left[\frac{\partial\phi}{\partial t}+2\mu\phi\right]_{z=0} \tag{1}$$

as a condition which must be satisfied at the free surface, provided q^2 is neglected, and $F(t)$ and the additive constant are supposed to be merged in $\partial\phi/\partial t$. The kinematical condition on the surface is

$$\frac{\partial\zeta}{\partial t}=-\left[\frac{\partial\phi}{\partial z}\right]_{z=0}. \tag{2}$$

Accordingly, for $z=0$, we must have

$$\frac{\partial^2\phi}{\partial t^2}+2\mu\frac{\partial\phi}{\partial t}+g\frac{\partial\phi}{\partial z}=0 \tag{3}$$

from (1) and (2).

On the other hand, if we assume the motion to be of symmetry about an axis (0_z) and use the cylindrical co-ordinates z,ϖ, the continuity-equation is given by

$$\frac{\partial^2\phi}{\partial z^2}+\frac{\partial^2\phi}{\partial\varpi^2}+\frac{1}{\varpi}\frac{\partial\phi}{\partial\varpi}=0. \tag{4}$$

§3 : 1. *The case of initial impulse*

First, let us consider the wave caused by an initial local impulse, following Lamb's method[3], and especially we need the solution at a distant place from the source of initial disturbance. If the initial conditions are supposed to be

$$\left.\begin{array}{ll}\text{elevation :} & \zeta=0\\ \text{impulse :} & \rho\phi_0=F(\tilde{\omega})\end{array}\right\} \quad \text{at} \quad t=0 \quad \text{and} \quad z=0\,, \tag{5}$$

the solution which satisfies (3), (4) and (5) is given by

$$\phi_t=-\frac{e^{-\mu t}}{\rho}\int_0^\infty\left(\cos\sigma t-\frac{\mu}{\sigma}\sin\sigma t\right)e^{kz}J_0(k\tilde{\omega})\,kdk\int_0^\infty F(\alpha)\cdot J_0(k\alpha)\alpha d\alpha \tag{6}$$

$$\zeta_t=-\frac{e^{-\mu t}}{g\rho}\int_0^\infty\frac{\sigma^2+\mu^2}{\sigma}\sin\sigma t J_0(k\tilde{\omega})kdk\int_0^\infty F(\alpha)\cdot J_0(k\alpha)\alpha d\alpha\,, \tag{7}$$

when the depth to the bottom is very large. Moreover, in (6) and (7), there must exist such a relation as .

$$\sigma^2+\mu^2=gk\,. \tag{8}$$

If the intensity of the initial impulse is constant in a limited extent, then assuming, instead of $F(\tilde{\omega})$ in (5),

$$\rho\phi_0=P\ (\tilde{\omega}\leqq l)^*\,, \qquad \rho\phi_0=0\ (\tilde{\omega}>l) \tag{9}$$

we have

$$\zeta_t=-\frac{Pe^{-\mu t}}{g\rho}\int_0^\infty\frac{\sigma^2+\mu^2}{\sigma}\sin\sigma t\cdot J_0(k\tilde{\omega})kdk\int_0^l J_0(k\alpha)\alpha d\alpha$$

$$=-\frac{Ple^{-\mu t}}{\rho}\int_0^\infty\frac{k}{\sigma}\sin\sigma t\cdot J_0(k\tilde{\omega})\cdot J_1(kl)dk\,.$$

Since $$J_0(k\tilde{\omega})\fallingdotseq(2/\pi k\tilde{\omega})^{1/2}\cdot\sin(k\tilde{\omega}+\tfrac{1}{4}\pi)$$

in the case when $k\tilde{\omega}$ is large, it is

$$\zeta_t=-\frac{2^{1/2}Pl\,e^{-\mu t}}{\pi^{1/2}\rho\tilde{\omega}^{1/2}}\int_0^\infty\frac{k^{1/2}}{\sigma}\sin\sigma t\cdot\sin\left(k\tilde{\omega}+\frac{1}{4}\pi\right)\cdot J_1(kl)dk$$

$$=-\frac{2^{1/2}\pi^{1/2}Pl}{\rho\tilde{\omega}^{1/2}}e^{-\mu t}\cdot\Re\left[-\frac{1}{2\pi}\int_0^\infty\frac{k^{1/2}}{\sigma}e^{i(\sigma t-k\tilde{\omega}-\frac{1}{4}\pi)}J_1(kl)dk\right.$$

$$\left.-\frac{1}{2\pi}\int_0^\infty\frac{k^{1/2}}{\sigma}e^{i(\sigma t+k\tilde{\omega}+\frac{1}{4}\pi)}J_1(kl)dk\right]. \tag{10}$$

As it is seen in (10) that the circular functions go through a large number of periods within the range of integration, while $(k^{1/2}/\sigma)J_1(kl)$ changes comparatively slowly, Kelvin's method[8] as to the principle of stationary phase can be applied to. In this case, the integration of the second term in (10) vanishes. Accordingly,

* Strictly speaking, we must have $\rho\phi_0=P/2$ at $\tilde{\omega}=l$.

the elevation to be obtained is given by

$$\zeta_i=-\frac{2^{1/2}\pi^{1/2}Pl}{\rho\tilde{\omega}^{1/2}}\cdot e^{-\mu t}\cdot\frac{k^{1/2}}{\sigma}\cdot\frac{J_1(kl)}{\sqrt{2\pi t|d^2\sigma/dk^2|}}\cdot\cos\left(\sigma t-k\tilde{\omega}-\frac{1}{4}\pi-\frac{1}{4}\pi\right), \tag{11}$$

where k and σ should be determined by

$$\frac{d}{dk}\left(\sigma t-k\tilde{\omega}-\frac{1}{4}\pi\right)=0. \tag{12}$$

Considering (8) and (12), we have easily

$$\sigma=\frac{gt}{2\tilde{\omega}}, \quad k=\frac{1}{g}\left(\frac{g^2t^2}{4\tilde{\omega}^2}+\mu^2\right); \quad \frac{d\sigma}{dk}=\frac{\tilde{\omega}}{t}, \quad \frac{d^2\sigma}{dk^2}=-\frac{2\tilde{\omega}^3}{gt^3}. \tag{13}$$

Hence, substituting (13) for (11), it is

$$\zeta_i=-\frac{2^{1/2}Pl\,e^{-\mu t}}{\rho g\tilde{\omega}}\left(\frac{g^2t^2}{4\tilde{\omega}^2}+\mu^2\right)^{1/2}\cdot\sin\left(\frac{gt^2}{4\tilde{\omega}}-\frac{\tilde{\omega}\mu^2}{g}\right)\cdot J_1\left(\frac{gt^2}{4\tilde{\omega}}\cdot\frac{l}{\tilde{\omega}}+\frac{l\mu^2}{g}\right). \tag{14}$$

In our case, since it is $g^2t^2/4\tilde{\omega}^2\gg\mu^2$, (14) becomes

$$\zeta_i=-\frac{Plt}{2^{1/2}\rho\tilde{\omega}^2}e^{-\mu t}\cdot\sin\left(\frac{gt^2}{4\tilde{\omega}}\right)\cdot J_1\left(\frac{gt^2}{4\tilde{\omega}}\cdot\frac{l}{\tilde{\omega}}\right) \tag{15}$$

approximately, and this is the solution which we have searched for. If the initial impulse is concentrated in the immediate neighbourhood of the origin, as was assumed by H. Lamb, it must be satisfied that

$$\lim_{t\to 0}\int_0^\infty F(\alpha)2\pi\alpha d\alpha=\lim_{t\to 0}\pi l^2\cdot P=1,$$

in (15). Hence, neglecting the frictional force ($2\mu=0$) and considering $J_1(\theta)\fallingdotseq\theta/2$ in case of $\theta\ll 1$, (15) becomes

$$\zeta_i\sim-\frac{gt^3}{2^{7/2}\pi\rho\tilde{\omega}^4}\cdot\sin\frac{gt^2}{4\tilde{\omega}}, \tag{16}$$

which just accords with what Lamb[3] obtained. Especially, if $gt^2l/4\tilde{\omega}^2$ is also large, we have

$$\zeta_i=-\frac{2Pl^{1/2}}{\pi^{1/2}\rho g^{1/2}\tilde{\omega}}e^{-\mu t}\cdot\sin\frac{gt^2}{4\tilde{\omega}}\cdot\sin\left(\frac{gt^2}{4\tilde{\omega}}\cdot\frac{l}{\tilde{\omega}}-\frac{1}{4}\pi\right) \tag{17}$$

from (15). But hereafter we shall discuss the solution (15) chiefly.

The node of "beats" shown in (15) is determined by

$$J_1\left(\frac{gt^2}{4\tilde{\omega}}\cdot\frac{l}{\tilde{\omega}}\right)=0 \tag{18}$$

and the period of individual waves is for $\sin(gt^2/4\tilde{\omega})$

$$\tau=\frac{4\pi\tilde{\omega}}{gt}\ . \tag{19}$$

An example of numerical calculation of (15) is shown in Fig. 1. D. In Fig. 1. E is shown also the elevation when the frictional force is neglected, i.e., when we put $\mu=0$ in (15).

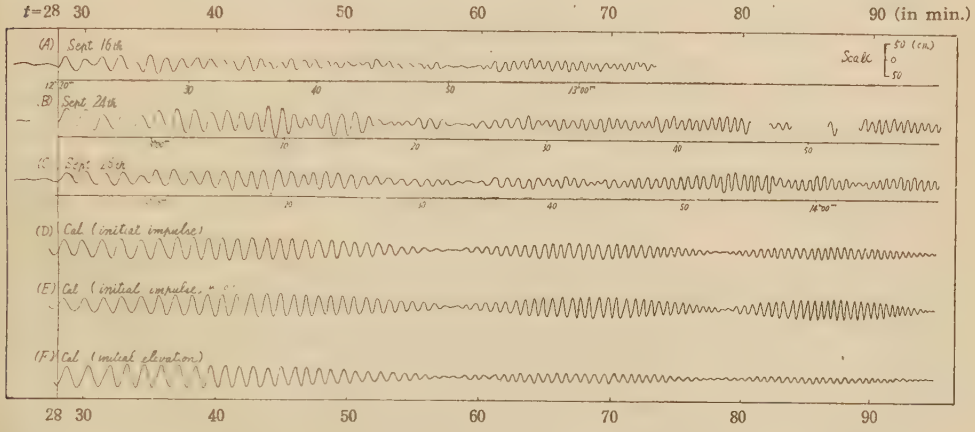
t=28 30 40 50 60 70 80 90 (in min.)
(A) Sept. 16th.
Scale
(B) Sept. 24th.
(C) Sept. 25th.
(D) Cal. (initial impulse)
(E) Cal. (initial impulse, μ=0)
(F) Cal. (initial elevation)
28 30 40 50 60 70 80 90

Fig. 1. (A), (B) and (C) are tsunami waves obtained by smoothing actual wave records in order to eliminate wind waves and swells. (D) shows the theoretical elevation caused by initial impulse and was calculated from Eq. (15); (E) was obtained by putting $\mu=0$ in Eq. (15). (F) shows the theoretical elevation caused by initial elevation and was calculated from Eq. (24).

§ 3 : 2. *The case of initial elevation*

In the case of an initial elevation applied to an undisturbed surface, with the initial conditions such as

$$\left.\begin{array}{ll}\text{elevation}: & \zeta=f(x)\\ \text{impulse}: & \rho\phi_0=0\end{array}\right\}\quad \text{at}\quad t=0\quad\text{and}\quad z=0\,, \tag{20}$$

the solution which satisfies (3) and (4) is easily seen to be

$$\phi_e=ge^{-\mu t}\int_0^\infty\frac{\sin\sigma t}{\sigma}e^{kz}J_0(k\tilde{\omega})kdk\int_0^\infty f(\alpha)J_0(k\alpha)\alpha d\alpha\ , \tag{21}$$

$$\zeta_e=e^{-\mu t}\int_0^\infty\left(\frac{\mu}{\sigma}\sin\sigma t+\cos\sigma t\right)J_0(k\tilde{\omega})kdk\int_0^\infty f(\alpha)J_0(k\alpha)\alpha d\alpha\ . \tag{22}$$

If the initial elevation whose height is uniform over the sea area of finite extent is given at the time $t=0$, then assuming

$$\zeta=Q\ (\tilde{\omega}\leqq L)\,,\qquad \zeta=0\ (\tilde{\omega}>L)\,, \tag{23}$$

we have from (22)

$$\zeta_e=\frac{2^{1/2}QL}{\tilde{\omega}}e^{-\mu t}\cos\left(\frac{gt^2}{4\tilde{\omega}}\right)\cdot J_1\left(\frac{gt^2}{4\tilde{\omega}}\cdot\frac{L}{\tilde{\omega}}\right) \tag{24}$$

approximately, by using Kelvin's method as well as in the case of initial impulse. In particular, for a concentrated elevation at the origin such that

$$\lim_{L\to 0}\int_0^\infty f(\alpha)2\pi\alpha d\alpha=\lim_{L\to 0}\pi L^2Q=1\,, \tag{25}$$

we have, neglecting the frictional force in (24),

$$\zeta_e\sim\frac{gt^2}{2^{5/2}\pi\tilde{\omega}^3}\cos\frac{gt^2}{4\tilde{\omega}}\,, \tag{26}$$

which is the same with what Cauchy and Poisson obtained. In the case of initial elevation also, the node of (24) which means an interference wave form is determined by (18) and the period of individual waves is given by (19), as well as in the case of initial impulse. This is shown in Fig. 1. F.

In the above discussions, in order to avoid mathematical difficulties, we have assumed the depth of the sea to be infinitely deep. Fortunately, as was stated in the first paper, the travel time of a deep water wave progressing with group velocity from Myojinsho Reef to the wave recorder is very near the value of actual travel time of tsunami waves caused by the eruption of a submarine volcano, and this fact suggests that we can assume the wave to be a deep water one as was done above.

§ 4. *Discussions*

Comparing the solution (15) and (24) obtained by us with the solution (16) and (26) obtained by Lamb respectively, it is seen that we have in (15) and (24) such new factors as $e^{-\mu t}$ and $J_1(gt^2/4\tilde{\omega}\cdot l/\tilde{\omega})$. The former factor means the effect of frictional force and the latter the beat-phenomenon caused by interference of the waves generating from various parts of the initial disturbance of finite area.

The period of individual waves is given by

$$\tau=\frac{4\pi\tilde{\omega}}{gt}\,, \tag{19}$$

which is quite the same with the formula obtained in the case of one dimension

when l or $L \ll \tilde{\omega}$. Accordingly, as stated in the first paper, it is concluded that, in the case of two dimensions also, the agreement between the theory and observations is excellent in the period and variation of it with time. The period of interference wave form is about $(\tilde{\omega}/l)$ times as large as that of individual waves.

First, we shall take up the case of initial impulse. Considering (18), the first node of wave groups will be seen for

$$\frac{gt_0^2 l}{4\tilde{\omega}^2} = 3.832.$$

Since $\tilde{\omega} = 130$ km and $t_0 = 58$ min in actual cases, we have $l = 2.2$ km, after all; that is, the initial impulse has acted on the surface area whose radius is about 2.2 km. Similarly, we have also $L = 2.2$ km in the case of initial elevation. On the other hand, we have obtained l(or L) $= 1.8$ km in the case of one dimension, as stated in the first paper.

Considering the observations made on the 23rd of September, the value l(or L) obtained here seems to be somewhat larger than what is generally conceived, especially it is so in the case of initial elevation. However, according to some reasons stated in the first paper, this value seems to be not so unreasonable in the case of inital impulse.

Now, putting l(or L) $= 2.2$ km, the results of numerical calculation of the equations (15) and (24) are shown in Fig. 1. D and F respectively. For the purpose of reference, the theoretical elevation when $\mu = 0$ in (15) is also shown in Fig. 1. E. Comparison of these theoretical curves with the observed wave records A, B and C of Fig. 1 shows an accordance in the aspect of variation of wave, especially the accordance is excellent in the first stage from the beginning ($t = 28$ min) to the first node ($t = 58$ min). However, paying attention to the mode of decrease of wave height with time, it is distinctly recognized that the curve D in case of initial impulse is more consistent with observed ones than the curve F in case of initial elevation, because the decrease of F with time is too rapid. Therefore, it may be considered that, for the generation of our waves the action of initial impulse was more effective than that of initial elevation in all cases on the 16th, 24th and 26th.

On the other hand, the distribution of waves with the distance from the disturbing source is shown in Fig. 2. A and B. The interval between two successive nodes of beat becomes longer with larger distance, as well as that of individual waves, i.e. wave length which is given by

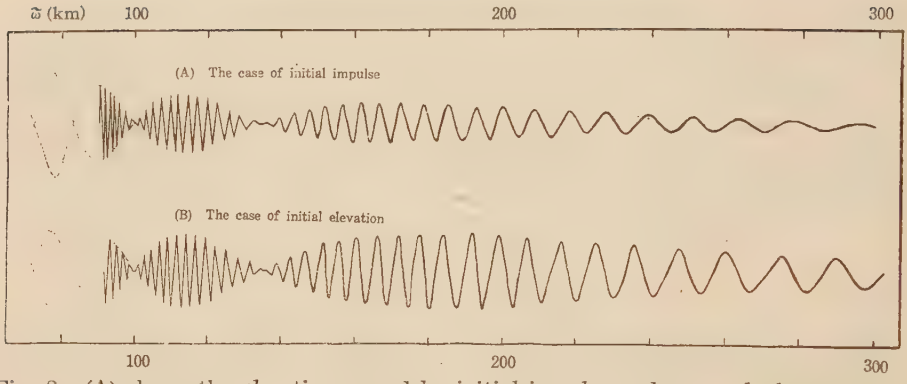

Fig. 2. (A) shows the elevation caused by initial impulse and was calculated by Eq. (15); (B) the elevation caused by initial elevation and was calculated by Eq. (24); case when l(or L)=2.2 km and t=60 min.

$$\lambda=\frac{8\pi\tilde{\omega}^2}{gt^2}\,.$$

Hence, it is important that the decrease of wave height with distance is more rapid in the case of initial impulse than in the case of initial elevation as shown in Fig. 2, conversely the decrease of wave height with time is more rapid in the latter case than in the former as shown in Fig. 1.

Next, the intensity P of initial impulse per unit area and the height Q of initial elevation are obtained by

$$P=\frac{\rho\tilde{\omega}^2H_{\max}}{2^{1/2}l[te^{-\mu t}J_1(gt^2/4\tilde{\omega}\cdot l/\tilde{\omega})]_{\max}}\,, \tag{27}$$

$$Q=\frac{\tilde{\omega}H_{\max}}{2^{3/2}L[e^{-\mu t}J_1(gt^2/4\tilde{\omega}\cdot L/\tilde{\omega})]_{\max}} \tag{28}$$

from (15) and (24) respectively, where $H_{\max}=2\zeta_{\max}$.

In calculating P or Q, it should be considered that (27) or (28) was obtained by assuming the sea to be uniform and the motion of wave to be of symmetry about the axis of z; accordingly, for $H_{\max}$ in (27) and (28) we should substitute the corrected value of observed maximum wave height. This coefficient of correction K will be due to the convergence of orthogonal lines in a refraction diagram and the non-uniformity of the depth.

Assuming that the energy contained between two orthogonal lines is kept constant, as well as the assumption in the case of surf forecasting[9], the coefficient of correction due to the convergence of orthogonal lines is given by $\sqrt{\widehat{CD}/\widehat{AB}}$ in

Fig. 3, that is, square root of the ratio of the interval $\widehat{CD}$ between two actual orthogonals in the vicinity of a wave station W to the interval $\widehat{AB}$ between two imaginary orthogonals obtained by assuming that the wave would not be refracted. Referring to the refraction diagram shown in Fig. 4 of the first paper, this coefficient seems to be about 1/3 for our waves.

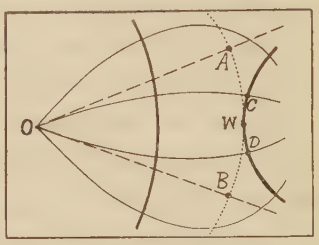

Fig. 3.
wave crests
actual orthogonals
imaginary orthogonals

And, the coefficient of correction due to the non-uniformity of the depth to the bottom will be given by the application of Green's formula[10], which shows that the elevation varies inversely proportional to 1/4 root of the depth of the place when the sea is shallow and the variation of depth is small. From the contours of depth shown in Fig. 4 of the first paper, it seems to be about 1/2.

Accordingly, the coefficient of correction K which has been searched for becomes about $1/3\times 1/2=1/6$. However, owing to the unsatisfactory assumptions and the unavoidable uncertainty produced in making use of the refraction diagram, this value is not so decisive, and may be to be revised. But in this place we dare to use this value of K owing to unavoidable circumstances. Thus, $1/6\times$ (actual maximum wave height) means the maximum wave height which will be found at the wave station when the wave travels over the sea of deep and uniform depth without refraction. Substituting it for $H_{\max}$ in (27) and (28), calculated values of P and Q are represented in Table 1, where we put l (or L)$=2.2$ km, $\tilde{\omega}=130$ km, $[e^{-\mu t}J_1(gt^2/4\tilde{\omega}\cdot L/\tilde{\omega})]_{\max}=0.31$ and $[te^{-\mu t}J_1(gt^2/4\tilde{\omega}\cdot l/\tilde{\omega})]_{\max}=7.2\times 10^2$. And it should be borne in mind that P and Q were obtained under the assumption that the initial impulse or initial elevation acted on the water surface independently, but not simultaneously.

Table 1

Sept. 1952	A (16th)	B (24th)	C (26th)
H*(cm)	56	92	71
P (dyne·sec/cm^2)	7.0×10^6	11.6×10^6	8.9×10^6
Q (m)	6.3	10.3	8.0
E (erg)	3.0×10^{19}	7.9×10^{19}	4.8×10^{19}

* observed maximum wave height

In Table 1, the calculated height of initial elevation is near the observed height 5 m of the water dome on the 23rd stated in § 1, but the radius of the area which was occupied by initial elevation is likely to be rather large.

On the other hand, according to the report[11] with regard to the causes of the disaster of the "Kaiyo-maru No. 5", it has been said that the sinking of the ship is possible if the pressure of the magnitude 10 kg/cm^2($\fallingdotseq 10^7$ dyne/cm^2) acts on the body of the vessel in the interval of 1/100 sec. Consequently, the values of P obtained by us will not necessarily be quite unreasonable, because each of them is powerful enough to cause the sinking.

Moreover, it will be interesting to know the total energy of wave motion. In the case of initial elevation, the total energy of all wave motions is equal to the potential energy of initial column of water, whose height is Q and whose radius of the base is L. Consequently it is given by

$$E=\tfrac{1}{2}\rho\pi g L^2 Q^2 ,$$

and the calculated values are shown also in Table 1. According to the report[12] as to the explosion of an atomic bomb at Bikini Atoll, the total energy of waves generated by this explosion has been $2.6\times10^{18}\sim3.4\times10^{18}$ erg. However, since the waves of our consideration due to volcanic explosion of larger scale reached farther, it is never unreasonable to consider that our waves must have rather great amount of energy than in the atomic bomb explosion and that the energy is of the order of 10^{19} erg as shown in Table 1. In the case of initial impulse, the total energy of our wave motion would be obtained by using the velocity potential at the time $t=0$. However, on account of mathematical difficulties, we could not execute the calculation. Moreover, the potential energy of the water dome observed on the 23rd by Dr. Niino comes to be about 4×10^{16} erg, which is far smaller than what was obtained here as already suggested in the first paper.

According to volcanologists[11], an explosion at Myojinsho Reef is supposed to have issued the same amount of energy as the energy of explosion at Mt. Asama, one of the most active volcanos in Japan, where the energy of an explosion has been calculated to be of the order of 10^{19} erg in violent cases[13]. Accordingly, if the above obtained energy of wave motions are admissible, the energy of waves is to have occupied a considerable part of all energy in the explosion.

§ 5. *Summary*

Whether the observed Cauchy-Poisson waves have been chiefly generated by

the action of initial impulse or initial elevation is not so decisive, but from some reasons it seems that the action of initial impulse was rather effective than that of initial elevation in our cases. Moreover, it is seen that the strong impulse enough to cause the sinking of the "Kaiyo-maru No. 5" acted on the water surface at the moment of explosion.

The energy of wave motions has been calculated to be of the order of 10^{19} erg, and this energy corresponds to a considerable part of all energy issued by the explosion at Myojinsho Reef.

Acknowledgement

In conclusion, the authors wish to express their thanks to Dr. R. Takahashi for his kind advices and to Mr. T. Yusa who assisted in numerical calculations.

Literature

1) S. Unoki and M. Nakano: On the Cauchy-Poisson Waves Caused by the Eruption of a Submarine Volcano (1st paper), *Oceanogr. Mag.* Vol. 4, No. 4, p.p. 119~141, 1953.
2) H. Niino: Some Problems on the Explosion of the Myojinsho Reef. *Kagaku Asahi* (in Japanese), Dec., 1952.
3) H. Lamb: *Hydrodynamics*, sixth edition, § 255, 1932; or *Lond. Math. Soc. Proc.* Vol. 2 (2), p. 371, 1904.
4) H. Lamb: On Water Waves due to Disturbance beneath the Surface, *Proc. Lond. Math. Soc.*, (2) XXI, p. 359~372, 1923.
5) K. Terazawa: On Deep-Sea Water Waves Caused by a Local Disturbance on or beneath the Surface, *Proc. Roy. Soc. A.* XCII, p.p. 57~81, 1915.
6) S. Unoki: On the Variation of Sea Level Caused by the Variation of Atmospheric Pressure, *Oceanogr, Mag.* Vol. 2, No. 1, p.p. 1~15, 1950.
7) M. Nakano: On the Secondary Undulations of Tides Caused by Cyclonic Storms, *Oceanogr. Mag.* Vol. 1, No. 1, p.p. 13~32, 1949.
8) H. Lamb: *Hydrodynamics*, § 241.
9) Hydrographic Office, U. S. Navy: Breakers and Surf; Principles in Forecasting, p. 18, 1944.
10) H. Lamb: *Hydrodynamics*, § 185.
11) The report presented by the Commitee of Investigation for the cause of the disaster of the "Kaiyo-maru No. 5", 1952, Hydrographic Office of Japan.
12) Los Alamos Scientific Laboratory: *The Effect of Atomic Weapons*, § 4.56, 1950.
13) T. Minakami: Some Problems on Physical Volcanology, (in Japanese), *Proc. Phy. Math. Soc.*, Vol. 16, No. 1, p.p. 6~32, 1942.

海水の泡沫性の研究（その5）
海水及び無機電解質水溶液の泡沫性について

阿部友三郎

中央気象台　海洋報告　第3巻　第1～2号　別刷
昭和25年6月

海水泡沫性の研究（その5）
海水及び無機電解質水溶液の泡沫性について

阿部友三郎
（気象研究所海洋研究室）

A study on the foaming of sea water and inorganic electrolyte solutions (Part 5)

By
Tomosaburo ABE
(*Oceanographic Laboratory, Meteorological Research Institute.*)

Abstract:— The state of sea is commonly expressed by Beaufort Scale. Foam of the sea is one of the basic evidence of this scale. Experiments have been performed on the foaming natures of sea water and of solutions of various inorganic electrolytes at varying temperatures and concentrations. The results are summarized as follows:

1. When the chlorinity of sea water is held at a constant value, "*foam height*" (H) of sea water increases slightly with increasing temperatures in a linear relation.
2. Under a constant temperature, "*H*" increases exponentially with chlorinity.
3. The mean thickness of the membrane surrounding bubbles is about 20μ, when foaming has occurred in sea water whose temperature is 20°C and chlorinity is 18.93‰.
4. Inorganic acids are almost non-foamy.
5. On the other hand, the foam height in solution of salts or alkalies increases with incneasing concentration, up to a maximum. It decreases with further increase of the concentration. The maximum value has been observed in concentration below I N in the majority of solutions tested, although the concentration varies with kinds of electrolytes.

§1. 緒　　言

海洋学的な立場から，海水の泡沫性を考察すると，海水が淡水と異つて著しい泡沫性を有することは，一般に水面状態の観測に対して大きな問題を提供している。例えば，ビューフォート波浪階級は白波の有無と云うことに，相当重きを置いているが，水面の等しい擾乱によつて生ずる白波の程度は海水，淡水によつて著しく異つているのに，従来，湖水等における観測にもこの階級をそのまま用いている，併しその階級数に対応する水面の擾乱の程度，従つて風速の程度は海におけるより大きくなければならないことは既に当所の三宅泰雄博士及び筆者により指摘されている。更に筆者はこの泡沫

性の問題の考察を進めて，海水泡沫層の高さと温度，溶存塩素量との関係等を求めた。又これに関連して，海水溶存塩類水溶液の泡沫性につき，海水の場合と同様な実験を行いての如き結果を得たので報告する。*

§2. 海水の泡沫性

i） 泡沫層の高さと水温との関係.……十分洗滌した新鮮な約 4 cm³，長さ約 14cm のガラス製試験管に，一定量のよく濾過した新鮮な海水を封じ，これを恒温器にて，振幅 20mm，毎秒 15 回の振盪を与え，生ずる泡沫状態がほぼ平衡になる時間，即ち 30 秒後に振盪を止め，振盪後 1 秒後に火花放電光により，泡沫状態を瞬間撮影した。この際，室温はほぼ一定に保つて置いた。

濃度を一定に保ち水温を 3° C より 33° C までの範囲で，泡沫層の高さ（以後泡高と呼ぶ）を測定した。結果，泡高は水温の増加すると共に，直線的に増すことがわかつた。

即ち，泡高，水温をそれぞれ H（mm），t（°C）とすれば，次の如き関係にある。

$$H = A + Bt$$

ここに A, B は海水塩素量濃度に依存する常数である。第1図に Cl. 18.93‰ の場合を示した。この際，$A=10.5$, $B=0.2_1$ である。即ち泡高は 3° C で約 11mmであり，水温が増すと共に直線的に増加して行き 33° C で約 16mm になつている。泡高は水温によつて影響されるが，その程度は余り大きくはない。

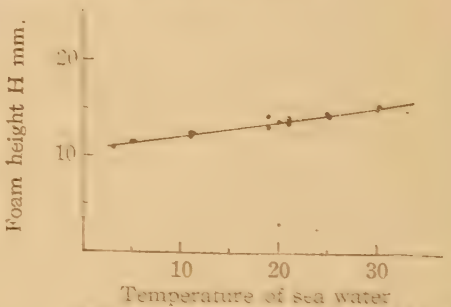

Fig 1. Relation between foam height and temperature of sea water.

ii） 泡高と濃度との関係.……Cl 濃度 19.37‰ の海水を基準水として，種々の濃度のものを作り水温をほぼ一定に保つて（± 1° C の精度）泡高と Cl 濃度との関係を求めた。水温一定のとき，海水の Cl 濃度を増加して行くと，泡高は指数函数的に増加して行く。水温 10° C，20° 及び 30° の場合につき，この関係を図示すれば，第2図の如くなる。

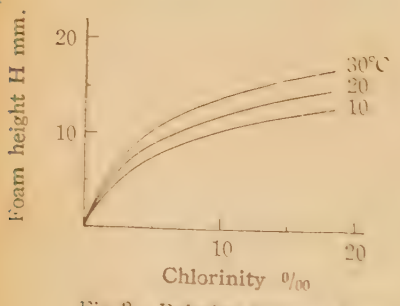

Fig 2. Relation between Foam height and Chlorinity

Cl 濃度 3‰ 位までの稀い海水では，濃度によつて，泡高は比較的に大きな変化があるが，濃度が大になると，この変化の程度は比較的少なくなる。

以上の関係を用いて，任意の温度，任意の Cl 濃度の場合に生ずる泡高を計算することができる。

* この研究は筆者の当所地球化学研究室勤務中に行つたものであり，当所研究報告会及び日本化学会の年会等において発表済のものである。

iii) 泡粒の平均の厚さ.……海水泡沫層を形成する泡粒について，その膜の平均の厚さの程度を実験的に求めてみた。使用した海水は Cl 濃度 18.93‰ のものであり，水温は約 20°C の場合である。その方法は次の如くである。

振盪管内における振盪前の海水面と，振盪停止直後，泡沫層が形成されて下つた海水面との差から，振盪によつて泡沫に変つた海水量 v を求める。次に泡沫層の全体積 V を求め，又従来の方法で泡沫層の写真から計測して平均半径を求めこれを r とすれば，泡沫層中に存在するこの r の泡粒の個数 N は $V/\frac{4}{3}\pi r^3$ である。所が一個の泡粒を形成するために使用された海水の体積 dv は v/N であるから，泡粒の膜の平均の厚さを dr とすれば，次の如くなる。

$$dr = \frac{dv}{4\pi r^2}$$

斯様にして，20回の実験値から，dr を求めると，約 20μ となる。

この方法で dr を求めることには色々と不合理な点がある。例えば泡粒相互間に存在する海水量を除いてないこと，実験中管の上部に泡沫が，往々附着して了うことがあるが，この影響も除いてない等々。併し大略の程度は示すものと思われる。

§3. 無機電解質水溶液の泡沫性

元来，海水は一種の無機電解質水溶液であり，三宅及び筆者の実験によると，無機電解質だけで造つた人工海水がほぼ天然海水に近い起泡力をもつことは，この電解質が海水の起泡力の主原因であると考えられる。

そこで，海水の泡沫性の物理化学的機構を明かにする第一歩として，無機電解質水溶液の泡沫性を調べることにした。実験に用いた資料は主に海水中に存在する塩類であり，4 N までの濃度につき，又無機酸に至つては 6N までにつき，海水の場合と同様な方法で実験を行つた。

§. 4 濃度と泡高との関係

無機電解質水溶液の濃度と泡高との関係を図示すれば第3図の如くなる。即ち，泡高は濃度が増すに従つて増加して行き，溶質特有の一定の極大値に至つて，以後は減少して行く。この極大値を示す濃度は溶質により異つているが，概して，濃度の比較的小さい所，即ち，大体 1N 以内にある。この極大値における濃度と泡高を示せば第1表の如くなる。この泡高の極大値を示す濃度は，その泡沫の性質を特徴づける他の量例えば，安定度等と密接な関係を持つらしい。

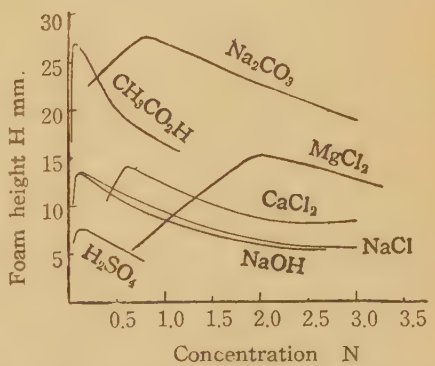

Fig 3. Relation between foam height and concentration of electrolyte solution.

次に，これ等の泡沫の様相を調べるため，極大値辺の平均直径を求めてみると第2表の如くなる。表からわかる如く，Na OH の泡沫は比較的大きく，安定度もよく十数秒の寿命がある。以上の図，表

Table 1.

Substance	K_2SO_4	$MgCl_2$	$CaCl_2$	Na Cl	Na OH	CH_3CO_2H
Concentration at. Max. F.H.	0.05N	2.0	0.6	0.5	0.5	0.05
Foam Height	7.5mm	15.5	12.0	13.5	13.5	26.5

に醋酸の場合を示したのは，単に比較のためであり，これは周知の如く無機電解質に比較して，非常に泡立ち易く，いわゆる，さらさらした感じの細かい，一様な泡沫が多量にできる。

Table 2.

Substance	Concentration	d
Na Cl	0.1 N	0.83 mm
$MgCl_2$	2.0	0.62
$CaCl_2$	0.6	0.73
Na OH	0.1	1.45
K_2SO_4	0.5	0.75
CH_3CO_2H	0.05	0.64

§ 5. Na Cl, $MgCl_2$ 水溶液の泡沫性

次に，海水の主成分の Na Cl, $MgCl_2$ 水溶液の泡沫性につき，多少，精しく考察してみる。

先ず Na Cl 水溶液 3.54 N のものにつき，実験した。泡沫層は 15° C で約8秒の寿命を持ち，毎秒の泡沫状態を撮影した。

先ず，泡高の時間的変化を図示すると第4図の如くなる。即ち，最初約 6mm の泡高は殆んど直線的に時間の経過と共に減少して行く。

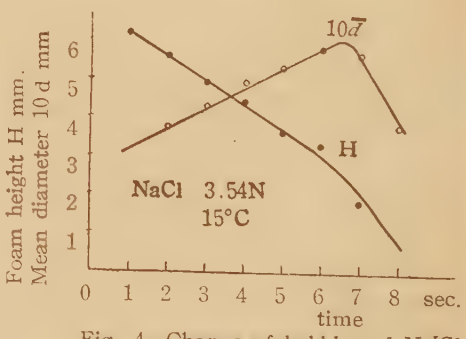

Fig. 4 Change of bubbles of NaCl solution

次に，この間の平均直径 d を求めてみると，d は最初約 0.3mm から，6.5秒後の約 0.6mm まで殆んど直線的に，時間と共に増加して行くことがわかる。これは，細かい泡程不安定で，凝集し易く，互に凝集して大きくなつて行くためか，或いは，比較的破裂し易くて，破裂して失われて行くかであろう。この際，泡を形成していた気体は泡粒が破れて遊離すると，泡沫間を通つて上昇して行くのであろう。この機構は明かでない。結局，比較的大きな泡粒が多数残留して行く結果となるためであろう。なお，この場合 0.6mm 以上の泡粒は存在し得ないのである。6.5秒以後は大きな泡粒も崩壊して行くのであろう。これ等の点に関しては，更に実験的又は理論的に確めたい。

次に泡粒の大きさと濃度との関係を求めてみると第5-A図の如くなる。この分布は濃度 0.1N から 2 Nまでの範囲で求めた。この分布は既報の海水の場合と同様な形態であり，Gauss の正規分布の

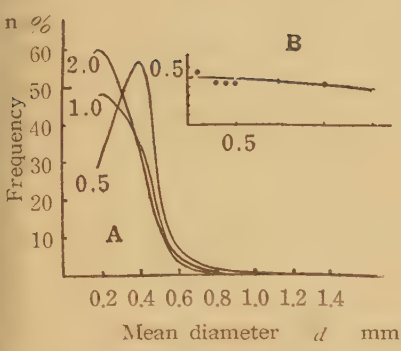

Fig 5. Distribution of the size of foam and concentration of NaCl solution.

形である。泡粒は大部分 0.6 mm 以内にある。分布の極大は濃度 0.5N では，d が0.4mm の処にあり，頻度は 56.5% である。更に濃くなると，この極大は 0.2 mm 以下に移る。この曲線の極大附近の形は，濃度が増すと共に，鋭くなつて行く傾向にある。即ち，溶液が濃くなつて行くと，泡粒は次第に細かくなり，一様な泡粒の揃つたものが多くなる傾向にある。

次に全般的にみると d は大体 0.4 mm 程度であり，濃度によつて殆んど変らないが，大体濃度が増すと共に僅かではあるが減小する傾向がある(第 5-B 図)。

次に $MgCl_2$ の場合を考察する。$MgCl_2$ は周知の如く吸湿性が甚だしいため等で実験に誤差が入り易く決定的な結論は云えぬが，NaCl の場合と大体同様な傾向にある。即ち，溶液の濃度の増加と共に，分布の極大を示す d は，小さな方向に移る。又泡粒の大きさは，濃度が増すと共に小さくなり，粒の揃つた大きさのものが多くなる傾向である。

§6. 結 果 の 考 察

以上海水及び無機電解質水溶液の泡沫性につき述べたが，海水の場合における泡高につき多少考察してみる。

実際の海洋現場においては，以上の実験の閉管の場合ではなく，むしろ開管の形式で泡沫層が形成される。又海水は色々な夾雑物も含んでいるのであろうから，以上の結果を直ぐ海洋現場にあてはめるのは甚だ危険である。開管の場合については，筆者は多くの実験は行つていないが，開管の際，最も泡沫に影響すると考えられるものは蒸発であろう。この点に関して鮫島実三郎氏等によつて行われた液体膜の安定度の実験がある。これによると，蒸発の行われる場合は，蒸発の行われぬ場合に比較して，液体膜の安定度は 2 倍若しくは 3 倍位よくなることを報告している。従つて恐らく，蒸発の影響の多分にある海洋現場では，泡沫層の安定度は相当よくなるものと考えられる。

§7. 要　　約

以上要約すれば，

海洋観測の精度を向上させるため，海水泡沫性を実験的に調べた。又これに関連して泡沫の物理化学的機構を明かにする第一歩として無機電解質水溶液の泡沫性につき実験的に調べて次の結果を得た。

I. 海水泡沫につき

1. 濃度一定なるとき，泡高は温度と共に直線的に僅かであるが増加する。(Fig. 1)

2. 温度一定なるとき，Cl 濃度が増加すると泡高は指数函数的に増加する。これを温度 10° C, 20° 及び 30° の場合につき求めた。この関係を用い任意な温度，Cl 濃度の場合に生ずる泡高を計算することができる (Fig. 2)。

3. 泡粒の平均の膜の厚さを，20° C 18.93 ‰ Cl の場合につき求め，約 20μ であることがわかつた。

II. 主に海水中溶存の無機電解質水溶液の泡沫性につき，濃度と泡高の関係を求めた。即ち，温度一定なるとき，泡高は濃度と共に増加し，一定の極大値に至り，以後減小する。この極大値を示す濃度は，比較的小さい所 1N 以内にある。無機酸は殆んど泡立たぬ (Fig. 3, 4, 5, Table 1, 2)。

終りに臨み，本研究を行うにあたつて，地球化学研究室長三宅泰雄先生からは，有益な御教示を頂き，又実験及び計算には，岡野政広，松村泰及び吉村照子の三氏に御助力を頂いた。ここに厚く御礼申上げる。

参 考 文 献

1. 三宅泰雄，阿部友三郎：海と空，第24巻9号 昭和19年. p. 291～295
2. 〃 〃 ：海戸海洋要報 第4号 昭和20年. p. 1～2
3. Y. Miyake and T. Abe: *Journ. Mar. Res.* Vol. VII, No. 2, 1948. p. 67～73.
4. 鮫島実三郎等. 膠質学論叢 第一輯 日本化学会編 昭和17年 p. 75～88

海水の泡沫性の研究（その6）
海水泡沫層の崩壊機構について

阿部友三郎

中央気象台　海洋報告　第3巻　第1～2号　別冊
昭和28年6月

海水泡沫性の研究(その6)
海水泡沫層の崩壊機構について

阿部友三郎

(気象研究所海洋研究室)

A study on the foaming of sea water (Part 6)
On the mechanism of decay of foam layer in sea water

By

Tomosaburo ABE

(Oceanographic Laboratory, Meteorological Research Institute)

Abstract : In order to improve the precision in applying the Beaufort scale to oceanographic observations, the decay of foam layer in sea water, as the fundamental problem, was experimentally studied, and the following results were obtained.

1. The velocity of the decay is proportional to the foam height at the time moment considered, namely, it is of the type of the 1st order chemical reaction {§. 3. (i)}.

2. Stability of foam layer on the white crested waves in situ was considered at varions points by using τ, *i. e.* half life of foam layer of sea water { §. 3. (ii) }.

3. Several characteristic considerations up to this time for general foam stability were stated briefly { §. 4. }.

§. 1. はしがき

現在，海洋及び湖沼観測等において，水面状態の観測には，ビ氏波浪階級が使用されている。所が困つたことには，この階級数が水域によつては，風力に一対一に対応して明確に決定できぬことである。このことは既に Pettersen 等も指摘している。しかし，その原因については，従来，殆んど触れられておらず，不明のままに残されていた。この階級をきめる際，白波の有無と云うことに相当重きを置いているので，本研究第2報において，三宅泰雄博士と筆者は，水面の擾乱によつて如何に海水が泡立つか等の問題に一応の知見を発表した。今回は，この問題に関連して，海面に生じた泡沫層が時間的に如何なる経過をたどるか，つまり，如何に消失して行くかを，主問題として，泡沫層の崩壊機構を実験的に調べ，又この泡沫層の安定度について，多少の考察を行つた。

§. 2. 泡沫層崩壊の実験

既に，三宅及び筆者は海水泡沫層の構造につき，形態学的考察を行つて報告している。即ち，海水

泡沫層は成長，崩壊及び残留の三層より成り立つと考えた。これ等の泡沫層を作り上げている泡粒につき，その膜の平均の厚さも実験的に求めて，塩素量18.93‰の外洋水では，約20μであることを第5報に述べている。

さて，この泡沫層の崩壊現象を取扱う場合，先ず対象として，泡沫層の何を選ぶかが問題になる。つまり，対象として泡沫層内にある泡粒の大きさ，或いは個数等の変化も考えられるが，筆者は色々と試みた結果，泡沫層自体の高さ（或いは厚さ），即ち泡高を対象とすることにした。つまり泡高が時間の経過と共に，如何に変化して行くかを調べることにしたのである。

実験方法は次の通りである。

断面がほぼ正方形（約4×4cm²）長さ約15cm（即ち容量約200cc）の共栓附ガラス容器を十分よく洗滌し，これに予め濾過した試料海水を6/10（これが最も泡立ち易い比率である）を注入してまた。これを第2報に述べた振盪装置にて上下に

振　　幅　　15mm

振　動　数　　15回/秒

にて約30秒間振盪する。これで泡立ちは平衡状態になる。次に振盪を停止し，停止後2秒毎に，泡沫層の状態を予め装置して置いたライカ型カメラにて，連続撮影した。この際，照明によつて泡沫層が暖められぬ様特に注意して，写真撮影用電球等は使用せず，超高圧水銀燈を使用して，これでてるだけ短時間泡沫層を照射した。この撮影は14秒間位まで行い終ると直ちに海水温を測定した。おこの装置は全部空気恒温室に入れてあり，ほぼ±1℃で恒温に保たせておいた。使用した資料海水は外洋で採水した塩素量19.26‰のものをよく濾過し，これを蒸溜水で稀めて

18.46‰，16.05，14.42，12.82及び9.63の5種類の濃度のものを作つた。実験に使用した海水以上6種の濃度のものである。

実験した海水温は29℃，21，14，4の四ツの場合である。実験は各場合につき3乃至5回行い，その平均値を以て各場合の代表値とした。

§. 3.　実験結果とその考察

（i）崩壊の形式

時間（t）の経過と共に，泡高（h）は，以上の種々な場合につき類似な変化傾向を示すことがかつたので，ここには，一例として，塩素量14.42‰，水温14℃の場合を述べる。

写真はこの際の泡沫層の経過を示す。この場合 $\log h$ と t との関係を示すれば，第1図の如くなる。から明かな如く，$\log h$ は t の増加と共に直線的に減少している。ただし，ここで泡高の初期はまず下方から盛んに泡の供給の行われているため，泡沫層の最下端，つまり海水と接する境界面はたえ

Changes of Foam layer height of Sea Water

Sea Water : Cl. 14.42‰,
Temp. 14°C
(×2)

Foam layer

2 Sec

4 Sec

6 Sec

8 Sec

10 Sec

Scale (mm)

12 Sec

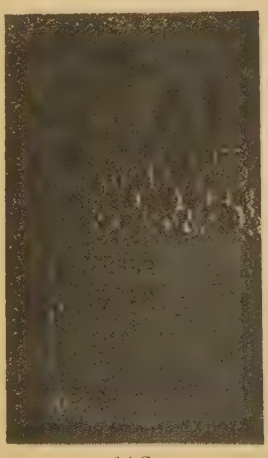

14 Sec

16 Sec

$h=h_0e^{-kt}$

Where h_0 : Initial foam height

k : Decay constant

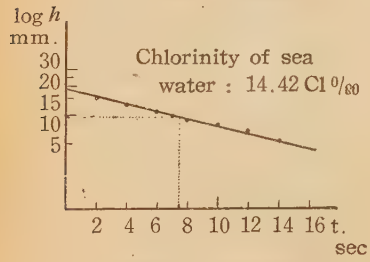

Fig. 1 Relation between the foam height (h) and time (t)

変動している。又，末期では数個の泡粒が器壁に附着して，偶然長く残留することもある。以上の理由で初期と末期との泡高の値は，泡粒以外の周囲の影響が大であり，不適当であると考え無視することにした。

従つて，泡沫層崩壊の実験式として次の如く置いた。

$$h=h_0e^{-\kappa t}\cdots\cdots\cdots\cdots(\mathrm{I})$$

ここに，h は泡高，h_0 は $t=0$ のときの泡高であり，図から求める。κ は崩壊恒数ある。（1）式を t につき微分すると，次の如くなる。

$$\frac{dh}{dt}=-h_0\,\kappa e^{-\kappa t}=-\kappa h\cdots\cdots\cdots\cdots(2)$$

即ち，泡沫層の消失する速さは，その時の泡高に比例していることがわかる。これはいわゆる化学反応における一次反応の形式に外ならない。（1）の函数型から直ぐわかる如く，変化中の任意な時刻から，h の大きさが半分になるまでに要する時間は等しく，一定である。この時間，即ち放射性原子崩壊の際，用いられている半減期を τ とすれば（1）式より，次の如くなる。

$$\frac{h_0}{2}=h_0\,e^{-\kappa\tau}$$

$$\therefore\quad 0.5=e^{-\kappa\tau}$$

或いは $$0.693=\kappa\tau\cdots\cdots\cdots\cdots(3)$$

第Ⅰ表に，実験値及び計算値を挙げる。表より計算値 $\kappa\tau$ はほぼ（3）式の 0.693 に近くほぼ一定であることがわかる。泡沫層の崩壊が純粋に確率論的問題として取扱い得る放射性原子の崩壊と同様な形式を採ることは興味あることである。

Table 1

Water temp.	Concentration ‰ Cl.	h_0 (mm)	k (Calc.)	τ (sec)	$k\tau$ (Calc.)
29.°C	19.26	22.5	0.143	4.8	0.685
	18.46	24.6	0.170	4.1	0.697
	16.05	24.4	0.166	4.2	0.696
	14.42	19.3	0.137	5.1	0.698
	12.82	18.5	0.145	4.8	0.696
	9.63	20.0	0.200	3.6	0.690
21°C	19.26	23.8	0.124	5.5	0.682
	18.46	25.5	0.128	5.4	0.691
	16.05	19.3	0.099	7.1	0.702
	14.42	23.0	0.131	5.3	0.695
	12.82	19.0	0.109	6.4	0.697
	9.63	14.3	0.214	3.2	0.685
14°C	19.26	17.4	0.071	10.0	0.710
	18.46	17.4	0.071	9.1	0.646
	16.05	16.4	0.084	8.2	0.776
	14.42	18.5	0.094	7.5	0.705
	12.82	—	—	—	—
	9.63	—	—	—	—
4°C	19.26	16.2	0.071	10.0	0.710
	18.46	13.7	0.047	14.5	0.686
	16.05	15.2	0.058	11.8	0.790
	14.42	14.7	0.049	12.6	0.713
	12.82	—	—	—	—
	9.63	15.8	0.097	7.4	0.722

(ii) 海水泡沫層の Stability

次に第1表から海水の塩素量と τ の関係を調べてみる。この関係を図示したのが第2図である。図からわかることは，塩素量 13‰ 以上，即ち，比較的濃い海水では，大体 τ は比較的大きく，つまり泡沫層の寿命が長く，これ等の泡沫層は消失し難いことがわかる。所が，第2報で

述べた如く，ある程度以上，塩素量が大きな海水は泡沫が出来易いのであるから，結局，泡沫が生じ易くて生じた泡沫は持続し易いのであるから，斯様な海域では白波が立ち易いことになる。

これに反して，塩素量 9‰ 以下の比較的稀い海水ではτは小さく，つまり泡沫層は寿命が短かく，消失し易いし，その上既報の如く泡沫は生じ難いのであるから，結局，泡沫は生じ難くて，生じた泡沫は持続し難いのであるから，斯様な海域では，白波は立ち難いことがわかる。以上の傾向は，水温が低い程顕著に現われる。これは第2表から明かである。即ち，第2図における各温度についての値を，矢印の如き直線にて近似的に置換えて，この矢印直線の勾配より，$\frac{\partial\tau}{\partial Cl}$ 即ち，塩素量の変化に対するτの変化を求めたのが第2表である。$\left(\frac{\partial\tau}{\partial Cl}\right.$ とせず表には，$\left.\frac{\Delta\tau}{\Delta Cl}\right)$ として置いた），表からわかる如く，$\frac{\Delta\tau}{\Delta Cl}$ は 29°C における 6×10^{-2}deg/‰Cl の値から，温度が減ずると共に増加し，4°C にてたその約9倍の値に激増している。$\frac{\Delta\tau}{\Delta Cl}$ は水温の高い処では小さく，塩素量濃度によつて，τ は余り大きな変化のないことを示す。つまり水温が高いと，塩素量が多かろうが，少なかろうが生じた泡沫の寿命は，殆んど同様であることを示している。これに反して水温が低くなると，$\frac{\Delta\tau}{\Delta Cl}$ の値は非常に大きくなり，塩素量濃度によるτの変化が極めて著しいことを示している。つまり水温が低いと，塩素量濃度の大小に泡沫の寿命は非常に影響されることを示している。この傾向は水温とτとの関係を示す第3図を見ると，更に明かである。

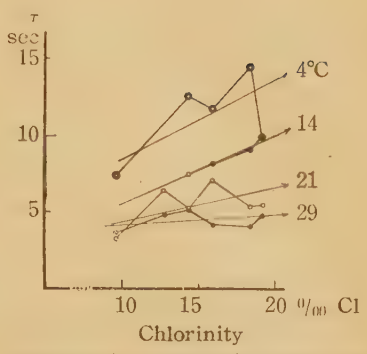

The straight lines with arrows are drawn to show the general tendency

Fig. 2 Relation between the half-life (τ) of foam height and the chlorinity (Cl) of sea water.

Table 2

Temp. °C	$\frac{\Delta\tau}{\Delta Cl}\times10^{-2}\frac{Cl.‰}{deg}$
29	6
21	23
14	45
4	51

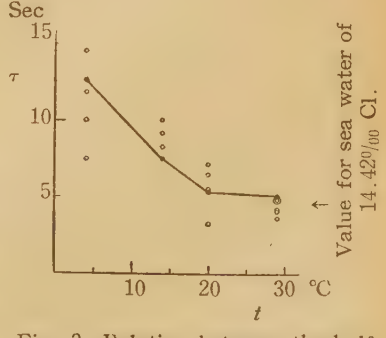

Fig. 3 Relation between the half-life of foam height and the tamperature (t) of sea water.

以上は閉管内の泡沫層の崩壊について述べたのであるが，実際の海洋現場では，閉管の場合でなく，むしろ開管の場合であり，鮫島実三郎教授等の薄膜の実験によると，この場合は蒸発が自由に行われるため等で，恐らく泡沫は安定度を増し，その上実際の海洋現場では海水に不溶性物質の微粒子等が海面附近に存在することもあろうから，これ等の物質表面の性質によつては，泡沫に強固に附着して著しく安定な，い

わゆる多相泡沫の形態をとるだろう。このときは泡沫の安定度は非常によくなるものと思われる。しかし斯様にして寿命は長くなるが泡沫層の崩壊する形態は以上述べた閉管実験の場合とほぼ同様な過程をとるものと思われる。

§4. 泡沫安定度に関する二，三の説

従来泡沫，特に筆者の取扱つている海水によつて作られる不安定泡沫の安定度についての明確な理論は殆んど無い現状にある。おもに有機物質の安定泡沫については，工業上の要請から，浮游選鉱法，石鹸製造等に関連し比較的多くの実験や説もあるが，取扱う対象が彷徨偏倚的現象であり，取扱いの困難さも手伝つて殆んど定性的説明以上を余り出ていない。次に二，三の説を挙げてみる。1931年 Foulk 等によつて Balanced layer theory が発表され，液体の薄膜の安定度の問題を取扱つている。即ち液体膜とは二つの液体表面が互に相近づいてできるものであり，両者が合致すると膜は消失する。この二つの液面が，或る距離以内に接近するとこれを妨げる力が働くため，それ以上二面は接近することができなくなり，液体膜が形成されるのである。この抵抗力は，この膜面の吸着によつて膜面における溶質の濃度と，液の内部の濃度とに差ができるために生ずると考えている。これで彼等は泡の安定度を論じている。しかし彼等の実験は不正確で信用できぬと云う非難も一部にある。現九州大学の佐々木恒孝教授も泡沫形成と吸着とは密接な関係があると云つている。同教授は表面張力と液の濃度との関係を調べ，表面張力が濃度によつて急激に変化する処で，泡沫層の安定度は極大になることを実験的に求めている。最近では Kirkwood や Harkins 等は，泡沫の安定度をきめる最も大きな要素は，膜表面における溶質の輸送の問題であると云つているが，これも安定性的説明以上を出ていない。

§5. 結　　語

以上要するに，泡粒の物理的性質が解明されればよいのであつて，この解明によつて雨粒，霧粒等の物理的性質への良き知見ともなるものと考えられる。しかし問題はなかなか難しいものである。筆者はこの解明の一助として，泡沫の安定度の尺度として τ 又は κ を用い，泡沫を形成する液体の粘性，表面粘性，表面張力，吸着等との関係を攻究して，海水泡沫の力学的性質を考えて行きたい。

§6. 要　　約

海洋観測等において，ビ氏波浪階級を使用する場合，その精度を向上させるための基礎的問題として，海水泡沫層の崩壊機構を実験的に調べ次の結果を得た。

1. 海水泡沫層における崩壊速度は，その時の泡高に比例している。即ち一次化学反応の形式であることを認めた。(§3. (1), (2),)
2. この際の半減期 τ を安定度の尺度として，海洋現場における白波につき多少の考察を行つた。
3. 一般の泡沫の安定度につき，従来行われた定性的考察を若干述べた。

終りに本研究を行うにあたつて，当所地球化学研究室長三宅泰雄先生から何かと御教示を賜いた。ここに厚く御礼申上げる。又測定用写真の引伸等に関して御援助を賜いた金沢五寿雄技官に深謝する。

参 考 文 献

1. 三宅泰雄，阿部友三郎，海と空 24，9 号 昭和 19 年
2. 〃 〃 神戸海洋要報 4 号 昭和 20 年
3. 阿部友三郎 本誌 3，昭和 28 年
4. C. W. Foulk and J. W. Miller. *Ind. Eng. Chem.* **23** No. 11, 1931.
5. W. E. Ewers and K. L. Sutherland. *Austr. Journ. Sci. Res. Ser. A.* **5** No. 4.
6. C. N. Hinshelwood, The Kinetics of chemical change, Oxford Univ. Press. 1940.
7. 佐々木恒孝 泡沫現象 河出書房 昭和 15 年.
8. 鮫島実三郎等 膠質学論叢 日本化学会編 昭和 17 年.

Reprinted from "papers in Meteorology and Geophysics" VOL. IV

551.460.189

An Improvement on the Case of Forel's Sea Color Scale

by

T. Nan'niti

Meteorological Research Institute

(Recieved June 20, 1953)

The author made an improvement on the case of Forel's sea color scale, that is, its case was reformed as shown in the following figure. Holes were made through the case which holds the ampoules of standard color solutions. The holes and ampoules are alternately drawn up in two lines as shown in the figure.

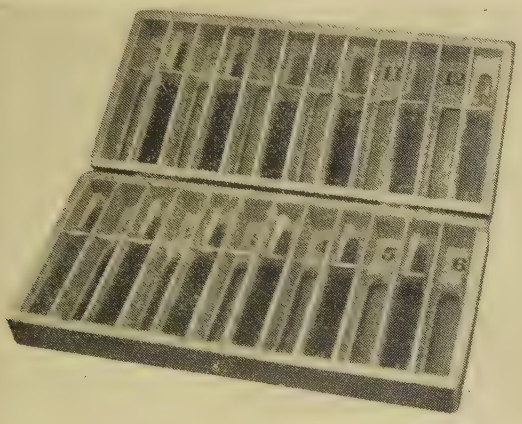

Note the holes which have been made beside each ampoule of standard color solutions.

If we observe the sea surface through these holes with one eye, we see the water surface in the same shape as the ampoule and on the same plane as Forel's standard, our sense of distance being lost. So we can determine the sea color more strictly and rapidly, avoiding our mental illusion, for the comparison can be done between the colors very near to each other.

Acknowledgement——The author wishes to express his hearty thanks to the Turumi Seiki Co. for the construction of the instrument.

Reprinted from the *Papers in Meteorology and Geophysics* Vol. IV No. 2, 1953
Published by the Meteorological Research Institute

How to Select the Observation Points

by
T. Nan'niti

Published by the Meteorological Research Institute,

Mabashi, Suginami, Tokyo, Japan

September 1953

551.460.18

How to Select the Observation Points

by
T. Nan'niti

Meteorological Research Institute
(Received June 20, 1953)

Abstract

In selecting time intervals and spacings between stations systematically, the author calculated theoretically and applied them to some examples.

1. Introduction

To observe temperature, chlorinity and other oceanographical elements, i.e. the object of oceanographic surveys, is to represent them as a function of a location (x, y, z) and time (t).

Now let a function, $F(x, y, z, t)$, represent some oceanographical element, and suppose it can be expanded as follows:

$$(1)\quad F(x+\alpha, y+\beta, z+\gamma, t+\delta) = F(x, y, z, t) + \left(\alpha\frac{\partial}{\partial x}+\beta\frac{\partial}{\partial y}+\gamma\frac{\partial}{\partial z}+\delta\frac{\partial}{\partial t}\right)F(x, y, z, t) + \frac{1}{2!}\left(\alpha\frac{\partial}{\partial x}+\beta\frac{\partial}{\partial y}+\gamma\frac{\partial}{\partial z}+\delta\frac{\partial}{\partial t}\right)^2 F(x+\theta\alpha, y+\theta\beta, z+\theta\gamma, t+\theta\delta),$$
$$0<\theta<1.$$

As values observed at points (x, y, z, t) and $(x+\alpha, y+\beta, z+\gamma, t+\delta)$ are equal or nearly so to each other, the author may take $F(x, y, z, t)$ as the representative value of the domain of the circle, its radius being $\sqrt{\alpha^2+\beta^2+\gamma^2}$ miles and $\pm\delta$ hours. Of course, $\alpha, \beta, \gamma, \delta$ are determined by the accuracy which the observation needs. By the above assumption, we have

$$(2)\quad \alpha F_x+\beta F_y+\gamma F_z+\delta F_t=0,$$

$$\text{error}\quad R=\frac{1}{2!}\left(\alpha\frac{\partial}{\partial x}+\beta\frac{\partial}{\partial y}+\gamma\frac{\partial}{\partial z}+\delta\frac{\partial}{\partial t}\right)^2 F(x+\theta\alpha, y+\theta\beta, z+\theta\gamma, t+\theta\delta),$$

$$\text{where,}\quad F_x=\frac{\partial F}{\partial x},\quad F_y=\frac{\partial F}{\partial y},\quad F_z=\frac{\partial F}{\partial z},\quad F_t=\frac{\partial F}{\partial t}.$$

In subsequent sections we shall discuss the above equation in various cases.

2. The y–z plane

Suppose a stationary and the homogeneous sea to the x-axis direction, $F_t=0$,

$F_x=0$; or a very variable sea $\alpha=0$, $\delta=0$, then from the equation (2) we have

$$\beta F_y+\gamma F_z=0. \tag{3}$$

Now let the points adjoining to each other be A and B, and the distance betwee them be l, and we have

$$\begin{cases} \beta_A F_{yA}+\gamma_A F_{zA}=0 \\ \beta_B F_{yB}+\gamma_B F_{zB}=0 \\ \sqrt{\beta_A{}^2+\gamma_A{}^2}+\sqrt{\beta_B{}^2+\gamma_B{}^2}=l. \end{cases} \tag{4}$$

If the observation layers have been selected beforehand, i.e. γ_A and γ_B are know and $\gamma_A=\gamma_B=\gamma$, the distance between the points will be decided as follows:

$$l_y=\gamma\{\sqrt{1+(F_{zA}/F_{yA})^2}+\sqrt{1+(F_{zB}/F_{yB})^2}\}. \tag{5}$$

Especially when the points A and B are on the same plane, $F(y, z)$ is t representative value of the quadrilateral domain. So we have,

$$\begin{aligned} l_y&=\beta_A+\beta_B \\ &=-\gamma(F_{zA}/F_{yA}+F_{zB}/F_{yB}). \end{aligned} \tag{6}$$

If we put $F_{yA}=F_{yB}=F_y$, $F_{zA}=F_{zB}=F_z$, we have the approximate solution,

$$l_y=-2\gamma\frac{F_z}{F_y}. \tag{7}$$

Here 2γ is the distance between the successive observation layers, and the spacin between observation points may be different from those of each layer as γ, F_z, will be changed. So if we plan to take observation layer roughly, i.e. γ is lar we may also observe the oceanic elements roughly along the y-axis direction. F_z/F_y is large, i.e. F_z is large and F_y is small, then l_y is large, that is, the distar between the successive stations may be taken to be large. But when F_z/F_y is sm i.e. F_z is small and F_y is large, we must take many stations along the y-a direction. If $F_y=0$, the sea condition will vary only in the z-axis direction, t $l_y=\infty$, so we may take only one point in the y-axis direction at that layer. $F_y=$const., then $l_y=$const$\times F_z$, so the spacing between stations will be governed F_z. If $F_y=\infty$, l_y is zero, we must take many stations along the y-axis directi On the other hand, if we plan to take the spacings of stations, 2β, along the axis direction beforehand, we must select observation layers according to $2\beta F_y$ densely in an upper and roughly in a lower layer as F_z will be large in the form

For example, put the function of elements as

$$F=F_0\left(B\cos\frac{\pi}{D}y-Cx\right)f(z)g(t) \quad [1], \tag{8}$$

then from the equations (7) and (8) we have

$$l_y=2\gamma\frac{D}{\pi}\cot\frac{\pi}{D}y\frac{\frac{\partial f(z)}{\partial z}}{f(z)}. \tag{9}$$

So we must take observation points densely at $y=\frac{D}{2}, \frac{3D}{2}, \frac{5D}{2}, \cdots\cdots,$

3. The x–y plane

Next we take $rF_x=0$, $\delta F_t=0$, then from the equation (2) we have the next equation, as in the above case.

$$l_y=-2\alpha\frac{F_\infty}{F_y}. \tag{10}$$

Putting the equation (8) into (10) we have

$$l_y=-2\alpha\frac{CD}{B\pi}\operatorname{cosec}\frac{\pi}{D}y. \tag{11}$$

Putting $D=120'$, $2B/C=120'$ in winter or $90'$ in summer (see Fig. 1)[1], we have

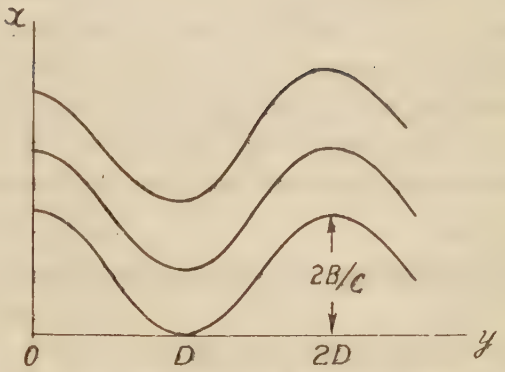

Fig. 1. The pattern of the distribution of the oceanographic element.

$$\begin{cases} l_y=-2\alpha\dfrac{2}{\pi}\operatorname{cosec}\dfrac{\pi}{D}y & \text{(in winter)} \\ l_y=-2\alpha\dfrac{8}{3\pi}\operatorname{cosec}\dfrac{\pi}{D}y & \text{(in summer)} \end{cases} \tag{12}$$

$$l_y \text{ (in summer)}/l_y \text{ (in winter)}=1.3. \tag{13}$$

From the equation (13) we may take a distance between successive stations in summer about 1.3 times as large as in witer. From the equation (12) we have the next results: $2\alpha\frac{2}{\pi}\leq l_y\leq\infty$ in winter or $2\alpha\frac{8}{3\pi}\leq l_y\leq\infty$ in summer. So we may select the observation points which have their mutual distance, in winter, 0.64 times

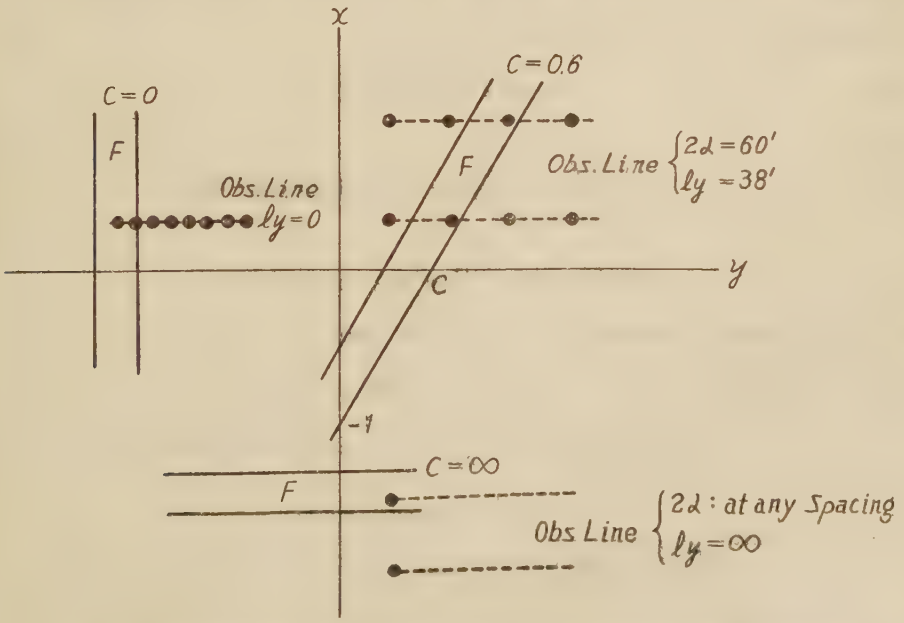

Fig. 2. The patterns of the distribution of the oceanographic element and the distribution of stations selected.

or, in summer, 0.85 times as large as the distance between the adjoining observation lines, 2α. For instance, take the distance, 2α, to be one degree, and we may select the stations at intervals of 38 miles in winter or 51 miles in summer. These values are rational ones considering the present actual observations. Furthermore if we take stations more closely along the y-axis direction, we must take adjoining observation lines more closely by the equation (10). If we take

$$F=F_0+Bx-\frac{B}{C}y, \tag{14}$$

for the equation (8), from the equations (10) and (14) we have

$$l_y=2\alpha C. \tag{15}$$

For example, putting $C=0.61$, -0.23, 0.64* and $2\alpha=60'$, we have $l_y=37'$, $14'$, $38'$. We have $l_y=0$ or ∞ as C is 0 or ∞ (see Fig. 2). In this case, we may change the x-axis for the y-axis for convenience' sake.

4. The non-stationary case

From the equation (2) we have the following equation

$$l_y=-2\frac{\alpha F_x+\gamma F_z+\delta F_t}{F_y}, \tag{16}$$

as above. If v denotes the average speed of the ship in knots, taking into account the duration of the stations, the position at time t is given by

$$y=vt. \tag{17}$$

Of course δ will be determined by the accuracy which we need, but we can not help taking the value $\frac{l_y}{v}$ for the minimum value of δ as we use only one ship. So putting this into the equation (16) we have

$$l_y=-2v\frac{\alpha F_x+\gamma F_z}{vF_y+2F_t}. \tag{18}$$

If we put

$$F=F_0\left(B\cos\frac{\pi}{D}y-Cx\right)\{1+\cos\omega(t-\varepsilon)\}, \tag{19}$$

or

$$F=\left(F_0+Bx-\frac{B}{C}y\right)\{1+\cos\omega(t-\varepsilon)\}, \tag{20}$$

then we have from the equations (17) (18) (19) and (20)

$$l_{y\omega}=-2\alpha\frac{vC\left\{1+\cos\omega\left(\frac{y}{v}-\varepsilon\right)\right\}}{\frac{vB\pi}{D}\left\{1+\cos\omega\left(\frac{y}{v}-\varepsilon\right)\right\}\sin\frac{\pi}{D}y+2\omega\left(B\cos\frac{\pi}{D}y-Cx\right)\sin\omega\left(\frac{y}{v}-\varepsilon\right)}, \tag{21}$$

$$l_{y\omega}=2\alpha\frac{vB\left\{1+\cos\omega\left(\frac{y}{v}-\varepsilon\right)\right\}}{\frac{vB}{C}\left\{1+\cos\omega\left(\frac{y}{v}-\varepsilon\right)\right\}+2\omega\left(F_0+Bx-\frac{B}{C}y\right)\sin\omega\left(\frac{y}{v}-\varepsilon\right)}. \tag{22}$$

* Calculated from Ten-Day Marine Report, State of the Sea Adjacent to Western Japan Nos. 181–183 issued by the Nagasaki Marine Observatory.

When $\omega \to 0$, these equations (21) and (22) coincide with the equations (11) and (15), respectively. From the equations (11) (21) and (15) (22), we have

$$l_{y\omega} \leq l_y. \tag{23}$$

Also letting $\omega \to \infty$, we have $l_{y\omega} \to 0$. So we must select spacings between stations smaller along oceanic profiles as periods of oceanic variations become smaller.

Reference

[1] Nan'niti, T. 1951; On the Austausch Coefficient in the Sea. The Oceanographical Magazine **3**, (1) p. 49.

Reprinted from the *Papers in Meteorology and Geophysics* Vol. IV No. 2, 1953
Published by the Meteorological Research Institute

A Current Meter Using a Phototube (II)

— Experiment on a Wind Drift Current in a Rising State —

by
T. Nan'niti

Published by the Meteorological Research Institute,

Mabashi, Suginami, Tokyo, Japan

September 1953

551.460.183 : 551.465

A Current Meter Using a Phototube (Ⅱ)

— Experiment on a Wind Drift Current in a Rising State —

by

T. Nan'niti

Meteorological Research Institute

(Received August 14, 1953)

Abstract

The author observed a drift current in a rising state using his newly designed current meter [1], and he could distinguish in a recorded chart a rising drift current, a proper ocean current and an apparent ocean current caused by a swing of the current meter due to the yawing, pitching and rolling of the research ship "Asasiwo Maru" in bad sea conditions.

1. Materials

The experiment was performed in Sagami Bay on board the research ship "Asasiwo Maru" on May 15, 1953, using three current meters of different kinds simultaneously, such as an Ekman-Merz, an Ono's (Hydrographic Office) and the author's current meters. Their relative positions in the experiment are shown in Fig. 1.

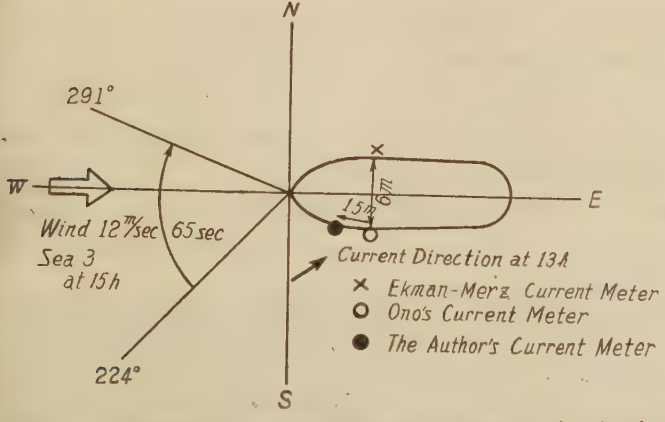

Fig. 1. Positions of the three current meters in the simultaneous observation. The arrows show the directions of wind, sea and current as observed by vision.

Just before the ship reached a station the wind had risen to a gale at about 10h40m~50m, and then the sea surface began to be covered with white horses. The ship reached the station (34° 59'.5N, 139°05'.7E) at 11h 10m.

The observation was done at a layer of 5m depth. The direction of current, as seen from the deck, was NE or NNE and turned to the east gradually, perhaps by the westerly wind. Oceanographical data obtained by the Ekman-Merz current

meter, meteorological data and others are tabulated in Table 1.

Table 1. Oceanographical observation taken in Sagami Bay.

Station 34°59′.5 N, 139°05′.7 E. Date May 15, 1953. Mag. Var. 5°W.
Tide (at Itô) H.W. 4h45m, 18h55m; L.W. 12h10m. Lunar Age 1.9 day

(1) Direct current measurement taken by an Ekman-Merz current meter
Depth 5m

Time	Speed	Dir.	Distribution of balls
h m	cm/sec	°	
13 23	19.3	218	12/1, 14/1, 20/2, 21/1, 34/1, 35/1
13 40	15.8	55	1/1, 14/1, 17/1, 18/1, 33/2, 34/1
13 59	14.6	60	0/1, 1/2, 9/1, 11/1, 17/1
14 50?	?	40	0/2, 1/1, 2/1, 5/1, 7/2, 8/2, 13/1, 34/1

(2) Marine-meteorological observation

Time	Air temp.	Wind	Clouds	Sea	Swell
h m	°C	dir. speed			
8 00		SW 2 (in Beaufort's)	clear sky		
12 00		W 5 (in Beaufort's)	clear sky		
15 00	21.5	W 12.0 m/sec	1 Ci, 0 Ac	W 3	none
16 00		W 6 (in Beaufort's)	clear sky		

(3) Movement of the ship

Time taken for yawing from 224° to 291° .....65 sec.
Period of rolling..... 5 sec.
Period of pitching ..... 3 sec.

From a bad record obtained by the Ono's current meter, it is very difficult to read any speed or direction of the current, due to bad sea conditions. Balls of the Ekman-Merz current meter are also distributed in various directions due to bad sea conditions, so the average direction is uncertain.

Next, a part of the chart recorded by the author's cnrrent meter at a 5m layer is shown in Fig. 2. As mentioned in the previous paper [1], the speed calibration

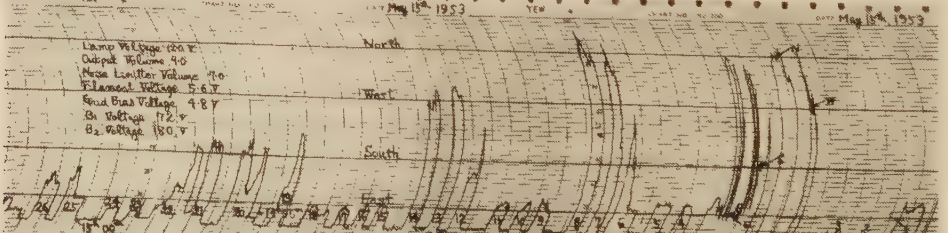

Fig. 2. A record of current obtained at a 5m layer from 14h38m till 15h00m.

was not done. So a comparison about current speed obtained by simultaneous

observations with the Ekman-Merz and the author's current meters was done, and the result is shown in Fig. 3. From the figure we may add 1.8 cm/sec to the calculated speeds by the author's current meter. We must also add this value to the results obtained in the previous paper [1]. Adding this correction to the values calculated from Fig. 2, we get the results tabulated in Table 2 and shown in Figs. 4 and 5. In this table and the figures, the records obtained when the light path was opened were numbered in time order. After this, at about 15h03m, the sea surface became more and more rough, so we stopped the observation.

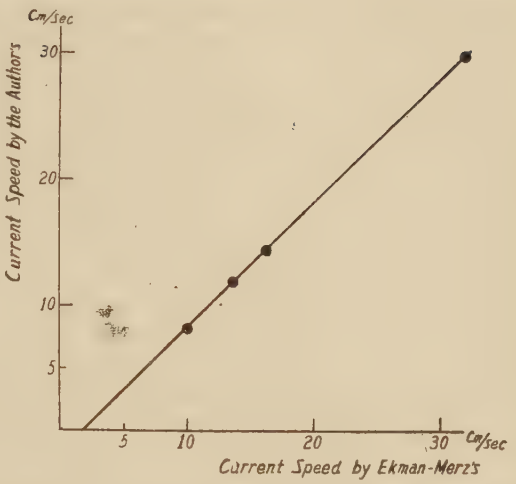

Fig. 3. Relation between the speeds obtained by a Ekman-Merz and by the author's current meters.

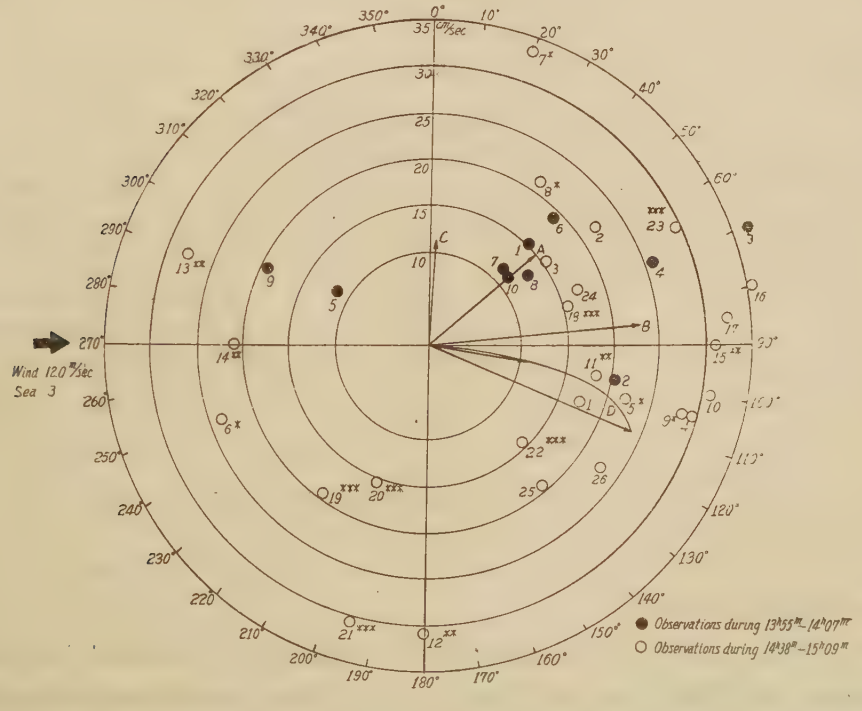

Fig. 4. Vectors of velocities of the recorded current at every instance and the mean currents at 14h (A) and at 15h (B); and the proper (C) and the wind currents deduced from them. A hodograph of rising wind current (D) is also shown.

Table 2. Direct current measurement taken by the author's current meter at a 5m layer from 14h38m till 15h00m.

No.	Time	Speed	Dir.	No.	Time	Speed	Dir.
	h m	cm/sec	°		h m	cm/sec	°
1	14 38	17.6	110	14	14 50.6	21.0	270
2	39	22.2	55	15	51.5	31.1	90
3	39.8	15.7	55	16	52	35.5	80
4	43.8	29.6	105	17	52.5	32.5	85
5	44.4	22.2	105	18	53	15.7	75
6	45.2	23.7	250	19	54.2	19.6	215
7	46	33.6	20	20	55.2	15.6	200
8	46.5	21.3	35	21	56.4	30.6	195
9	47.4	28.7	105	22	57.6	14.7	135
10	47.9	31.0	100	23	58.3	29.6	65
11	48.6	18.5	100	24	58.9	17.2	70
12	49.6	30.9	180	25	15 00	19.7	140
13	50.1	27.7	290	26	00.9	22.9	125

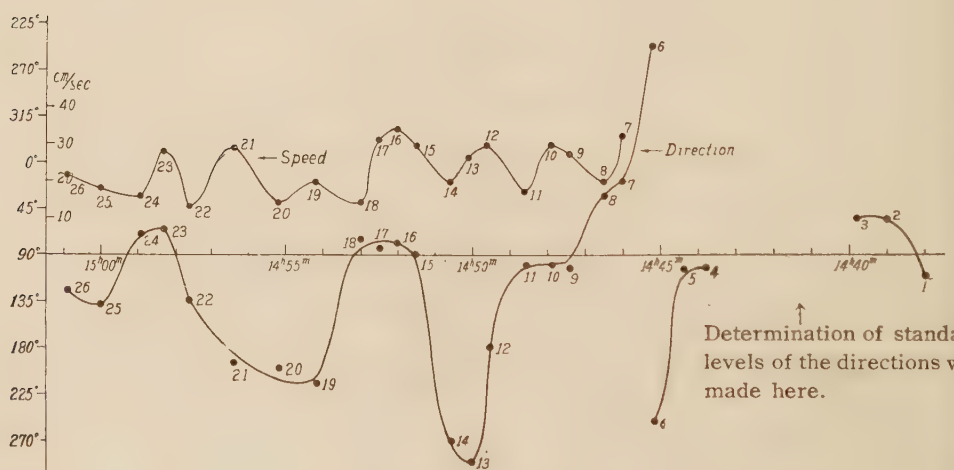

Fig. 5. Oscillation of the current meter caused by the ship's yawing due to the gale.

2. Analysis of materials

From Figs. 4 and 5, we can find that the current meter changed its directio remarkably about four times in 15 minutes. We have marked the records of eac cycle by affixing to the numbers the signs*,**,*** in Fig. 4. It might not occu that the real ocean current changed its speed rapidly and its direction widely i such a manner. And the observation was carried out in bad sea conditions, so w

:an suspect that the instrument was swung with a period of two or three minutes ıround its main direction, the east. And as the current ran towards NE, the ship ɔscillated anti-symmetrically with reference to the E–W direction, i.e. it oscillated arger towards NE. (See Fig. 1). For, we can see that recorded speeds decreased n their values on that chart at points 2–3, 4–5, 7–8, 10–11, 13–14, 16–17–18, 19–20, 21–22, 23–24; and increased in their values at the points 1–2, 5–6–7, 8–9–10, 11–12–13, 14–15–16, 18–19, 20–21, 22–23, 24–25–26. We can explain these facts by supposing :hat the ocean current itself did not change just as was recorded, but that the instrument was swung by the ship's movement, namely speeds in increasing state were recorded when the instrument was swung strongly, being suspended from a meter wheel as the ship was yawing by the strong wind, and speeds in decreasing state were recorded as the instrument was nearly free from oscillation, or it was near the turning points of its pendulum motion.

At 15h00m the ship itself was yawing from 224° to 291° taking 65 sec as shown in Table 1, so it took about 2 min 10 sec in order for the spip to swing one cycle. The record in Fig. 2 shows that the instrument was swung in two or three minutes and then rested about equal minutes and again swung as before. And recorded currents in Fig. 4 pointed mostly towards the direction between 44° (=224°−180°) and 111° (=291°−180°). As shown in Figs. 2 and 5, the swing of the current meter was damped and its direction gradually tended to the east for more than 15 minutes. The damping oscillation shown in Fig. 5 would not be caused by a real variable current speed and direction as the meter wheel, the suporting point of the current meter, did not swing, because its amplitude was too large. But it could be caused by the swing of the supporting point due to the ship's yawing. In this observation, the ship dropped only one anchor, so the above-mentioned yawing occured, which we could put an end to by dropping one more anchor.

Furthermore, we can see the fluctuation in the direction of the order of 20°～40°, 5 sec in Fig. 2. These periods of the fluctuation coincided with the periods of rolling or pitching of the ship.

By a complex combination of an apparent current induced by the ship's rolling, pitching and yawing and the ocean current, the recorded chart mentioned above was obtained; and in these disturbances, the apparent current, the effect of yawing was the largest.

We get the mean value, 23 cm/sec 85°, as the ocean current omitting the apparent current and averaging the values obtained at such points as 2–3, 4–5, 10–11, 16–17 and 23–24, where recorded directions were kept constant for about one or two minutes. At these points, it seems that the instrument was nearly at rest, being free from the ship's swinging around (see Figs. 4, and 5).

Next we investigate the current condition before 14h38m. We tabulate the results in Table 3 calculated from Fig. 6 obtained at a 5m layer from 13h55m till 14h07m. Plotting these values in Fig. 4, we get the mean value, 15 cm/sec 50°, as the ocean current.

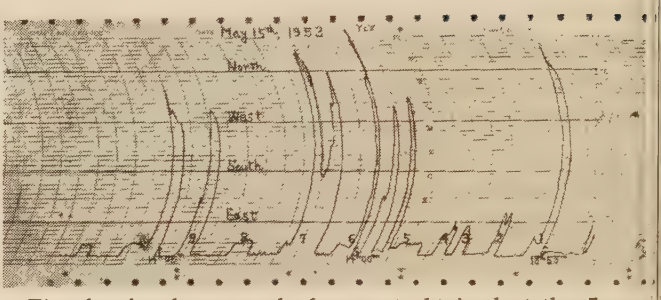

Fig. 6. Another record of current obtained at the 5m layer from 13h55m till 14h07m.

Table 3. Direct current measurement taken by the author's current meter at a 5m layer from 13h55m till 14h05m.

No.	Time	Speed	Dir.	No.	Time	Speed	Dir.
	h m	cm/sec	°		h m	cm/sec	°
1	13 55	15.3	45	6	14 00	19.3	45
2	56.3	20.6	100	7	01.8	11.5	45
3	57.1	36.9	70	8	03	13.2	55
4	57.8	25.8	70	9	04.4	19.3	295
5	59	11.4	300	10	05.5	11.3	50

3. Discussion of the above section

As shown in Table 1, the distribution patterns of balls of the Ekman-Merz current meter were very irregular. Assuming that 7 balls were dropped in 5 minutes, the current meter kept a constant direction, less than 10 degrees, only for 43 sec or 86 sec, because we found only one or two balls in each compartment of the compass box, and the angular velocity of yawing was $(291-224)/65=1.03$ deg/sec. If we assume that the current meter was swung with an angular velocity 1.0 deg/sec, the current meter changed its direction by 30° in 30 sec. And when it came to the turning point, or it was nearly free from oscillation, it was at rest for 120 sec, so it dropped one or two balls in one compartment. It is not quite probable that two balls were dropped in one and the same compartment in the going and coming of the swing. So it would be natural that the balls were spread in such a wide extent as they were observed to be. Time for one cycle of yawing was four to five minutes and the time interval taking for one current observation by the Ekman-Merz's was also five minutes. So the values observed by the Ekman-Merz's were not so widely different from the average values obtained by the author's. But if the period of yawing was larger, the time interval for one observation by the Ekman-Merz's had to be taken also larger.

The wind began to blow hard from the west at 10h40m~50m. At 14h00m, 3 hours after the rising of the gale, the speed of the ocean current was 15 cm/sec

its direction was 50°; and at 15h00m, 4 hours after the rising of the gale, the current speed was 23 cm/sec, its direction was 85° (see Fig. 4).

4 hours after the rising of the gale, the speed of wind current would have been almost developed. And it is well known that the average value of wind factor is 0.02. So let the speed of wind current be $1200 \times 0.02 = 24$ cm/sec and its direction be 105° or 110° or 115° as $h/D = 1/4$, ($D = 150$m) [2]. Though the depth of the station, 15m, was estimated from a sea chart, its position was near the coast and the depth of its offing was 30m~60m. So we take $h/D = 1/4$ as the representative value of this sea. We have the proper ocean current in Table 4.

Table 4. The proper ocean current calculated when the wind current is assumed.

Assumed wind current (speed 24 cm/sec)	Direction					
	105°		110°		115°	
Proper ocean current	speed cm/sec	dir. °	speed cm/sec	dir. °	speed cm/sec	dir. °
	8.6	359	10.5	3	12.4	5

At 14h, the resultant ocean current was 15 cm/sec, 50°, and if the proper ocean current at 14h was also 10.5 cm/sec, 3°, the wind current at 14h was 11.2 cm/sec, 94°; and if the proper current was 12.4 cm/sec, 5°, the wind current was 10.8 cm/sec 104°. So the wind current increased its speed by $24 - 11.2 = 12.8$ cm/sec and turned its direction by $110 - 94 = 16°$ to the right for an hour, or increased its speed by $24 - 10.8 = 13.2$ cm/sec, and turned its angle by $115 - 104 = 11°$ to the right.

But the culculated wind current at 14h was smaller than the theoretical one. Perhaps the disagreement was caused by the assumption that the proper current was stationary. The directions in this paper are all mentioned referring to the geomagnetic axes. The magnetic variation at the station is 5°W.

The periods of rolling and pitching were 5 sec and 3 sec respectively (see Table 1). Though we did not observe the period of the sea, we calculated it [3] and got 3 sec. As the period of the sea has an intermediate value between the periods of rolling and pitching, the yawing will be damped [4], though the bow of the ship was fastened by the chain, and it was restricted in its movement in some degree and received the force of the ocean current from the port. Thus the yawing had been damped as shown in Fig. 5.

There were no recording instruments for meteorological elements, and the data of the ocean current in initial condition were not obtained, so we can not discuss them further.

4. Conclusion

The author observed a current on a strong windy day, and he could observe

it successfully. The proper ocean current was 11.5 cm/sec, 4°. 3 hours after th rising of the gale, 12 m/sec, 90°, the wind current was 11.0 cm/sec, 99°, and 4 hour after the beginning it was 24 cm/sec, 113°, it increased its speed by 13 cm/sec, an turned its direction by 14° to the right for an hour.

Acknowledgement ——The author wishes to express his hearty thanks to D M. NAKANO for his kind advice, and to the members of the Oceanographical Sectio of the Central Meteorological Observatory for their help during the observation.

References

[1] NAN'NITI, T., 1953: A Current Meter Using a Phototube (I). Papers in Meteorolo and Geophysics, **3**, p. 286.

[2] HIDAKA, K., 1933: Non-Stationary Ocean-Current, Part 1. Memoirs of the Kobe Mari Observatory, **5**, p. 141.

[3] SVERDRUP, H.U. and W.H. MUNK, 1947: Wind, Sea and Swell; Theory of Relations f Forecasting. Contribution from the Scripps Institution of Oceanography. N Series No. 303.

[4] SEZAWA, K., 1935: The Theory of Oscillations (in Japanese). Tokyo, Iwanami-Shote p. 467.

海水の泡沫の研究 第七報
海水泡沫層の崩壊機構について (その 2)

阿部友三郎
(気象研究所海洋研究室)

A Study on the Foaming of Sea Water (7th report)
—On the Mechanism of Decay of the Foam Layer of Sea Water (Part 2)—

By

Tomosaburo ABE

(Oceanographical Laboratory, Meteorological Research Institute)

Abstract: The mechanism of decay of bubbles in the foam layer of sea water was studied and the following results were obtained.

(1) If the ordinates of the upper and lower boundary surface be y_1 and y_2, respectively, and t the time, the following relations hold good:

$$4.44 \geq \left|\frac{dy_1}{dt}\right| \Big/ \left|\frac{dy_2}{dt}\right| \geq 2.22$$

That is, the decay speed at y_1 is larger than that at y_2, i.e. a little more than four times in the initial stage and a little more than twice even in the last stage.

(2) In the frequency distribution of foam sizes at various periods, there exists some maximum frequency. Foam sizes of maximum frequency increase with time up to a certain limit.

(3) The mean radius of foam linearly increases with time as expressed by the following empirical formula:

$$\bar{r} = 0.33 + 0.018\, t \text{ mm},$$

where $\bar{r}$ is the mean radius of foams in the layer at the temperature 20 ± 1°C and with the chlorinity 14.42 ‰.

(4) By using the relationships obtained in (2) and (3), the mean lives of various radius of foam are calculated. Foams with diameters less than 0.2 mm are the most unstable ones, coagulate with each other, and then grow up.

§1. 緒　言

先に，筆者は海水泡沫層の崩壊が一次化学反応の形式で行われることを発表した。この崩壊の際，求まる崩壊恒数，半減期等を用いて，海水泡沫層の安定度等を多少論じた。

今回は，この崩壊の際，定時間毎に撮影した泡沫層写真を基にして，定時間毎に泡粒

子の大きさの頻度分布を求め，これから，泡沫層内の種々の大きさの泡粒につき，平均寿命を計算してみた。又，この種々の大きさの粒子が次第に成長して行き，終に崩壊する形式についても考察してみた。尙，この取扱いは，14.42‰ Cl の海水の 20±1°C の場合につき行つた。併し，我々が従来発表してきた，泡沫性に対する液の濃度及び温度の影響等の関係を考慮すれば，他の濃度及び温度の場合の泡沫層についても大略の様相は知れよう。次に結果の大略を述べる。

§2. 海水泡沫層の時間的変化

a) 境界面の時間的変化

我々の取扱つている泡沫層には一般に，次の二面が考えられる。即ち，

1. 液体（即ち，現在は海水）に接する面
   {y_2 面と呼び，坐標 y_2 にてその位置を示す}
2. 気体（即ち，現在は空気と水蒸気）に接する面
   {y_1 面と呼び，y_1 にてその位置を示す}

この y_1, y_2 は一般に異つた速度で変化して行くが，直ぐにわかる如く，泡沫層が崩壊するため y_1 は下降即ち減少して行き，これとは反対に泡沫が液に変つて行くため，y_2 は上昇即ち増加して行くのである。この二面の時間的変化を図示したのが Fig. 1 である。ここで横軸に時間（sec）をとり，縦軸に界面の位置（mm）をとつた。図から明かな如く，y_1, y_2 は時間と共に指数函数的に変化する。即ち，一般にこれ等界面の位置を y で表わせば $y=y_0e^{kt}$ の形になる。ここに y_0 は最初の y の位置，k は恒数，t は時間とする。この y の代りに $\log y$ をとつたのが Fig. 2 である。これから，y の函数形を求めると次の如くなる。

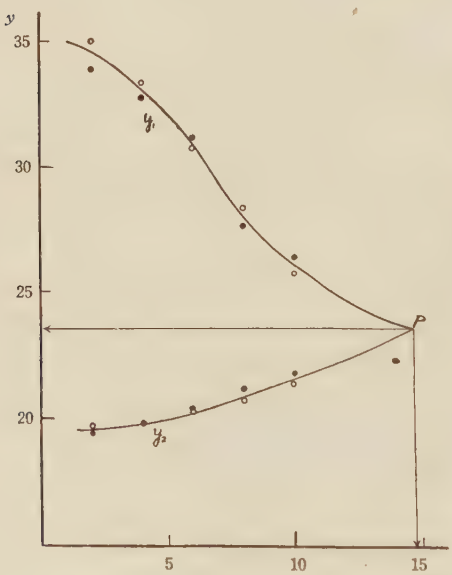

Fig. 1.

$$y_1=y_{0.1}e^{k_1t}=37.5\,e^{-0.0328\,t} \qquad (1)$$

$$y_2=y_{0.2}e^{k_2t}=19.0\,e^{+0.0146\,t} \qquad (2)$$

ここに $y_{0.1}, y_{0.2}$ は夫々最初の y の位置を示し，k_1, k_2 は恒数であり，変化の程度を示す量である。

明らかに $k_1<0$, $k_2>0$ である。(1), (2) から，直ぐわかる如く，

$|k_1|>|k_2|$ であり

$|k_1|/|k_2|\fallingdotseq 2.25$ である。

即ち，y_1 面の変化の方が，y_2 面の変化より甚だしいことがわかる。この変化を更に明瞭に

するため，(1)，(2) 式を t につき微分すると

(1) より $$\frac{dy_1}{dt}=-k_1g_1y_{0.1}e^{k_1t}=-37.5\times0.0328\,e^{-0.0328\,t} \qquad (1')$$

(2) より $$\frac{dy_2}{dt}=k_2y_{0.2}e^{k_2t}=19.0\times0.0146\,e^{0.0146\,t} \qquad (2')$$

依つて $$\frac{dy_1}{dt}-\frac{dy_2}{dt}=\frac{37.5\times0.0328}{19.0\times0.0146}e^{-0.0474\,t}\fallingdotseq4.44\,e^{-0.0474\,t}$$

これを σ と置けば，

$$t=0 \quad \text{のとき} \quad \sigma=4.44$$

Fig. 2 から明かである如く，$t=14.7$ sec にて $y_1=y_2$ であり，泡沫層は，14.7 sec で完全に消え去つて了うのであるから，$t=14.7$ sec における σ を求めると

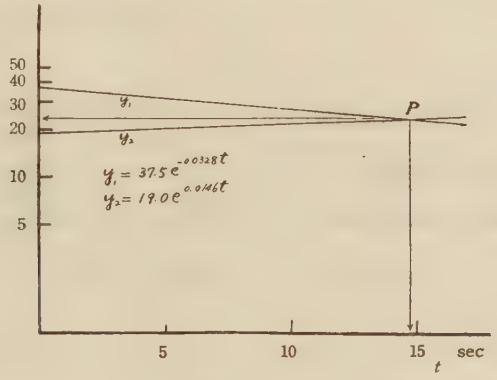

Fig. 2.

$$\sigma_{14.7}=4.44\,e^{-0.0476\times14.7}\fallingdotseq4.44\times0.5=2.22$$

即ち，t の値如何に関らず次の関係が成立つ

$$4.44\geqq\sigma\geqq2.22$$

即ち，y_1 面は y_2 面に比較し非常に早く変化し，初期では y_2 の変化の 4 倍強の速さであり，末期でも 2 倍強の速さ変化するわけである。この y_1 と y_2 とを組合すと前報で述べた，所謂，泡沫層の高さ，即ち泡高 (h) が求まるわけである。

即ち， $$h=y_1-y_2=h_1e^{-k_1t}-h_2e^{k_2t}=h_0e^{-kt}=18.5\,e^{-0.131\,t} \qquad (3)$$

ここの記号は従来の形式通りとする。

b) 頻度分布の時間的変化

従来通りの方法によつて，2 sec 毎に撮影した泡沫層を引伸し拡大した写真より，計測して，2 sec 時，4 sec 時等，2 sec 毎における泡粒の頻度布図を作ると，Fig. 3 の如くなる。泡粒の計測は直径 0.2 mm 毎にその数を数えた。又各範囲内の中央値を以つて，その範囲内の泡粒を代表させることにした。例えば，直径 0～0.2 mm まで範囲の泡粒の頻度を求めたときは，その値を以つて，その範囲の中央値直径 0.1 mm の頻度とした。尚，図

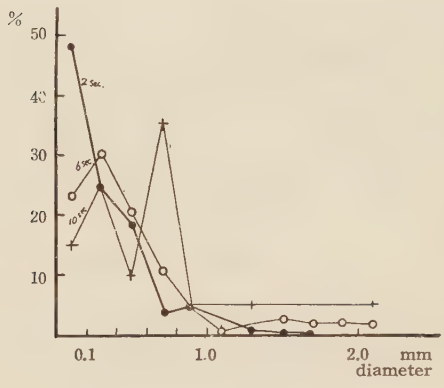

Fig. 3.

が重なつて不明瞭になることをさけるため，図には便宜上，2 sec, 6 sec 及び 10 sec の頻度分布だけを掲げた。この図から明かな如く，各時刻において，頻度の極大値が存在し，その極大値を示す泡粒の大きさが，時間の経過と共に，次第に大きくなつて行くことがわかる。これは Table 1 を見ると更に明かである。即ち，表では，時刻 2 sec にては 0.1 mm 辺が頻度の極大値を示し，48.0% であり。略々，存在する泡粒の半数が直径 0～0.2 mm 内の微小泡粒である。時間が経過して 6 sec になると，この極大頻度を示す直径は増して 0.3 mm

Table 1.

Time	2 sec	6	10
Diameter of at max. frequency	0.1 mm	0.3	0.7
Max. frequency	48.0%	30.5	35.0

になり，30.5% となる。更に時間が経過して 10 sec に到ると，この直径は更に増大して 0.7 mm になり 35% になつて了う。

次に，この図を基にして，ある特定の大きさの泡粒の数が時間的に如何に変化するかを求めてみる。今，例えば，泡粒直径 0.2 mm につき，各時刻毎の頻度を求め，求まつた値を頻度と時刻とを夫々坐標軸とした図上にプロツトすれば，Fig. 4 の如くなる。直径 0.2 mm より 2.0 mm までについて作図したが，図には，重複して不明瞭になるのをおそれて 0.2 mm, 0.6 mm, 1.0 mm 及び 2.0 mm の場合だけを掲げた。

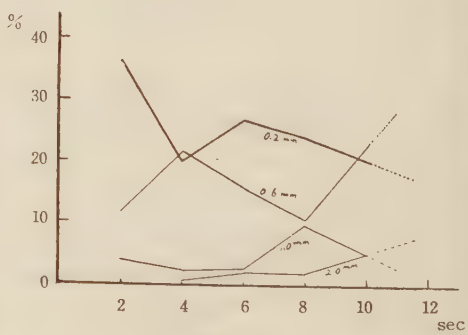

Fig. 4.

今，時刻 n sec における頻度を p_n で表わすことにし，便宜上，奇数時刻につき，泡粒の大きさと p_n との関係をこの図から求めると Table 2 の如くなる。Fig. 4 及び Table 2 から顕著なことは，時間の経過と共に，次第に頻度は減少するとは云え，0.2 mm までの泡粒のものは比較的多量（約 20% 位）に，常に存在する。0.4～0.6 mm のものは比較的多量に存在するが，時間的の変動が大であり，崩壊末期に到るにつれて反つて増加する傾向さえある。更に大粒の 1.8 mm～2.0 mm のものは，崩壊途中から生産され，絶対量は比較的少ないが，時間と共に増加している。

c) 平均半径の時間的変化

前2節で泡粒が時間的に，互に結合又は凝集して成長して行くことは明かであるので，ここでは其の変化の様相の一端として，平均半径の時間的変化を求めてみることにした。便宜上，これまでの方法と趣を多少変え，或る時刻における平均半径 $\bar{r}$ として $\sqrt{\frac{\sum n_i r_i^2}{\sum n_i}}$ で算出することにした。ここに r_i は半径，n_i はその個数である。斯様な平均半径を各時刻につき求めると，時間 t と $\bar{r}$ との間には次の関係が実験的に成立つ

$$\bar{r}=0.33+0.018\,t\ \text{mm} \qquad (4)$$

但し，　　海水　14.42‰ Cl　　温度　20±1°C

未だ，計算は全部終つてはいないが，他の濃度，温度においても同様な，t につき一次の関係が成立つらしい。

§3. 泡粒子の平均寿命

次に，前章で得られた結果を利用して，泡沫層中に存在する種々の大きさの泡粒につきその平均寿命を計算してみる。原理の大略は次の通りである。

一定温度，一定濃度の海水を振盪して生成された泡沫層の等時間毎の泡粒の頻度分布を Fig. 5-A とする。ここに d は泡粒の直径，p はその頻度である。t_1, t_2 及び t_3 は夫々接近した時刻を示し，$t_1<t_2<t_3$ であり，$t_2-t_1=t_3-t_2\{=2\delta$ とおく$\}$ であるとする。

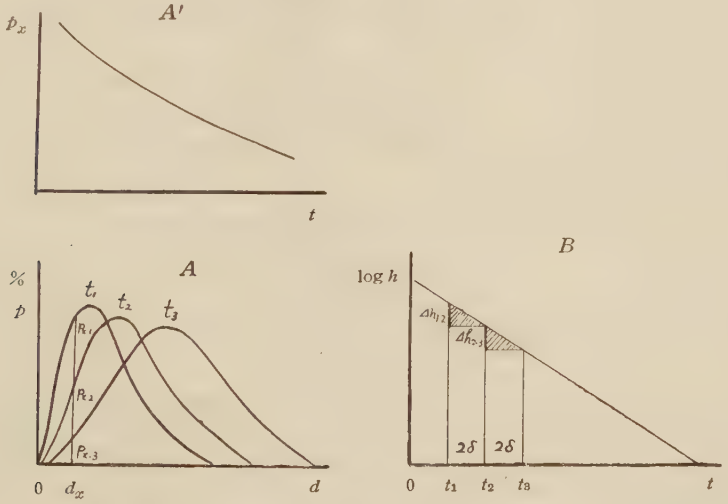

Fig. 5.

今，平均寿命を求めようとする泡粒を d_x とし，A 図から，各時刻における頻度を

t_1　では　$p_{x\cdot1}$

t_2　では　$p_{x\cdot2}$

t_3　では　$p_{x\cdot3}$

として，これ等を A 図より求めると，d_x に関する頻度の函数形が t の函数として $p_x(t)$ が求まる (A' 図)。一方，これまでの実験結果として，泡高を h とすれば，$\log h$ は t の経過と共に，一次的に減少する故，この関係を図示すれば，Fig. 5-B の如くなる。

今，t_1, t_2 及び t_3 における h を夫々 h_1, h_2 及び h_3 とすれば

$$h_1 = h_0 e^{-kt_1}$$
$$h_2 = h_0 e^{-kt_2}$$
$$h_3 = h_0 e^{-kt_3}$$

である。ここに h_0 は $t=0$ の h の値である。

さて，
$$h_2 - h_1 = \Delta h_{1\cdot 2}$$
$$h_3 - h_2 = \Delta h_{2\cdot 3}$$

とおけば，$\Delta h_{1\cdot 2}$ 及び $\Delta h_{2\cdot 3}$ は夫々 t_1 から t_2 までの間，及び t_2 から t_3 までの間の泡高の減少を示し，斜線をほどこした面積は，この間に崩壊した泡沫数に比例する。今，この間に崩壊した数を夫々 $n_{1\cdot 2}, n_{2\cdot 3}$ とおけば

$$n_{1\cdot 2} = K \cdot \Delta h_{1\cdot 2} \cdot 2\delta / (\bar{d}_{1\cdot 2})^2$$
$$n_{2\cdot 3} = K \cdot \Delta h_{2\cdot 3} \cdot 2\delta / (\bar{d}_{2\cdot 3})^2$$

ここに，K は比例恒数，$\bar{d}_{1\cdot 2}, \bar{d}_{2\cdot 3}$ は夫々 t_1, t_2 間，t_2, t_3 間の平均泡沫直径である。

故に
$$\frac{n_{2\cdot 3}}{n_{1\cdot 2}} = \frac{\Delta h_{2\cdot 3} \cdot 2\delta / (\bar{d}_{2\cdot 3})^2}{\Delta h_{1\cdot 2} \cdot 2\delta / (\bar{d}_{1\cdot 2})^2} \tag{5}$$

所が，明かな如く

$$\frac{\Delta h_{2\cdot 3}}{\Delta h_{1\cdot 2}} = e^{-2k\delta}$$

であるから，(5) は次の如くなる

$$\frac{n_{2\cdot 3}}{n_{1\cdot 2}} = e^{-2k\delta} \cdot \frac{(\bar{d}_{1\cdot 2})^2}{(\bar{d}_{2\cdot 3})^2} \tag{6}$$

又は
$$n_{2\cdot 3} = e^{-2k\delta} \cdot \frac{(\bar{d}_{1\cdot 2})^2}{(\bar{d}_{2\cdot 3})^2} \cdot n_{1\cdot 2} \tag{6'}$$

同様にして
$$n_{3\cdot 4} = e^{-2k\delta} \cdot \frac{(\bar{d}_{2\cdot 3})^2}{(\bar{d}_{3\cdot 4})^2} \cdot n_{2\cdot 3}$$

故に，一般に

$$n_{s(s+1)} = e^{-2k\delta} \cdot \frac{(\bar{d}_{(s-1)\cdot s})^2}{(\bar{d}_{s\cdot(s+1)})^2} \cdot n_{(s-1)\cdot s} \tag{7}$$

なる所謂，漸化式が成立つ。

次に特定の大きさの泡粒の平均寿命を考えてみる。$t_1 \sim t_2$ 間で崩壊した泡沫数 $n_{1\cdot 2}$ の内で大きさ d_x の泡粒の数は $n_{1\cdot 2} \cdot p_x$ で与えられ，これ等は $\frac{1}{2}(t_1+t_2)$ 即ち $(t_1+\delta)$ 時間の寿命があつたと考えられる故，確率論における希望値の考えから，泡粒 d_x の寿命を τ_x とすれば，次の関係が成立つ

$$\tau_x = \frac{\int_0^T t \cdot n_t p_x \cdot dt}{\int_0^T n_t \cdot p_x \cdot dt} \tag{8}$$

ここに T は泡沫層が完全に消え去る時間であり，n_t は t における泡粒の個数である。

(7) 式を取扱いの便宜上，次の如き形式に改める

$$\tau_x = \frac{\sum t_i \cdot n_i \cdot p_i}{\sum n_i \cdot p_i} \tag{8'}$$

而して，(4), (6) 式及び Table 2 を用いて (8′) 式より τ_x を計算するのである。

Table 2.

Diameter	0～0.2 mm	0.2～0.4	0.4～0.6	0.6～0.8	0.8～1.0	1.4～1.6	1.8～2.0
p_3	28.2%	22.2	16.5	7.1	3.0	1.1	—
p_5	23.3	24.2	18.5	8.8	2.2	2.0	1.2
p_7	25.4	22.0	13.0	7.9	6.0	3.0	1.8
p_9	22.0	17.5	16.5	13.8	7.4	4.4	3.5
p_{11}	18.4	15.4	28.7	24.4	2.8	5.8	6.8

今，計算例として $d_{0.1}$ mm の場合を示せば次の如し。

	崩壊する数（$n_i \cdot p_i$ に相当する）	$t_i \cdot n_i \cdot p_i$ に相当する
2～ 4 sec	$n_{2.4} \cdot p_3 = e^{-2\lambda\delta} \cdot \frac{(\bar{d}_{0.2})^2}{(\bar{d}_{0.4})^2} \cdot n_{0.2} \cdot p = 18.0 \cdot n_{0.2}$	$3 \cdot n_{0.2} \cdot 18.0 = 54.0 \cdot n_{0.2}$
4～ 6	$n_{4.6} \cdot p_5 = 0.411 \cdot n_{0.2} \cdot p_5 = 9.57 \cdot n_{0.2}$	$5 \cdot n_{0.2} \cdot 9.57 = 47.85 \cdot n_{0.2}$
6～ 8	$n_{6.8} \cdot p_7 = 0.270 \cdot n_{0.2} \cdot p_7 = 6.85 \cdot n_{0.2}$	$7 \cdot n_{0.2} \cdot 6.85 = 47.95 \cdot n_{0.2}$
8～10	$n_{8.10} \cdot p_9 = 0.178 \cdot n_{0.2} \cdot p_9 = 3.92 \cdot n_{0.2}$	$9 \cdot n_{0.2} \cdot 3.92 = 35.28 \cdot n_{0.2}$
10～12	$n_{10.12} \cdot p_{11} = 0.118 \cdot n_{0.2} \cdot p_{11} = 2.17 \cdot n_{0.2}$	$11 \cdot n_{0.2} \cdot 2.17 = 23.87 \cdot n_{0.2}$
∴	$\sum n_i \cdot p_i = 40.51 \cdot n_{0.2}$	$\sum t_i \cdot n_i \cdot p_i = 208.95 \cdot n_{0.2}$

$$\therefore \quad \tau_{0.1} = \frac{\sum t_i \cdot n_i \cdot p_i}{\sum n_i \cdot p_i} = 5.16 \text{ sec}$$

同様にして，他の大きさの泡粒につき計算した結果を表にすれば，Table 3 の如くなる。

Table 3.

Size	0～0.2 mm	0.2～0.4	0.4～0.6	0.6～0.8	0.8～1.0	1.4～1.6	1.8～2.0
life	5.16 sec	8.06	5.65	6.42	6.06	6.99	8.50

Table 3 から明かな如く粒径 0～0.2 mm の泡粒は平均寿命 5.16 sec で最も短命であり，1.8～2.0 mm のものが 8.50 sec で最も長命である。概して，粒径の大きなもの（1.4 mm 以上のもの）程，寿命は長くなつている。併し 0.2～0.4 mm のものも比較的長命である。次に以上の結果をもとにして泡粒の性質につき多少考えてみる。

現在取扱つている泡沫層が全部崩壊し去る時間は約 15 sec である。所が 0～0.2 mm

径のものの平均寿命は 5.16 sec であり，この種の大きさの泡粒は泡沫層中に常に存在する所から考えると，この大きさの泡粒は非常に活潑で，よく互に凝集し合い，泡粒は盛に成長して行く。他方，比較的大粒のものが破裂する時等には，新しくこの範囲の大きさの泡粒が再生産もされるものらしい。海水の表面張力を σ，粒の半径を r，粒の内外の圧力を夫々 p_i, p_0 であるとすると，周知の如く $p_i - p_0 = \frac{4\sigma}{r}$ であるから，この圧力差 $(p_i - p_0)$ は r に逆比例することからも，r の小さな泡粒は不安定であり，従つて活潑になることもうかがい知れる。0.2～0.4 mm の泡粒のものが比較的長命であるのは興味あることである。次に大粒のものの絶対的の数は小さいが，時間と共に或る限度まで増加して行くことは，比較的小粒のものが凝結して成長して行くことを示すのであろう。

この泡粒の成長につき，凝結個数の点を考えてみる。今，或る時刻の泡沫層内の泡粒の平均の半径を r とし，これ等同志が互に n 個宛結合して，平均半径が R になつたとする。但しこの結合の際，泡粒内の気体は外部へは逃げ出さず，全部次の大きな泡粒を造るに使われると仮定すれば，次の式が成立つ

$$n \cdot \frac{4}{3}\pi r^3 = \frac{4}{3}\pi R^3$$

或は

$$R^3 = nr^3$$

$$\therefore \quad \frac{R}{r} = n^{1/3} \tag{9}$$

この n を 3 sec から 5 sec の間の変化につき計算してみると．Table 4 の如くなる。n としては元来 2 より大なる正の整数であるから，計算の結果から n に最も近い正整数をと

Toble 4,

Conc.	k/r	3 sec～5 see		n	Sea water temp. 20°±1°C	
		$\log k/r$	$3 \log k/r$		n's round number	r mm
9.63 ‰ Cl	1.30	0.1139	0.3417	2.197	2	0.550
12.82	1.32	0.1206	0.3618	2.300	2	0.40
14.42	1.31	0.1173	0.3519	2.249	2	0.39
16.05	1.18	0.0719	0.2157	1.644	2	0.37
18.46	1.12	0.0492	0.1476	1.405	2	0.32
19.26	1.12	0.0492	0.1476	1.405	2	0.33

ると大体2になる。即ち結合は2個づつ行われるのが最も probable であるらしい。勿論，結合の過程が仮定通りには行われないだろうし，r と R との時間々隔が，その時取扱つている泡粒子の寿命に比して不適当であること等で，n としては奇麗な値は得られないのだろう。特に海水濃度が大になると，例えば，18.46, 19.26 ‰ Cl になると，n の値は小さくなつて了う。やはり，凝結の問題等を取扱う場合，時間尺度に関しては，泡粒の大きさ，寿命等できまる適当な時間尺度で測ることが必要であろう。熱力学でよく知られた Van der Waals の状態式を適当に変形すると物質による常数の現われない各物質に共通の形

になる（所謂，対応状態の考えを導入したのである）。又，卑近な例であるが，生物の成長等を取扱う場合に，生物個有の寿命を一応の尺度の標準として，これの何分の一かで測定することにし．所謂，同一対応時間で各生物の状態等を比較検討すれば便利であろう。

§4. 結　語

以上，要約すれば，

海水泡沫層について，次の諸点を明かにした。

（1） 境界面の内，海水に接する面と，空気（水蒸気で満たされている）に接する面の位置坐標を夫々 y_1, y_2 とし，時間を t とすれば，

$$4.44 \geqq \left|\frac{dy_1}{dt}\right| \Big/ \left|\frac{dy_2}{dt}\right| \geqq 2.22$$

である。即ち，y_1 面は y_2 面に比較し変化が速かであり，崩壊初期では約4倍強であり，末期でも 2 倍強の速さである（§2. a）。

（2） 各時刻における泡粒の大きさの頻度分布を作ると，各時刻において極大の頻度を示す泡粒があり，この極大頻度を示す泡粒は，時間と共に或る限度まで大きくなる（§2. b, Fig. 3, Table 1）。

（3） 平均半径は時間につき一次の関係で増大して行く，

$$\bar{r} = 0.33 + 0.018\, t \text{ mm}$$

ここに，r は平均半径，t は時間である。但し，これは 14.42 ‰ Cl の海水で，温度 20±1°C の場合である（§2. c）。

（4） (2), (3) で得られた関係を用い，種々な泡粒につき平均寿命を計算した。直径 0～0.2 mm のものが最も不安定で，寿命は 5.16 sec であり，一般に泡粒が大になると，或る限度まで比較的寿命は長くなる。1.8～2.0 mm のものは 8.5 sec である。泡粒の寿命に関聯して，その凝結及び成長の様相等につき多少の考察を行つた（§3. Table 3）。

終りに臨み，本研究に興味を持たれ，屢々有益な御教示を頂いた海洋研究室長中野猿人先生に厚く御礼申上げる。又，計測用の写真の引伸の労を快くとられた金沢五寿雄技官に深謝する。

参　考　文　献

（1） Y. MIYAKE and T. ABE: Journ. Mar. Res., Vol. VII, No. 2 (1948).

（2） 阿部友三郎： 中央気象台海洋報告，3 巻 1 号，昭和 28 年.

Reprinted from the *Papers in Meteorology and Geophysics* Vol. IV Nos. 3~4, 1953
Published by the Meteorological Research Institute

On the Result of Wave Observations at Jogashima Island and Its Application to Wave Forecasting (I)

by

M. Nakano,

S. Unoki and Y. Kuga

Published by the Meteorological Research Institute,

Mabashi, Suginami, Tokyo, Japan

December 1953

551.465 : 551.55

On the Result of Wave Observations at Jogashima Island and Its Application to Wave Forecasting (I)

by

M. Nakano,

Meteorological Research Institute

S. Unoki and Y. Kuga

Central Meteorological Observatory

(Received October 13, 1953)

Abstract

Some investigations were made on the wave height and wave period of wind waves and swells, based on the data of continuous observation of ocean waves with a self-registering wave gauge at Jogashima Island, Kanagawa Prefecture, Japan, duriug a year from September, 1951 to August, 1952. and the characteristics of variations of wave height and wave period and their relations to meteorological conditions were made clear. These results of analysis are also available for forecasting ocean waves. The variations of wave height and wave period can be classified into six types as shown schematically in Fig. 5, and each of these types corresponds to a particular meteorological change. The points which have become known up to now are as follows:

1) In case a cyclone moves eastward on the Pacific side of Honshu, Japan, the change of wave of "Type I" or "Type II" occurs at Jogashima Island, and the positions of the cyclonic centre at the time when the waves begin to become high, at the time when the wave height becomes maximum and at the time when the waves begin to decay at Jogashima Island are shown in Fig. 8. Again, the positions of the cyclonic center at the time when the wave period becomes maximum are shown in Fig. 9. Further, the maximum wave height, the duration of higher waves, etc. and their relations to the intensity and distance of the cyclone are shown in Figs. 10~12.

2) In case a cyclone moves eastward on the Japan Sea side of Honshu, the change of waves of "Type III" or "Type

IV" occurs at Jogashima Island, and the maximum wave height, the duration of higher waves, etc. in that case, are shown in Figs. 16~19.

3) In case a migratory anticyclone covers Honshu, the change of waves of "Type V" or "Type VI" occurs at Jogashima Island. And Fig. 23 shows the extent of area covered by this migratory anticyclone when the sea is calm at Jogashima Island.

4) In case the station under consideration is within the sphere of influence of Ogasawara Anticyclone, the change of waves is complicated, depending upon the nature of the sphere of influence. In this case, the change of waves of "Type V" or "Type VI" generally occurs, with incidental occurrence of the change of "Type III". And we can see from Fig. 25 the extent of area under the influence of this anticyclone when the sea is calm at Jogashima Island.

1. Introduction

Since 1951, ocean wave observations have been made by the Central Meteorological Observatory of Japan with self-registering wave gauges at Jogashima Island in Kanagawa Prefecture, Omaezaki in Shizuoka Prefecture, Choshi in Chiba Prefecture and Hachijo Island (Fig. 1). The present paper reports on a part of the results obtained by analysing the data of observations at Jogashima Island during the year from September 1951 to August 1952.

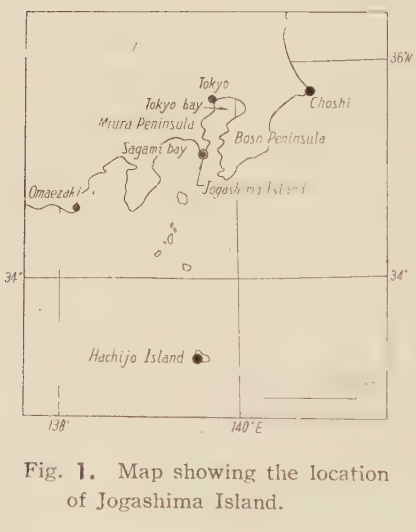

Fig. 1. Map showing the location of Jogashima Island.

Since SVERDRUP and MUNK's excellent paper [1] was published, investigations on the theory of ocean waves and its application to quantitative wave forecasting have been very striking. Recently, NEUMANN [3] has also published an interesting paper. However, in practising wave forecast by their methods, the accurate determination of wind direction, wind speed, fetch and duration is necessary, but it is difficult to determine these quantities uniquely. Again, according to their methods, wave forecast where the wind changes with time is very difficult. In the neighbourhood of Japan, for instance, the change of cyclones and anticyclones is frequent, and accordingly the change of ocean waves is also complicated and rapid, so that it is

fairly difficult to practise quantitative wave forecast. In order to avoid these difficulties, we have first made a continuous observation of ocean waves, and investigated their time-variation.

Fig.1 shows the position of Jagashima Island where the observation was made. As seen from this figure, Jogashima Island is located at the southern end of Miura Peninsula where Tokyo Bay meets Sagami Bay, and those waves observed there that come from the south represent with comparative correctness the state of wave in the open sea, but it is not the case with other waves.

Now, refraction diagrams were drawn on a supposition that a train of waves of the period 10 seconds or of the wave length 156 m off shore approaches from

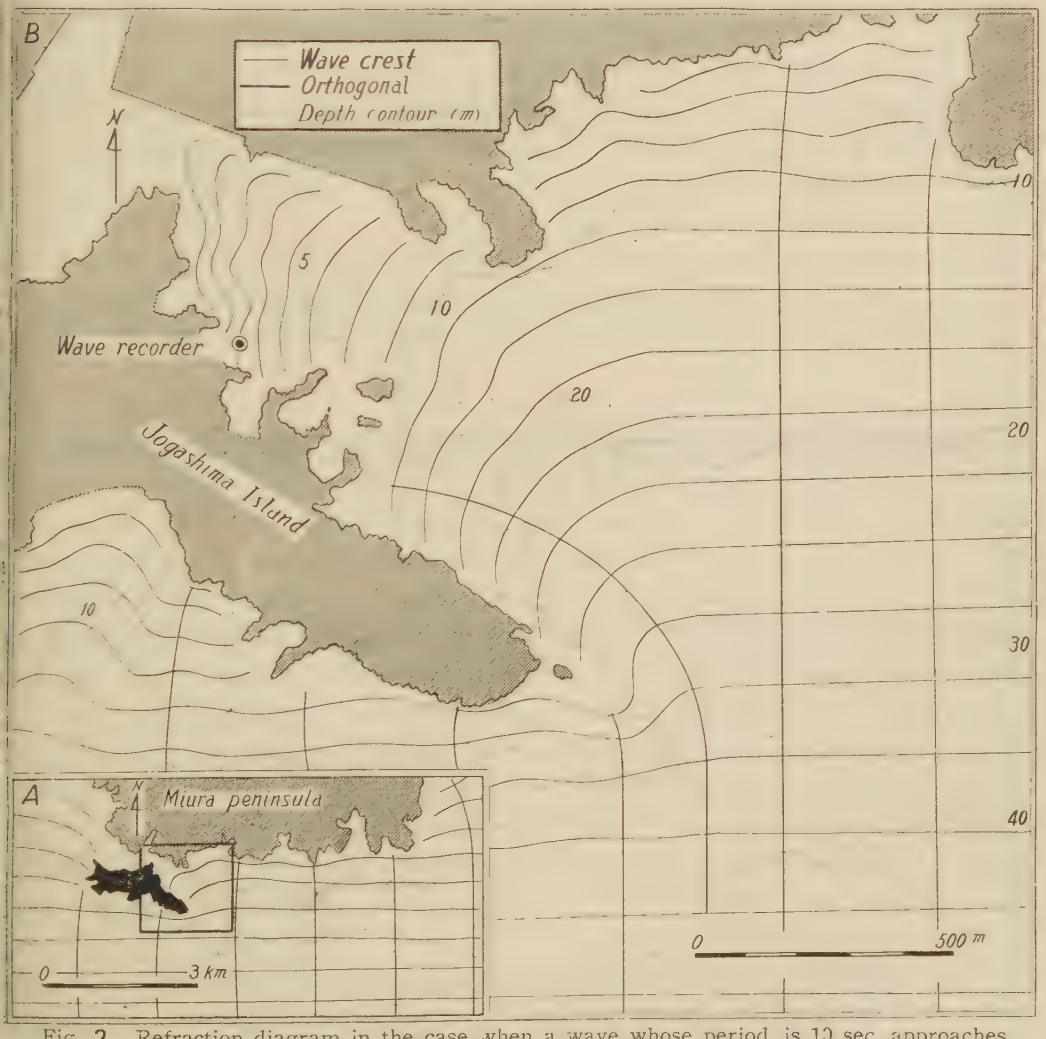

Fig. 2. Refraction diagram in the case when a wave whose period is 10 sec approaches Jogashima Island from the south; in (A) crest interval means four wave lengths, and in (B) one wave length.

the south toward Jogashima Island, and are shown in Fig. 2, where thin full lines represent the wave crests ("crest lines"), thick full lines the "orthogonals", and dotted lines the depth contours. In Fig. 2 (A), the crest lines are drawn at the interval of four wave-lengths, while in Fig. 2 (B) at the interval of one wave-length. As seen from Fig. 2 (B), a sudden refraction of waves or great divergence of orthogonals is occurring in the vicinity of Jogashima Island. If we assume that the wave energy within two adjoining orthogonals is conserved, and that the wave height varies as the square root of the mean wave energy per unit area (Hydrographic Office, U.S. Navy [4]), the wave height in the vicinity of the wave gauge would be reduced to about several percent of the height in the open sea. As a matter of fact, however, the reduction of the wave height is of the order of one-fifth or thereabouts, showing that the above assumption does not hold good and that the effect of diffraction is considerable. As for the refraction and diffraction of actual waves in such a complex sea or day as this, mere calculation can not be expected to solve the problem; we have no choice but to rely on actual observations, and the present authors intend to make such observation when they get a chance.

At any rate, the waves observed at Jogashima Island are fairly local ones, and it is somewhat difficult to compare these with those observed in the open sea, nevertheless it is considered that a general tendency of the latter can be inferred from the former.

2. The method of observation and the instrument

The apparatus of observation is constructed as follows: At a point in the sea about 50 m distant from the beach, where the depth of water is about 2 m at low tide, an iron pipe of about 5 cm inside diameter and of about 4 m length, closed at the upper end and open at the lower, was erected vertically, the lower end of the pipe being situated about 50 cm above the bottom of the sea. To the upper end of this pipe, a small cylindrical mouthpiece is attached horizontally, and a thick rubber tube of about 0.7 cm inside diameter and of about 50 m length connects this mouthpiece with the wave gauge, which is of the pressure recorder type, set up on the shore. Thus, when the height of the sea level changes with wind waves, the pressure change within the pipe induced thereby is transmitted to the bellows of the wave gauge through the rubber tube, and is recorded mechanically. It is to be mentioned here that the "time-lag" of the present instrument is 0.5 sec or so, which is not large.

Fig. 3 shows a schematical view of the apparatus. A represents the iron pipe, B the wave gauge, C the rubber tube, and D a slow-leak device with a capillary glass tube, which is attached in order to eliminate the wave of longer periods such as tides, etc.

Now, two types of wave gauges were used in the present observation. One was designed by Y. Ota [5] of Omaezaki Weather Station (to be called "Pattern I"), the other was reconstructed from a statoscope, which is in ordinary use for recording microbarographic oscillations (to be called "Pattern II"). The wave gauge of "Pattern I" is equipped with two kinds of recording drums, which are interchangeable with each other; one rotates once a day, the other once in 5 minutes. (A) and (B) of Fig. 4 respectively show the examples of wave records obtained by means of the 5-minute and the one-day rotating drums. However, as the wave gauge of "Pattern I" was unfit for continuous observing of variations of wave height and wave period

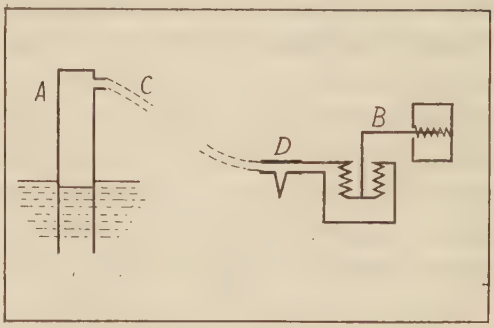

Fig. 3. Schematical view of the wave gauge.

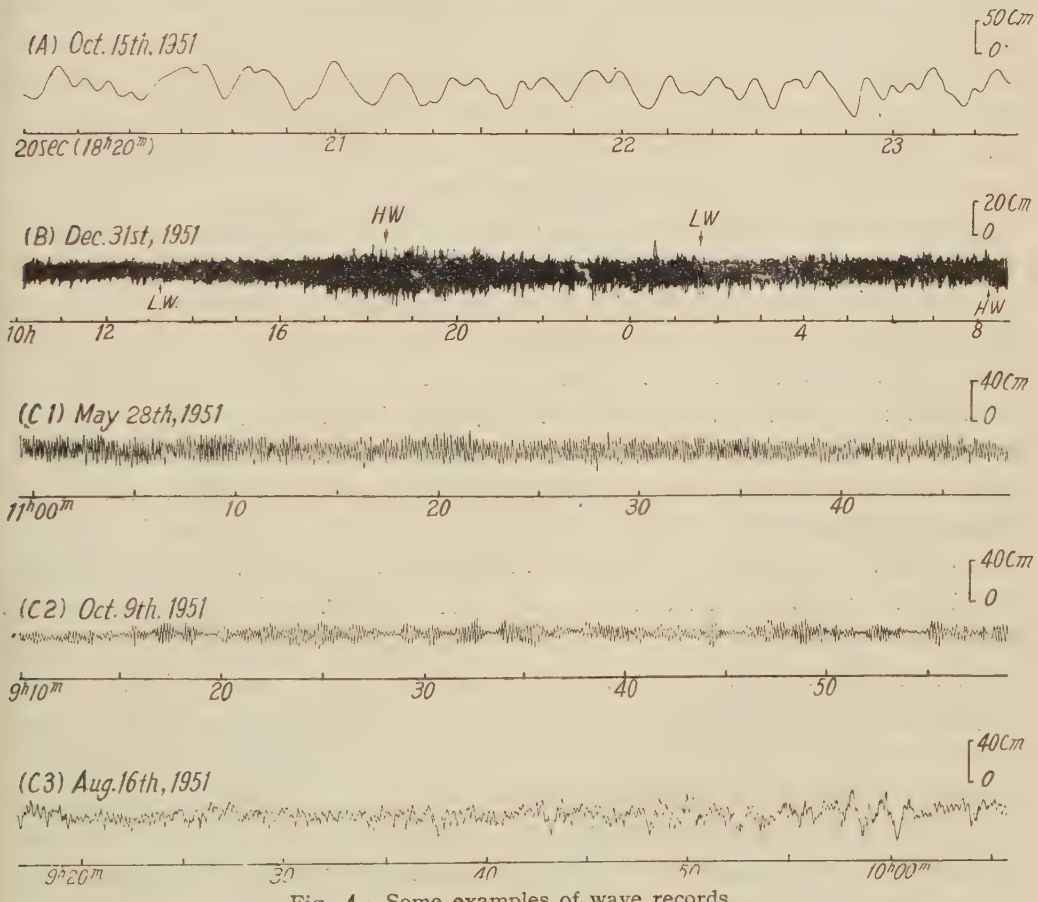

Fig. 4. Some examples of wave records.

lasting many hours, the wave gauge of "Pattern II" was coustructed and used afterwards. This instrument was, as mentioned above, reconstructed from a statoscope, and the recording part of it is designed as follows: The curve which graphically represents the pressure change, corresponding to the rise and fall of the sea level, is automatically traced by a fountain pen on a roll of paper, which is sent out from an idler roller and is wound upon a uniformly rotating drum at a speed of about 33 cm per hour. This device is capable of obtaining a continuous record of waves lasting about half a day. Fig. 4 (C) shows a part of such records.

3. Observed data and the method of analysis

It was on the 1st of September, 1951, that the present wave observation was commenced at Jogashima Island. At first, the observation was made with the wave gauge of "Pattern I" alone, but after the middle decade of March, 1952, the wave gauge of "Pattern II" was also used. The observational data used for the analysis are those for one year from September, 1951, to August, 1952. For the former period, i.e. before the middle decade of March, 1952, when the wave gauge of "Pattern II" was not yet used, the wave-period data used are only those of the observations, each covering about 5 minutes, usually taken once a day, while the wave-height data used are those of continuous observation. For the latter period, i.e. after the middle decade of March 1952, the data used are those of continuous observations both for wave height and wave period.

Now, as seen from Fig. 4 (A), the form of the waves appearing on the self-registering wave gauge is very complex, being neither a mere sine curve nor a trochoid, and the wave height and wave period of successive waves never change continuously but fluctuate rather irregularly. So it is difficult to determine the wave height and wave period at a given time correctly, and hence, for convenience' sake, the maximum wave height appearing in an interval of 10 minutes previous to a certain time was adopted as a measure of the wave height corresponding to that time, and also the mean wave period taken for the same interval of 10 minutes was regarded as the wave period corresponding to the time in question. Accordingly, some difficult points exist as to the wave period. For instance, the actual waves are composed of many waves of different periods and origins, so that, strictly speaking, investigations should be made by using the result of periodogram analysis. Unfortunately, no wave-analyser could be used, so in the present investigation the mean wave period as mentioned above was adopted. And, as it is usual that in a wave record a certain wave period prevails, the said mean wave period was obtained by watching such a prevalent one. Although this method is not free from its defects it will enable us to know the general state of things. Moreover, the wave height and wave period were read off every three hours in the case of the wave gauge of "Pattern I," and hourly in the case of "Pattern II."

Fig. 4 (B) shows an example of wave records obtained by a one-day rotating drum, where the effect of the tide is seen, namely, the wave height tends to become larger at high water, and smaller at low water. As regards this variation, we may mention two causes of it; namely, one is a mechanical cause depending upon the construction of the wave gauge, and the other is the fact that the wave height actually changes with the ebb and flow of the tide. As these effects are difficult to eliminate perfectly, care must be taken when we treat the wave height.

Fig. 4 (C2) shows an example of wave records, where the phenomenon of "beat" is conspicuously occurring. It is an interesting problem waiting for future investigation to know in what cases such a phenomenon occurs.

Fig. 4 (C3) shows an example of wave records, where longer waves of the period about 1~3 minutes occur, superposed on ordinary wind-waves or swells. M. NAKANO [6], one of the present authors, formerly discussed the waves of the period about 1~3 minutes which sometimes appear on tide gauge records, but it is not yet clear whether the said longer waves of about 1~3 minute period are of the same nature as what he calls "very long swells" or as what W.H. MUNK [7] calls "surf beats", or in other words, whether the said longer waves came out from the vicinity of a cyclonic centre or were produced near the seashore, a problem which also requires future investigation. Besides, some tsunamis (seismic sea waves) were also recorded on our wave gauge.

Now, if we construct the diagrams showing the variations of wave height and wave period, we can see that these variations can be classified into several types, and that each of these types corresponds to a particular meteorological change. Thus, the variations of wave height and wave period were classified into six types (Type I~Type VI) as shown schematically in Fig. 5. In this figure the abscissa represents the time, the full line H the variation of wave height, and the dotted line T the variation of wave period; the broken line D represents, in the cases of "Type I" and "Type II", the distance of Jogashima Island from the cyclonic centre for each value of time, while in the cases of "Type III" and "Type IV", where a cold front stretching from NE to SW moves eastwards, it means the shortest distance from Jogashima Island to the cold front, thus the point of intersection of the curve D with the axis of time corresponding to the instant when the cold front passes Jogashima Island. For instance, the change of waves of Type I occurs when a cyclone moves eastwards along the Pacific coast of Honshu, and we can see from the figure that both the wave height and the wave period become maximum when the cyclonic centre comes nearest to the station. If a cyclone moves eastwards on the Japan Sea side of Honshu, the change of waves of Type III or Type IV occurs.

Now, from the standpoint of the passing of cyclones and anticyclones, the meteorological changes occurring in the neighbourhood of Japan may be classified

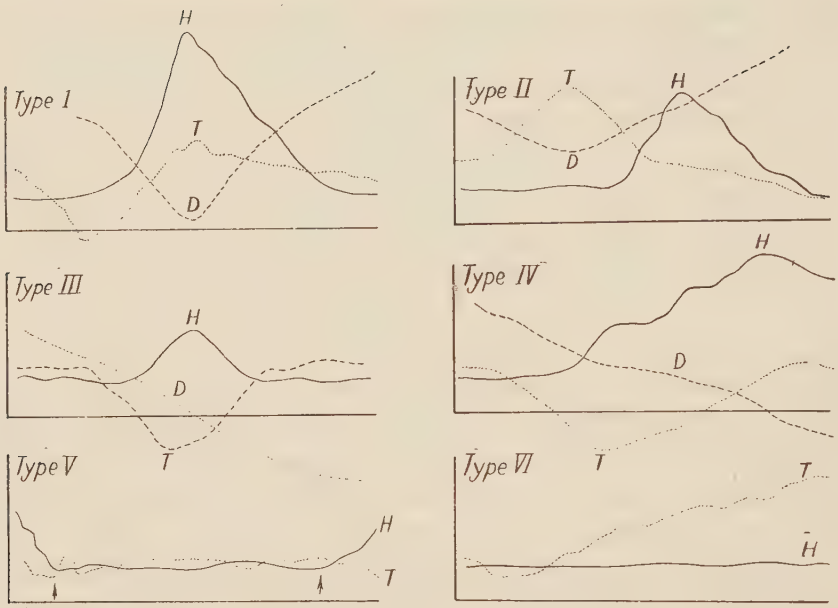

Fig. 5. Six types of the variation with time of wave-height and wave-period. The full line H represents the variation with time of wave-height, and the broken line T that of wave-period; the dotted line D represents the distance from Jogashima Island to a cyclone in the cases of Types I and II, or to a cold front in the cases of Types III and IV.

into the following several types: namely, (1) the case where a cyclone moves on the Pacific side of Japan, (2) the case where a cyclone passes on the Japan Sea side, (3) the case where Japan is covered with a migratory anticyclone, (4) the case where Japan is covered with Ogasawara Anticyclone (subtropical maritime air mass), (5) the case where Japan is visited by a typhoon, (6) the case where the monsoon from the continent prevails, and (7) the case where a stationary front stretching from east to west stagnates in the vicinity of Japan, as is the case in the rainy season, and the weather is unsettled, etc. In the present paper, discussions will be made on the characteristic variations of wave height and wave period and on their relations to meteorological conditions as regards the cases (1)~(4) above. As for the remaining cases, discussions will be reserved for the authors' second report.

4. The case where a cyclone moves on the Pacific side of Japan

In the case where a cyclone moves eastwards along the Pacific coast of Honshu, the variations of waves produced thereby can be classified into two types as illustrated by "Type I" and "Type II" in Fig. 5. The actual examples of Type I and Type II are shown in Figs. 6 and 7, respectively, and the corresponding examples of weather maps in Fig. 13 (D) and (E), respectively.

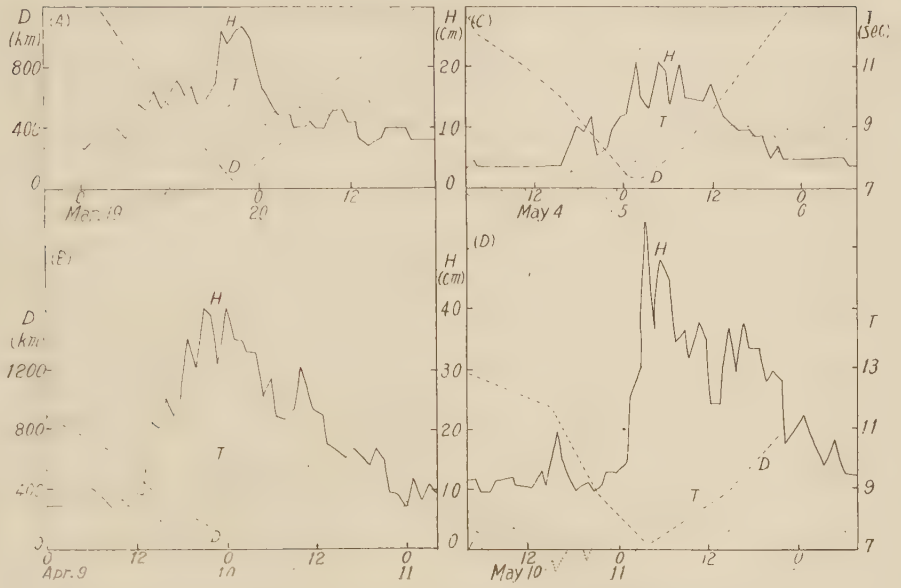

Fig. 6. Examples of variation of waves of Type I, observed when a cyclone moves closely along the Pacific coast of Honshu. The full line H and the dotted line T represent the variations of wave-height and wave-period, respectively, and the broken line D that of distance from Jogashima Island to the center of the cyclone. The weather map corresponding to the example (D) is shown in Fig. 13 (D).

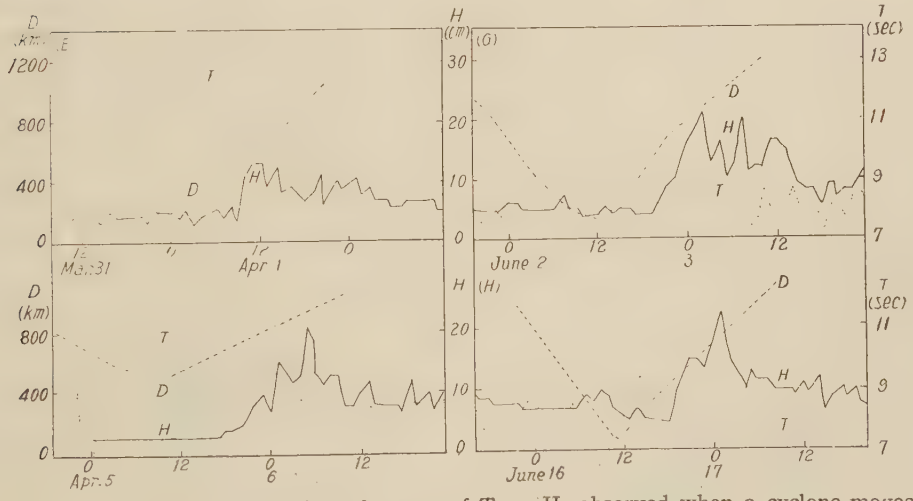

Fig. 7. Examples of variation of waves of Type II, observed when a cyclone moves eastwards at a tolerable distance in the south of Honshu. The curves H, T and D are of the same meaning as in Fig. 6. The weather map corresponding to the example (E) is given in Fig. 13 (E).

Now, the variation of waves of Type I occurs when a cyclone moves eastwards along and close to the Pacific coast of Honshu. A special feature of this type is

that both the wave height and the wave period become maximum when the cyclonic centre comes nearest to the station. Moreover, it is usual that, owing to the effect of the cyclone, when the wave height begins to grow, wind-waves of shorter periods prevail, and hence the wave period becomes somewhat shorter.

Next, the variation of waves of Type II occurs when a cyclone moves eastwards at a tolerable distance to the south of Honshu (viz. south of Hachijo Island shown in Fig. 1). A special feature of this type is that the wave period becomes maximum towards the time of the nearest approach of the cyclonic centre to the station, while the maximum of wave height occurs fairly later.

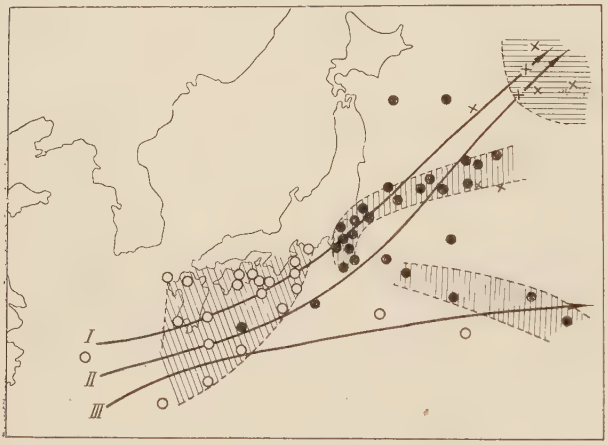

Fig. 8. Three representative paths of cyclones and the positions of the cyclonic centres corresponding to particular phases of change of wave-height at Jogashima Island.

In Fig. 8, the curves I, II and III show three representative paths of cyclones belonging to the cases under consideration, and the points marked with ○, ● and × show the positions of the centre of each cyclone at the time when the wave height at Jogashima Island begins to be conspicuous, attains maximum, and begins to be reduced to its ordinary value, respectively. The time of these phases can be determined fairly accurately as seen in Figs. 6 and 7. Again, Fig. 9 shows the positions of the centre of each cyclone at the time when the wave period at Jogashima Island becomes maximum ; the curves I, II and III are of the same meaning as in Fig. 8.

Now, glancing at Fig. 8, we can recognize that the points with the marks ○, ● and × are distributed, with few exceptions, in their respective domains shown with different hatches. Also we can see from this figure that in the

Fig. 9. Three representative paths of cyclones and the positions of the centre of the respective cyclones at the time when the maximum wave-period occurs at Jogashima Island.

case when a cyclone travels close to the Pacific coast of Honshu (Path I), the wave height becomes maximum when the cyclonic centre comes nearest to the station, while in the case when it travels at a tolerable distance from the coast (Path II or III), the maximum wave height occurs fairly later than the time of the nearest approach of the cyclonic centre to the station.

On the other hand, as for the wave period, it can be recognized from Fig. 9 that the maximum wave period occurs nearly at the time when the cyclonic centre comes nearest to the station, regardless of the path of the cyclone. Thus it is considered that the time interval between the time of the maximum wave period and that of the maximum wave height will become longer as the distance of the cyclonic centre from Jogashima Island becomes larger when a cyclone approaches. This relation can be clearly seen from Fig. 10, where the abscissa represents the time interval mentioned above, that is, the time interval from the occurrence of the maximum wave period to that of the maximum wave height, and the ordinate represents the "effective distance" D_m of a cyclone. The effective distance D_m, so named here provisionally, means the distance between Jogashima Island and the point of intersection of the path of the cyclone with a line joining Jogashima Island with Hachijo Island, but not the distance of the nearest approach of the cyclone to the station. Generally speaking, when a cyclone crosses the said line eastwards, it tends to change its course considerably. Thus, even if a cyclone travels fairly south of Hachijo Island, it frequently changes its course towards north abruptly after it has crossed the said line, and passes immediately east of Jogasima Island. In such a case, indeed, the distance of the nearest approach of the cyclone to the station is very small, but the effective distance of it responsible for the waves near Jogashima Island will be somewhat larger. For this reason, the said distance D_m has been adopted as a measure representing the effective distance of the nearest approach of the cyclone to the station. From Fig. 10, we can see that, if the effective distance D_m for a cyclone and the time of occurrence of the maximum wave period be known, it will be possible to forecast how many hours later the wave height will attain its maximum value.

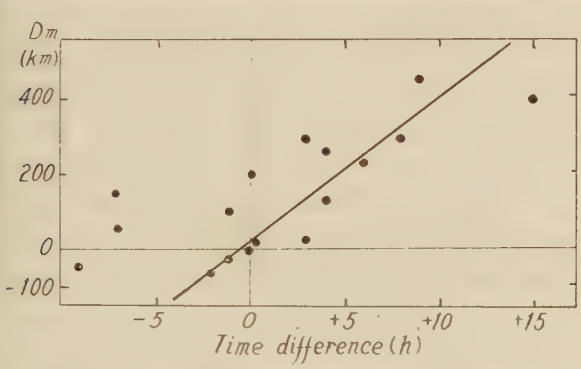

Fig. 10. Relation between the "effective distance" D_m and the time interval from the time of occurrence of the maximum wave-period to that of the maximum wave-height.

The next problem to be discussed concerns the value of the maximum wave height. Various factors can be considered as relating to this quantity, but the

distance and intensity of a cyclone may be regarded as leading factors. Let us now take, for convenience' sake, the effective distance D_m mentioned above as the distance of the nearest approach of a cyclone, and the difference in pressure Δp between the outside and the centre of the cyclone as a measure for the cyclonic intensity. It will not be superfluous to mention here that, as the said pressure difference Δp is equivalent to (pressure gradient) × (scale of the cyclone), to consider the pressure difference Δp is to consider the pressure gradient and the scale of the cyclone, and is also to consider indirectly the velocity of wind and the fetch, etc. Fig. 11 shows the relation between the maximum wave height and the quantities D_m and Δp. From this figure we can see that the sea is naturally high when a strong cyclone passes near the station, and low when a weak one passes far from it. Since, of course, the maximum wave height depends more or less upon various factors other than those considered above, it is impossible to determine the maximum wave height accurately from the above diagram. Nevertheless its approximate value can be inferred from the given values of D_m and Δp, as indicated by the contour-lines in the diagram. Besides, the values of the maximum wave height in Fig. 11 seem to be fairly small, but it must be noticed that, as is already remarked, the wave height in the open sea is several times as large as that observed near the station.

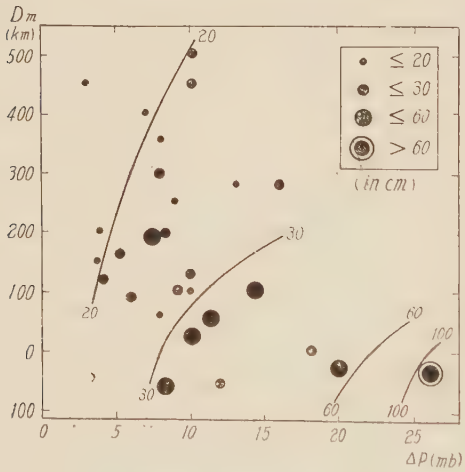

Fig. 11. Relation between the maximum wave-height and the quantities D_m and Δp.

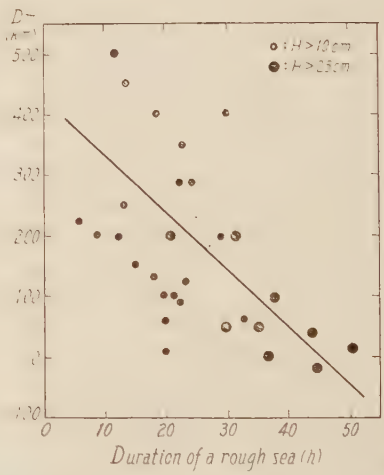

Fig. 12. Relation between the "effective distance" D_m of a cyclone and the duration of a rough sea at Jogashima Island.

Fig. 12 shows the relation between the "effective distance" D_m of a cyclone and the duration of a rough sea. (Here the cases where the wave height H is larger than 10 cm are regarded as corresponding to a rough sea. It may be thought that the wave height of 10 cm is too small as the lowest value for a rough sea,

but that is not the case. If we consider the peculiarity of the sea near the station as mentioned before, it will be recognized that the above value is rather appropriate. In fact, no waves of a wave height exceeding 10 cm appear on our wave gauge, unless something unusual occurs in the meteorological state.) From Fig. 12 we can see that, as might be expected, the closer to the station the cyclone passes, the longer the duration of a rough sea is, although the distribution of the points plotted show a considerable fluctuation.

5. The case where a cyclone passes on the Japan Sea side of Honshu

When a cyclone travels on the Japan Sea side of Honshu, it is almost always accompanied by a cold front stretching from the cyclonic centre towards SW, as

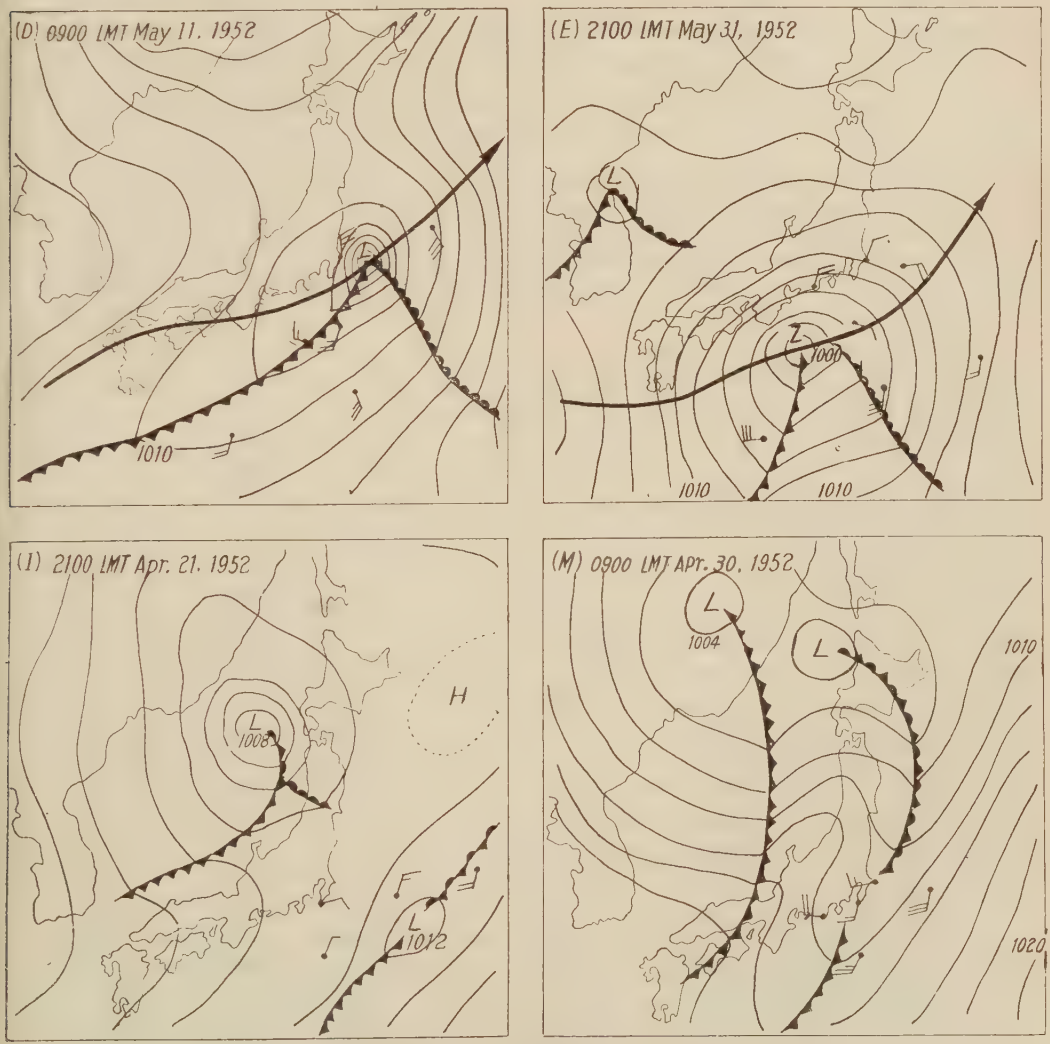

Fig. 13. Examples of the weather maps when a cyclone passes on the Japan Sea.

shown on the weather maps (I) and (M) of Fig. 13. As this cyclone moves eastwards and the cold front approaches Jogashima Island, strong southerly winds

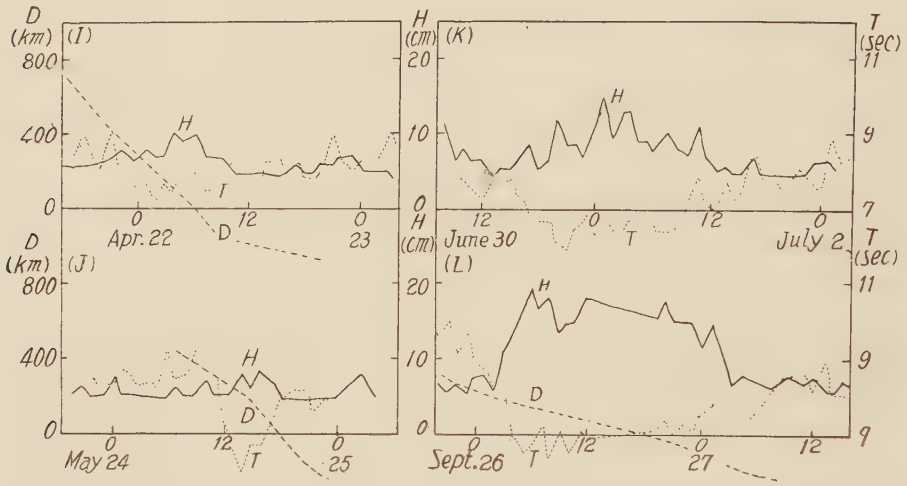

Fig. 14. Examples of variation of waves of Type III, observed in case when a cyclone travels eastwards through the Japan Sea. The full line H and the dotted line T represent the variation of wave-height and wave-period, respectively, and the broken line D that of the distance from Jogashima Island to the cold front accompanying the cyclone. An example of the corresponding weather maps is shown in Fig. 13 (I).

begin to prevail there and waves begin to grow. The variations of the waves in this case can be classified into two types as shown schematically by "Type III" and "Type IV" in Fig. 5. The actual examples of these two types are shown in Figs. 14 and 15, respectively, and the corresponding examples of weather maps are shown in Fig. 13 by (I) and (M) respectively.

Type III is characterized by the fact that towards the time when a cold front passes the station wind

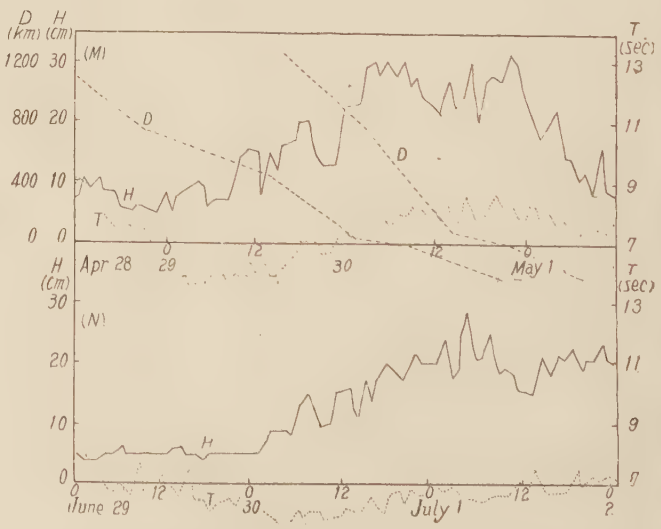

Fig. 15. Examples of variation of waves of Type IV, observed in case when a cyclone travels eastwards through the Japan Sea. The curves H, T and D are of the same meaning as in Fig. 14. An example of the corresponding weather maps is shown in Fig. 13 (M).

waves grow and the wave height becomes larger, while the wave period becomes shorter. On the other hand, if we compare the weather maps (I) and (M) in Fig. 13 with the corresponding variations of ocean waves, we can recognize that in the case where the cyclone (cold front) is strong and the neighbouring sea of Jogashima Island is under its influence for a long time, wind waves continue to grow and the wave height becomes gradually larger, and also the wave period, which was temporarily short, gradually extends, resulting in a parallel increase of wave height and wave period, and this type of variation was designated as Type IV. Thus, no substantial difference exists between Type III and Type IV, but the latter may be regarded as an advanced stage of the former. And these variations of wave height and wave period can be explained by considering the fetch and duration of wind.

Now, the time interval from the time of passing of the cold front over Jogashima Island to the time when the wave height becomes maximum was examined, and the result is shown in Fig. 16, whence it is known that the mean value of the time interval is 0.35 hours. In other words, we can see that the case where the wave height becomes maximum towards the time of passing of the cold front at the station is of the most frequent occurrence.

We shall now take the quantity $t_{W>10} \cdot W_m$ as a measure for intensity of the cold front as viewed from the generation of waves, where $t_{W>10}$ denotes the dura-

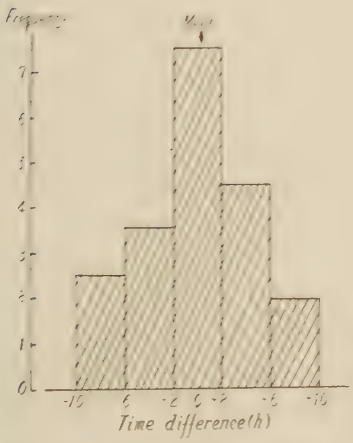

Fig. 16. Histogram showing the distribution of time interval from the time of passing of a cold front over Jogashima Island to the time of occurrence of the maximum wave-height.

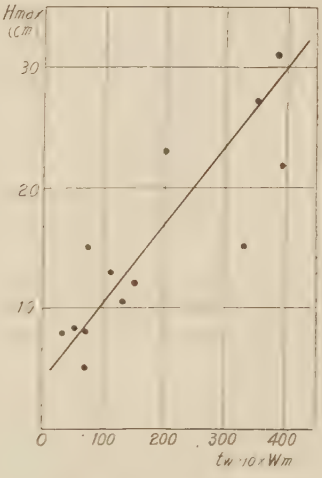

Fig. 17. Relation between the intensity of a cold front $t_{W>10} \cdot W_m$ and the maximum wave-height H_{max}. $t_{W>10}$ denotes the duration of wind whose velocity W exceeds 10 m/sec., and W_m the maximum wind velocity.

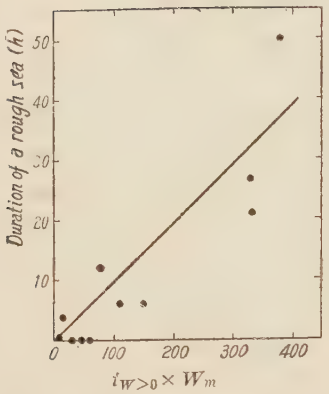

Fig. 18. Relation between the intensity of a cold front $t_{W>10} \cdot W_m$ and the duration of a rough sea.

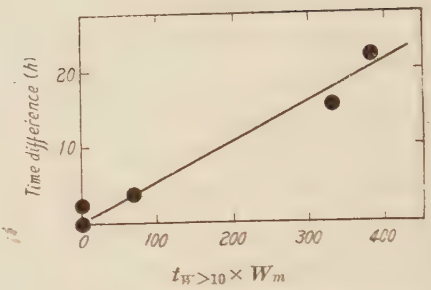

Fig. 19. Relation between the intensity of a cold front $t_{W>10} \cdot W_m$ and the time interval from the time of occurrence of the maximum wave-period to the time of passing of a cold front over Jogashima Island.

tion of southerly wind whose velocity W exceeds 10 m/sec, and W_m the maximum wind velocity. Unfortunately, at Jogashima Island no data of continuous observation of wind direction were available, although those of wind speed were, so that the value of $t_{W>10}$ referred to the above was obtained on the basis of an assumption that winds with south components continued to blow until the passing of the cold front over the station.

Fig. 17 shows the relation between the quantity $t_{W>10} \cdot W_m$ and the maximum wave height, and Fig. 18 that between $t_{W>10} \cdot W_m$ and the duration of waves whose wave heights exceed 10 cm (rough sea). From these figures we can recognize that there exists a tendency that the stronger the cold front is, the higher is the wave height and the longer the duration of higher waves, although the distributions of the points plotted show considerable fluctuations. Again, in the case where the cyclone (cold front) is strong, since it has already generated wind waves when it is still far away from the station, it follows that the shortest wave-period appears long before the passing of the cold front over the station. This relation is shown in Fig. 19; namely, we can see from this figure that when the cold front is weak, the shortest wave-period appears towards the time of its passing over the station, while, on the contrary, when the cold front is strong, the shortest wave-period appears long before its passing. These circumstances explain well the difference between Figs. 14 and 15, that is, between Type III and Type IV.

6. The case where Japan is covered by a migratory anticyclone

So far we have treated the case where the sea becomes high. However, it is also important to investigate the contrary case, viz. the case where the sea remains calm. The latter case, which is equivalent to the case where the wind is gentle, nearly corresponds to the case where Japan is within the sphere of influence o

an anticyclone. And, this may be divided into two cases; namely, one is the case where Japan is covered by a migratory anticyclone, and the other is the case where Japan is covered by Ogasawara Anticyclone (subtropical maritime air mass). The migratory anticyclones are more frequent in spring and autumn in the neighbourhood of Japan, and they are accustomed to travel nearly from west to east over Japan, after leaving the Asiatic Continent. Some examples of conspicuous migratory anticyclones are shown in Fig. 20 (Weather maps (P) and (S)).

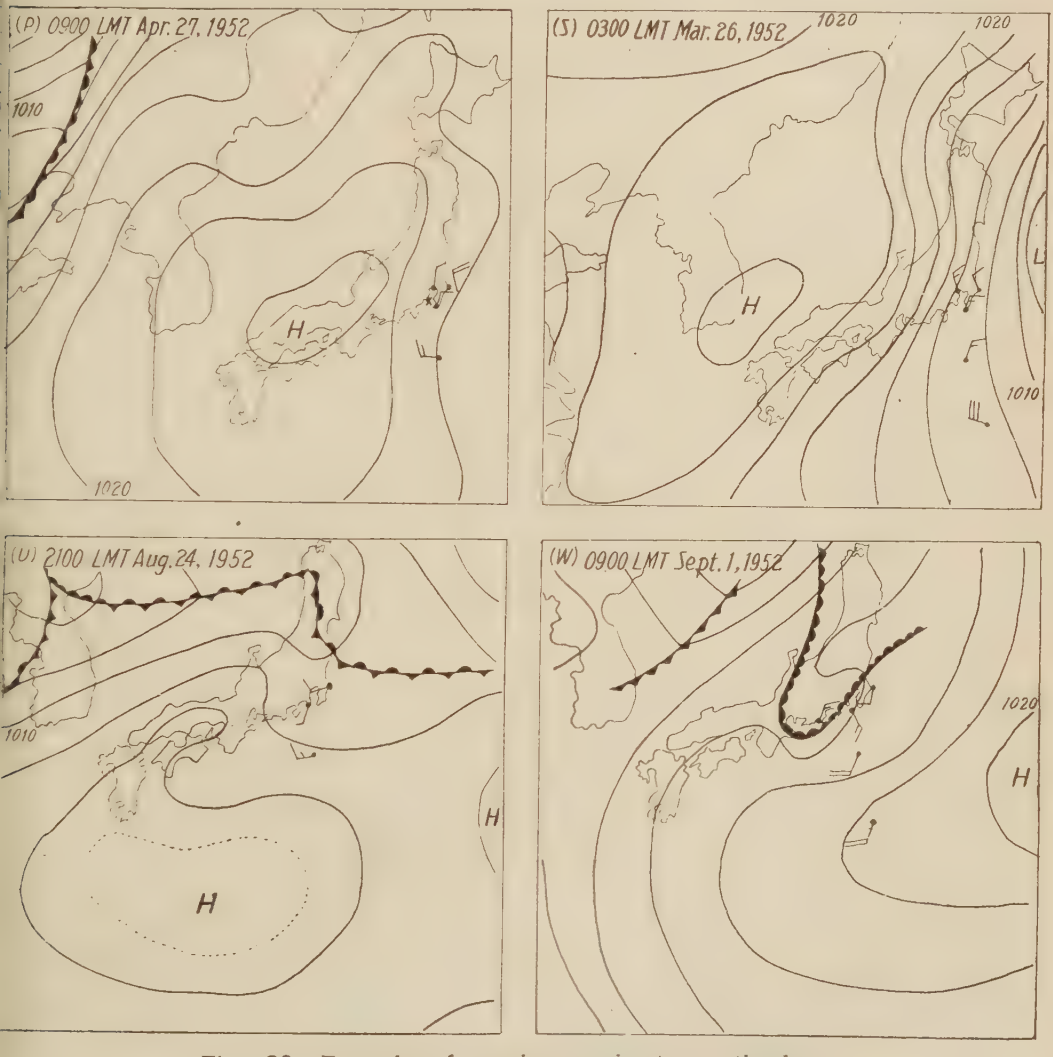

Fig. 20. Examples of conspicuous migratory anticyclone.

Again, some typical examples of the variation of waves at Jogashima Island when Japan is covered by a migratory anticyclone are shown in Figs. 21 and 22, where the full lines indicate the variations of wave height, and the dotted lines

the variations of wave period. Moreover, the arrows in Fig. 21 indicate the time when the sea begins to become calm by entering within the sphere of the anticyclone and the time when the sea begins to become high owing to the departure of the anticyclone.

Now, the variations of waves shown in Fig. 21 are characterized by the fact that, within the interval limited by the said arrows, both the wave height and the wave period remain nearly constant, to say nothing of the smallness of the wave height. This type of variation of waves, which is shown schematically in

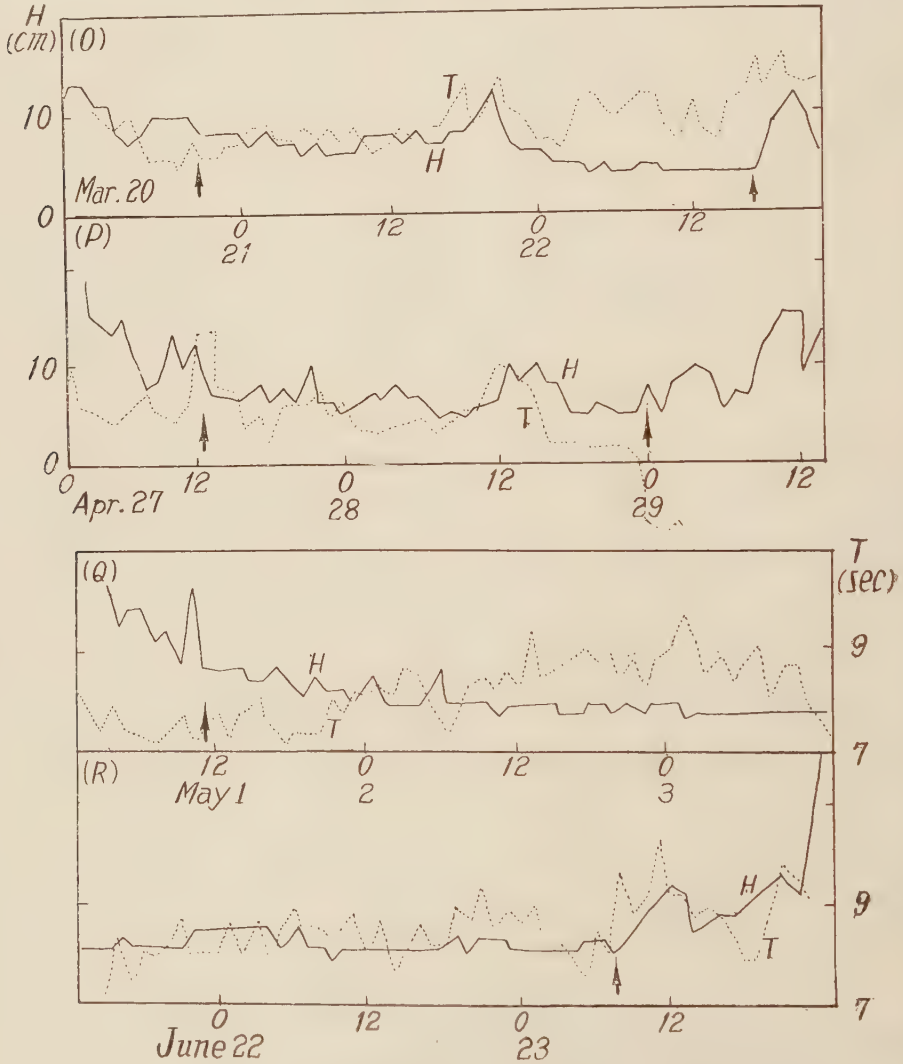

Fig. 21. Examples of variation of waves of Type V, observed in case when a migratory anticyclone covers Japan. The full line indicates the variation of wave-height, and the dotted line that of wave-period. An example of the corresponding weather maps is given in Fig. 20 (P).

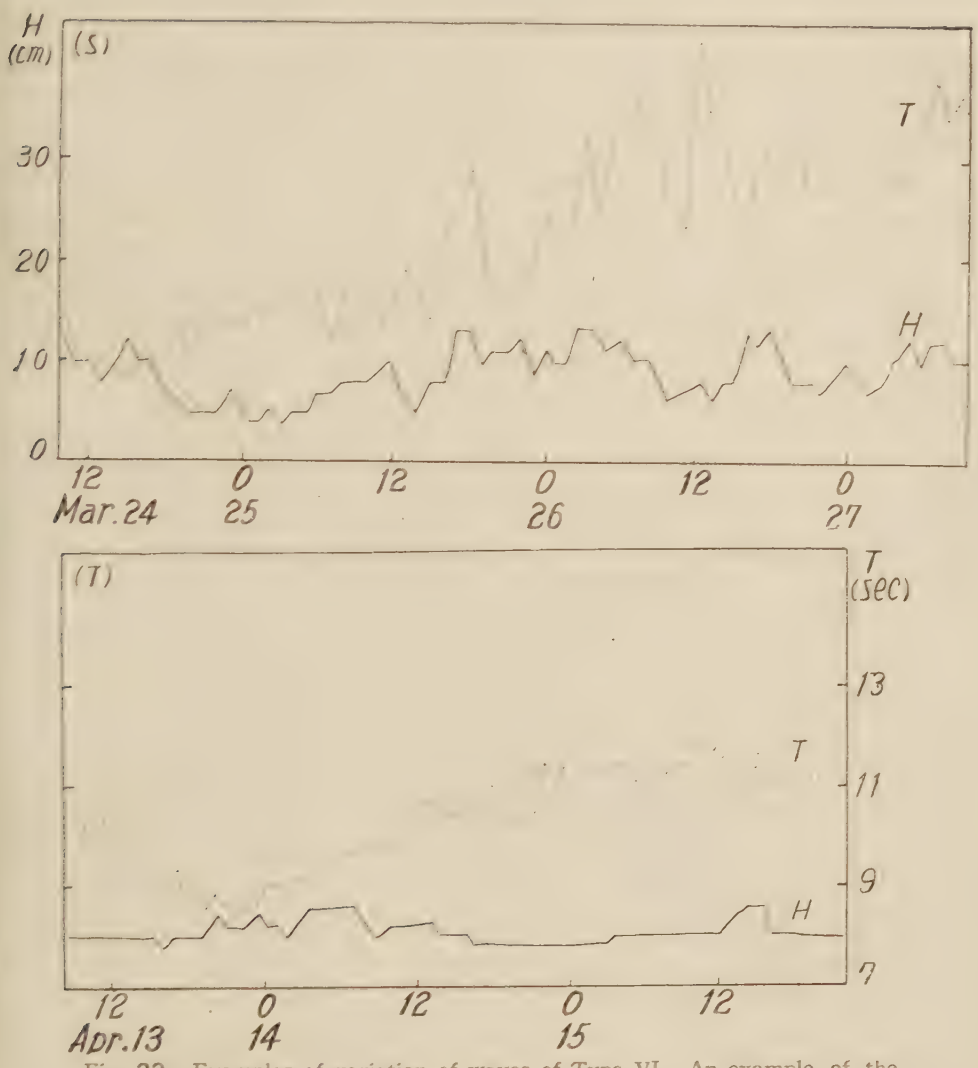

Fig. 22. Examples of variation of waves of Type VI. An example of the corresponding weather maps is shown in Fig. 20 (S).

Fig. 5 (left lower end), was designated as "Type V".

On the other hand, referring to Fig. 22, it is recognized that the aspect of variation of the wave is somewhat different from that of Type V; namely, in this case the wave period is gradually increasing with time, although the wave height remains nearly constant as well as small—this gradual increase of the wave period lasts until a next disturbing source appears. This type of variation of waves, which is shown schematically in Fig. 5 (right lower end), was designated as "Type VI". The variation of waves of Type VI occurs most frequently under the meteorological state such as shown by the weather map exemplified in Fig. 20 (S), namely in the case when a strong cyclone has travelled eastwards over Japan previous

to a migratory anticyclone; it sometimes occurs also in the case where there is a strong cyclone far to the south while Japan is being covered by a migratory anticyclone. In either case, from the areas where these strong and distant cyclones are located, waves of longer periods or swells will be sent out to the station. When the sea is running high near the station, however, these waves of longer periods will not be conspicuous, being concealed by the waves of shorter periods and of larger wave heights. But, as the sea goes down near the station by entering within the sphere of the anticyclone, these waves of longer periods gradually stand out, resulting in a gradual increase of the wave period. The characteristic variation of waves of Type VI as shown in Fig. 5 (or Fig. 22) can thus be explained.

Now, as a matter of practical importance, an investigation was made as to within what extent of area a migratory anticyclone draws near when the sea begins to be calm, and how far it recedes when the sea begins to get rough, and the result is shown in Fig. 23. In this figure, the points marked with ○ represent

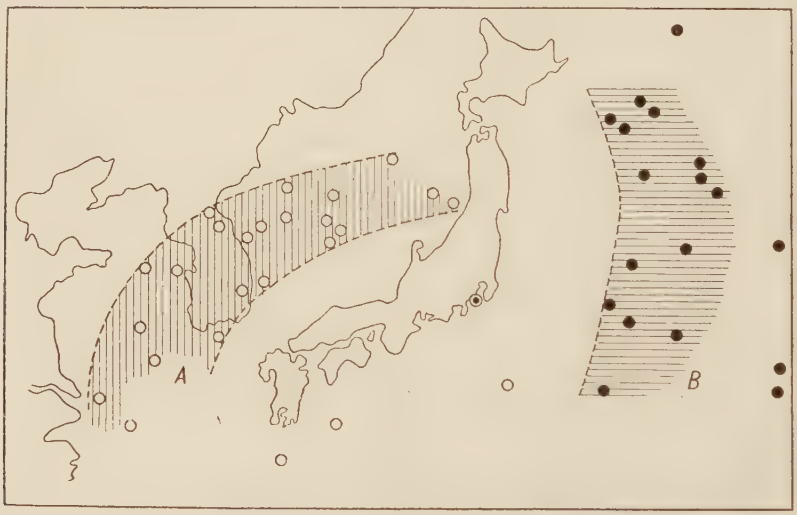

Fig. **23.** Map showing the interval in which the sea is calm at Jogashima Island; case when a migratory anticyclone travels through Japan.

the positions of the centres of the respective migratory anticyclones at the time when the sea begins to get calm at Jogashima Island, and those marked with ● the positions of the centres of the respective anticyclones at the time when the sea begins to get rough. Thus it appears that at Jogashima Island the sea usually begins to get calm when the anticyclone moves eastwards and comes up to the region designated as A and remains calm until the anticyclone recedes as far as the region designated as B. Examining the duration of this calm sea for conspicuous examples belonging to Types V and VI, we have the result as follows: for 8 cases out of 11 conspicuous examples belonging to Type V, the duration

ranges from 1.5 to 2.5 days, and the average of the durations taken for all the 11 examples examined is 2.1 days. Again, the cases belonging to Type VI are 4 in number, and the average of the said durations taken for these 4 cases is 2.0 days. Further, for the last-mentioned 4 cases, the durations of the "gradual increase of wave period" mentioned before are 2.0, 1.5, 2.0 and 2.3 days, respectively, with its average of 2.0 days.

7. The case where Japan is covered by Ogasawara Anticyclone

From late spring till early autumn, subtropical maritime air-mass develops over the North Pacific Ocean, and Japan falls within the sphere of its influence; thus the meteorological conditions near Japan are swayed by the movement of this air-mass, and the ocean waves are also influenced by it. "Ogasawara Anticyclone", as this air-mass is usually called, is fairly conservative in its nature, and yet it sometimes strengthens and sometimes weakens, or moves now eastwards, now westwards. And, since Japan is generally situated in the rear of this anticyclone, even a slight movement of it affects considerably the meteorological conditions near Japan, and consequently the state of the sea around it. For instance, in the cases of the weather maps shown in Fig. 20 (U), the greater part of Japan was within the sphere of the anticyclone, and the sea was calm, and the variation of wave period small at Jogashima Island. However, when the interval of this calm sea lasted long, the wave period gradually increased as seen in Fig. 24 (U), owing to the gradual prevalence of waves of longer periods or swells coming from a remote source of disturbance.

On the other hand, when the margin of the anticyclone is grazing against Japan as in the cases of weather maps shown in Fig. 20 (W), southerly wind blows on the Pacific coast of Honshu and consequently the sea becomes rough for a time. In this case, as seen in (V) and (W) of Fig. 24, the wave height becomes large while the wave period is small for a time, owing to the generation of wind waves; this type of variation of waves is the same as Type III (Fig. 14) mentioned above, which was seen in the case where a cyclone accompanied by a cold front stretching from the cyclonic centre to the southwest travels eastwards on the Japan Sea side of Honshu. And this is a matter of course, when we consider that when the margin of the anticyclone is grazing against Japan, there usually exists a low-pressure zone to the north of it, frequently accompanied by a cold front, though not so conspicuous as in the case of Fig. 14.

Now, the next problems to be discussed are: how near to the Island the Ogasawara Anticyclone comes when the sea goes down, and how far it recedes from it when the sea becomes rough. Although it is difficult to determine definitely the sphere of influence of the Ogasawara Anticyclone, here an isobar which seems to be the margin of the anticyclone was suitably selected on the weather map,

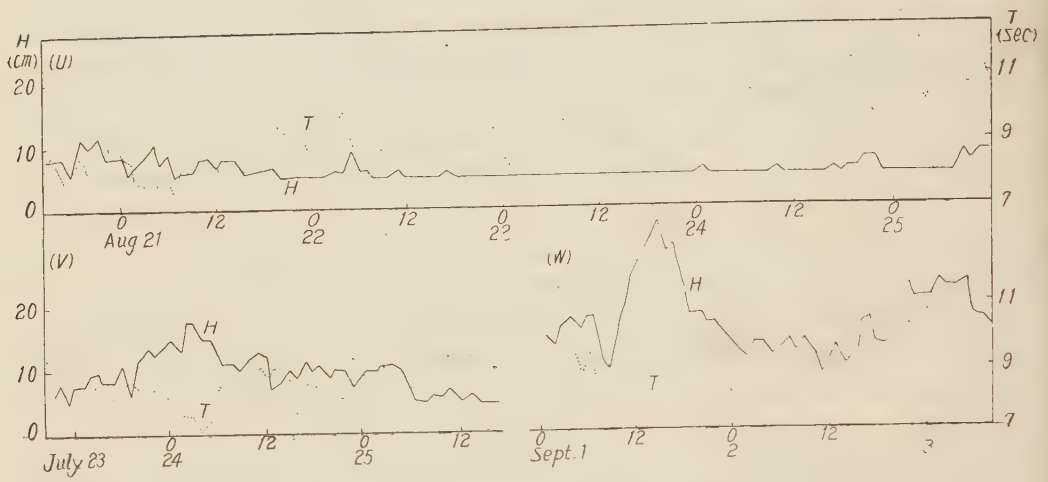

Fig. **24.** Examples of variation of waves observed at Jogashima Island in case when Ogasawara Anticyclone develops in the Northwestern Pacific. Examples of the corresponding weather maps are shown in Fig. 20 (U) and (V).

Fig. **25.** Map showing the interval in which the sea is calm at Jogashima Island; case when Ogasawara Anticyclone develops in the Northwestern Pacific.

and this was provisionally regarded as the boundary of the sphere.

In Fig. 25, the broken lines represent the positions of the boundary of the Ogasawasa Anticyclone when the sea is still running high at Jogashima Island. When this anticyclone extends northwestwards and its northwestern boundary goes to the Japan Sea, passing over Honshu, the sea usually goes down at Jogashima Island, and the dotted lines in Fig. 25 represent the positions of the boundary of the anticyclone in that case. Thus, we can see from Fig. 25 that the sea is still rough at Jogashima Island while the anticyclone remains within the region B, but when the anticyclone extends further and its northwestern boundary reaches as far as the region A, the sea usually goes down at Jogashima Island.

8. Concluding remarks

In the above sections, we have made an analysis of wave records of long con-

tinuance, and discussed the variations of wave height and wave period in various cases of cyclones and anticyclones. It was shown that the variations of waves are more regular than expected and can be classified into six types as shown schematically in Fig. 5, each of which corresponds to a particular meteorological change. And their relations to meteorological changes were given more or less quantitatively.

It is suggested that, if we use these relations, quantitative wave forecasting will be possible even in the case where the velocity and direction of wind change with time fairly rapidly; thus it seems that some weak points contained in the theoretical method of wave forecasting, developed by H. U. Sverdrup and W. H. Munk, etc, can be made up for, to some extent. It must be admitted, however, that the method of investigation adopted here also has its own fault and the results obtained still contain some problems.

In the first place, the results of the present analysis are only applicable to the station under consideration. Accordingly, in order to make wave forecasts for different places, similar investigations should be made, based on the observations taken at the respective stations. And, for this purpose, it is desirable that observations should be made at such a point as represents the state of the sea in an area as wide as possible. Unfortunately, Jogashima Island where the present wave observations were taken is of fairly conspicuous local character, and so it is rather difficult to make wave-forecasts for the open sea, based on the results of the present investigation. Nevertheless, the present authors believe that the utility of the method of wave forecasting based on the present method of analysis will never be small.

In the second place, the present analysis has considered a cyclone or an anticyclone independently. As a matter of fact, however, in most cases these are closely combined with each other in such a manner that, when a cyclone passes by, a migratory anticyclone soon appears in its wake, and this in turn is followed by another cyclone. Hence, properly speaking, analyses should be made by considering the simultaneous effect of the two, and also in case of wave-forecasting this must be taken into consideration. Although this is comparatively easy in the case where conspicuous cyclones and anticyclones travel regularly, it is not so otherwise. And, for the latter case a more detailed analysis is necessary.

Acknowledgements ——The present authors wish to express their hearty thanks to Dr. K. Wadati, director of the Central Meteorological Observatory of Japan, for his interest and advice. Equal thanks are due to Messrs. Y. Ota and M. Amano, who assisted in constructing the wave gauge, to Messrs. J. Sugiura and H. Itakura, who assisted in observation, and to Messrs. J. Fukuoka and T. Yusa, who assisted in arranging the data of observation.

References

[1] Sverdrup, H.U. and Munk, W.H., 1947: Wind, Sea and Swell. Theory of Relations for Forecasting, U.S. Navy Hydrographic Office, Publication No. 601.

[2] U.S. Hydrographic Office, 1944: Wind Waves and Swell. Principles in Forecasting, U.S. Navy Hydrographic Office, Miscellaneous Publication No. 11.

[3] Neumann, G., 1952: On Wind-Generated Ocean Waves with Special Reference to the Problem of Wave Forecasting. Department of Meteorology, Collection of Engineering, New York University Publication May 1, 1952.

[4] U. S. Hydrographic Office, 1944: Breakers and Surf: Principles in Forecasting. U. S. Navy Hydrographic Office, Publication No. 234.

[5] Ota, Y., 1952: On the Ocean Waves Observed at Cape Omaezaki, (III) (In Japanese), Tokyo-Kanku Kisho-Kenkyukaishi, **11**.

[6] Nakano, M., 1939: On the Secondary Undulations of Tides Caused by Cyclonic Storms (I), Journal of the Meteorological Society of Japan, **17**, No. 4 (In Japanese); and 1949 Oceanographical Magazine, **1**, No. 1 (In English).

[7] Munk, W. H., 1949: Surf Beats. Transaction of the American Geophysical Union, **30**, No. 6.

Spawning in the Tridacnid Clams

Seiji K. WADA

Oceanographical Laboratory, Meteorological Research Institute, Tokyo

---

Reprinted from
JAPANESE JOURNAL OF ZOOLOGY
Vol. 11, No. 2
March 1954

Spawning in the Tridacnid Clams

Seiji K. WADA

Oceanographical Laboratory, Meteorological Research Institute, Tokyo

The tridacnid clams are protandric functional hermaphrodites (Wada, 1942, 1952). In the functional hermaphrodite gonads of the adults, female and male follicles lie side by side throughout the whole extent, and both eggs and sperm mature simultaneously. In the majority of functional hermaphrodite bivalves, eggs and sperm are discharged at the same time, and self-fertilization is usual; while in the tridacnid clams, simultaneous spawning never occurs. As far as the writer knows, such spawning behavior is not known to occur in any other bivalves. The mechanisms involved in the spawning of American oysters have been elaborately studied by Galtsoff (1938a, 1938b, 1940) and Nelson and Allison (1940); and it is very probable that a similar situation also obtains in other bivalves in which the sex is apparently or strictly separate, However, as would be expected from the peculiar behavior in spawning, a somewhat different principle may rule the mode of reproduction in the tridacnid clams.

n the following will be presented the results of observations and experiments on the spawning of these hermaphrodite molluscs. The experiments were performed in 19 8, 1940 and 1941 at the Palau Tropical Biological Station on Korrol Island and, mainly, on the sandy beach called Nghus, on the Island of Ngrektable, which is reached by some 30 miles' sailing southwards from the Station.

The writer wishes to express his indebtedness to Dr. Shinkishi Hatai, former director of the Station. His hearty thanks are also due to the staff of the South Sea Pearl Culture Co., for residence facilities at Nghus, and to Dr. Jean C. Dan for her kind guidance in the preparation of the manuscript.

Materials

Three species of the Tridacnidae were mainly used in experiments; these are *Tridacna squamosa*, *T. serrifera* and *Hippopus hippopus*. Clams of the first two species are found on reef flats, loosely attached to dead broken corals or shells by means of the byssus, while *Hippopus* inhabits sandy areas, lying unattached. The animals used ranged in size from 10 to 30 cm in shell length.

Besides these species, some observations were also made on *T. crocea*. Although this is the smallest and commonest form among the family, it is rather difficult to collect the animals in an intact condition because the mollusc lives as a borer into coral rocks around the low water mark, attaching firmly by

strong byssus threads.

Mode of Spawning

The tridacnid clams live normally with the edges of the shell valves pointing directly upwards. The pedal aperture (where this is present) lies close to the umbo. The hinge side of the shell is morphologically ventral, the free edge being dorsal; the relations are the exact opposite of those in other bivalves, The mantle is greatly developed; in *Tridacna*, when the animal is feeding, thick and fleshy mantle lobes are seen to be reflected over the edge of the shell-valves. The mantle-lobes are fused for the greater part; connection between the mantle cavity and the surrounding sea water is made through an inhalent and an exhalent aperture, in addition to a pedal one in certain forms. Regarding the position of the mouth as indicating the anterior end of the animal and that of the anus the posterior end, the exhalent aperture is situated a little to the anterior of the mid-dorsal line, while the inhalent aperture opens rather ventrally, near the posterior end. The former is circular in cross-section and situated on the end of a conical siphonal process. The inhalent aperture is a longitudinal slit girdled by numerous tentacles. The feeding bebavior of *T. crocea* has been elaborately studied and illustrated by Yonge (1936).

When the animal is feeding, the shell-valves are opened widely and the mantle-lobes are stretched out to their full extent. Water enters the pallial cavity through the inhalent aperture and, after being strained through the branchial structures, is expelled from the exhalent opening to the outside. Both the inhalent and exhalent apertures can be closed or opened freely without contraction of the adductor muscle. The closure of the valves rarely occurs; it takes place probably in order to expel debris or faeces to the ontside.

In *T. crocea*, in which a large pedal vent is present, it has been shown by Yonge (1936) that waste matter rejected by the labial palps is carried to the extreme anterior end of this vent, where it accumulates into masses, and that it is removed from the inhalent chamber through this opening, water expelled by the sudden contractions of the adductor muscle making its way upward between the shell and the sides of the burrow and carrying the waste matter with it. In animals in which the pedal vent is lacking or very small, as *Hippopus* or *T. squamosa* or *T. serrifera*. waste matter is carried to the posterior end of the inhalent cavity, and expelled from time to time by way of the inhalent opening. It has been observed that this is done either by a water current produced by the contractions of the adductor muscle or by an everting motion of a portion of the mantle surrounding the aperture which is charged with waste matter; the latter case seems to take place when the mass of waste is small.

When spawning begins, the valves are first opened more widely with the relaxation of the adductor, then the exhalent siphon which has been directed anteriorly is stretched to its full extent and raised upwards. The contraction of the adductor muscle then ensues, producing closure of the inhalent aperture, by which a vigorous jet of water, charged with sex cells, is ejected upwards

through the exhalent opening ; the shell-valves are again parted as far as possible with opening of the inhalent aperture and relaxation of the erected exhalent siphon. The process is repeated with great regularity and may continue for more than one and a half hours, its duration depending on the amount of ripe sex cells in the gonads and on the nature of the spawning stimulus. The shell movement is at first repeated at from 15 to 30 second intervals, slowing down gradually as spawning approaches the end, until it finally ceases entirely.

No differences in the spawning behavior were observable between shedding of eggs and ejaculation of sperm. Spawning in the tridacnid clams may be divided into three distinct phases ; the discharge of sex cells from the gonads, the rhythmical contactions and relaxations of the adductor, and the motion of the mantle. The last-mentioned involves closing and opening of both inhalent and exhalent apertures, and raising and relaxing of the exhalent siphon. In animals which have a large pedal vent, closing the vent during spawning must be executed by bringing together of the mantle-lobes in that region, although this has not been affirmed by observation.

Of these three phases, the first is obviously the principal sexual reaction of the organism, while phases two and three may be considered as accessory reactions providing a mechanism for the dispersal of the sexual cells. However, it should be noted that the last two phases are very closely related to each other, and, as will be stated later, it has not been possible to provoke them separately, although under certain conditions, they have been observed to occur independently of the discharge of sex cells.

When spawning takes place copiously, the sexual product is discharged continuously, though more or less rhythmically, by way of the exhalent opening, while in a lighter spawning, it is discharged to the outside sea water only when water is ejected. At the beginning and toward the end of spawning, it has been not infrequently observed that the inhalent aperture is not closed during the contraction of the adductor muscle and, therefore, water is expelled through both the exhalent and the inhalent openings ; this is one of the typical reactions in the case of a light spawning. On the other hand, a heavy spawning is usually inaugurated with ejection of water only through the exhalent aperture.

The force of the jet during spawning is very great, as will be seen in the following observation : when a spawning animal (*T. squamosa*) measuring about 20 cm long was placed in a glass jar so as to be just covered by water, the jet of water then produced attained a height of 2 meters or more.

Experimentally, discharge of sperm can be provoked several times in the same individual until the ripe sex cells are exhausted. If spawning is interrupted by exposing the animal to air, it is resumed immediately when the mollusc is put into water again, unless the exposure to air lasts for more than several hours.

Relation to Temperature

In the laboratory, spawning was observed to occur at temperatures ranging from 28° to 31°C. It was also observed that ejaculation of sperm could not be interrupted by transferring spawning *Hippopus* to water of 16°–17°C. Clams of this species were found to survive in water of temperature as low as 9°–10°C for more than an hour, although spawning could not be induced at a temperature of 14°–15°C by the addition to the water of a suspension of macerated gonad tissue.

When the water temperature was raised gradually from 13°C, the rate of the rise being 0.06°C/min. or 3.6°C/hour, under constant chemical stimulation for spawning, *Hippopus* was induced to discharge sperm at a temperature of 21°C in 2 hours 13 minutes after the commencement of the experiment, and thenceforth spawning continued. Since such a low temperature as 21°C will not usually be encountered in the shallow waters around the Palau Islands, water temperature in nature will never be a limiting factor in the spawning (at least of sperm) of these clams.

So far, the experiments show that thermal stimulation alone is not effective; no individuals of *T. crocea* could be induced to spawn by quickly raising the water temperature from 22.5°C to 33.5°C.

In another experiment on *Hippopus*, sperm ejaculation was observed to be induced by gonad suspension at 28°C without the rhythmical contractions of the adductor, although some undulating movements of the mantle surrounding the exhalent and inhalent openings were observed; this animal had previously been exposed to low temperature (7.5°–10.0°C) for one and a half hours. In the same individual, typical spawning behavior was observed at 28°C after 160 minutes' exposure to temperature of 14.2°–14.6°C.

Stimulation of Spawning by Sex Cells

Since adult animals of the Tridacnidae are functional hermaphrodites, and, in the gonads, female and male acini lie side by side, a mixed suspension of eggs and sperm is produced when sex cells expressed from the excised gonad are diluted by sea water. As the eggs are very fragile, a filtrate of the suspension through chemical filter paper always contains spermatozoa and egg granules, besides water-soluble substances.

When such suspension is introduced to a feeding clam with ripe gonads, the discharge of sperm can easily be induced. The animal responds first by further opening of the shell-valves, followed immediately by sudden closure; a jet of water charged with sperm is ejected by way of the exhalent siphon. Opening and closing of the shell-valves are repeated with great regularity by rhythmical relaxations and contractions of the adductor.

The latent period, i.e., the duration between the time of introduction of the gonad suspension and that of the first occurrence of shell-movement varies from 20 seconds to 19 minutes according to conditions. The results of observations

along this line are presented in Table 1. In these experiments, the gonad suspension was introduced gently into the pallial cavity of feeding animals by a glass pipet inserted through the inhalent aperture, care being taken not to inflict any mechaninical disturbances on the animal.

Table 1.

Latent periods in stimulation by gonad suspension.

	Temperature °C	Latent period	
		Jet of water from exhalent aperture	Discharge of sperm
T. squamosa:	29.3	155 sec.	240 sec.
	29.3	140	175
	30.0	50	160
	29	55	160
	29	60	160
	29	35	—
	30	20*	—
	31.3	85*	—
	29.5	1140	1235
	29.5	300	310
	29.5	555	600
	29.5	36	240
	30.5	140*	—
	30.5	150*	—
	30	20	960
	30	70*	—
Hippopus:	28.1	—	120
	28.1	50	375
	28.1	140*	—
	28.2	120	235
	28.2	60	105
	28.2	—	200
	28.1	—	180
	27.9	85	120
	27.7	310	380
	27.8	340	705
	27.2	155	340
	29.3	115	165
	28.6	75	100
	27.2	135	315
	29.0	110	125
	28.4	295	390

Discharge of sperm did not occur in the cases marked with an asterisk.

When a fully ripe animal is employed, the first sudden closure of the valves usually occurs within 50 to 60 seconds (temperature : 27-31°C) after injection of gonad suspension. In the majority of cases, discharge of sperm began at the third time of shell closure, in from 50 to 120 seconds after the first shell movement.

It has not infrequently observed that although the rhythmical movement of the adductor and the ejection of water through the exhalent opening occur in quite the same manner as in the usual spawning, and these frequently last even for 20 or 30 minutes, no reproductive cells are discharged. Eleven such cases have been observed with *T. squamosa*, and 4 cases with *Hippopus*. The majority of the animals which behaved in this way were found to have rather poorly developed gonads ; hence, the condition of the gonads is supposed to be largely

responsible for such behavior. However, the strength of the spawning stimulus is also believed to be a contributory factor, as indicated by the following experiment. *T. squamosa* was placed in a glass jar which contained 10 l of sea water in which 0.05 g of ripe gonad was included as suspensoid; only rhythmical adductor motions, with no shedding of sex cells, were induced; on addition of a further dose of ripe gonad suspension, discharge of sperm was provoked immediately.

In this connection, it should be noted that, in a typical spawning, prior to the shedding of gametes, the rhythmical adductor movements and the resultant jet of water, not charged with sex cells, through the exhalent aperture are almost always observed to occur. These behaviors are never observed in any other cases than spawning, and they really constitute a part of the spawning pattern.

In order to obtain some evidence as to the limits of the effective concentration of gonad suspension, the following experiment was set up. 5 g of well developed gonad of *T. squamosa* was minced and ground thoroughly in a glass mortar with a small amount of sea water, and diluted by sea water to 500 ml; 1 ml of this suspension is assumed to be equivalent to 0.01 g of the gonad. A certain aliquot of the suspension was mixed thoroughly with 10 l of sea water in a glass jar, in which an experimental animal, *T. squamosa*, was placed. The water which was contained within the mantle cavity of the animal had been drained as much as possible before the experiment, a wooden wedge being inserted between the shell-valves to prevent them from closing.

Spawning occurred in all the animals which were exposed to gonad suspensions of 0.005%, 0.0025%, or 0.001%. In one case in which a gonad suspension of 0.0005% was employed, of two animals, one individual did not respond in any way, while, in the other clam, rhythmical movements of the adductor with ejection of water through the exhalent opening were induced, but no shedding of sperm was observed. On exposure to a more concentrated gonad suspension, a light spawning took place in the former individual; and, on addition of 5 ml more of the original gonad suspension to the surrounding water, a typical spawning was provoked in the latter mollusc.

Judging from these facts, it is postulated that the threshold concentration of effectiveness of the gonad suspension for *T. squamosa* is around $0.5-1\times10^{-5}$ (0.05—0.1 g of ripe gonad in 10 l of sea water).

In the tridacnid clams, as previously stated, eggs or sperm are discharged completely separately; egg-sea water or sperm suspension, therefore, can be prepared from discharged sex cells.

The supernatant fluid of a suspension of shed eggs of *T. squamosa* was introduced into the pallial cavity of animals of the same species. Two series of experiments, involving 6 animals, were attempted. A copious ejaculation was induced in all the animals.

On the other hand, sperm suspension prepared from discharged sperm has been found to be non-effective. Negative results have always been obtained in the experiments hitherto performed: 3 times with *T. squamosa*, 3 times with *Hippopus*, and once with *T. serrifera*. Control tests with hermaphroditic gonad

suspension were always positive in these animals.

Judging from these facts, it is very certain that the active principle is carried by the eggs and not by the spermatozoa. Since egg sea water is effective, it is almost certain that the active principle borne by the eggs is soluble in sea water.

Further experiments have shown that sperm suspension prepared from discharged sperm of different species is also ineffective in provoking spawning.

The tridacnid clams being protandric, sperm suspension can also be prepared from the male phase gonads of young animals. Experiments in which such spermatic tissue suspension was employed have revealed that the suspension is sometimes effective and sometimes not.

In the experiments with *Hippopus*, out of 16 cases, typical spawning was observed in 8 cases, only rhythmical shell movements occurred in 2, and no responses were observed in the rest. In *T. serrifera*, out of 9 cases, typical spawning was observed in one case, and only shell movements were induced in another whereas in two series of experiments with *T. crocea*, none of the animals responded to sperm suspension. In the control tests with hermaphrodite gonad suspension, positive results were always obtained.

The suspension of spermatic tissues which were found effective in the above experiments was prepared from rather large-sized male-phase clams; the effective suspension of *Hippopus* was made from the gonad of a clam of 15.1 cm in shell-length, the largest among the male-phase animals examined. The effective suspension of *T. serrifera* was also obtained from animals measuring about 23.5 cm in shell-length.

It is highly probable that in the gonads of such large-sized male-phase animals, the primordial ovarian tissues have commenced developing. Since the sperm suspension of discharged sperm and the spermatic tissue suspension of small-sized male-phase animals are not effective, it is almost certain that the active principle in the effective suspension of the male-phase gonad is borne by some tissue cells other than those involved in the production of spermatozoa. Very probably, it is borne by the primordial ovarian cells, and the active principle is therefore, believed to be produced in the early stages of ovarian development.

Some Properties of the Gonad Suspension

In the tridacnid clams, spawning of sperm cannot be provoked by a gonad suspension of a different species; the reaction is species specific. Experiments show that *T. squamosa* could not be induced to spawn by a gonad suspension of *Hippopus* or of *T. serrifera*, and *T. serrifera* not by that of *Hippopus* or of *T. squamosa*; whereas, all the clams used in these experiments were found to respond typically in control tests with self-species gonad suspensions. Moreover, when a gonad suspension of a different species was introduced into the pallial cavity of animals, it was observed that the inhalent aperture was closed tightly, as if to prevent further introduction of the suspension.

Gonad suspension of a different species is found to include some substance

or substances which act antagonistically to the active principle in the self-species gonad suspension, as indicated in the following experiment. Two clams of *T. squamosa* which had been proved not to respond to the suspension of *Hippopus* gonad were stimulated by a mixed suspension of the gonads of *Hippopus* and *T. squamosa*. In one of the animals, spawning was induced immediately, while the other clam showed no reaction. When the latter animal was subsequently exposed to a suspension of self-species gonad, an immediate discharge of sperm resulted.

In these respects, the mechanisms involved in the induction of discharge of sperm in the Tridacnidae seem to be more or less different from those in *Crassostrea virginica*, in which the males can be induced to spawn, Galtsoff (1940) shows, by egg water of such varied species as *Pecten*, *Mya*, *Mytilus*, *Asterias*, etc.

The active gonad principle is not destroyed by distilled water. A portion of well ripened *Hippopus* gonad was ground thoroughly in a glass mortar with clean fine sand, and mixed with distilled water, the sand being entirely removed; after one hour's standing, the suspension was proved to be as effective as ever. Therefore, it is thus proved that the active principle remains intact on and after the death of the sex cells.

A gonad suspension of *T. squamosa* which had been boiled for 5 minutes or heated to 55–60°C for 15 minutes was found to have become ineffective. The animals used in these experiments were afterwards induced to spawn by fresh suspension. Moreover, it was observed that the animals closed the inhalent aperture tightly as soon as the heat treated suspension was added, and that they remained in this state for a while.

Three individuals of *T. squamosa*, in which no spawning reactions could be induced by heat treated gonad suspension, were stimulated by a mixed, fresh and heated, suspension of gonad. The heat treated suspension was prepared by warming at about 57°C for a quarter of an hour. After the animal had been exposed to this mixture for 22 min. 15 sec., one of them ejected water 5 times through the exhalent opening at intervals of from 30 seconds to 5 minutes; the two others did not respond. Soon afterward, fresh suspension was added; in the first animal, the rhythmical shell movements occurred in 80 sec., and light spawning was observed later; of the other two clams, one discharged sperm with shell movements which were inaugurated in 150 sec.; while in the other animal, only movements of the adductor were observed, beginning at 225 sec. Judging from these results, it is certain that some substance(s) which prevent the action of fresh gonad principle are formed by heating; it remains unsolved whether these are produced from disintegration of the active principle or of other materials in the fresh gonad, and whether the active principle is destroyed by heat or not.

The activity of effective suspensions of male-phase gonad is lost by heating, although it has been found to persist, although weakened, after boiling for one and half minutes. The results of the experimental run in this respect are presented in the following:

Type of suspension	*Number of animals*	*Mode of response*
Boiled 10 min.	5	No response.
Boiled 1 1/2 min.	5	Frequent shell movements at intervals of 0.5–2 min., ejection of water through exhalent opening, in 2 animals (1 in 10 min.; the other in 36 1/2 min.), no discharge of sex cells.
Heated to 75°C, cooled immediately	5	3 responded with frequent shell-movements, no discharge of sex cells.

Species of experiment animal: *Hippopus hippopus.*

In control tests, typical spawning was induced in the clams used in these experiments.

Spawning Induced by Other Stimuli

T. crocea burrows into solid coral boulders, so that the edges of the shell-valves lie flush with the surface of the rock. They attach firmly to the rock by an immense byssus. For collection of the clams, it is necessary to break the rock by a hammer and loosen the byssus.

When animals, whose byssus had been detatched by hand from the substratum, were reared in a laboratory tank, discharge of eggs or sperm was not infrequently observed. In this case, the cutting-off of the byssus is supposed to be the stimulus responsible for spawning. Tearing out the byssus causes secretion of a large amount of mucus from the byssus gland, as seen in other cases of bodily injury. The stimulus in this case might be of a similar nature to the case of "swarming" of nauplius larvae in *Lepas* or *Balanus* which is caused by the release of the animal from the substratum.

In several cases, discharge of eggs or sperm occurred in succession with a short pause between. In all cases of such successive spawning, shedding of eggs always occurred previous to ejaculation of sperm.

Discussion

In most cases of functional hermaphroditism, in which both female and male sex cells mature concurrently, simultaneous spawning takes place and self-fertilization is usual; while, in hermaphroditic tridacnid clams, as already stated, simultaneous spawning never occurs. On one occasion, however, it was observed that, in *T. squamosa*, both kinds of sex cells were discharged simultaneously, and in this case the rhythmical movements of the adductor were not observed; moreover, the eggs discharged, like ovarian ones, were provided with a well-defined membrane at the outermost surface, and the underlying gelatinous coating was rather thin. These facts show that the eggs were in a less mature condition than those normally discharged. In the latter, a very thick gelatinous coating develops on standing in sea water, the outermost membrane being

rendered obscure. Furthermore, the clam died soon after spawning. Hence, it is very certain that this abnormal mode of spawning was caused by an unhealthy condition of the animal.

In the tridacnid clams, spermatozoa expressed from the excised gonad are as intensely active as those discharged, and no morphological or physiological differences were appreciable between spermarian and discharged sperm. It is generally believed that ripe sperm in the gonad are always ready to be discharged under proper stimulus.

The fact that discharge of eggs cannot be induced by sperm suspension or egg water may indicate that primarily different mechanisms of stimulation are involved in discharge of eggs and in ejaculation. On the other hand, the fact that successive spawning was induced by tearing out the byssus in *T. crocea* may show that a common stimulus is sometimes effective for both sexual reactions.

In normal spawning patterns of *Ostrea echinata* and *Pinctada martensii*, in which spawning is readily provoked by sperm suspension or egg-sea water, it has been observed that eggs or sperm in the gonads attain at a certain stage of maturity on receiving the spawning stimuli. When an animal is subjected to spawning stimuli, nuclear dissolution takes place in the ovarian eggs and an increase in potential motility is caused in the spermarian spermatozoa.

Iwata (1953) also reports that, when a mantle piece of *Mytilus edulis* with female follicles is subjected to certain chemical stimuli, shed of eggs occurs after the nuclear breakdown has been accomplished in the follicles.

In case of the tridacnid clams, probably, the sperm suspension does not induce the maturity of eggs in the gonads.

Although failure in the induction of egg discharge by gonad suspension can be explained by the assumption that the principle in the eggs and sperm is not effective for ovulation, it seems very difficult to explain by what mechanism or mechanisms differential spawning occurs in animals whose eggs and sperm are concurrently "fully mature", as indicated by the occurrence of successive spawning. In this connection, it is worth mentioning that ovulation was always followed by ejaculation in cases of successive spawning. The ejaculation of sperm might be suppressed by a sphinctor-like mechanism around the spermiduct, although the presence of such has not been affirmed at all. The problem is left to be solved in the future.

In the American oyster, Nelson and Allison (1940) show that the receptors for the stimulation of spawning of the male animal by eggs are located on the surface of the demibranchs, and that the shedding of sperm results from a relaxation of the sphinctor of the distended sperm duct.

Spawning phenomena in the American oyster have also been elaborately studied by Galtsoff (loc. cit.). According to this author, spawning in the female oyster is readily provoked by the sperm suspension of the same species; and that in the male by various agents, e.g., egg-water, sperm suspension, thyroxin, etc. The present author has found that this is also the case in the Japanese pearl oyster. It is very probable that similar factors are working in other

bivalves in which the sex is apparently or strictly separate. In the tridacnid clams, however, conditions seem to be somewhat different.

In these molluscs, the spawning of eggs and of sperm are accompanied by the same behavior, with rhythmical contraction of the adductor; whereas, in *Crassostrea virginica*, muscular contraction of the adductor plays no rôle in the release of sperm and, moreover, there is no increase in the rate of pumping of water during male spawning (Galtsoff, 1940).

In the tridacnid clams, the discharge of sex cells is nearly always preceded by two or three movements of the adductor, and it was not infrequently observed that the typical rhythmical spawning motions of the shell valves occurred without being followed by the discharge of sex cells. The latter case was observed when gonads were poorly developed, or a weak stimulus was employed. Further, in several particular cases, it was observed that the discharge of sperm occurred without accompanying the shell movements. These facts seem to suggest that the discharge of sex cells and the rhythmical movements of the adductor are differently controlled, although a close relationship exists between the two reactions.

The independence of the rhythmic spawning contractions and ovulation is also shown in oyster. Loosanoff and Davis (1952) report that, when some American oysters, probably females, which had been reared at 15°C for 25 or 30 days were subjected to chemical and thermal stimuli, they moved their shells in typical rhythmic spawning motions, but no eggs were discharged. This seems to have been due to a poor condition of the gonads, since spawning was successfully induced in a few oysters for the first time on the 35th day of exposure to 15°C. Nelson and Allison (1940) also report that four sterile "spawnings" have been observed in female oysters.

As was already stated, a clam in which only shell movements were induced by a gonad suspension of low concentration responded typically to a suspension of higher concentration. This seems to show that the discharge of sperm in *Tridacna* does not follow the "all-or-none" principle unlike the female spawning of *C. virginica* (Galtsoff, 1938 b). Concerning spawning in the male oyster, Galtsoff (1940) states that the amount of sperm released and the duration of ejaculation greatly varied, depending upon the state of ripeness of the male and the strength of the stimulus employed.

The discharge of eggs in oviparous oysters or pearl oysters can be readily induced by a suspension of self sperm; the shedding of eggs in hermaphroditic tridacna, on the other hand, could not be provoked by sperm suspension, according to the foregoing experiments.

The active principle in gonad suspension is species specific in the tridacnid clams, and the suspension prepared from different species is not only ineffective for the induction of spawning, but is antagonistic to self-gonad suspension; while, in American oysters, the males display no specificity in their spawning reaction and can be stimulated by eggs of other Pelecypoda or echinoderms, and also by thyroidin or other chemicals or by the sperm of the self species.

In this connection, it should be noted that specificity is also observed in the case of the jelly of tridacna eggs; in experiments on interspecific fertilization,

it has been observed that foreign sperm do not penetrate through the egg jelly, but are arrested at its outer layer, while the self-species sperm readily reach the egg membrane.

From the results of the foregoing experiments, it has been postulated that the active principle in gonad suspension comes from both the eggs and the primordial ovogonia or other ovarian tissue cells. Galtsoff (1940) is of the opinion that the stimulating substance of oyster egg suspension is not derived from the ovarian tissue cells or juices which may be present in suspension, although he has not presented any data which directly corroborate this conclusion.

The activity of gonad suspension was found to be affected by heating. Marked loss of potency was recognized by heating to 75°C or by boiling for 90 seconds, and the activity was completely lost by heating to 55°-60°C for 15 minutes or by boiling for 5 minutes. However, it cannot be confirmed whether the active principle is destroyed by heat, whereas it is certain that some substance or substances are formed by heating, which arrest the activity of the gonad suspension.

The active principle of egg suspension of oysters can withstand boiling for 30 seconds or heating at 68°C for 10 minutes (Galtsoff, 1940).

Judging from the facts observed in successive spawning and in chemical stimulation, it may be postulated that, in nature, molluscs respond first to spawning stimulus or stimuli with shedding of eggs, and a certain water-soluble substance borne by the eggs stimulates the discharge of sperm in other individuals. Fertilization will thus be effected.

Summary and Conclusion

1. The tridacnid clams are protandric functional hermaphrodites. Throughout the whole extent of the hermaphroditic gonads, female and male acini are found side by side, and both kinds of sex cells mature simultaneously, while in spawning they are discharged completely separately.

2 Spawning reactions are similar in shedding of eggs and sperm ejaculation. The reaction involves discharge of the sex cells, rhythmical motions of the adductor muscle, and characteristic movements of the mantle in the region of the inhalent aperture and exhalent siphon. Water containing the sex cells is squirted vigorously from the erected exhalent siphon with the contraction of the adductor. In the early phase of spawning the shell movements are performed at intervals of from 15 to 30 seconds, which become longer as spawning approaches its end.

3. The discharge of sex cells is almost always preceded by two or three shell-movements; not infrequently, only the rhythmical motions of the adductor were observed, without subsequent discharge of sex cells. This was observed in animals with poorly developed gonads, or when a weak stimulus was employed. In an animal which had been exposed to low temperature, it was observed that the dischage of sex cells occurred without accompanying shell-movement.

Hence, it is supposed that the discharge of sex cells and the rhythmical movements of the adductor are, while closely related, regulated by different physiological controls; and the spawning (of sperm) does not follow the "all-or-none" principle.

4. Discharge of sperm can easily be induced by the addition to the water of gonad suspension. The latent period varies from 20 sec. to 19 min., mostly lying between 50 sec. and 2 min. Shedding of eggs could not be induced by gonad or sperm suspension.

5. Discharge of sperm can be induced at temperature as low as 21°C. Such a low temperature will never be encountered in the natural habitat of these animals.

6. The lowest limit of effective concentration of gonad suspension seems to lie between 0.5×10^{-5} and 1×10^{-5} (for *T. squamosa*).

7. The active principle is carried by eggs and also by primordial ovogonia or other ovarian tissue cells; suspension of sperm or spermatic tissue cells is not effective in inducing spawning reactions.

8. The action of gonad suspension is species specific, and suspensions of different species of the family are not only ineffective, but deter the action of the self species suspension.

9, The active principle is soluble in water, and is destroyed neither by distilled water, nor by the killing of eggs or sperm. By rather long heating, the potency of gonad suspension is completely lost. It is very certain that some substance(s) are formed by this treatment which deter the effect of the fresh suspension. However, it cannot be decided whether the active principle is destroyed by heating.

References

Galtsoff, P.S. 1938a, Physiology of reproduction of *Ostrea virginica*. I. Spawning reactions of the female and male. Biol. Bull., **74**: 461-486.

——— 1938b, Physiology of reproduction of *Ostrea virginica*. II. Stimulation of spawning in the female oyster. Biol. Bull., **75**: 286-307.

——— 1940, Physiology of reproduction of *Ostrea virginica*. III. Stimulation of spawning in the male oyster. Biol. Bull., **78**: 117-135.

Iwata, K.S. 1952, Mechanism of egg maturation in *Mytilus edulis*. Biol. Jour. Okayama Univ., **1** (1/2): 1-11.

Loosanoff, V.L., and H.C. Davis. 1952, Temperature requirements for maturation of gonads of northern oysters. Biol. Bull., **103** (1): 80-96.

Nelson, T.C., and J.B. Allison. 1940, On the nature and action of diantlin; a new hormone-like substance carried by the spermatozoa of the oyster. Jour. Exp. Zool., **85**: 298.

Wada, S.K. 1942, Notes on the tridacnid clams in Palau. Kagaku-Nan'yo (Science in the South Seas), **5** (1): 62-69 (in Japanese).

——— 1952, Protandric functional hermaphroditism in tridacnid clams. Oceanogr. Magazine (Tokyo), **4** (1): 23-30.

Yonge, C.M. 1936, Mode of life, feeding, digestion and symbiosis with zooxanthellae in the Tridacnidae. Sci. Rep. Great Barrier Reef Exped. 1928-29, **1** (11): 283-321.

Reprinted from the *Papers in Meteorology and Geophysics* Vol. IV Nos. 3~4, 1953
Published by the Meteorological Research Institute

On the Cauchy-Poisson Waves Caused by the Eruption of a Submarine Volcano (III)*

S. Unoki

and M. Nakano

Published by the Meteorological Research Institute,

Mabashi, Suginami, Tokyo, Japan

December 1953

550.342:550.345

On the Cauchy-Poisson Waves Caused by the Eruption of a Submarine Volcano (Ⅲ)*

S. Unoki

Central Meteorological Observatory

and M. Nakano

Meteorological Research Institute

(Received November 30, 1953)

Abstract

Peculiar tsunami waves produced by the eruption of a submarine volcano at Myojinsho Reef on March 11, 1953 were recorded by wave gauges installed on Hachijojima Island, Cape Omaezaki and Jogashima Island, which are distant from the volcano by 130, 336 and 356 km, respectively. Moreover, from the 11th to the 25th of March tsunami waves were recorded about fifty times at Hachijojima Island. From these data we could make clear the features of the variation of waves with distance as well as with time, and it was proved that the theory of Cauchy-Poisson wave explains these waves satisfactorily. It was also shown that these waves were caused by an initial impulse rather than by an initial elevation at the moment of explosion, and that the waves progressed with group velocity. In order to understand two kinds of tsunami waves, one of which shows a conspicuous beat phenomenon while the other does not, discussions were made on the effect of initial impulse of different types.

1. Introduction

In the previous papers [1], we investigated peculiar tsunami waves caused by the eruption of Myojinsho Reef on the 16th, the 24th and the 26th of September, 1952, which were recorded by the wave gauge installed on Hachijojima Island, and showed that the Cauchy-Poisson wave actually exists in the ocean. However, since our discussions were based on the data at only one station, the theory was not

* This investigation has been carried out as a part of the "Microseism and Ocean Wave Research Project" of the Central Meteorological Observatory of Japan during 1951~1953.

verified by observations as to the change of the wave with distance.

Fortunately, on March 11, 1953, a tsunami wave caused by a volcanic explosion at Myojinsho Reef was recorded not only at Hachijojima Island, but also at Cape Omaezaki, Shizuoka Prefecture, and Jogashima Island, Kanagawa Prefecture, where wave gauges similar to that installed on Hachijojima Island had been operating. Moreover, at Hachijojima Island, tsunami waves were recorded about fifty times in the period from the 11th to the 25th of March. These data give us some interesting new facts that help us to answer several questions still unsolved.

Fig. 1. Map showing the locations of Jogashima Island, Cape Omaezaki, Hachijojima Island and Myojinsho Reef.

2. Observed data

According to the reports of the crewmen who have been in the vicinity of Myojinsho Reef, the shape of the reef have frequently varied since the eruptions in September 1952. Though these reports suggest that the submarine volcano was as active as before, tsunami waves were not recorded by the wave gauge of Hachijojima Island till the 11th of March 1953.

The waves caused by a vigorous eruption on the 11th of March, 1953, were recorded at Jogashima Island, Cape Omaezaki and Hachijojima Island, and the records are shown in Fig. 2 (A), (B) and (C). On the other hand, a peculiar type of seismic waves with small amplitude was recorded by a portable seismograph of the Hachijojima Weather Station at 07h 28m 29.4s on March 11, and it is somewhat doubtful whether this seismic wave was

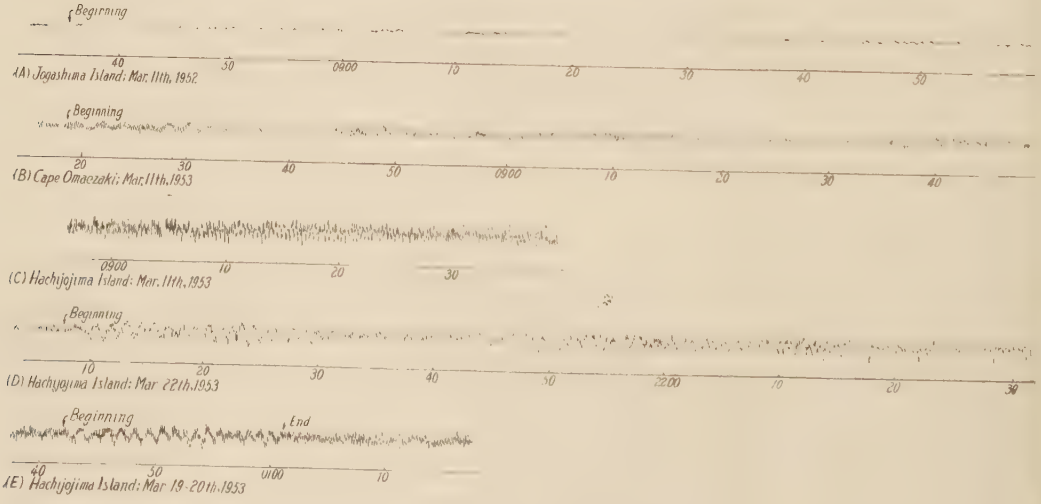

Fig. 2. Wave records.

due to the explosion of Myojinsho Reef or not, according to seismologists. However, in default of proof that it was not due to the explosion, we shall consider this wave to have been produced by the explosion which caused the tsunami wave. Assuming the velocity of this wave to be several kilometers per second, the eruption can be assumed to have occured at about 07 h 28 m.

At Jogashima Island the tsunami wave began to appear at 08 h 33 m, the period of which was 114 seconds and the maximum wave-height was only 13 cm. At Cape Omaezaki, the first wave with the period of 125 seconds occurred at 08 h 19 m and the maximum wave-height was only 15 cm. Strictly speaking, however, the time of beginning of the tsunami wave could not be determined so definitely ; of course, the wave-height was measured after the effects of wind waves and swell were eliminated by smoothing the wave records. At these two stations the tsunami wave shows the phenomenon of beat, but the time of occurrence of its nodes can not be determined so definity.

At Hachijojima Island, as shown in Fig. 2 (C), we can not know the time of beginning of the tsunami wave, owing to the lack of the records in early stages. Since the maximum wave-height is 58 cm even in the rear part of this tsunami wave, it is considered that the present tsunami wave was very large compared with those on other days. The distance from Myojinsho Reef to Cape Omaezaki and to Jogashima Island is respectively 336 and 356 km, and it is not so unreasonable to consider that the wave traveled almost along straight paths, because the sea is deep and the depth uniform, as a whole, except in the vicinity of the stations.

Moreover, similar tsunami waves with comparatively small wave-height were recorded at Hachijojima Island successively during the half-month after the 11th of March. The values of some elements read off from the wave records are shown in Table 1.

When wind waves and swell due to cyclones prevail, it is difficult to detect the tsunami wave out of wave records, because the period of the tsunami wave is long and its wave-height is comparatively small. Accordingly, the actual frequency of our wave seems to be more than what is shown in Table 1.

Of these records, twelve cases show a conspicuous "beat" and the duration of tsunami is very long, while the remaining cases do not show any beat phenomenon and the duration of tsunami is short. Fig. 2 (D) and (E) are representative examples of these waves, observed at 21h on the 22nd and at about 01h on the 20th of March, respectively. So far as the tsunami waves which occurred in the said March are concerned, except that on March 11, tsunami waves observed at Hachijojima Island were not recorded by the wave gauges of the stations at Cape Omaezaki and Jogashima Island, and this may be due to the fact that the wave was too faint to appear at these stations. In our first paper [1] it was said that at Cape Omaezaki and Jogashima Island no tsunami waves accompanying the eruptions of Myojinsho

Table 1. Results of wave observations at Hachijojima Island*.

d	t_0 h	m	τ_1 sec	H_1 cm	H_2 cm	H_3 cm	t_d min	t_n min
Sept. 1952								
16	12	20	96	56	27	24	80	31
24	12	53	(93)	92	39	30	90	30
26	13	03	86	71	54	36	80	30
Mar. 1953								
11	—	—	—	—	—	58	—	—
12	16	09	88	55	—	—	60	—
14	10	03	92	57	44	—	60	29
〃	14	11	68	27	—	—	10	—
〃	16	47	73	32	—	—	20	—
〃	18	40	70	37	—	—	20	—
〃	21	05	71	30	—	—	5	—
15	03	49	72	36	21	—	60	24
〃	13	08	84	31	—	—	15	—
〃	15	16	74	25	—	—	5	—
〃	17	15	91	33	—	—	20	—
〃	18	42	83	36	—	—	40	—
〃	22	09	100	32	—	—	20	—
16	00	24	78	24	—	—	15	—
〃	00	49	93	33	—	—	15	—
〃	03	47	90	32	—	—	20	—
〃	07	34	88	50	25	—	50	26
〃	09	37	76	28	—	—	20	—
〃	11	23	78	29	—	—	20	—
〃	13	43	108	35	—	—	15	—
〃	18	46	75	37	—	—	15	—
Mar. 1953								
17	02	24	58	36	—	—	15	—
〃	04	40	92	47	—	—	25	—
〃	12	36	86	42	—	—	15	—
〃	15	45	77	63	—	—	35	28
〃	19	18	90	48	—	—	15	—
〃	21	51	100	30	—	—	30	—
18	00	15	107	30	24	—	60	35
〃	02	44	83	30	—	—	35	—
〃	03	56	71	28	—	—	15	—
〃	11	06	69	25	—	—	10	—
〃	14	07	85	34	—	—	20	—
〃	16	25	88	27	—	—	20	—
〃	19	27	91	28	—	—	20	—
〃	21	39	86	40	—	—	25	—
〃	22	5	95	37	—	—	15	—
19	02	05	95	40	—	—	20	—
〃	05	06	69	42	—	—	45	—
〃	10	35	74	32	—	—	25	—
〃	13	16	102	28	—	—	15	—
〃	16	33	76	34	—	—	20	—
〃	20	15	95	60	28	—	50	30
20	00	42	85	47	—	—	20	—
22	21	08	106	57	40	26	120	30
23	02	23	95	58	—	—	60	27
〃	13	56	119	38	—	—	60	28
25	01	02	95	50	—	—	25	—
〃	07	13	93	54	—	—	40	—

t_0: Time of beginning of the tsunami wave.

t_d: Duration of the tsunami wave (from the beginning to the end).

t_n: Time-interval from the first wave to the first node.

τ_1: Period of the first wave.

H_1, H_2, H_3: Maximum wave-heights in the first, second and third groups of a wave train, respectively, where the latter two groups appear when the wave record shows a conspicuous beat.

* In the case of Hachijojima Island, owing to the lack of a master clock for time checking, it is probable that there might be errors of about 10 minutes, except the cases of the 16th, the 24th and the 26th of September 1952 and the 11th of March 1953.

Reef were seen in September, 1952. But, according to a more careful examination afterwards, faint traces of tsunami waves could be perceived in the wave records at Jogashima Island occurring at about 15h of the 24th, 08h of the 25th and 20h of the 25th of September, 1952, although the details are unknown on account of their too small amplitudes.

3. Variation of wave period

According to equation (19) in our second paper [1], when the point of observation is very far from the disturbance source, the wave-period is approximately represented by

$$\tau = \frac{4\pi\varpi}{gt} \quad (1)$$

where ϖ denotes the distance of the observing point from the centre of the disturbance source, and t the time elapsed since the explosion; that is, τ is linearly proportional to $\frac{\varpi}{t}$. This theoretical straight line is shown in Fig. 3, where $\frac{\varpi}{t}$ is taken as abscissa, and τ as ordinate. In Fig. 3, there are also shown the actual data observed at Jogashima Island, Cape Omaezaki and Hachijojima Island on March 11, 1953. In the calculation of $\frac{\varpi}{t}$, the origin of time was taken at 07h 28m, which was determined by the occurrence of the seismic wave mentioned above. Comparison of the theoretical straight line with observed values gives a fair agreement for all the stations under consideration, showing that equation (1) is satisfied with the values of time and distance concerned. Conversely speaking, it may be said that the said seismic wave observed at Hachijojima Island was due to an explosion of the submarine volcano at Myojinsho Reef.

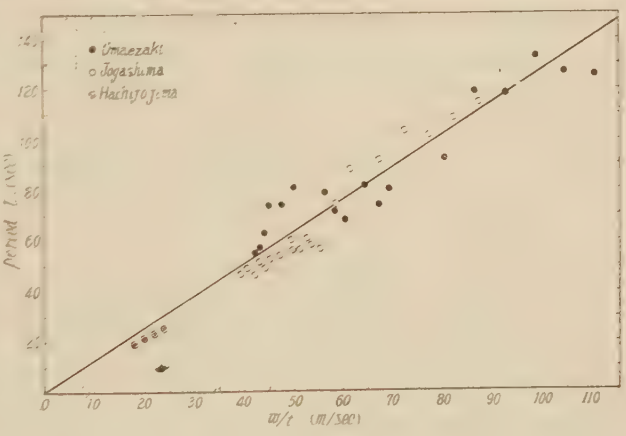

Fig. 3. The variation of wave-period τ with the value of $\frac{\varpi}{t}$. The straight line denotes the theoretical values calculated by Eq. (1). The points marked with ●, ○ and + correspond to the observed values; the observed values are based on the wave records of March 11, 1953.

4. Variation of wave-height

According to the second paper, under the initial conditions such as

$$\zeta=0, \quad \rho\phi_0=P(\varpi\leqq l), \quad \rho\phi_0=0(\varpi>l) \quad \text{at} \quad t=0 \quad \text{and} \quad z=0, \quad (2)$$

the wave-height is approximately given by

$$(3) \qquad \zeta_i = -\frac{Pl}{2^{1/2}\rho\bar{\omega}^2} e^{-\mu t} \cdot \sin\left(\frac{gt^2}{4\bar{\omega}}\right) \cdot J_1\left(\frac{gt^2}{4\bar{\omega}} \cdot \frac{l}{\bar{\omega}}\right),$$

where 2μ is the coefficient of frictional force and is equal to 5.5×10^{-4} sec^{-1}. On the other hand, in the case of initial elevation, the solution is approximately

$$(4) \qquad \zeta_e = \frac{2^{1/2}QL}{\bar{\omega}} e^{-\mu t} \cdot \cos\left(\frac{gt^2}{4\bar{\omega}}\right) \cdot J_1\left(\frac{gt^2}{4\bar{\omega}} \cdot \frac{L}{\bar{\omega}}\right),$$

under the conditions of

$$(5) \qquad \zeta = Q\ (\omega \leqq L),\ \zeta = 0\ (\omega > L),\ \rho\hat{\phi}_0 = 0 \quad \text{at} \quad t = 0 \quad \text{and} \quad z = 0.$$

From the theory it is known that the wave-height decreases with time, showing a phenomenon of beat as clearly seen in Fig. 1 (D) and (F) of the second paper [2]. In Table 1, we can find nine examples showing conspicuous "beat". In this table are also shown the maximum wave-heights H_1, H_2 and H_3 in the first, second and third wave groups, respectively, which appeared as the consequence of beat and are separated from each other by nodes. In every case we have calculated the values of H_2/H_1 and H_3/H_1, which mean the rate of decrease of wave-height. The averaged values of them are given in Table 2, Theoretical values can be calculated by (3) or (4) according to the case of initial impulse or initial elevation, and are shown also in the table. In the theoretical calculation we used $\bar{\omega}=130$km and l or $L=2.2$km.

Table 2. Average values of H_1/H_1, H_2/H_1 and H_3/H_1.

Rate of decrease of wave-height with time		H_1/H_1	H_2/H_1	H_3/H_1
Observation at Hachijojima Island		1.00	0.61	0.43
Theoretical Values	the case of initial impulse	1.00	0.62	0.44
	the case of initial elevation	1.00	0.36	0.20

Strictly speaking, the time of occurrence of the actual maximum wave-height does not always agree with the theoretical one, but we did not consider it. According to Table 2, the agreement between theory and observation is quite satisfactory in the case of initial impulse. In the second paper [1] we stated that the action of initial impulse, rather than that of initial elevation, seems to have been effective on the formation of our waves at the moment of explosion at Myojinsho Reef. Here we could prove the correctness of our judgement.

At Jogashima Island and Cape Omaezaki, the rate of decrease of wave-height could not be determined so distinctly as at Hachijojima Island on account of small wave-height and obscure beat, as shown in Fig. 2 (A) and (B). Roughly speaking, however, at Omaezaki the decrease of wave-height seems to have been slower than it is shown in Table 2, and at Jogashima Island, the maximum wave-height in the first wave group seems, to our surprise, to have been rather smaller than those in the second and the third wave groups. But the cause of this is not yet

nown. In order to make it clear, more data of observation would be necessary.

Now, according to Table 1, we can recognize that the largest wave with aximum wave-height 92cm occurred on September 24, 1952. Though the explosion hich caused this wave was strong enough to cause the sinking of the *Kaiyo-maru* o. 5, the wave hardly appeared at Jogashima Island.

On the other hand, in spite of the lack of the wave records at early stages, the ave of March 11, 1953, can be considered to have been far larger than that of eptember 24, 1952, because the former reached Jogashima Island with larger nplitude. Moreover, at Hachijojima Island the maximum wave-height H_3 in the ird group of the former wave is larger than that of the latter. Using the xperimental (and also theoretical) formula $H_3/H_1=0.43$ represented in Table 2, we n guess the maximum wave-height H_1 of the first wave group at Hachijojima land; namely,

$$H_1=58/0.43=135\text{ cm},$$

r March 11, 1953, which is far larger than 92cm of September 24, 1952, just as e expected.

So far, we have discussed the time-variation of wave-height. We shall now nsider the decrease of wave-height with distance. Table 3 gives the ratio of the aximum wave-height H_1 of the first wave group at Cape Omaezaki and Jogashima land to that at Hachijojima Island, using the data of March 11, 1953. The eoretical values which are also shown in the same table were calculated by (3) (4) according to the case of initial impulse or initial elevation.

Table 3. Rate of decrease of wave-height with distance.

Station	Maximum wave-height (cm)	Observational values	Theoretical values	
			case of initial impulse	case of initial elevation
Hachijojima Island	(135)	1.00	1.00	1.00
Cape Omaezaki	15	0.11	0.15	0.25
Jogashima Island	8	0.06	0.14	0.19

In comparing observational with theoretical values, it must be borne in mind at (3) and (4) were obtained by assuming the sea to be very deep everywhere nd the motion of wave to be symmetrical with respect to the axis of Z. In actual ses, however, the waves are subject to refraction and diffraction in the neighourhood of the wave gauge station, where the sea is shallow and the depth is t uniform. Consequently, the wave-height varies locally. Thus, at Hachijojima land, as has already been shown in the second paper, the wave-height bemes considerably large owing to the effect of refraction, etc. And similar

circumstances seem to hold for the cases of Cape Omezaki and Jogashima Island, but we can not estimate the magnitude of local variation of wave-height quantitatively.

Leaving the said local variation of wave-height out of consideration and comparing the observation with the theory, though this may be a rather rough-and-ready procedure, it might be provisionally concluded that the rate of decrease with distance of actual wave-height is rather nearer to what was obtained theoretically for the case of initial impulse than for the case of initial elevation, and that it endorses the result stated at the beginning of the present section.

5. Two kinds of tsunami waves

According to equation (3), which is represented in Fig. 1 (D) of the second paper [1], the wave-height increases gradually with time in the first stage. In actual cases, however, the wave tends to begin suddenly with considerable amplitude and with a period of about 90 seconds, as shown in Fig. 2 (D) and (E) of the present paper and Fig. 2 (A), (B) and (C) of the first paper [1]. A part of the causes of this disagreement may be attributed to the fact that our solution is only an approximate one under the condition that $\frac{gl^2l}{4\pi^2}$ is large, and also to the fact that wind-waves and swell frequently happen to conceal the tsunami wave in the first stage, because the latter is too small. But this is not enough to make the question clear.

Now, from Table 1, we obtain Fig. 4 (A) which represents the frequency distribution of the period τ_1 of the first wave. From this figure we can recognize that the wave with the period of about 90 seconds was the first to reach Hachijo-jima Island most frequently. What does this fact mean? Again, Fig. 4 (B) gives

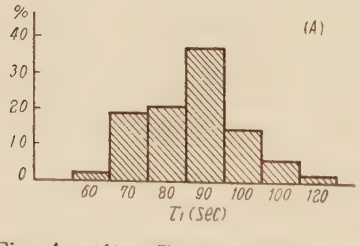

Fig. 4. (A): Frequency distribution of the period τ_1 of the first wave.

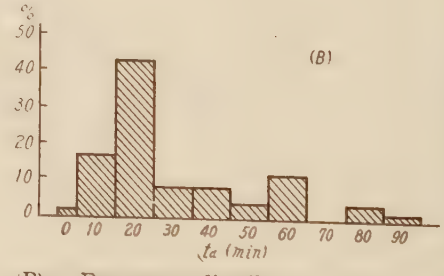

(B): Frequency distribution of the duration t_d of a wave train.

the frequency distribution of duration t_d, viz. the time interval from the beginning to the end of a wave train. And we can seen from this figure that there exist two maximum frequencies centering at 20 min. and 60 min., respectively. Why? Further, referring to Table 1, it is seen that in some cases the wave shows a conspicuous beat phenomenon, while in other cases no beat occurs. Each of their examples is shown in Fig. 2 (D) and (E), respectively. Thus it appears that there

ist two kinds of tsunami waves. This is also an interesting fact.

We shall now answer the above questions. According to equation (7) in the cond paper [1], when the initial conditions are given by

(6) $$\zeta=0,\quad \rho\phi_0=Pe^{-\frac{\varpi^2}{4r^2}},\qquad \text{at } t=0 \text{ and } z=0,$$

e solution is

$$\zeta^*=-\frac{Pe^{-\mu t}}{\rho}\int_0^\infty \frac{k^2}{\sigma}\sin\sigma t\cdot J_0(k\varpi)\,dk\int_0^\infty e^{-\frac{\alpha^2}{4r^2}}J_0(k\alpha)\,\alpha d\alpha,$$

here

$$\sigma^2+\mu^2=gk\,.$$

nce

$$\int_0^\infty e^{-\frac{\alpha^2}{4r^2}}J_0(k\alpha)\,\alpha d\alpha=2r^2e^{-r^2k^2},$$

om WEBER's infinite integral and

$$J_0(k\varpi)\fallingdotseq\left(\frac{2}{\pi k\varpi}\right)^{1/2}\sin\left(k\varpi+\frac{\pi}{4}\right),$$

hen $k\varpi$ is large, we have

$$\zeta^*=-\frac{2^{3/2}\pi^{1/2}r^2}{\rho\varpi^{1/2}}e^{-\mu t}\Re\left[\frac{1}{2\pi}\int_0^\infty\frac{k^{3/2}}{\sigma}e^{i(\sigma t-k\varpi-\frac{\pi}{4})}\,e^{-r^2k^2}dk\right.$$

$$\left.-\frac{1}{2\pi}\int_0^\infty\frac{k^{3/2}}{\sigma}e^{i(\sigma t+k\varpi+\frac{\pi}{4})}\,e^{+r^2k^2}dk\right].$$

sing KELVIN's method [2] as to the principle of stationary phase as in the second aper, it becomes

(7) $$\zeta^*=-\frac{Pgr^2t^3}{2^{\frac{3}{2}}\rho\varpi^4}e^{-\mu t}\sin\left(\frac{gt^2}{4\varpi}\right)\cdot e^{-\left(\frac{gt^2}{4\varpi}\cdot\frac{r}{\varpi}\right)^2}.$$

In comparing this solution with (3), we have only to consider such formulas as

(8) $$\zeta_i=A\theta^{1/2}J_1(\theta)\,,$$

nd

(9) $$\zeta^*=B\theta^{3/2}e^{-\theta}\,,$$

stead of original equations where A and B are constant, and we put

(10) $$\theta=\frac{gt^2}{4\varpi}\cdot\frac{l}{\varpi}\quad\text{or}\quad\frac{gt^2}{4\varpi}\cdot\frac{r}{\varpi},$$

cording to (3) or (7), respectively.

The results of numerical calculations are shown in Fig. 5. Two insets (A) and 3) in the figure represent the distribution of initial impulse given by (2) and (6), spectively.

In the first stage, the wave-height given by ζ_i increases gradually, while the ave-height given by ζ^* suddenly reaches its maximum value. Accordingly, by

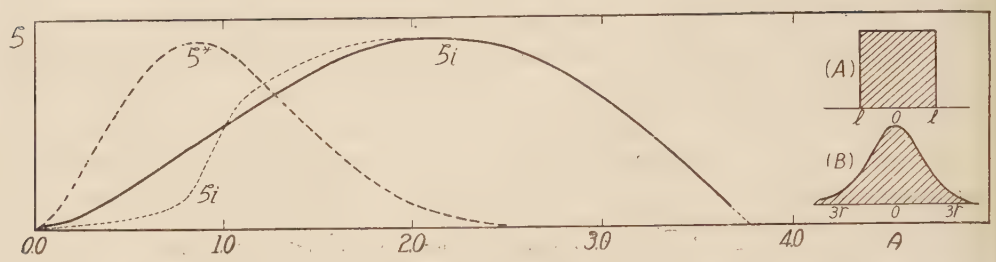

Fig. 5. Results of numerical calculations of equations (8) and (9), which are shown by the curves ζ_i and ζ^*. Two insets (A) and (B) reprasent the distribution of initial impulse given by (2) and (6), respectively.

assuming a suitable distribution of initial impulse, we shall be able to explain the fact that the wave under consideration occurs suddenly at a certain time with a considerable amplitude and with a given period.

Moreover, the wave represented by ζ_i shows a beat phenomenon and its duration is long, while that represented by ζ^* does not show a beat and its duration is short. Accordingly, it is considered that the type of waves accompanied by a conspicuous beat and represented by Fig. 2 (D) may have been produced by an initial impulse whose distribution is something like (2). On the other hand, another type of wave which shows no beat and represented by Fig. 2 (E) may have been due to an initial impulse whose distribution is rather near to (6). In order to complete our idea, it is most desirable to find the form of initial impulse which causes such tsunami wave as ζ_i' in Fig. 5, but we could not do it.

According to Table 1, the time t_n elapsed since the occurrence of the first wave till that of the first node is almost thirty minutes in all the cases amounting to twelve in number. Referring to the theory given in the previous paper, this means that the area affected by an initial impulse was nearly of the same magnitude in all the cases, its radius l being about 2.2 km.

6. Volocity of tsunami waves

In the first paper, we could not ascertain that the wave progressed with group velocity as the theory demands, owing to the fact that there was not much difference between the phase velocity and the group velocity while the distance of travel was not sufficiently large, and that the accuracy of the time-marks was not necessarily satisfactory.

In the case of March 11, 1953, the mean velocity of propagation of the wave $\bar{C}$ obtained from the observations is as shown in Table 4. In this table are also shown the values of the phase velocity C and the group velocity C_g of a medium wave (elliptic trochoidal wave) given by

$$C=\left\{\frac{g\lambda}{2\pi}\tanh\left(\frac{2\pi d}{\lambda}\right)\right\}^{\frac{1}{2}} \quad \text{and} \quad C_g=\frac{C}{2}\left\{1+\frac{\frac{4\pi d}{\lambda}}{\sinh\left(\frac{4\pi d}{\lambda}\right)}\right\},$$

spectively, and of the group velocity C_{og} of a deep-water surface wave, together ith the values of the period of the first wave τ_1, the distance of travel ϖ, the avel-time t_{ϖ} and the mean depth $\bar{d}$.

Table 4. Mean velocity of propargation of the wave $\bar{C}$ obtained from observations.

Station	τ_1 sec	ϖ km	t_{ϖ} min	$\bar{d}$ km	$\bar{C}$ m/s	C_g m/s	C m/s	C_{og} m/s	λ km
Cape Omaezaki	125	336	51	1.6	109	102	117	98	14.6
Jogashima Island	114	356	65	1.1	91	88	98	89	11.2

Now, comparing $\bar{C}$ with C or C_g, it seems that in the case of Jogashima Island he wave progressed with group velocity rather than with phase velocity. In the ase of Omaezaki, however, it appears that we can not give any decision as to hether the wave traveled with group velocity or with phase velocity. In order hat we can give a decisive answer to this question, it is necessary above all that the me of start of the wave from its source or the time of the corresponding explosion t Myojinsho Reef is accurately known, but as mentioned in Section 2, there exists kind of uncertainty as to this point. Such being the case, the present tsunami ata are also insufficient for the solution of our question. The present section has nly be added by way of a suggestion.

Moreover, referring to the above table, it can be seen that the group velocity $_{og}$ of deep-water surface wave is near to $\bar{C}$ or the actual velocity of propagation f the wave. This fact suggests that we can not so unreasonably go on with our iscussions by assuming the wave to be a deep-water one as already pointed out n the first paper [1]. The wave-length λ of these waves is more than ten killo- heters !

. Nature of volcanic eruptions which caused tsunami waves

It has already been proved in Section 4 that our tsunami waves were produced y an initial impulse at the moment of explosion at Myojinsho Reef. According to Table 1, these tsunami waves occurred successively during the latter halves of September, 1952 and March, 1953. and in other periods no tsunami was recognized. On the other hand, it is seen that eruptions occurred frequently even when no sunami wave was recorded as stated in Section 2. Strictly speaking, this fact was ecognized even in September, 1952, as stated in the first paper [1].

The above facts suggest that the eruptions which changed the features of the eef are of a different kind from the eruptions which caused tsunami waves, though n some cases they may be active in both actions. The latter action will be most iolent when the eruption occurs under the sea and with strong impulse. That a trong impulse really acts on the water surface at the moment of an explosion of

a submarine volcano is confirmed by the fact that a vessel which happened to pass over a submarine volcano in explosion received a violent shock, a "sea-shock" as it is called.

Moreover, according to Table 1, it appears that tsunami waves occurred several times a day in the most active period from the 14th to the 19th of March, 1953. Such frequent occurrence of volcanic explosions has already been reported by many volcanologists in the case of volcanoes on land.

Acknowledgement———In conclusion, the present authors wish to express their hearty thanks to Mr. S. Daidoji, Director of the Hachijojima Weather Station, Mr. Y. Ota, Director of the Omaezaki Weather Station, and Mr. Y. Kuga of the Central Meteorological Observatory, who kindly furnished the authors with their valuable wave records. Equal thanks are due to Mr. Y. Fujii, Chief of the Oceanographical Section of the Central Meteorological Observatory, for his interest and advice, and to Mr. K. Kajiura of Tokyo University, for his helpful informations and suggestions.

References

[1] Unoki, S. and Nakano, M. 1953: On the Cauchy-Poisson Waves Caused by the Eruption of a Submarine Volcano (I) and (II), Oceanographical Magagine **4.** p. 119 and **5.** p. 1.

[2] Lamb, H. 1932: Hydrodynamics, S. 241.

A STUDY ON THE FOAMING OF SEA WATER ON THE MECHANISM OF THE DECAY OF FOAM LAYER OF SEA WATER

Abe Tomosaburo

Reprinted from

Records of Oceanographic Works in Japan

Volume I, No. 2, New Series,

December 1954

Published by

Japanese National Commission for Unesco

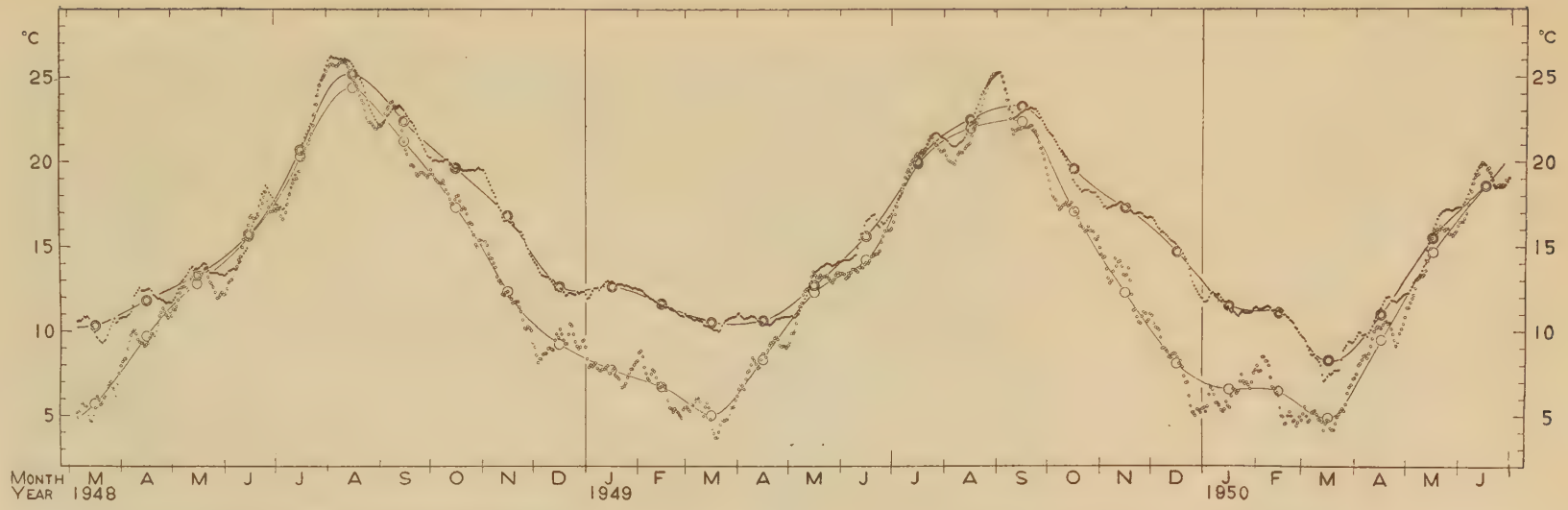

Fig. 1. The variations of the air and sea-surface temperatures at the fixed station "Extra" (30° N, 153° E) in the North Pacific Ocean from March 1948 to June 1949. The small circles represent the moving averages of 11 days, the open being for air temperature and the solid for sea-surface temperature. The large open circles and large double circles represent the monthly means of air and sea-surface temperature respectively.

Records of Oceanographic Works
in Japan, Vol. 1, No. 2,
New Series, December 1953

A study on the foaming of sea water
On the mechanism of the decay of foam layer of sea water

By Tomosaburo Abe

Oceanographic Laboratory, Meteorological Research Institute

§1. *Introduction*

In observation of surface conditions of the sea, Beanfort's scale is mainly used at present. Existence of white-chops produced by wind is the most important factor on this scale.

It is considered from our experimental results that the degrees of white-chops change with the chlorinity concentration of sea water, the temperature and the stability of foam. These experimental relationships have already been reported by Y. Miyake and T. Abe. In the present paper, the mechanism of the decay of foam layer of sea water has been experimentally studied.

§2. *Experimental procedure.*

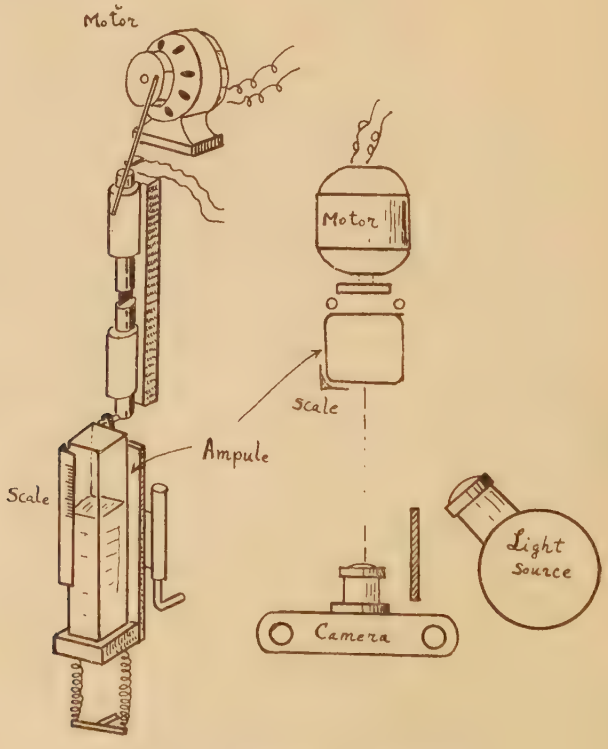

Fig. 1. Diagram of Apparatus

The glass ampule used in the present experiments has a square section of about $4 \times 4\,cm^2$ and about 15 cm in length. The ampule containing filtered sea water was vibrated up and down about 15 time per second in the amplitude 15 mm for about 30 seconds (Fig. 1). After the vibration was over, the features of foam layers were taken photograph illuminated by ultra high pressure mercury lamp. As soon as above procedures were over, the temperature of sea water was measured. All the apparatus were contained in a constant temperature room and kept at constant temperature within errors of $\pm 1°C$.

For the samples, the filtered natural sea water (19.26‰°Cl) and various ones which were prepared by diluting natural sea water in various degrees, were used. The experiments were done under the temperature of 29, 21, 14, and 5°C.

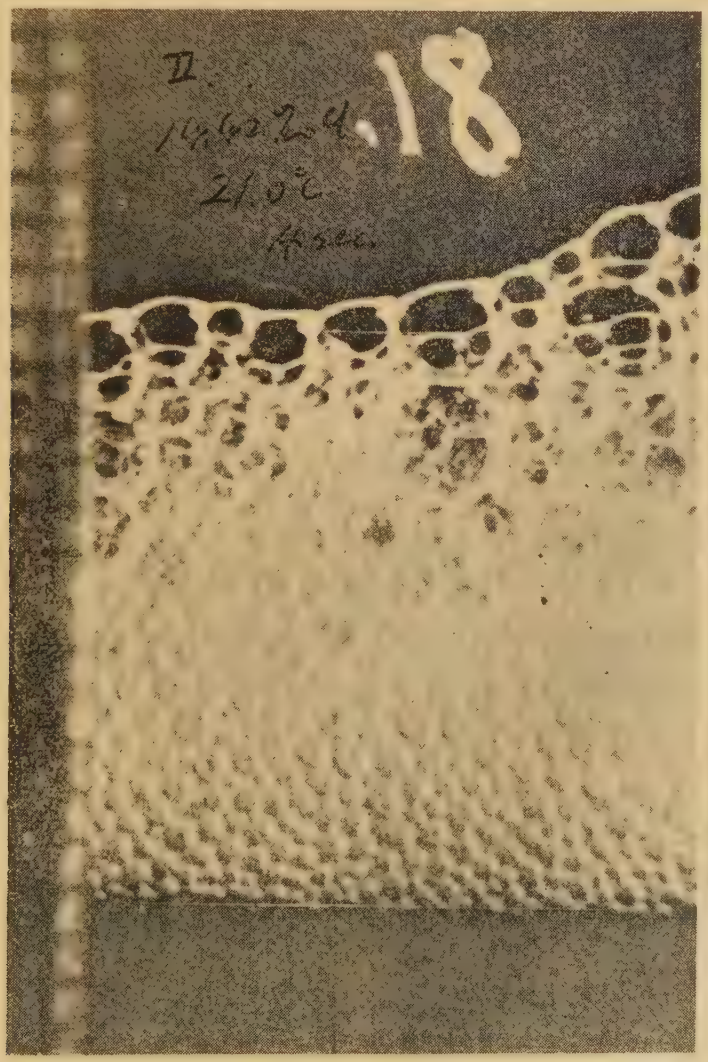

Photograph of Foam layer of Sea Water Cl. 14.42‰, after 4 sec.

§3. *Results and discussions.*

[1] **Relation between the height of foam layer and the time.**

All the samples show the analogous tendencies in reference to time, and so, for example, the case of sea water having the chlorinity concentration 14.42‰ at temperature of 28°C, is as follows:

The empirical relation between log h and t is shown in Fig. 2, where h is the height of foam layer (mm.) and t the time (sec.).

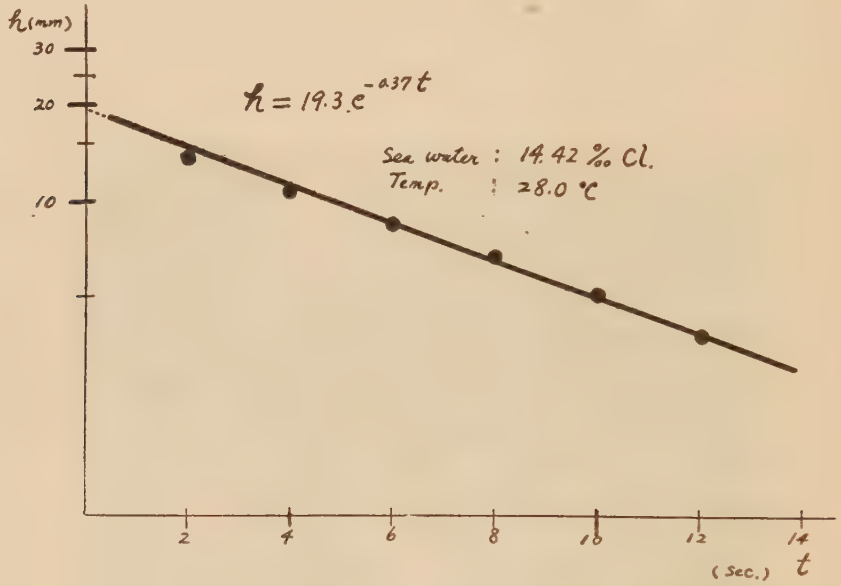

Fig. 2. Relation between the height of foam layer (h) and time (t)

Log h decreases linearly with increasing t, i.e.

$$h = h_0 e^{-kt} \tag{1}$$

where h_0 is the value of h at t=o, and k the decay constant of foam layer.

Hence by differentiating Eq. (1) with t, we have

$$\frac{dh}{dt} = -h_0 k e^{-kt} = -kh \tag{2}$$

That is, the speed of decay of foam layer is proportional to its height, and thus the type of the decay is that of the so-called "lst order chemical reaction". From Eq. (1), we can see that the time required for the height of foam layer to reduce to its half value, is constant. This corresponds to the half life τ, which is often used in the decay of radioactive elements. Hence from Eq. (1), we have

$$\frac{h_0}{2} = h_0 e^{-kt} \qquad \therefore \quad kt = \text{const} = 0.693$$

The results of measurements are given in Table 1.

Table. 1.

Chlorinity concentration ‰	Initial height of foam layer h_0(mm)	Decay const (k)	Half life τ(sec.)	Calculated value of kt
19.26	22.5	0.143	4.8	0.685
18.46	24.6	0.170	4.1	0.697
16.05	24.4	0.166	4.2	0.696
14.42	19.3	0.137	5.1	0.698
12.82	18.5	0.145	4.8	0.696
9.63	20.0	0.20	3.6	0.690

In the cases of sea water having chlorinity concentrations higher than 13‰, the value of τ is larger than that in the case of lower concentrations; that is, the foam layer is more stable in the former case than in the latter, and it does not decay easily. It was previously reported by us that foam is easily produced when the chlorinity of sea water has a comparatively large value, i.e. a value larger than 13‰ Cl., and the foam produced lasts longer. Thus, it is considered that in the sea regions with large chlorinity concentration, the white-chops easily appear, while in the sea regions with comparatively low chlorinity, i.e. lower than 9‰ Cl., the white-chops do not easily appear.

[2] **Changes in frequency distribution of the size of bubbles in foam layer.**

Frequency distributions of the size of bubbles at every 2 seconds were obtained, which are shown in Fig. 3. The size ranges of the bubbles were represented by

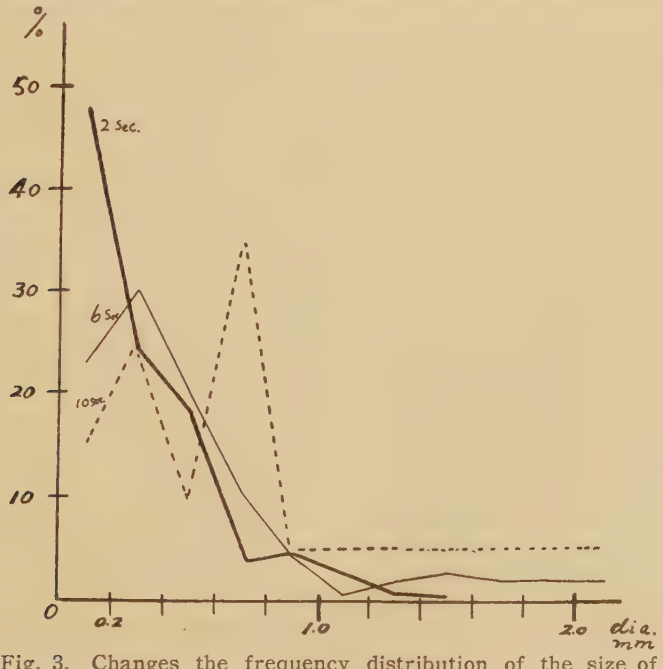

Fig. 3. Changes the frequency distribution of the size of bubble of foam layer

their median values. As seen in this figure, there is the bubble having maximum frequency at each stage and the size of it increases with time to a certain value

Table. 2.

Time (sec)	2	6	10
Dia. at max. frequ. (mm)	0.1	0.3	0.7
Max. frequ. (%)	48.0	30.5	35.0

(see Table 2). From Fig. 3, the changes of frequencies with time for various sizes of bubbles can be obtained, which are shown in Fig. 4.

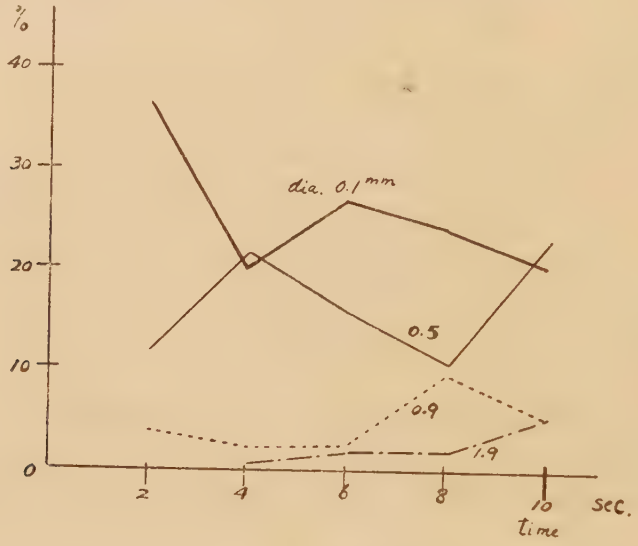

Fig. 4. Relation between the frequency distribution of bubble and time

[3] **Changes of the mean radius of bubbles in foam layer.**

The mean radius r was calculated by the following formula:

$\bar{r}=\sqrt{\frac{\sum n \cdot r^2}{\sum n}}$, where r is the radius of each bubble, and n the number of bubbles.

An empirical formula was found as follows:

$\bar{r}=C_1+C_2 \cdot t$, where C_1 and C_2 are const. and t is time.

In the case of sea water having chlorinity 14.42‰ at the temperature of 21°C, C_1 and C_2 are 0.33 and 0.018, respectively.

[4] **The mean life of a bubble in the foam layer.**

The distribution of the size of bubbles in the foam layer changes its form as shown in Fig. 8-a, where d is the diameter of the bubble, p the frequency and t the time ($t_1<t_2<t_3$, $t_2-t_1=t_3-t_2=2\delta$, δ is time element).

Let the frequencies of bubbles having diameter d_x, be $p_{x\cdot1}$ at t_1, $p_{x\cdot2}$ at t_2 and $p_{x\cdot3}$ at t_3. Eq. (1) gives:

$$h_1=h_0e^{-kt_1} \quad h_2=h_0e^{-kt_2} \quad h_3=h_0e^{-kt_3}$$

Put $h_1-h_2=\Delta h_{1\cdot2}$, $h_2-h_3=\Delta h_{2\cdot3}$; $\Delta h_{1\cdot2}$ is the decrease in foam height between

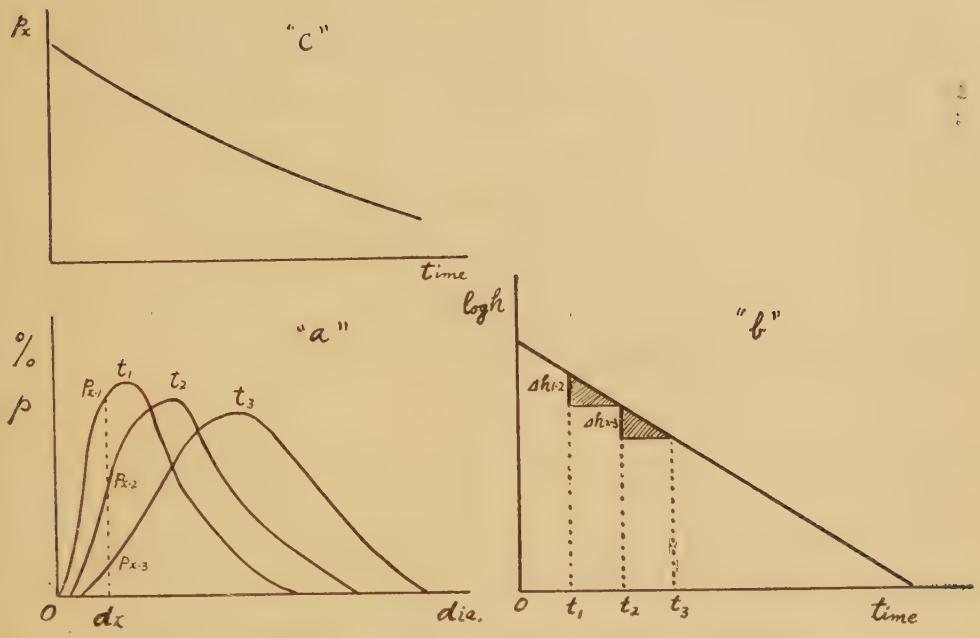

Fig. 5. Schematic diagram of determination of bubble life

t_1 and t_2, and the shaded parts of Fig. 5–b represent the amount proportional to the numbers of bubbles decayed in this time interval.

Then
$$n_{1\cdot2}=k\cdot\Delta h_{1\cdot2}\cdot 2\delta/(\bar{d}_{1\cdot2})^2 \tag{5}$$

where k is a certain constant, $\bar{d}_{1\cdot2}$ the mean diameter corresponding to the time interval.

In a similar manner, we have:

$$n_{2\cdot3}=k\cdot\Delta h_{2\cdot3}\cdot 2\delta/(\bar{d}_{2\cdot3})^2 \tag{6}$$

Therefore from Eqs. (5) and (6), we have,

$$\frac{n_{2\cdot3}}{n_{1\cdot2}}=\frac{\Delta h_{2\cdot3}}{\Delta h_{1\cdot2}}\left(\frac{\bar{d}_{1\cdot2}}{\bar{d}_{2\cdot3}}\right)^2 \tag{7}$$

Further, from
$$\frac{\Delta h_{2\cdot3}}{\Delta h_{1\cdot2}}=e^{-2k\delta}$$

Eq. (7) becomes

$$\frac{n_{2\cdot3}}{n_{1\cdot2}}=e^{-2k\delta}\left(\frac{\bar{d}_{1\cdot2}}{\bar{d}_{2\cdot3}}\right)^2 \quad \text{or} \quad n_{2\cdot3}=e^{-2k\delta}\left(\frac{\bar{d}_{1\cdot2}}{\bar{d}_{2\cdot3}}\right)^2\cdot n_{1\cdot2}$$

Similarly,
$$n_{3\cdot4}=e^{-2k\delta}\left(\frac{\bar{d}_{2\cdot3}}{\bar{d}_{3\cdot4}}\right)^2\cdot n_{2\cdot3}$$

therefore, the following recurrence formula is generally obtained:

$$n_{s\cdot(s+1)}=e^{-2k\delta}\left(\frac{\bar{d}_{(s-1)\cdot s}}{\bar{d}_{s\cdot(s+1)}}\right)^2\cdot n_{(s-1)\cdot s} \tag{8}$$

Among the number of bubbles which decayed between t_1 and t_2, the number of those whose diameter is d_x, is $n_{1\cdot 2}\ p_{x_1}$, and the life of them are considered as $\frac{1}{2}(t_1+t_2)$ or $(t_1+\delta)$. And so if the mean life of the bubble is represented by τ_x, by the idea of expectation in probability,

$$\tau_x = \frac{\int_0^\infty t \cdot n_t p_x \cdot dt}{\int_0^\infty n_t \cdot p_x \cdot dt} \fallingdotseq \frac{\Sigma t_i \cdot n_i \cdot p_i}{\Sigma n_i \cdot p_i} \tag{9}$$

τ_x can be calculated by substituting the values obtained in Eqs. (4), (8) into Eq. (9). The results of calcuration are given in Table (3).

Table 3.

Dia. (mm) median	0.1	0.3	0.5	0.7	0.9	1.5	1.9
Mean life (sec)	5.1_6	8.0_5	5.6_5	6.4_2	6.0_6	6.9_9	8.5_9

This table shows that a bubble of diameter 0.1 mm has the shortest mean life, and that of diameter 1.9 mm the longest.

Generally speaking, the larger the diameter of a bubble, the longer the mean life, but there is a certain upper and lower limiting value of the diameter.

Though the life of the bubble of diameter 0.1 mm is only 5 seconds, there is always the bubble of this size (see Fig. 4). It is therefore supposed that such a small bubble is in a very activated state and hence easily coagulates with each other and grows up to a larger one, and when larger ones burst, smaller ones are newly produced.

§4. *Acknowledgement*

The author wishes to express his sincere thanks to Dr. Y. Miyake as well as to Dr. M. Nakano for their discussions on the points dealt with in this paper.

References

1. Y. Miyake and T. Abe, 1948: A study on the foaming of sea water. Part 1, (Journ Mar. Res. Vol. VII, No. 2, pp. 67–73).
2. T. Abe, 1953: On the mechanism of the decay of foam layer of sea water, Part 1, Oceanogr. Report. Vol. 3, No. 1 C.M.O.
3. T. Abe, 1953: On the mechanism of the decay of foam layer of sea water, Part 2, Journ. Oceanogr. Soc. Japan. Vol. 9, No. 2.
4. T. Abe 1953: On the foaming of sea water and inorganic electrolyte solutions. Oceangr. Report, C.M.O. Vol. 3, No. 1.

ON THE OCEANOGRAPHIC AND METEOROLOGICAL CONDITIONS AT THE FIXED STATION "EXTRA" IN THE NORTH PACIFIC OCEAN I

Koizumi Masami

Reprinted from

Records of Oceanographic Works in Japan

Volume I, No. 2, New Series,

December 1954

Published by

Japanese National Commission for Unesco

Records of Oceanographic Works
in Japan, Vol. 1, No. 2,
New Series, December 1953

On the oceanographic and meteorological conditions at the fixed station "Extra" in the North Pacific Ocean (Part 1)

By Masami Koizuni

Oceanographical Laboratory, Meteorological Research Institute, Tokyo

1. Since October 1947, maritime meteorological as well as oceanographic observations have been performed without interruption in spite of various diffculties by the Central Meteorological Observatory of Japan at a fixed station in the western part of the North Pacific Ocean, centered at 39°N, 153°E and called "Extra" or abbreviatedly "X". And an enormous amount of data has already been accumulated. If these abundant data are dealt with corresponding to the respective purposes of various kinds of investigations, many interesting and worthy results will be obtained.

A weather ship is not always fixed at the center but in most cases drifted here and there within the permissible circle of 50sm radius. Meteorological observations have been carried out every hour up to quite recently but afterwards 8 times a day. The points where the meteorological observations were performed are more or less scattered, but it will be allowed to consider that the distribution of these points has a parttern similar to that of the oceanographic stations, in regard to which the author described in the previous reports [1] [2]; the stations are so densely distributed around the center that 90% of them are within the area of 38°30′–39°30′N and 152°30′–153°30′E. However, in this paper the distribution of the stations will not be taken into consideration in particular except those which are located within the same limits as previously reported, *viz.* 38°–40°N and 152°–154°E.

2. Sea-surface temperature is most frequently observed in any region of the sea because of the simplicity of measurement, and also very ofted used in order to obtain informtion on a general trend of oceanograhic conditions. Therefore, it seems to be most necessary that the properties of sea-surface temperature are examined in detail from various points of view.

Here the sea-surface temperature as well as air temperature at the "Extra" are dealt with. In the first place, the daily means and then the moving averages of 11 days are computed for the two elements. Also, the monthly and yearly means are obtained. The moving averages and the monthly means are plotted in Figure 1. Some characteristic figures of the annual variations of both elements,

based on the monthly means, for instance, in the case of 1949, are given in Table 1, in which the corresponding figures for the fixed point "Tango" or shortly "T" (29°N, 135°E) [3] are also inserted for the sake of comparison, but they are based

Table 1 Some characteristic figures in the annual variation of air and sea-surface temperatures

St.	Element	Max. (time of occur.)	Min. (time of occur.)	Ann. range	Year. mean	Remarks
"X"	t_w	23.32 (Sept.)	10.46 (Mar.)	12.86	15.93	1949
	t_a	22.36 (Sept.)	4.99 (Mar.)	17.37	13.00	
"T"	t_w	27.58 (Aug.)	18.74 (Feb.)	8.84	22.95	From Jun. 1950 to May 1951. By Masuzawa [3]
	t_a	27.25 (Aug.)	15.86 (Feb.)	11.39	21.28	

t_w: sea-surface temperature in °C
t_a: air temperature in °C

on the data from June 1950 to May 1951. However, it is to be noted that the year of 1949 showed generally lower temperatures among the five years from 1948 to 1952, and in this year, the extremes and the annual range of the surface temperature were smaller than those of the monthly means of the five years. The annual ranges of air and sea-surface temperatures, especially of the former, are much greater at the "Extra" than at the "Tango". Since, in the North Pacific Ocean, the annual range of the sea-surface temperature generally reaches a maximum of about 10°C in the zone of about 40°N [4], the vicinity of the "Extra" with a range of more than 12°C is probably one of the regions with the greatest annual range of the sea-surface temperature in the whole ocean. The maximum of the sea-surface temperature occurred in September in the year of 1949, but in the remaining cases among the five years it took place in August, and the latter case as this may be considered as normal. The minimum of the surface temperature takes place ordinarily in March, but sometimes in February. The extremes of the air temperature occur generally in accordance with those of the surface temperature. The time of occurrence of the extremes at the "Extra" seems to be somewhat different from that of the "Tango".

In Table 2 are given the differences between the air and sea-surface temperatures, based on the monthly means. For the sake of comparison the differences for the "Tango" are also shown in Table 2. The sea-surface temperature is, as far as the monthly means are concerned, higher than the air temperature, though, as shown in Figure 1, in the moving averages the latter is sometimes higher than the former in summer season. Therefore, heat is, on a average, given off from the ocean to the atmosphere. The difference, $t_w - t_a$, is markedly large from late autumn to early spring, and in summer it is generally very small. With dry prevailing wind, such a large difference of temperature is expected to increase the evaporation in a marked degree. The period in which the surface temperature

Table 2 Differences between air and sea-surface temperatures (°C)

(By the monthly means)

$t_w - t_a$

St.	Jan.	Feb.	Mar.	Apr.	May	Jun.	Jul.	Aug.	Sep.	Oct.	Nov.	Dec.
"X"	5.0	4.9	5.5	2.3	0.4	1.4	0.1	0.5	1.0	2.4	5.0	6.6
"T"	3.3	2.9	2.8	1.0	0.8	0.6	0.2	0.3	0.4	1.4	1.8	4.6

t_w: sea-surface temperature.
t_a: air temperature.

is lower than the direct subsurface temperature almost coincides with that of the said large difference. The large amount of evaporation and the air temperature much lower than the surface temperature are to be very effectual on the rapid cooling of the sea surface.

Now, at a glance upon Figure 1, it is found that the series of the moving averages rise and fall with a shorter and more or less distinct period, being superimposed on the general annual variation. This may be associated with the meandering of the ocean currents, but still affords a scope for further investigation. The author intends to touch on this problem in a subsequent paper. Again, it is recognized that in the series of the moving averages the sea-surface temperature varies more smoothly than the air temperature. It is perceived from this that the air temperature is liable to fluctuate in a marked degree compared with the sea-surface temperature. In fact, the plotted daily means of the air temperature are particularly in winter notably scattered, whereas those of the sea-surface temperature generally deviate little from the course of its moving average. The larger fluctuation of the air temperature will be understood, if we consider the magnitudes of the density and specific heat of air and sea water, and also the speeds of the movements of air and water masses.

Finally, the monthly means of the surface temperature computed from all the observed values are compared with those obtained only from the values at the oceanographic stations where serial observations of oceanographic elements were made. The result for the year of 1949 is shown in Table 3. The difference, $t'_w - t_w$, falls mostly within the range of ± 0.5°C, while the case where the difference, $t'_a - t_a$, exceeds this range occur very frequently. The accuracy of such a mean as $t'_a(t'_w)$ in Table 3 may be unsatisfactory for some special purposes and for a better accuracy more abundant data will have to be taken into consideration in computation. J. Masuzawa [5], using the data of the sea-surface temperature at the "Tango", calculated the ranges within which the deviations of the mean temperature of several observations in a day from the daily mean (average of hourly observations) take place with the probability of 95%. According to his calculation, it is shown, for instance, that if we average four observations the probability with which the deviation of this mean from the daily mean exceeds the range of ±

Table 3

Comparison of monthly mean of hourly-observed sea-surface (air) temperatures with mean of the observed sea-surface (air) temperatures at the time of oceanographic observations, $t'_w(t'_a)$.

1949	Jan.	Feb.	Mar.	Apr.	May	Jun.	Jul.	Aug.	Sep.	Oct.	Nov.	Dec.
(°C)												
t_w	12.6	11.6	10.5	10.6	12.7	15.6	20.0	22.5	23.3	19.6	17.3	14.7
t_w'	13.0	11.7	10.2	10.9	12.8	16.2	20.3	22.3	23.4	19.6	17.4	15.1
$t_w'-t_w$	0.4	0.1	−0.3	0.3	0.1	0.6	0.3	−0.2	0.1	0.0	0.1	0.4
t_a	7.7	6.7	5.0	8.3	12.3	14.2	19.9	22.0	22.4	17.1	12.3	8.1
t_a'	7.9	6.3	6.0	7.7	12.4	14.6	20.6	21.7	22.5	16.9	11.4	7.7
$t_a'-t_a$	0.2	−0.4	1.0	−0.6	0.1	0.4	0.7	−0.3	0.1	−0.2	−0.9	−0.4
n	9	9	5	8	13	20	17	21	17	15	10	5

n: Numbers of oceanographic stations.

0.3°C is only 5%. Of course, the case he treated is concerned with the diurnal variation, and it is applicable to the regions such as the "Tango" where any variation besides the diurnal one is only small as a rule. For the case of the "Extra" where different water masses contact with each other and accordingly the variations of meteorological and oceanographic phenomena are intense and intricate, the more complicated methods will have to be applied. Anyhow it will be certain that in this case we must increase the number of data to be used in order to gain such an accuracy as mentioned above.

References

[1] Koizumi, M. (1951): On the oceanographical conditions around the fixed point "X-Ray" (39°N, 153°E) (1948–1949) (in Japanese). *Oceanogr. Rep. C.M.O.*, **2** (4).

[2] Koizumi, M. (1953): On the annual variation in oceanographic elements at a fixed point (39°N, 153°E) in the Pacific Ocean. *Records of Oceanographic Works in Japan, new series* **1** (1).

[3] Masuzawa, J. (1952): The heat exchange between sea and atmosphere in the southern sea of Japan (in Japanese). *Journ. Oceanogr. Soc. Japan*, **7** (3/4).

[4] Sverdrup, H. U. et al. (1942): *The Oceans*. Prentice-Hall, New York. pp. 129–130.

[5] Masuzawa, J. (1951): Diurnal variations of the surface water temperature in the open sea (in Japanese). *Journ. Oeanogr. Soc. Japan*, **6** (3).

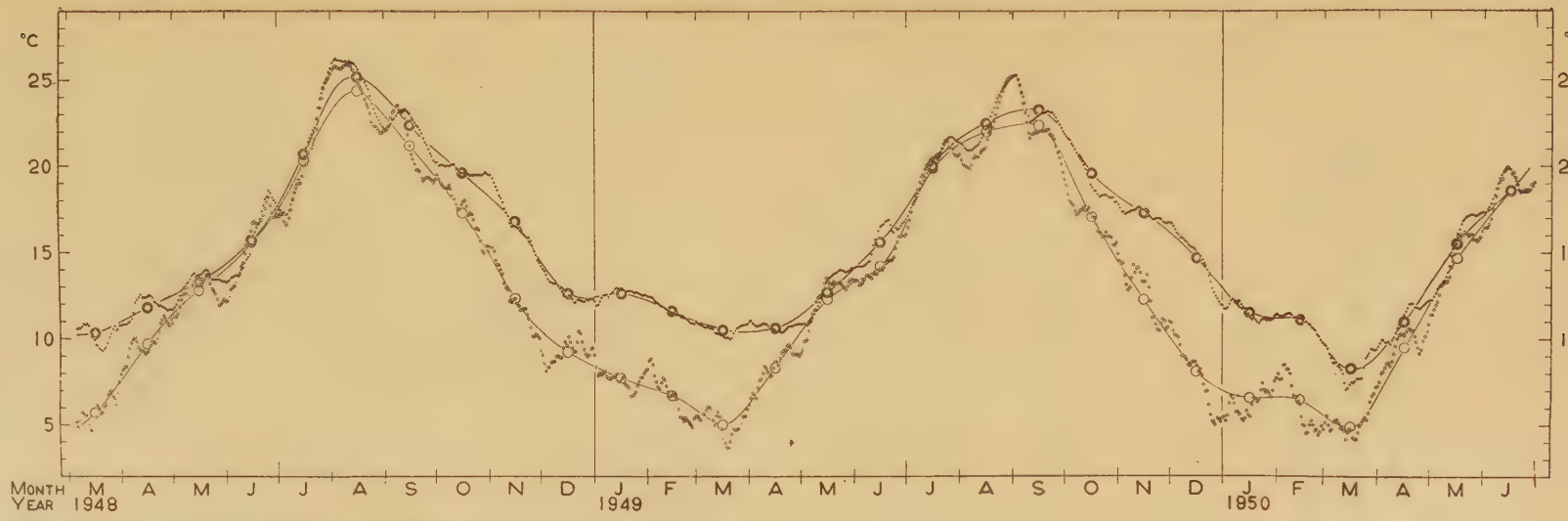

Fig. 1. The variations of the air and sea-surface temperatures at the fixed station "Extra" (30° N, 153° E) in the North Pacific Ocean from March 1948 to June 1949. The small circles represent the moving averages of 11 days, the open being for air temperature and the solid for sea-surface temperature. The large open circles and large double circles represent the monthly means of air and sea-surface temperature respectively.

Records of Oceanographic Works
in Japan, Vol. 1, No. 2,
New Series, December 1953

A study on the foaming of sea water
On the mechanism of the decay of foam layer of sea water

By Tomosaburo Abe

Oceanographic Laboratory, Meteorological Research Institute

§1. *Introduction*

In observation of surface conditions of the sea, Beanfort's scale is mainly used at present. Existence of white-chops produced by wind is the most important factor on this scale.

It is considered from our experimental results that the degrees of white-chops change with the chlorinity concentration of sea water, the temperature and the stability of foam. These experimental relationships have already been reported by Y. Miyake and T. Abe. In the present paper, the mechanism of the decay of foam layer of sea water has been experimentally studied.

§2. *Experimental procedure.*

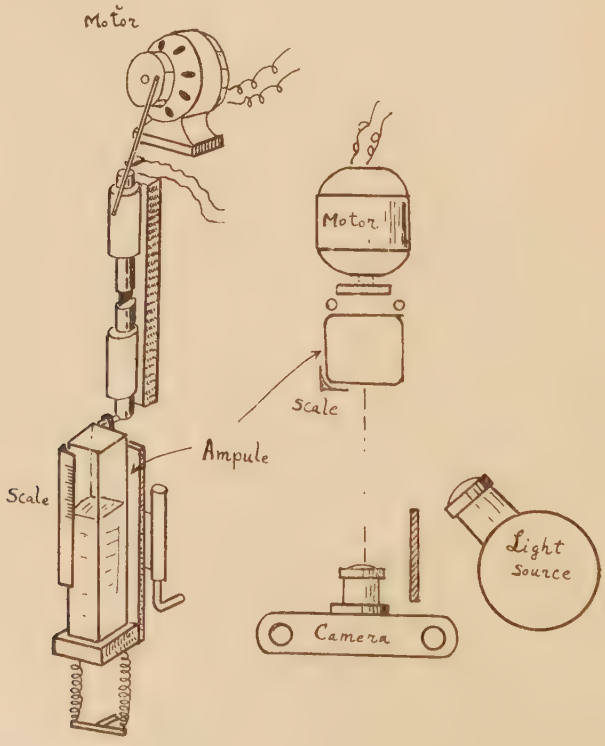

Fig. 1. Diagram of Apparatus

LARVIPAROUS OYSTERS FROM THE TROPICAL WEST PACIFIC

Wada Seiji

Reprinted from

Records of Oceanographic Works in Japan

Volume I, No. 2, New Series,

December 1954

Published by

Japanese National Commission for Unesco

be prepared for the new species (*Hachijomopalia*). It seems to be natural to treat the new group as a subgenus of *Mopalia*, because it will be the nearest akin to *Mopalia* s. str. of all groups of Mopaliidae in many points, as decribed above.

Type. The Holotype and 2 paratypes are preserved in the Zoological Department, National Science Museum, Tokyo. Coloration. Holotype: central area of tegmentum painted with dark brown, white and green patches on the posterior boundary and on some jugal regions on the ground color of yellowish buff; lateral area finely mottled with small white and green patches and large vermilion maculations; girdle generally brownish buff, light buff at sutures, caudal end and at base of bristle-tufts.

Paratype (a): blue and dark brown patches on the apex and the 2nd jugal region on the ground color of milky white; central area of the 2nd valve streaked with 3 brown maculations on each side; jugal boundaries of other valves mottled with blue, dark brown on the light blue ground color: girdle light buff throughout.

Paratype (b): shell colored with purplish brown all over the surface, freckled sparsely with deep blue, especially on the jugal region; girdle brown throught.

Records of Oceanographic Works
in Japan, Vol. 1, No. 2,
New Series, Decembeber 1953

Larviparous Oysters from the Tropical West Pacific

By Seiji K. Wada

Oceanographical Laborotory, Meteorological Research Institute

Out of about 100 species of oysters inhabiting tropical or temperate regions, about 10 species are known to be larviparous. In a previous paper (1942), the author reported that oysters of four species from the Palau Islands, *Ostrea cristagalli, O. cumingiana, O. crenulifera* and *O. hyotis*, are larviparous. After that, additional observations were made on *O. crenulifera* at Misaki, Japan, and further scrutiny of the data reveals doubt as to whether *O. hyotis* is a larviparous species, although occurrence of the larviparous mode of reproduction in the other three species is unequivocal.

Since the previous paper was written in Japanese, some of the results presented in that paper will be reproduced here, with a description of further findings on *O. crenulifera* and an amendment of the previous report.

The works was carried out at the Palau Tropical Biological Station, Palau, West Carolines, in 1940 and at the Misaki Marine Biological Station, Misaki, in 1943.

Materials were obtained from the vicinity of these stations.

Results

Ostrea crista-galli Linné. Oysters of this species inhabit the lagoon waters of the Palau Islands. The animal is found in the water from the low water mark to the bottom. It is never found in tidal regions. The animals not infrequently live gregariously, fixing to coral rocks near the upper edges of coral cliffs which border the water channels between the islands. The shell-height commonly reaches about 8 cm.

Observation of gonads was made in May and August. Generally speaking, the gonads were found to be not fully developed in May. Of 16 animals examined in May, 9 were found in the male phase, 2 in the female phase and 3 individuals showed a hermaphroditic condition, while 2 were found to be in a spent condition. In August, animals with well matured gonads were commonly found. Of 20 individuals, 13 were in the male phase, 3 in the female phase, and 4 were hermaphroditic. One small individual, measuring 35×25 mm, was found to be still sexually undifferentiated.

In August, two individuals were found carrying veligers on their gills. In one of them, the veligers were in an early stage of development, white in color with D-shaped shells. The shell, measuring 110 μ in length, 85 μ in height and 50 μ in hinge-length, did not yet cover the whole soft part of the body. In the other animal, the veligers were well-grown, being old-rose in color. The shell-valve measured 153 μ in length, 137 μ in height and 70 μ in hinge-length. Three pairs of teeth had made their appearance on each side of the hinge. The hinge was tinted reddish brown. The umbo had just begun to protrude above the hinge line.

On being released into sea water, these veligers swam about actively, forming columns in a glass jar, as is commonly observed in free-living veligers of other bivalves. In this species, the veligers seem to be released from the maternal branchial cavity at this stage of development.

As in other larviparous oysters, "sperm-balls" of motile spermatozoa were always observed when male gonads were expressed in sea water. Gonadal eggs, when mature, are spherical in form, and 85 μ in diameter; although the germinal vesicle is present, it cannot be seen through a microscope in intact eggs, owing to the heavy accumulation of yolk matter in the cytoplasm.

It is noted that all individuals measuring under 50 mm in shell-height were found in the male phase, while in larger forms, all the cases of sexuality were represented.

Ostrea cumingiana Dunker. Oysters of this species generally show a habit similar to that of *O. crista-galli*. Sometimes animals of these two species were found forming a clump together. Molluscs of the present species were also found in tidal regions near the low water mark.

Examinations on the conditions of the gonads were made from May to August. During these months, animals well developing gonads were common, while in some specimens, the gonads had developed only slightly. The observation included 29 individuals in the male phase, 6 in the female phase and 8 hermaphrodites. Sperm-balls were always found in male or hermaphroditic follicles. Eggs occurring in mature gonads were oval in shape, measuring about 175×165 μ on an average. This probably is the largest among the eggs of the larviparous oysters. Eggs were heavily laden with yolk granules and opaque under a microscope, the germinal vesicle present. The vitelline membrane was very fragile, as in cases of other larviparous oysters. In the middle of June, one animal carrying embryos in an early developmental stage was found.

Ostrea crenulifera Sowerby. Oysters of this species are commonly found on reef flats, attaching to coral boulders or dead corals.

Although examination of gonadal conditions was not made at Palau, the swarming of veligers, that is, the release of veligers from the parental mantle cavity, was observed in the laboratory in the middle of September. The shell-valve

of the veliger measured 180 μ in length, 160 μ in height and about 85 μ in hinge-length. The veliger was tinted light green all over the body; the larval liver was lightly yellowish brown in color. A pair of eye-spots were very prominent. The veliger was D-shaped, the umbonal region not yet protruding.

Oysters of this species are also commonly found around the low water mark in the vicinity of the Misaki Marine Biological Station. On these oysters, observations were made during the months from May to August.

The results of observation on the ripeness of the gonads and the number of gravid oysters are summarized in Table 1. In the table, the condition of the gonads is expressed by the terms, A, B, C, D and Spent, in the order of ripeness.

Table 1. Reproductive activity of O. crenulifera (Misaki, 1943).

Date	Gonadal conditions					Total	Gravid oysters			
	A	B	C	D	Spent		Black-sick	White-sick	Total	%
May 20	10	7	2	2	0	21	0	0	0	0
June 5	13	2	0	0	0	15	0	0	0	0
June 19	2	6	4	7	10	29	3	4	7	24
29	2	5	5	1	15	28	1	0	1	3.5
July 2	6	9	13	15	11	54	1	6	7	13
3	4	8	15	18	23	78	1	4	5	6.5
5	3	7	8	13	10	41	1	11	12	29
Aug. 12	4	9	6	4	26	49	0	1	1	2
16	3	5	6	5	25	44	3	7	10	23
Total						359			43	

The figures represent the number of oysters. Ripeness of the gonads is conventionally expressed by the terms A, B, C, D and Spent in the order of their development.

Inspection of the table clearly shows that spawning was inaugurated about the middle of June and lasted through July and August. It is noted that, with only one exception among 43 cases, all of the gonads of the gravid animals were graded into one of the classes, C, D or Spent. The smallest individual among the embryo-bearing oysters was 15 mm in shell-length.

Sperm balls were always observed if the male gametes were recognized. On one occasion, spawning of sperm occurred in an oyster which was observed to have previously discharged veligers. This fact indicates that the animal functioned as a female immediately before shedding sperm. The freshly shed spermatozoa were all aggregated in speam balls, measuring about 20–50 μ in diamater, and no free spermatozoa were present.

Ripe gonadal eggs are oval or spherical, the diameter measuring 104 μ on an average (mean of 12 measurements). The germinal vesicles of these eggs were broken down when the eggs were exposed to ammoniacal sea water. Breakdown occurs at 60–70 minutes in 1×10^{-3} N NH_4OH sea water. If insemination occurs in such hyperalkaline sea water, fertilization can be accomplished artificially. Formation of first and second polar lobes was observed in eggs fertilized in this manner. According to Seno (1929), formation of polar lobes does not occur in the development of eggs of *O. denselamellosa*.

Black pigment appears in the liver when the shell of the embryo grows to 175 μ in length, 145 μ in height and 85 μ in hinge-length; at this stage, an eye-spot has appeared on the left side, but the intestine has not yet formed a loop. The aggregation of larvae at this stage is still designated as "white-sick", the larvae appearing opaque because of abundant yolk granules.

In a "black-sick" veliger measuring 185×160 μ, in which the eye-spot is still one-sided, the crystaline-style sac is formed, the intestine looped, the hinge-teeth making their appearance. From these stages on, the larvae are still retained in the mantle cavity of the parent oyster. The stomach of these veligers was observed to contain minute bits of food matter.

Swarming of the larvae was observed in the middle of August. These larvae measured 184–204 μ in shell-length, 163–177 μ in shell-height and 78–82 μ in the length of the hinge line. The mean is 192 μ, 171 μ and 81 μ respectively. However, the size at which the larvae are released from the maternal branchial cavity appears to very with the brood. One brood was found being retained in the mantle cavity which consisted of veligers measuring, on an average, 203 μ in shell-length, 180 μ in shell-height and 87 μ in hinge-length, these being considerably larger than the just mentioned, discharged veligers.

At the stage when it is released, the veliger has developed a pair of large, black eye-spots, and two pairs of interlocking teeth are present on each sides of the hinge. An individual tooth measures 4–7 μ in base-diameter and ca. 3 μ in height. The distance between neighboring teeth of the left and right sides is about 45 μ. These teeth persist throughout the following development of the veligers. In the style sac, cilia beating in waves towards the stomach are not infrequently observed.

Further development of the shelled larvae was traced from an examination of plankton samples collected in August. The free-swimming veliger can be indentified by the presence of prominent eye-spots at the base of the foot and the black color of the liver; a yellowish brown tinge which occurs in an antero-dorsal area of the liver also presents a useful feature for species identification.

Fully-grown veligers, which were observed crawling on the bottom of the glass

dish, measured 325–340 μ in shell-length and 315–325 μ in shell-height (measurements on the left valve). Spat fall was observed to have occurred on slates submerged in August. On the young spat thus obtained, measurements of the larval shell were made: left, i.e. underside, valve measured 314–331 μ (average 319 μ) in length, and 334–367 μ (av. 347 μ) in height (5 measurements each), while the right, upper valve measured 308–328 μ (av. 314 μ) in length and 314–334 μ (av. 327 μ) in height (8 measurements each).

Discussion

Judging from the facts presented above, it is certain that oysters of the three species, *O. crista-galli*, *O. cumingiana* and *O. crenulifera*, are larviparous. As far as the writer knows, excluding these three species, a larviparous mode of reproduction is known to occur in the following 9 species:

O. edulis, O. denselamellosa, O. angasi, O. circumpicta, O. futamiensis, O. equestris, O. lurida, O. lutaria, O. plicata.

(Amemiya, 1933; Gutsell, 1926; Orton, 1937; Seki, 1929, 1934).

All of these oysters are inhabitants of temperate waters. This fact leads Orton (1937) to the erroneous conclusion that larviparous oysters "occur in temperate regions", while oviparous species "occur in warm to tropical regions".

Amemiya (1933) listed a species-unknown oyster of the South Seas in the list of larviparous oysters. Since no description was given about this, it is quite uncertain to what species this oyster belongs However, it is highly probable that further search would bring to light many other larviparous forms in the tropical waters.

Seno (1936) was of the opinion that *O. crista-galli* is oviparous. Since no evidence has been presented in this support, however, his conclusion seems to be imaginary. The old-rose color of veligers retained in the branchial chamber of this species is very unusual. No such coloration occurs in veligers of other forms. If a similar terminology to "black-sick" or "white-sick" is applied to this species, *O. crista-galli* gravid with veligers should be called "rose-sick", although, in this case, the color is primarily contributed by the shell-valves and not by the liver.

In the freshly released veligers of *O. crenulifera*, a very marked difference has been observed in the tinge of the liver between a brood from oysters of Palau and that from oysters of Misaki. No black tinge was observed in the Palau batch. Moreover, the size of the veligers at release is smaller in the tropical batch than in the Misaki batch. At present, nothing can be said as to whether these differences are individual or ecological, or genetical. This is left for further examination.

As has already been stated, the size of veligers at release varies considerably between broods of oysters of the same habitat. A similar fact is also reported in *O. lurida* by Hopkins (1937) and Davis (1949).

Further, it has been shown by the writer (1942), through a feeding experiment on *O. glomerata*, that the liver of a D-shaped veliger can readily change its color, the color depending on the nature of the food digested. Differences in the tinge of the veliger liver between broods, though less marked than in the case of *O. crenulifera*, are also reported in *O. lurida* by Hopkins (1937).

The appearance of the eye-spot in an early veliger stage seems to be unique to *O. crenulifera*. In other larviparous oysters, in which the development of the veliger is known, eye-spots appear at a rather late umbone-stage of the free-swimming period. In *O. denselamellosa*, the eye-spot (pigment spot) does not make its appearance in veligers in which the shell-length measures less than 310 μ (Seki, 1930). Similar is also the case in *O. futamiensis*, *O. lurida* and *O. edulis* (Davis, 1948; Hori, 1933; Horst, 1882; Seki, 1930).

In the previously cited paper (Wada, 1942), it was reported that *O. hyotis* Linné is larviparous, because of the discovery of a "white-sick" individual. In this specimen fertilized ova were found between the lamellae and filaments of the gills. However, since the animal had been previously been exposed to the air for several hours before examination, it is not improbable that shed ova might have been retained in the branchial cavity without being discharged to the outside sea water.

In *O. echinata*, an oviparous oyster, it is usually observed that if a spawning female is removed from the sea water, the ova shed from the genital openings are accumulated in the branchial cavity through the ostia of the gills. This will give the "white-sick" appearance of the larviparous oysters.

In *O. hyotis*, hermaphroditic animals were frequently observed. However, this cannot be an unequivocal criterion for larviparous reproduction. Moreover, sperm balls were never observed in this species, while free motile spermatozoa were present in abundance.

Judging from these facts, it is precocious to conclude that *O. hyotis* is larviparous. The problem is left to be solved in the future. Unfortunately, oysters of this species were only sparsely found in the vicinity of the Tropical Biological Station.

Summary and Conclusion

1. Oysters of three species which inhabit tropical water are larviparous. These are *Ostrea crista-galli* Linné, *O. cumingiana* Dunker and *O. crenulifera* Sowerby; the last-named is also found along the southern coast of Japan.

2. Veligers of *O. crista-galli* which are believed to be ready for release from the brachial cavity are old-rose in color.

3. The size of veligers of *O. crenulifera* discharged into the sea water is variable. These veligers are provided with a pair of very distinct eye-spots. The appearance of eye-spots at such an early veliger stage does not occur in other

larviparous oysters. A fully-grown veliger which set as a spat measures about 320 μ in shell-length and 350 μ in shell-height.

4. A marked difference has been observed in the tinge of the larval liver at the time of release between veligers of *O. crenulifera* from Palau and those from Misaki.

5. Whether *O. hyotis* is larviparous or not, cannot be decided at present.

The writer wishes to express his indebtedness to Dr. Shinkishi Hatai, the former director of the Palau Tropical Biological Station, and to the Director of the Misaki Marine Biological Station. He is also deeply indebted to Dr. Jean C. Dan in the preparation of the manuscript.

Literature

Amemiya, I. 1933 Reproduction of Oysters. Tokyo. (In Japanese).

Davis, H. C. 1949 On cultivation of larvae of *Ostrea lurida*. Anat. Rec., **105** (3): 111.

Gutsell, J. S. 1926 A hermaphroditic viviparous oyster of the Atlantic coast of North America. Science, **64**: 450.

Hopkins, A. E. 1937 Experimental observations on spawning, larval development, and setting in the Olympia oyster, *Ostrea lurida*. Bull. Bureau Fish., **68** (23): 439–503.

Hori, J. 1933 On the development of the Olympia oyster, *Ostrea lurida* Carpenter, transplanted from United States to Japan. Bull. Jap. Soc. Sci. Fish., **1**: 269–276.

Horst, R. 1882 A contribution to our knowledge of the development of the oyster (*Ostrea edulis L.*). Bull. U. S. F. C., **2**.

Orton, J. H. 1937 Oyster Biology and Oyster-Culture, being the Buckland Lectures for 1935. 211 pp. London.

Seki, H. 1929 Description of a new species of oyster from Japan. Proc. Imp. Acad., **5** (10).

Seki, H. 1930 Identification on the larva of *Ostrea denselamellosa* Lischke. Jour. Imp. Fish. Exp. Sta. (Tokyo), **1** (1): 233–240.

Seki, H. 1934 Description of *Ostrea nippona*, n. sp., with remarks on *Ostrea circumpicta* Pilsbry. Venus, **4** (5): 375–284.

Seno, H. 1929 A contribution to the knowledge of the development of *Ostrea denselamellosa* Lischke. Jour. Imp. Fish. Inst. (Tokyo), **24** (5): 129–135.

Seno, H. 1936 Oyster-culture in the world. Shokubutsu oyobi Dobutsu, **4** (3): 577–586. (In Japanese)

Wada, S. 1942 Notes on the oysters of Palau. Science in the South Seas (Kagaku Nan'yo), **5** (1): 69–73. (In Japanese).